

# Effective Theories in Cosmology

## ACADEMISCH PROEFSCHRIFT

ter verkrijging van de graad van doctor  
aan de Universiteit van Amsterdam  
op gezag van de Rector Magnificus  
prof. dr. D.C. van den Boom  
ten overstaan van een door het college voor promoties  
ingestelde commissie,  
in het openbaar te verdedigen in de Agnietenkapel  
op dinsdag 24 september, om 10:00 uur

door

**Sander Johannes Nicolaas Mooij**

geboren te Haarlem

Promotor: prof. dr. E.L.M.P. Laenen  
Co-promotor: dr. M.E.J. Postma

Overige leden: prof. dr. A. Achúcarro  
prof. dr. J.-W. van Holten  
prof. dr. F.L. Linde  
prof. dr. J. Smit  
prof. dr. E.P. Verlinde  
dr. D. Roest  
dr. J.P. van der Schaar

Faculteit der Natuurwetenschappen, Wiskunde en Informatica

This work is part of the research programme of the Foundation for Fundamental Research on Matter (FOM), which is part of the Netherlands Organisation for Scientific Research (NWO). It has been part of the research project “*The early universe as a particle laboratory*” (file number 680-47-229). The research has been carried out at the National Institute for Subatomic Physics Nikhef.

Cover design by Yannick Nory ([cargocollective.com/YNy](http://cargocollective.com/YNy))  
Printed by Ipskamp Drukkers

This thesis is based on the following publications:

S. Mooij and M. Postma,  
*Hybrid inflation with moduli stabilization and low scale supersymmetry breaking*,  
JCAP **1006**, 012 (2010) [arXiv:1001.0664 [hep-ph]].

S. Mooij and M. Postma,  
*Goldstone bosons and a dynamical Higgs field*,  
JCAP **1109**, 006 (2011) [arXiv:1104.4897 [hep-ph]].

A. Achúcarro, S. Mooij, P. Ortiz and M. Postma,  
*Sgoldstino inflation*,  
JCAP **1208**, 013 (2012) [arXiv:1203.1907 [hep-th]].

D. P. George, S. Mooij and M. Postma,  
*Effective action for the Abelian Higgs model in FLRW*,  
JCAP **1211**, 043 (2012) [arXiv:1207.6963 [hep-th]].

A. Linde, S. Mooij and E. Pajer,  
*Gauge field production in SUGRA inflation: local non-Gaussianity and primordial black holes*,  
Phys. Rev. D **87**, 103506 (2013) [arXiv:1212.1693 [hep-th]].



# Contents

<b>I</b>	<b>Introduction</b>	<b>11</b>
<b>1</b>	<b>Cosmology and inflation</b>	<b>13</b>
1.1	Cosmology . . . . .	13
1.1.1	The metric of the universe . . . . .	15
1.1.2	The dynamics of the universe . . . . .	15
1.1.3	The CMB radiation . . . . .	16
1.2	Inflation: why and how . . . . .	17
1.2.1	Naturalness problems . . . . .	17
1.2.2	Expansion from negative equation of state . . . . .	19
1.2.3	Slow-roll variables . . . . .	20
1.3	Inflating quantum perturbations . . . . .	21
1.4	Inflationary observables . . . . .	24
1.5	Inflationary model building and the $\eta$ -problem . . . . .	27
1.5.1	Small field models . . . . .	28
1.5.2	Large field models . . . . .	28
1.5.3	Hybrid models . . . . .	28
1.5.4	Symmetries . . . . .	29
1.5.5	Lyth's bound . . . . .	29
1.6	Inflation in supergravity . . . . .	29
1.7	Higgs inflation . . . . .	30
<b>2</b>	<b>Effective field theory and the in-in formalism</b>	<b>33</b>

2.1	In-out formalism . . . . .	33
2.1.1	Propagators and Wightman functions . . . . .	33
2.1.2	Path integral method . . . . .	35
2.2	Effective action for the real scalar field . . . . .	36
2.2.1	Quantum fluctuations modify the classical theory . . . . .	36
2.2.2	Computation of $\Gamma$ . . . . .	37
2.3	Free mass split . . . . .	39
2.4	Effective equation of motion for the real scalar field . . . . .	41
2.5	In-in formalism . . . . .	43
2.6	Effective equation of motion in the in-in formalism . . . . .	45
2.6.1	Effective action in the in-in formalism . . . . .	47
2.7	Scalar field with time dependent mass . . . . .	47
2.7.1	Perturbative approach . . . . .	47
2.7.2	Non-perturbative approach . . . . .	48
2.7.3	Effective action . . . . .	50
<b>II</b>	<b>Rolling fields</b>	<b>51</b>
<b>3</b>	<b>Effective action for the U(1) Abelian Higgs model</b>	<b>53</b>
3.1	Motivation: Goldstone bosons in a rolling background . . . . .	53
3.1.1	Goldstone's theorem . . . . .	54
3.2	Lagrangian . . . . .	55
3.3	Perturbative computation (in arbitrary gauge) . . . . .	57
3.4	Non-perturbative computation (in the gauge $\xi = 1$ ) . . . . .	62
3.5	Discussion: on-shell gauge invariance and the trouble of unitary gauge . . . . .	66
<b>4</b>	<b>Extension to FLRW</b>	<b>69</b>
4.1	Real scalar field . . . . .	69
4.2	Action . . . . .	71
4.3	Effective equation of motion . . . . .	74
4.3.1	First order contribution $\mathcal{A}^{(1)}$ . . . . .	76

<i>CONTENTS</i>	7
4.3.2 Second order contribution $\mathcal{A}^{(2)}$	76
4.3.3 Third order contribution $\mathcal{A}^{(3)}$	77
4.3.4 Summary of graphs	78
4.4 Effective action	78
4.4.1 Fermions and additional scalars	81
4.4.2 Initial conditions	83
4.5 Discussion	84
<b>III Inflation in supergravity</b>	<b>85</b>
<b>5 Sgoldstino inflation</b>	<b>87</b>
5.1 Introduction: single field sugra inflation	87
5.2 Decoupling of the sgoldstino	90
5.2.1 Mass matrix	90
5.2.2 Kähler invariant function for sgoldstino inflation	92
5.2.3 Inflationary trajectory	92
5.2.4 Separable Kähler function	94
5.3 Single field sgoldstino inflation	94
5.3.1 Large field inflation	95
5.3.2 Hybrid inflation	96
5.3.3 Small field inflation	97
5.4 Conclusions	102
<b>6 Gauge field production and non-Gaussianity</b>	<b>103</b>
6.1 Introduction	103
6.2 CMB scales: violations of Gaussianity and scale invariance	106
6.3 Very small scales: strong backreaction	109
6.4 Bounds from primordial black holes	111
6.5 Local non-Gaussianity from heavy vector fields	114
6.6 Stochastic approach	116
6.7 Gauge field production in sugra inflation: reheating	117

6.8	Conclusions . . . . .	119
<b>7</b>	<b>Moduli stabilisation</b>	<b>121</b>
7.1	Introduction . . . . .	121
7.2	The model: sugra hybrid inflation . . . . .	122
7.3	Adding the modulus sector . . . . .	124
7.3.1	General approach . . . . .	125
7.3.2	Discussion . . . . .	127
7.4	Inflation with a KL modulus sector . . . . .	128
7.4.1	Inflation . . . . .	129
7.4.2	Numerical analysis . . . . .	130
7.5	Conclusions . . . . .	131
<b>IV</b>	<b>Outlook</b>	<b>133</b>
<b>A</b>	<b>Mode functions for the time dependent scalar field</b>	<b>137</b>
<b>B</b>	<b>Abelian Higgs model</b>	<b>141</b>
B.1	Mixed propagator . . . . .	141
B.2	Mode functions . . . . .	143
<b>C</b>	<b>Vector loops</b>	<b>147</b>
C.1	Minkowski . . . . .	147
C.2	FLRW . . . . .	150
C.2.1	$\mathcal{A}_{\text{mass}}^{(2)}$ . . . . .	151
C.2.2	$\mathcal{A}_{\text{mass}}^{(2)}$ . . . . .	152
C.2.3	$\mathcal{A}_{\text{mix}}^{(3)}$ . . . . .	152
<b>D</b>	<b>Action for Abelian Higgs model in FLRW</b>	<b>155</b>
<b>E</b>	<b>Small spectral index for inflection point inflation</b>	<b>159</b>
<b>F</b>	<b>Effects of gauge field production in the CMB</b>	<b>161</b>

<i>CONTENTS</i>	9
F.1 Variance of $\vec{E} \cdot \vec{B}$ . . . . .	161
F.2 Power spectrum estimate . . . . .	162
F.3 Skewness of $\vec{E} \cdot \vec{B}$ . . . . .	165
F.4 Bispectrum and $f_{\text{NL}}$ estimate . . . . .	165
F.5 Black hole masses . . . . .	167
<b>G SUGRA Coleman-Weinberg potential</b>	<b>169</b>



## Part I

# Introduction



# Chapter 1

## Cosmology and inflation

This first chapter is meant to give some background information on cosmology in general and inflation in particular. The emphasis is on the material needed to appreciate the work done in our articles [1, 2, 3, 4, 5], which will be presented in the chapters 3-7. Much more comprehensive reviews can be found in, for example, [6, 7].

### 1.1 Cosmology

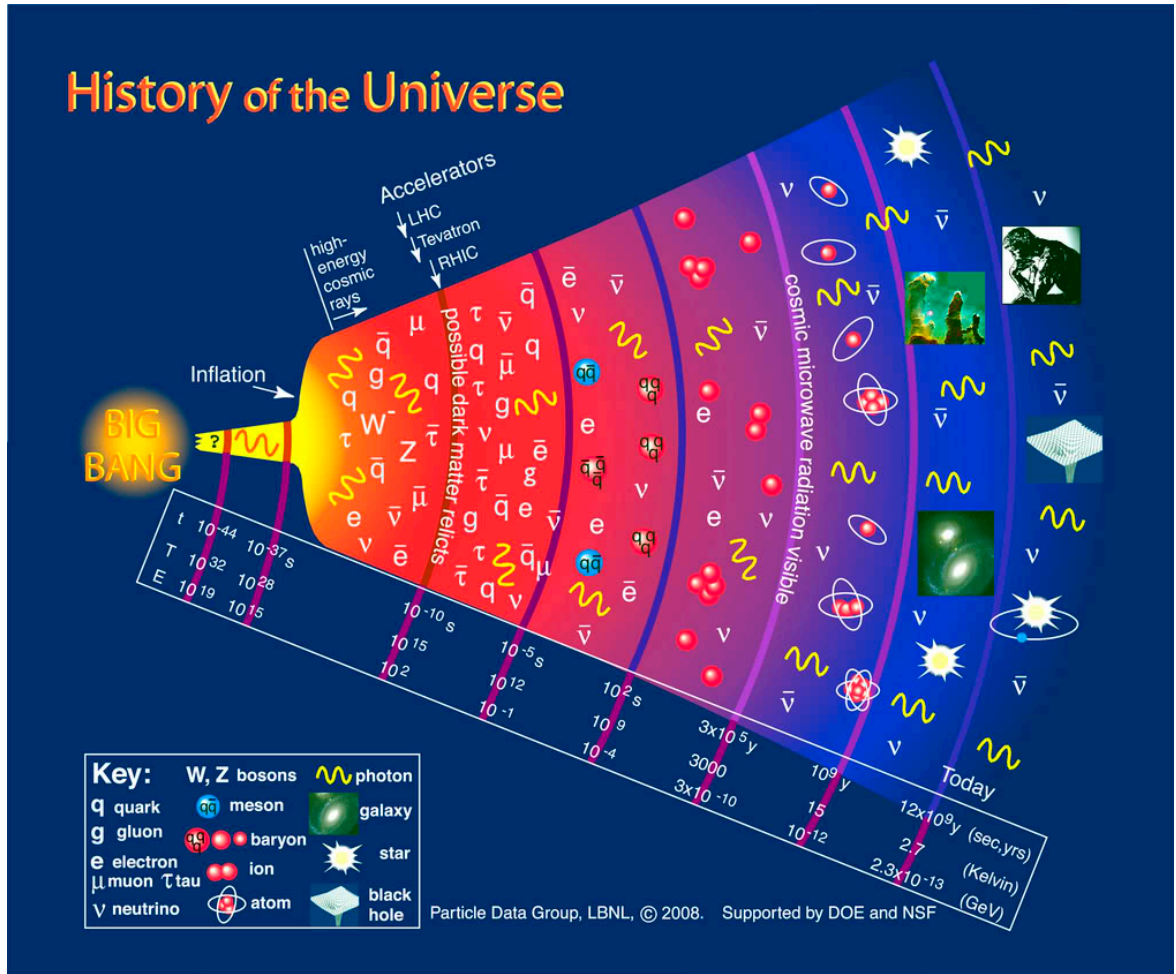
In this first section we provide a short chronological overview of the history of the universe, highlighting the parts relevant for cosmological inflation. With time passing by, the universe expands. As a result it cools down, and matter and radiation dilute. An intuitive sketch of this expansion history, provided by the Particle Data Group, is in figure 1.1.

At  $t = 0$  the Big Bang takes place. Much can be said, conjectured or dreamt about this beginning, but theories break down and nothing can be measured. Up to  $t = 10^{-43}$  s (the Planck scale,  $E = 10^{18}$  GeV), the universe should be described with a theory of quantum gravity. String theory is the most intensively pursued option. The only feature of string theory that we will deal with in this thesis is the fact that it predicts the existence of extra spacetime dimensions. At lower scales, these show up in quantum fields known as moduli fields. Below the Planck scale, gravity is much weaker than the three other fundamental forces (strong, weak and electromagnetic) and the universe can be described by a, possibly supersymmetric, quantum field theory in a curved background. It is widely conjectured that the three forces can still be described as one unified force in the framework of a Grand Unification Theory (GUT). However, so far no experimental evidence<sup>1</sup> has been found. After  $t = 10^{-36}$  s ( $E = 10^{16}$  GeV) we reach the Grand Unification scale. The three forces decouple from each other. (The energy scale of  $10^{16}$  GeV is suggested by the supersymmetrical (MSSM) running of the coupling constants. In non-supersymmetric theories the grand unification scale is rather  $10^{13}$  GeV, or there is no unification at all.)

Around this time, cosmological inflation takes place. This is a brief phase of accelerated expansion of the universe. The cosmological scale factor  $a(t)$ , defined in the metric (1.1), grows by a factor of at least  $e^{60}$ , but there is really no upper limit on this amount, see section 1.2. All pre-inflationary physics is therefore “washed out” (the universe is empty after inflation) and its observational features are extremely

---

<sup>1</sup>Scenarios of grand unification predict a finite lifetime for protons, but no decaying proton has been observed yet.

Figure 1.1: *The history of the universe.*

hard, if not impossible, to recover. On the other hand, the remnants of inflation itself leave a clear observational signal in the Cosmic Microwave Background (CMB) radiation, as we will discuss in section 1.3. Models of inflation in supersymmetric grand unification suggest that inflation took place at the Grand Unification scale as well, but we will see that so far only lower bounds on the inflationary energy scale have been found. After inflation and the subsequent process of reheating, during which the inflaton's energy is transferred to other degrees of freedom, the universe is filled with radiation: relativistic elementary particles.

At  $t = 10^{-10}$  s we reach the TeV-energy scale, so we enter the energy range observable by the Large Hadron Collider (LHC). From here on theories are comforted by experimental guidance. Given the current experimental results, the breaking of supersymmetry should already have taken place. Around 100 GeV we are at the scale of electroweak symmetry breaking: the  $W$ - and  $Z$ -bosons acquire a mass as the Higgs field settles down at its nonzero vacuum expectation value. The radiation that fills the universe now only consists of quarks, leptons, photons and gluons. After  $10^{-4}$  s, we reach the QCD-energy scale of about 200 MeV. From here on individual quarks are confined inside hadrons (protons and neutrons) and mesons.

After about three minutes ( $E = 0.1$  MeV), Big Bang Nucleosynthesis (BBN) takes place: protons and neutrons combine into the light elements (H, He, Li,...). BBN manages to predict the abundances of these elements very precisely. Therefore, from this time on we have a precise quantitative description of the universe. Inflation should for sure take place before BBN (and as well before baryogenesis, which is meant to break the matter-antimatter symmetry in the post-inflationary phase).

With time passing further, the matter component of the energy density of the universe (non-relativistic particles) grows more quickly than its radiation component (relativistic particles). Both densities dilute in an expanding universe, but for radiation there is the extra effect from its wavelength that gets stretched out as well. After about  $10^4$  years, the matter component becomes dominant. When the universe is about 380,000 years old, it becomes transparent as recombination takes place. Free electrons are caught by protons. Therefore, photons can begin to free-stream through the universe, as they do not scatter off free electrons anymore. There is light in the universe. After about  $10^9$  years stars, planets and galaxies begin to form. Also, the expansion of the universe begins to accelerate again. By now the universe is about 13.8 billion years old and the energy scale has dropped to about 1 meV. At least at one planet life has emerged. A subgroup of the population has begun to look up at the sky and to wonder where it all came from.

### 1.1.1 The metric of the universe

Already in the 16th century Copernicus has taught us that our position in the universe is not special at all. We are just one planet orbiting just one star in just some galaxy. In modern cosmology his principle has been translated in the notion that on large scales ( $> 100\text{Mpc} \approx 10^{24}\text{m}$ ) the universe is homogeneous and isotropic. It has been proven right time and again by CMB and large scale structure experiments.<sup>2</sup> In the (+ - - -) convention that we use in this thesis, the metric of the universe in spherical coordinates follows from the invariant interval

$$ds^2 = dt^2 - a^2(t) \left( \frac{dr^2}{1 - kr^2} + r^2 d\theta^2 + r^2 \sin^2 \theta d\phi^2 \right). \quad (1.1)$$

Here  $a(t)$  is the cosmological scale factor, which takes the expansion of the universe into account. The physical distance between two objects with fixed  $r$ ,  $\theta$  and  $\phi$  coordinates is given by the product of their fixed coordinate distance and this dynamical scale factor  $a(t)$ . The parameter  $k$  specifies the global metric of the universe. The universe can be open ( $k = 1$ ), flat ( $k = 0$ ) or closed ( $k = -1$ ).

In most of this thesis we will consider a flat universe, in line with the observations by Planck and earlier. (We will discuss the flatness of the universe further in the next section.) For a flat universe we can as well employ a Cartesian coordinate system, in which the metric follows from

$$ds^2 = dt^2 - a^2(t) (dx^2 + dy^2 + dz^2). \quad (1.2)$$

### 1.1.2 The dynamics of the universe

The mutual interaction between spacetime curvature and energy-momentum (“Matter tells space how to curve, and space tells matter how to move”) is encoded in the Einstein equations

$$R_{\mu\nu} - \frac{1}{2}g_{\mu\nu}R - \Lambda g_{\mu\nu} = 8\pi GT_{\mu\nu}. \quad (1.3)$$

---

<sup>2</sup>However, the apparent dimness of very far supernovas that is most often taken as an indication for the late-time accelerated expansion of the universe, can also be explained as the result of us living in the center of a local spherical underdensity (“void”), see [8] and references therein. Isotropy has also been questioned by “axis of evil”-scenarios [9].

Here the Ricci tensor  $R_{\mu\nu}$  and the Ricci scalar  $R$  encode the curvature of spacetime. These follow directly from the metric  $g_{\mu\nu}$ , see for example [10].  $\Lambda$  is the cosmological constant, which is most probably responsible for the late-time acceleration of the universe. Treating the matter in the universe as a homogeneous and isotropic “cosmic fluid” the energy-momentum tensor  $T_{\mu\nu}$  can be written as

$$T_{\mu\nu} = (\rho + p)u_\mu u_\nu - pg_{\mu\nu}, \quad (1.4)$$

where  $\rho$  denotes energy density and  $p$  stands for pressure. We will work in the rest frame where  $u_\mu = (1, 0, 0, 0)$ .

In this whole thesis our units are such that  $\hbar = c = 1$ . Apart from this subsection, we set the reduced Planck mass  $\tilde{M}_p \equiv \sqrt{\frac{\hbar c}{8\pi G}} = 1$  as well.

The (00) component of the Einstein equation gives, after inserting (1.4), the Friedmann equation

$$H^2 + \frac{k}{a^2} - \frac{\Lambda}{3} = \frac{8\pi G\rho}{3}. \quad (1.5)$$

Here  $H$  denotes the Hubble parameter,  $H \equiv \frac{\dot{a}}{a}$ . From the Friedmann equation we can deduce the behaviour of the scale factor during the various epochs of expansion the universe has undergone. We get

$$a(t) \sim \begin{cases} e^{\sqrt{(\Lambda/3)t}} = e^{Ht} & \text{(inflation, present day expansion)} \\ t^{1/2} & \text{(radiation domination)} \\ t^{2/3} & \text{(matter domination)} \end{cases}. \quad (1.6)$$

Here we have used that during radiation domination we have  $\rho \sim a^{-4}$ , while during matter domination  $\rho \sim a^{-3}$ . The latter is easy to understand: when volumes grow as  $a^3$ , energy densities drop as  $a^{-3}$ . The extra inverse power of the scale factor for radiation comes from the fact that its wavelength gets stretched out as well, as we already discussed above.

### 1.1.3 The CMB radiation

We can still observe the photons emitted at recombination in the Cosmic Microwave Background (CMB) radiation. The CMB provides a marvelous insight in early-universe cosmology, as it is literally a baby picture of the universe. Its study has led to the most precise determination of almost all cosmological parameters. Figure 1.2 shows a sky map of the measured CMB temperature, taken from the Planck results [11]. The background temperature is the same in all directions, but there are tiny fluctuations on top of that:

$$T_{\text{CMB}} = 2.73 \pm 10^{-4} \text{K}. \quad (1.7)$$

As we observe the CMB in a sphere around us, we are led to decompose the temperature fluctuations in spherical harmonics:

$$\frac{\Delta T(\theta, \phi)}{T} = \sum_{l=1}^{\infty} \sum_{m=-l}^{m=l} a_{lm} Y_{lm}(\theta, \phi), \quad (1.8)$$

with  $\theta$  and  $\phi$  angles at the sky. We assume that the fluctuations follow a Gaussian distribution and that each  $l$ -mode is unrelated to all others:

$$\langle a_{lm} \rangle = 0, \quad \langle a_{lm} a_{l'm'}^* \rangle = \delta_{ll'} \delta_{mm'} C_l. \quad (1.9)$$

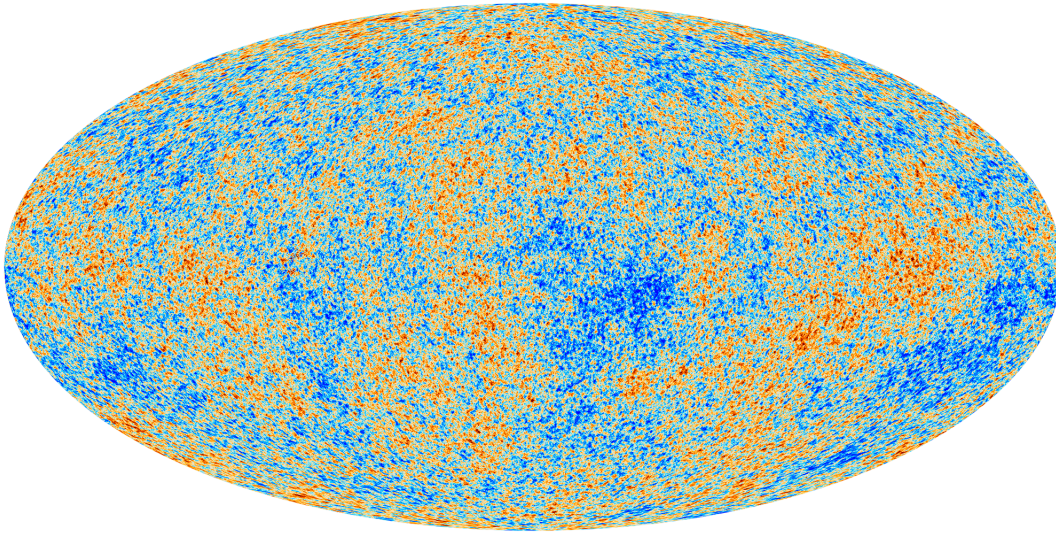


Figure 1.2: *CMB temperature fluctuations as measured by Planck [11]. The image shows a temperature range of  $\pm 500$  microKelvin. (The temperature increases from blue to red.)*

The collection  $C_l$ , the angular power spectrum, contains all information about the Gaussian temperature fluctuations. Per value of  $l$  we average over the  $(2l + 1)$  contributions. We have

$$\left\langle \frac{\Delta T(\vec{n})}{T} \frac{\Delta T(\vec{n}')}{T} \right\rangle = \frac{1}{4\pi} \sum_l (2l + 1) C_l P_l(\vec{n} \cdot \vec{n}'), \quad (1.10)$$

with  $P_l$  the  $l$ th Legendre polynomial. We have converted  $\theta$  and  $\phi$  into the unit vector  $\vec{n}$ , indicating the direction from which a CMB photon enters the telescope.

The measured angular power spectrum of the CMB temperature fluctuations is in figure 1.3. For  $l > 30$ , the data can perfectly be fit by the picture of the universe we have described so far. At larger scales, there is some discrepancy, which might hint to some unknown large scale physics. However, at these larger scales the uncertainty in the measurements increases dramatically. This is mainly due to “cosmic variance”: we can observe the universe only from our position, and per value of  $l$  we have less values of  $m$  that we can average over. Therefore there is, at least at the time of writing, no statistical evidence for new physics on scales  $l < 30$ .

## 1.2 Inflation: why and how

### 1.2.1 Naturalness problems

Inflation was originally proposed [12] to solve some naturalness problems. We will briefly review three of them in this section.

First there is the “horizon problem”. All over the CMB sky one measures one and the same background

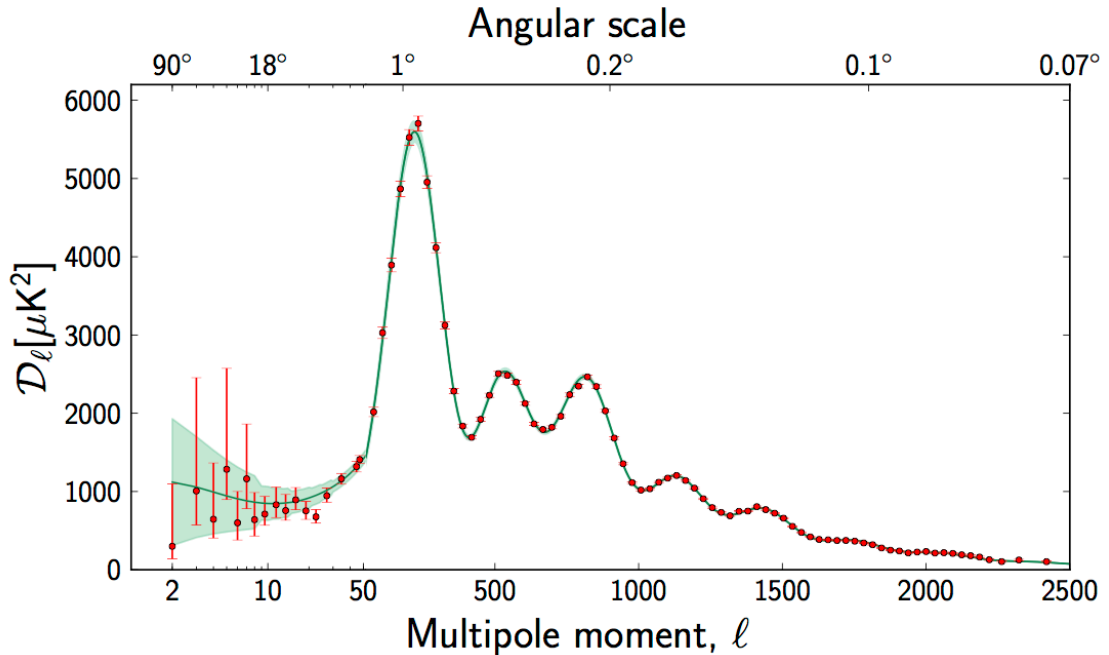


Figure 1.3: *Two point correlation function of the CMB temperature fluctuations [11]. The quantity plotted on the vertical scale is defined as  $\mathcal{D}_l \equiv \frac{l(l+1)C_l}{2\pi}$ .*

temperature<sup>3</sup>. Given the current age of the universe (and the finite speed of light), and the fact that the CMB came into existence after 380,000 years, one expects modes to be correlated only for  $l \geq 30$  (that is, on scales  $\leq 6^\circ$ ). The smaller  $l$ -modes correspond to scales that are too large to have been in causal contact already after 380,000 years. This is the horizon problem: how can it be that apparently all of the universe that we can see today has the same background temperature? Had the universe already been in causal contact in its infant days?

Next we have the “flatness” problem. The contributions to the total energy density  $\rho_{\text{tot}}$  coming from matter ( $\rho_m$ ), radiation ( $\rho_r$ ) and dark energy ( $\rho_\Lambda$ ) almost add up the critical density  $\rho_{\text{crit}} = 3H^2/8\pi G$  needed to have a perfectly flat universe (a universe with Euclidean geometry). Indeed Planck [13] finds, after switching to the normalized parameter  $\Omega \equiv \rho/\rho_{\text{crit}}$ ,

$$1 - \Omega_{\text{tot}} \equiv 1 - (\Omega_m + \Omega_r + \Omega_\Lambda) = -0.0005^{+0.0065}_{-0.0066}, \quad (2\sigma). \quad (1.11)$$

In other words: the data are perfectly compatible with a completely flat universe.

That is already an unnatural result, but it gets much worse when we go back in time. The Friedmann equation (1.5) can be rewritten in such a way

$$\Omega_m + \Omega_r + \Omega_\Lambda - \frac{k}{H^2 a^2} = 1, \quad (1.12)$$

that it lists the various contributions to the total energy density. Here we have introduced  $\rho_\Lambda \equiv \Lambda/8\pi G$ . We already discussed that in an expanding universe we have  $\Omega_m \sim a^{-3}$  and  $\Omega_r \sim a^{-4}$ . As its name

<sup>3</sup>Moreover, although this was not known when inflation was invented, we see in figure 1.3 that the temperature fluctuations are correlated on every scale.

suggests, the cosmological constant's contribution  $\Omega_\Lambda$  is constant. Therefore we see that the curvature contribution is increasing when the universe expands. To have a pretty flat universe now, one would need an extremely flat universe in the past. In slightly other words:  $\Omega_{\text{tot}} = 1$  is an unstable fixed point.

Furthermore it follows from the Friedmann equation that the immense flatness needed in the early universe to arrive at the current conditions is equivalent to having an enormous entropy in our Hubble volume:

$$\frac{k}{H^2 a^2} \approx \frac{k}{T^4 a^2} \approx \frac{k}{S^{2/3} T^2}. \quad (1.13)$$

Here  $S$  is the total entropy per Hubble volume, and we have used that  $H^2 \simeq \rho \simeq T^4$  and that  $S \sim a^3 s \sim a^3 T^3$ .

Inflation is by now regarded as a fundamental part of standard cosmology, as it solves the horizon problem, the flatness problem and the entropy problem in one go. One can compute that if inflation lasts at least 60–70 e-folds (if the scale factor increases by at least a factor  $e^{60-70}$ , the precise number depends on the energy scale of inflation) the current homogeneous CMB sky and flatness follow from natural order one initial conditions before inflation. Moreover, the reheating of the universe after inflation, a process in which the inflation energy density is released into other (Standard Model) degrees of freedom, causes an enormous increase in the entropy ( $T$  increases,  $a$  remains approximately constant).

### 1.2.2 Expansion from negative equation of state

Now let us see how we can get such an enormous expansion of spacetime itself. All we need is a scalar field  $\phi$  moving through an almost flat potential  $V(\phi)$ . For the energy density  $\rho$  and the pressure  $p$  we can then write, from evaluating the energy-momentum tensor in the cosmic rest frame,

$$\rho = \frac{1}{2} \dot{\phi}^2 + V(\phi), \quad p = \frac{1}{2} \dot{\phi}^2 - V(\phi). \quad (1.14)$$

Here we have neglected gradient terms, as we assume the field  $\phi$  to be homogeneous and isotropic.

If the potential is sufficiently flat,  $\dot{\phi}$  will be small, and the scalar field will have a negative equation of state:  $p \approx -\rho$ . From the conservation of energy-momentum it then follows that having such a negative equation of state leads to having a constant ( $a$ -independent) energy density:

$$\dot{\rho} + 3 \frac{\dot{a}}{a} (\rho + p) = 0 \quad \rightarrow \quad \rho \sim a^0. \quad (1.15)$$

Therefore we see that the energy density  $\rho$  of the scalar field  $\phi$  behaves exactly like the energy density contribution from the cosmological constant  $\rho_\Lambda$  we described before. From the analysis in section 1.1.2 it follows directly that indeed the scale factor will grow exponentially:

$$\left( \frac{\dot{a}}{a} \right)^2 = \frac{\rho}{3} \quad \rightarrow \quad a(t) = e^{\sqrt{\rho/3} t}. \quad (1.16)$$

Note that if the potential is perfectly flat, the inflaton does not move at all. As a result, there is no end to inflation. (However, this may describe the accelerated expansion that we are currently observing.)

### 1.2.3 Slow-roll variables

To get inflation, one imposes that the rate of change of the Hubble constant (i.e.  $\dot{H}/H$ ) be small over the Hubble time  $1/H$ :

$$\epsilon \equiv -\frac{\dot{H}}{H^2} \ll 1. \quad (1.17)$$

This is equivalent to demanding that the inflaton moves slowly through its potential, as we have  $\dot{H} = -\frac{\dot{\phi}^2}{2}$ . The number of e-folds that inflation generates follows from

$$dN = -\int H dt = -\int_{\phi_1}^{\phi_2} d\phi \frac{1}{\sqrt{2\epsilon}}. \quad (1.18)$$

Since inflation is defined as an accelerated expansion of spacetime, we see from the relation  $\frac{\ddot{a}}{a} = H^2 + \dot{H} = (1 - \epsilon)H^2$  that it stops when  $\epsilon = 1$ .

To keep inflating for a sufficient amount of time (or e-folds),  $\epsilon$  has to remain small. We need a second slow-roll parameter  $\eta$  that makes sure that  $\epsilon$  does not change too fast over the Hubble volume. For inflation to happen we therefore demand

$$\eta \equiv -\frac{\dot{\epsilon}}{H\epsilon} \ll 1. \quad (1.19)$$

(This could also be written as  $\eta \equiv -\frac{d \log \epsilon}{dN}$ .)

To avoid having to solve the inflaton's equation of motion, the slow-roll variables are often defined alternatively, in terms of the potential  $V(\phi)$ . We have

$$\tilde{\epsilon} \equiv \frac{1}{2} \left( \frac{V_\phi}{V} \right)^2, \quad (1.20)$$

$$\tilde{\eta} \equiv \frac{V_{\phi\phi}}{V}. \quad (1.21)$$

Here we used the notation  $V_\phi \equiv \partial V / \partial \phi$ . This “potential”  $\tilde{\epsilon}$  can be expressed in terms of the kinematical slow-roll parameters defined before:

$$\tilde{\epsilon} = \epsilon \left( 1 - \frac{\eta}{2(3 - \epsilon)} \right)^2 \approx \epsilon. \quad (1.22)$$

For  $\tilde{\eta}$  it follows that

$$\tilde{\eta} = \frac{1}{3 - \epsilon} \left[ 6\epsilon + \frac{3}{2}\eta + \dots \right] \approx 2\epsilon + \frac{\eta}{2}. \quad (1.23)$$

The last step assumes that kinematical  $\epsilon$  and  $\eta$  are small. We conclude that to have inflation, we need the kinematical slow-roll parameters  $\epsilon$  and  $\eta$  to be small (of order  $10^{-2}$ ), which implies that the “potential” slow-roll parameters  $\tilde{\epsilon}$  and  $\tilde{\eta}$  are small as well. In other words: the inflaton needs to be light.

Strictly speaking, however, having small potential slow-roll variables does not necessarily imply being in an inflationary phase. The behaviour of the cosmological scale factor depends on the path the inflaton follows through field space. Only when the field is slowly rolling, this path precisely follows the direction of steepest descent through the potential. Then the “potential” slow-roll variables can be used to extract information about inflation, like the number of e-folds that inflation lasts. When there is no slow-roll, the

field can for example use its kinetic energy to climb up to a higher potential value. It does not follow the direction of steepest descent through the potential anymore, so  $\tilde{\epsilon}$  and  $\tilde{\eta}$  become useless.

In the rest of this thesis, we will be using the kinematical slow-roll variable  $\epsilon$  and the potential slow-roll variable  $\tilde{\eta}$ , to which we will refer as  $\eta$  from now on.

### 1.3 Inflating quantum perturbations

As we reviewed in the previous section, the mechanism of cosmological inflation was originally proposed to solve naturalness problems. However, it was soon realized [14] that inflation can also explain the tiny temperature fluctuations in the CMB. It had been known for a long time that basic Newtonian physics suffices to describe how these fluctuations grow out to form stars and planets. Before inflation was studied these tiny CMB temperature variations, the seeds for the formation of all structure in the universe, had to be put in by hand as initial conditions. Inflation gives an explanation for the correlated fluctuations in the CMB. In this section we will quickly review how the inflation of fluctuations of the quantum inflaton field grow out to the temperature fluctuations in the CMB. For simplicity we will focus on single field inflation here.

We begin with the equation of motion for the quantum inflaton field  $\phi$ :

$$\ddot{\phi} + 3H\dot{\phi} - \frac{\nabla^2}{a^2}\phi + \frac{\partial V}{\partial\phi} = 0. \quad (1.24)$$

Now expand the field in a classical background field and a quantum fluctuation  $\phi(\vec{x}, t) = \phi(t) + \delta\phi(\vec{x}, t)$  and take the Fourier transform. In conformal time  $\tau$  (defined by  $dt = a d\tau$ ) we get, after rescaling the perturbations via  $v_k \equiv a\delta\phi_k$ , up to first order

$$\left( \partial_\tau^2 + k^2 - \frac{a''}{a} + a^2 \frac{\partial^2 V}{\partial\phi^2} \right) v_k = 0. \quad (1.25)$$

We will now first take a massless scalar field and work in exact de Sitter ( $\epsilon = \eta = 0$ ). For the moment we work with a fixed metric: later we will take gravity dynamical and consider the metric's perturbations as well. Now we have

$$\tau \equiv \int \frac{dt}{a} = \int dt e^{-Ht} = \left[ -\frac{1}{H} e^{-Ht} \right] = -\frac{1}{Ha}. \quad (1.26)$$

This means  $\frac{a''}{a} = \frac{-2/\tau^3 H}{-1/\tau H} = \frac{2}{\tau^2}$  and we get, after rewriting in terms of  $\rho \equiv -k\tau$  (not to be confused with the energy density),

$$\left( \rho^2 \frac{\partial^2}{\partial\rho^2} + \rho^2 - 2 \right) v_k = 0. \quad (1.27)$$

This equation is solved by

$$v_k = c\sqrt{\rho}\mathcal{H}_{3/2}^{(1)}(\rho), \quad (1.28)$$

where  $\mathcal{H}_\nu^{(1)}(\rho)$  denotes the Hankel function of the first kind. (Actually the solution contains a part proportional to a Hankel function of the second kind well, but that part should be set to zero if we want our solution to return the Bunch-Davies vacuum, defined below, in the infinite past.) For later reference we already notice that if we modify equation (1.27) a little bit into

$$\left( \rho^2 \frac{\partial^2}{\partial\rho^2} + \rho^2 - (2 + \alpha) \right) v_k = 0, \quad (1.29)$$

the solution is still given by  $v_k = c\sqrt{\rho}\mathcal{H}_\nu^{(1)}(\rho)$ , but now we need

$$\nu^2 - \frac{9}{4} - \alpha = 0 \quad \rightarrow \quad \nu = \sqrt{\frac{9}{4} + \alpha} \approx \frac{3}{2} + \frac{\alpha}{3}. \quad (1.30)$$

We set the integration constant to  $c = \frac{i}{2}\sqrt{\frac{\pi}{k}}$ . This makes  $v_k$  real in the limit  $(-k\tau) \rightarrow 0$ , as the Hankel function becomes purely imaginary there. Furthermore, for  $(-k\tau) \rightarrow \infty$  we get, using the Hankel expansion for large argument  $\mathcal{H}_\nu^{(1)}(z) \rightarrow \sqrt{\frac{2}{\pi z}}e^{iz}e^{-i\pi}$ ,

$$\begin{aligned} v_k &= \frac{i}{2}\sqrt{\frac{\pi}{k}}\sqrt{-k\tau}\mathcal{H}_{3/2}^{(1)}(-k\tau) \quad \rightarrow \quad \frac{i}{2}\sqrt{\frac{\pi}{k}}\sqrt{-k\tau}\sqrt{\frac{2}{\pi}}\frac{1}{\sqrt{-k\tau}}e^{-ik\tau} \times -1 \\ &= -i \times \frac{e^{-ik\tau}}{\sqrt{2k}}, \end{aligned} \quad (1.31)$$

which corresponds the Bunch-Davies vacuum.

To describe a more realistic situation, we need to consider a massive scalar field (but light compared to the Hubble scale). We should also acknowledge that inflation takes place in a “quasi-dS” spacetime:  $H$  does slowly change in time. In terms of kinematical  $\epsilon \equiv -\frac{\dot{H}}{H^2}$  and “potential”  $\eta \equiv \frac{V''}{V}$  the equation of motion for the modes  $v_k$  becomes

$$\left(\partial_\tau^2 + k^2 - \frac{1}{\tau^2}[2 - 3\eta + 3\epsilon]\right)v_k = 0. \quad (1.32)$$

Here we have used the quasi-dS result  $\tau = -\frac{1}{aH}\frac{1}{1-\epsilon}$  which leads to  $\frac{a''}{a} = \frac{1}{\tau^2}(2 - \epsilon)(1 + 2\epsilon) = \frac{1}{\tau^2}(2 + 3\epsilon)$ . After the discussion around (1.30) it is clear that the solution of (1.32) is given by

$$v_k = \frac{i}{2}\sqrt{\frac{\pi}{k}}\sqrt{\rho}\mathcal{H}_\nu^{(1)}(\rho), \quad \nu = \frac{3}{2} + \epsilon - \eta. \quad (1.33)$$

Plotting this solution, see figure 1.4, shows that for  $\rho > 1$ , which means inside the horizon<sup>4</sup> ( $\frac{k}{aH} > 1$ ) the function is oscillating, with constant amplitude. This is not surprising because for large  $k$  the equation of motion (1.32) reduces to

$$(\partial_\tau^2 + k^2)v_k = 0 \quad \rightarrow \quad v_k = A \sin(-k\tau) + B \cos(-k\tau). \quad (1.34)$$

Therefore: inside the horizon the modes  $v_k$  oscillate with constant amplitude, which means that the modes  $\delta\phi_k = \frac{v_k}{a}$  oscillate with an exponentially decreasing amplitude.

Outside the horizon, for  $\rho < 1$ , the solution grows exponentially. This can be seen from taking the small  $k$  limit of (1.32), which gives (again omitting slow-roll effects, reinserting  $\frac{a''}{a} = \frac{2}{\tau^2}$  and taking the growing solution)

$$\left(\partial_\tau^2 - \frac{a''}{a}\right)v_k = 0 \quad \rightarrow \quad v_k = c_1 a. \quad (1.35)$$

So: outside the horizon the modes  $v_k$  grow exponentially, proportional to the scale factor, which means that the modes  $\delta\phi_k = \frac{v_k}{a}$  freeze. That is what we would expect from causality as well. As soon as the typical wavelength of a fluctuation  $a/k$  becomes larger than the physical horizon  $H^{-1}$ , the wave can not evolve any further as its one end is not in causal contact anymore with its other end.

<sup>4</sup>The Hubble horizon  $1/H$  denotes the maximum distance over which physics can be in causal contact at a given point in time. When a mode crosses the horizon its physical wavelength  $a/k$  is equal to the horizon size  $1/H$ .

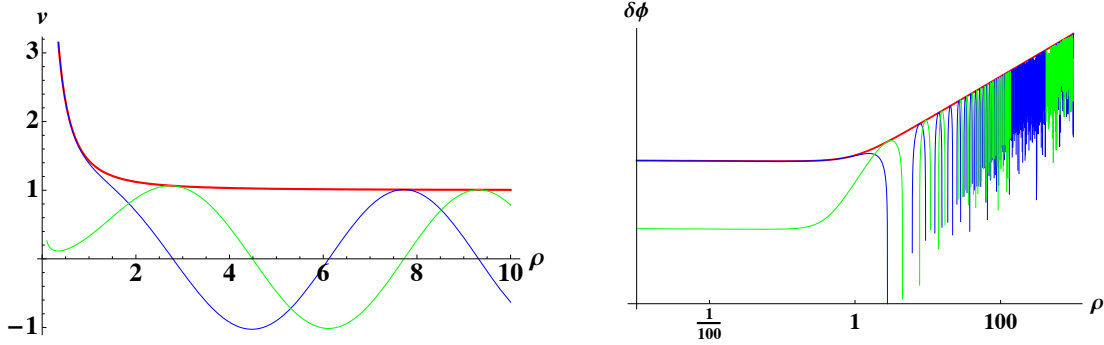


Figure 1.4: On the left the numerical solution to equation (1.32) for the modes  $v_k$ , on the right the associated solution for the modes  $\delta\phi_k$ . Absolute values in red, real and imaginary values in blue and green. Inside the horizon ( $\rho \equiv -k\tau > 1$ ) the modes  $v_k$  oscillate, outside the horizon ( $\rho < 1$ ) the modes  $\delta\phi_k$  freeze.

Finally, we should take general relativity (GR) into account. So far we have only considered fluctuations of the inflaton field. However, the metric fluctuates as well. We can write the perturbed metric as

$$g_{\mu\nu} = a^2 \begin{pmatrix} -(1+2A) & \partial_i B \\ \partial_i B & (1-2\psi)\delta_{ij} - D_{ij}E \end{pmatrix}. \quad (1.36)$$

This suggests that there are four scalar degrees of freedom in the metric. However, two of these are redundant. We can work in the longitudinal gauge where  $B = E = 0$ . Then we can use one of the off-diagonal components of the perturbed Einstein equations to show that we also have  $A = \psi$ . Finally we can use a diagonal Einstein equation to relate the scalar metric perturbations to the field perturbation  $\delta\phi$ . At the end of the day we are thus left with one degree of freedom, that we can take to be a linear combination of  $\psi$  and  $\delta\phi$ .

Now there are two frequently used diffeomorphism invariant variables to describe the fluctuations of inflaton and metric. We take the comoving curvature perturbation  $\mathcal{R}$  to be defined via

$$\mathcal{R} \equiv \psi + \frac{H}{\dot{\phi}} \delta\phi. \quad (1.37)$$

Alternatively, one often employs the curvature perturbation on uniform density hypersurfaces  $\zeta$ :

$$\zeta \equiv -\psi - \frac{H}{\dot{\rho}} \delta\rho. \quad (1.38)$$

Now we can use energy conservation  $\dot{\rho} + 3H(p + \rho)$ , the expressions (1.14) and the Klein-Gordon equation (1.24) to show that during inflation we have

$$\zeta = -\psi - \frac{H}{\dot{\rho}} \delta\rho = -\psi - \frac{H}{3H(p + \rho)} \delta(V(\phi)) = -\psi - \frac{H}{3H\dot{\phi}^2} V'(\phi) \delta\phi = -\psi - \frac{H}{\dot{\phi}} \delta\phi = -\mathcal{R}. \quad (1.39)$$

up to slow-roll corrections. Since after inflation  $\mathcal{R}$  and  $\zeta$  are frozen, this equality remains. Finally we can use an off-diagonal perturbed Einstein equation to find that on superhorizon scales one can approximate

$$\psi \simeq \epsilon H \frac{\delta\phi}{\dot{\phi}} \quad \rightarrow \quad \zeta \simeq -(1 + \epsilon) \frac{\delta\phi}{\dot{\phi}} \simeq -\frac{H}{\dot{\phi}} \delta\phi. \quad (1.40)$$

We will use this last approximation to compute  $\zeta$ 's two- and three point function in the next section and especially in chapter 6.

To compute  $\zeta$  itself, we still need to find out how the perturbation equation for  $\delta\phi$  changes once we allow the metric to fluctuate as well. We get (in cosmic time)

$$\delta\ddot{\phi}_k + 3H\delta\dot{\phi}_k + \frac{k^2}{a^2}\delta\phi_k + \frac{\partial^2 V}{\partial\phi^2}\delta\phi_k = -2\psi_k\frac{\partial V}{\partial\phi} + 4\dot{\psi}_k\dot{\phi}. \quad (1.41)$$

On superhorizon scales we have  $|4\dot{\psi}_k\dot{\phi}| \ll |2\psi_k\frac{\partial V}{\partial\phi}|$ . The remaining term can be rewritten using  $\frac{\partial V}{\partial\phi} = -3H\dot{\phi}$ . (We are still working up to first order in the perturbations, and up to first order in slow-roll.) Finally we use the superhorizon result  $\psi_k \approx \epsilon H \frac{\delta\phi_k}{\dot{\phi}}$  again. We get

$$\delta\ddot{\phi}_k + 3H\delta\dot{\phi}_k + \frac{k^2}{a^2}\delta\phi_k + \left(\frac{\partial^2 V}{\partial\phi^2} - 6\epsilon H^2\right)\delta\phi_k = 0. \quad (1.42)$$

Now we use

$$\frac{\partial^2 V}{\partial\phi^2} - 6\epsilon H^2 = V\frac{V''}{V} - 6\epsilon H^2 = 3H^2\eta - 6\epsilon H^2 = 3H^2(\eta - 2\epsilon), \quad (1.43)$$

and it is clear that on superhorizon scales we will get

$$\zeta_k = -\frac{H}{\dot{\phi}}\frac{v_k}{a}, \quad v_k = \frac{i}{2}\sqrt{\frac{\pi}{k}}\sqrt{\rho}\mathcal{H}_\nu^{(1)}(\rho), \quad \nu = \frac{3}{2} + 3\epsilon - \eta. \quad (1.44)$$

## 1.4 Inflationary observables

During inflation the modes  $\zeta_k$  freeze when they leave the horizon. After inflation, when time passes by, spacetime expands at a subluminal speed which makes that one by one the modes get back in causal contact. They begin to oscillate again. (Note however that during inflation the oscillations were of a quantum field, now they are classical oscillations of the pressure and the gravitational potential.) At the time the CMB radiation was emitted, the mode with  $l \approx 180$  had just reached its first extremum, which causes the large first peak in figure 1.3. Modes with smaller wavelengths (larger  $l$ ) had already done several oscillations, which generates the peak structure in the CMB in figure 1.3. For modes that were still frozen at that time ( $l \lesssim 30$ ), the temperature correlation functions are directly proportional to the curvature correlation functions that can be computed from the superhorizon result (1.44).

At the end of the day, CMB temperature measurements lead to precise values for the two- and three point correlation functions of the curvature perturbation  $\zeta_k$ . In this section we show how the solution (1.44) is connected to physical observables involving these correlation functions.

The power spectrum of  $\zeta$  is defined as the power per mode in  $\zeta$ 's two point function in momentum space:

$$\langle 0|\zeta(x)\zeta(x)|0\rangle = \int \frac{d^3k}{(2\pi)^3} |\zeta_k|^2 \equiv \int dk \frac{1}{k} \Delta_\zeta^2(k). \quad (1.45)$$

We therefore have

$$\Delta_\zeta^2(k) = \frac{k^3}{2\pi^2} |\zeta_k|^2. \quad (1.46)$$

This quantity is directly connected to the temperature fluctuations in the CMB, so this is what we need to compute (in the superhorizon limit). In passing by we also give the momentum space two point function

of  $\zeta$ :

$$\langle \zeta(\vec{k})\zeta(\vec{k}') \rangle \equiv (2\pi)^3 \delta^3(\vec{k} + \vec{k}') P(k). \quad (1.47)$$

Now we can write

$$\langle \zeta(x)^2 \rangle = \int \frac{d^3k}{(2\pi)^3} \frac{d^3k'}{(2\pi)^3} \langle \zeta(\vec{k})\zeta(\vec{k}') \rangle = \int \frac{d^3k}{(2\pi)^3} P(k) \quad (1.48)$$

to see that we have  $P(k) = |\zeta_k|^2$ .

Plugging our solution (1.44) in the definition (1.46) gives for the power spectrum of  $\zeta$  from slow-roll inflation

$$\Delta_\zeta^2(k) = \left( \frac{H^2}{2\pi\dot{\phi}} \right)^2 \left( \frac{k}{aH} \right)^{2\eta-6\epsilon}. \quad (1.49)$$

Therefore the picture is that every mode  $k_\alpha$  oscillates as long as it is inside the horizon. At the moment of horizon crossing  $t_\alpha$  we have by definition  $k_\alpha = a(t_\alpha)H(t_\alpha)$  and the power in this mode freezes at the value  $\left( \frac{H(t_\alpha)^2}{2\pi\dot{\phi}(t_\alpha)} \right)^2$ . If  $H$  and  $\dot{\phi}$  were exactly constant in time, all modes would freeze out at the same value and we would have a perfectly flat, scale invariant, spectrum. However,  $H$  and  $\dot{\phi}$  slowly decrease during inflation. Therefore we get a slightly red tilted spectrum: modes that leave the horizon later have smaller power. The most convenient way to describe this is to take a pivot scale  $k_0$ , compute the spectrum there, and compute the power on all other modes via

$$\Delta_\zeta^2(k) = \Delta_\zeta^2(k_0) \left( \frac{k}{k_0} \right)^{n_s-1}. \quad (1.50)$$

Unless stated otherwise, the pivot scale is taken at  $k_0 = 0.002 \text{ Mpc}^{-1}$ , which corresponds to (more or less) the scale that leaves the horizon 60 e-folds before the end of inflation, about the largest observable scale today. The tilt in the power spectrum is defined via the spectral index  $n_s$ . (A scale invariant spectrum would correspond to  $n_s = 1$ .)

Planck finds [15]<sup>5</sup>

$$\Delta_\zeta^2(k_0 = 0.05 \text{ Mpc}^{-1}) = (2.20_{-0.06}^{+0.05}) \cdot 10^{-9}, \quad n_s = 0.9643 \pm 0.0059, \quad (1.51)$$

where the quoted errors show the 68% confidence levels (the  $1\sigma$  bounds) on  $\Delta_\zeta^2$  and the 95% confidence levels (the  $2\sigma$  bounds) on  $n_s$ . Note that the spectral index is directly related to the slow-roll parameters:  $n_s = 1 + 2\eta - 6\epsilon$ .

In chapter 7 we will also look at the scale dependence of the spectral index itself.

Note that so far we have only looked at the scalar fluctuations observable in the CMB. However, there is also a tensor perturbation in the metric, denoted  $D_{ij}$  in (1.36). Such a perturbation can be detected as a gravitational wave coming from inflation itself. At the moment of writing, these have never been observed, and Planck [15] can only give an upper bound for the so-called tensor-to-scalar ratio  $r$ :

$$r \equiv \frac{\Delta_t^2(k_0)}{\Delta_\zeta^2(k_0)} = \frac{2\Delta_h^2(k_0)}{\Delta_\zeta^2(k_0)} < 0.12 \quad (95\% \text{ CL}). \quad (1.52)$$

Here  $\Delta_t^2(k)$  denotes the total tensor power spectrum. It gets two equal contributions  $\Delta_h^2(k_0)$  from the two possible gravitational wave polarizations. Computing the tensor wave power spectrum  $\Delta_h^2(k)$  is easier than computing  $\Delta_\zeta^2(k)$  since we only have to deal with metric fluctuations. The result is

$$r = 16\epsilon. \quad (1.53)$$

---

<sup>5</sup>Here we cite the result for a  $\Lambda$ CDM model with tensor waves and no running spectral index, acquired from both the Planck results and those from baryon acoustic oscillations.

The tensor to scalar ratio is connected to the energy scale of inflation  $V$  as well. One has

$$V^{1/4} \sim \left( \frac{r}{0.01} \right)^{1/4} \cdot 10^{16} \text{ GeV}. \quad (1.54)$$

The detection of a tensor wave signal of order  $10^{-2}$ , which is the expected sensitivity for Planck, would point to inflation at the GUT scale. As no nonzero value for  $r$  has been found at the time of writing, the inflation scale can still vary over many orders of magnitude.

After analyzing the two point function, it is a logical step to turn to  $\zeta$ 's three point function. Analogously to (1.47) one can define a momentum space three point function  $B(\vec{k}_1, \vec{k}_2, \vec{k}_3)$  (the bispectrum) via

$$\langle \zeta(\vec{k}_1) \zeta(\vec{k}_2) \zeta(\vec{k}_3) \rangle \equiv (2\pi)^3 \delta^3(k_1 + k_2 + k_3) B(\vec{k}_1, \vec{k}_2, \vec{k}_3). \quad (1.55)$$

It is clear that while  $P(\vec{k}_1, \vec{k}_2)$  depends only on the separation between its two arguments, the function  $B(\vec{k}_1, \vec{k}_2, \vec{k}_3)$  can be studied for all possible shapes of the triangle formed by  $\vec{k}_1$ ,  $\vec{k}_2$  and  $\vec{k}_3$ .

If inflation is indeed the result of a single scalar field slowly rolling down a potential, all three-point functions will be very small. Maldacena already computed [16] that they will be of the order of the slow-roll parameters. That was to be expected: if the inflaton can be approximated as a free field, there are no cubic or quartic terms in its action. Therefore there is no correlation between the modes  $\delta\phi_k$  at the linear level. The whole system can very adequately be described as a collection of uncoupled oscillators, that each follow a Gaussian distribution function.

However, if inflation is in fact the result of multiple fields conspiring together, the equation of motion (1.25) may not be a good approximation anymore<sup>6</sup>. Then we really have to consider the full system of coupled oscillators. The system is not linear and perturbations are not completely Gaussian. One often defines the non-linearity parameter  $f_{\text{NL}}$  via

$$\zeta(\vec{x}) = \zeta_g(x) + \frac{3}{5} f_{\text{NL}}^{\text{loc}} [\zeta_g(\vec{x})^2 - \langle \zeta_g(\vec{x})^2 \rangle], \quad (1.56)$$

where  $\zeta_g$  denotes the Gaussian part of  $\zeta$ . This version of non-Gaussianity is called local, since its definition is local in real space. Now that the system is not linear anymore, three point functions do not have to be negligibly small anymore. In the local case we have

$$B(\vec{k}_1, \vec{k}_2, \vec{k}_3) = \frac{6}{5} f_{\text{NL}}^{\text{loc}} \left[ P(\vec{k}_1)P(\vec{k}_2) + P(\vec{k}_2)P(\vec{k}_3) + P(\vec{k}_3)P(\vec{k}_1) \right]. \quad (1.57)$$

The bispectrum for local non-Gaussianity is largest when the smallest of the three vectors  $\vec{k}_1$ ,  $\vec{k}_2$  and  $\vec{k}_3$  is very small, such that the other two are almost equal (the squeezed limit).

Another shape for non-Gaussianity that we will compute in this thesis is the equilateral shape, which is largest when all three vectors are of equal size. In this case we can relate  $B_{\text{eq}}(k)$  to the position space three point function via (compare with (1.48))

$$\langle \zeta(\vec{x})^3 \rangle = \int d \log k \frac{8\pi^2}{(2\pi)^6} k^6 B_{\text{eq}}(k) \simeq \frac{8\pi^2}{(2\pi)^6} k^6 B_{\text{eq}}(k) \mathcal{O}(1). \quad (1.58)$$

Now it follows<sup>7</sup> that we can extract a value for  $f_{\text{NL}}^{\text{eq}}$  via

$$\langle \zeta(\vec{k}_1) \zeta(\vec{k}_2) \zeta(\vec{k}_3) \rangle_{\text{eq}} = (2\pi)^3 \delta^3(\vec{k}_1 + \vec{k}_2 + \vec{k}_3) \times (2\pi)^4 \frac{3}{10} f_{\text{NL}}^{\text{eq}} \Delta_\zeta^4(k) \frac{\sum_i k_i^3}{\prod_i k_i^3}. \quad (1.59)$$

<sup>6</sup>The same happens in models with higher order derivative terms, such as DBI inflation [17].

<sup>7</sup>Here we follow the convention employed in [18], but we modified some factors of  $(2\pi)$  to be consistent with our definition of the Fourier transform.

We therefore have

$$f_{\text{NL}}^{\text{eq}} = B_{\text{eq}}(\vec{k}_1, \vec{k}_2, \vec{k}_3) \frac{10}{3} \frac{1}{(2\pi)^4} \frac{1}{\Delta_\zeta^4(k)} \frac{\prod_i k_i^3}{\sum_i k_i^3} = \frac{10}{9} \frac{(2\pi)^2}{8\pi^2} \frac{\langle \zeta(\vec{x})^3 \rangle}{\Delta_\zeta^4(k)}. \quad (1.60)$$

The Planck results on these two shapes for non-Gaussianity are [19]:

$$-192 < f_{\text{NL}}^{\text{eq}} < 108, \quad -8.9 < f_{\text{NL}}^{\text{loc}} < 14.3, \quad (1.61)$$

where we have quoted the  $2\sigma$  bounds. Therefore, especially local primordial non-Gaussianity will be difficult to observe, as non-primordial physics gives a contribution of  $f_{\text{NL}} \sim 5 - 10$  to the measured CMB signal. One will need to go beyond linear order to disentangle an eventual primordial non-Gaussian signal.

Finally, let us look at one more observable that can constrain inflationary models: the non-detection of primordial black holes. These will form if at horizon re-entry (i.e. smoothing  $\zeta$  on scales of order  $H$ ) we have  $\zeta > \zeta_c$ , with  $\zeta_c \sim 1$  denoting the critical value leading to black hole formation. If one assumes that  $\zeta$  follows a Gaussian distribution (with  $\langle \zeta \rangle = 0$ ) one can express the probability of having  $\zeta > \zeta_c$  in terms of the variance  $\sigma^2 = \langle \zeta^2 \rangle$  by analyzing the Gaussian probability distribution function. This probability corresponds to the fraction of space  $b$  that can collapse to form horizon-sized black holes. We have

$$b \equiv \int_{\zeta_c}^{\infty} P(\zeta) d\zeta = \int_{\zeta_c}^{\infty} \frac{1}{\sqrt{2\pi}\sigma} e^{-\frac{\zeta^2}{2\sigma^2}} d\zeta. \quad (1.62)$$

Therefore, a given value for  $b$  leads to an upper bound on  $\sigma^2 = \langle \zeta^2 \rangle$ . Using (1.45) we find that  $\sigma^2$  is equal, up to an order one factor, to the power spectrum:

$$\sigma^2 = \langle \zeta(x)\zeta(x) \rangle = \int d\ln k \Delta_\zeta^2(k) \simeq \mathcal{O}(1) \Delta_\zeta^2(k). \quad (1.63)$$

Now the fraction  $b$  is constrained by Hawking evaporation and present day gravitational effects [20]. Taking a typical value of  $b = 10^{-20}$  we get an upper bound on the power spectrum [21]:

$$\Delta_\zeta^2(k) < 0.01. \quad (1.64)$$

Compared to (1.51) this bound is very weak. However, it is in principle valid on all scales. The experimental bounds coming from the CMB are much more precise, but are valid on a much smaller range of scales. In the usual Fourier decomposition of the CMB temperature fluctuations one gets information for multipole moments up to  $l \approx 2500$ . Let us make a rough estimate and state that the largest observable scale  $l = 2$  corresponds to the mode that left the horizon 60 e-folds before the end of inflation. Then we realize that the CMB gives only information on the modes that left between 60 and (about) 53 e-folds before the end of inflation, since  $\log(2500/2) \approx 7$ . In chapter 6 we will study models in which towards the end of inflation the power spectrum increases by many magnitudes. We will see that in such a case the non-detection of primordial black holes forms a realistic observational constraint. However, there we will need a more sophisticated analysis taking into account the non-Gaussianity of  $\zeta$ 's fluctuations and the scale dependence in the fraction  $b$ .

## 1.5 Inflationary model building and the $\eta$ -problem

To get inflation we need a scalar field rolling down a potential that is flat enough to generate 60 e-folds of inflation. This provides quite a challenge for model building, as scalar fields in general do not want

to be light. This is familiar from the case of the Higgs field in the Standard Model. The huge gap between its mass ( $\mathcal{O}(10^2)$  GeV) and the energy scale  $\Lambda$  up to which we tend to trust the theory ( $\mathcal{O}(10^{18})$  GeV) is the root of all evil. In the context of the Standard Model the problem is known as the hierarchy problem. Radiative corrections of order  $\Lambda^2$  modify the bare squared Higgs mass. At the end of the day the experimenter finds a physical Higgs mass of 125-126 GeV. The apparent enormous cancellation between bare mass and radiative correction leaves many physicists uneasy.

In the context of inflation, one talks about the  $\eta$ -problem which is really nothing else than the hierarchy problem rearing its head again. However, the situation is a bit more problematic than in the Standard Model. First, we want  $\eta$  to be small. (We will work with the “potential” definition  $\eta = (V''/V) = m_{\text{inf}}^2/3H^2$ ). That is just equivalent to trying to get the Higgs mass far below the cut-off scale. However, now that we are trying to say something about gravity, which is unrenormalizable, we should view the Standard Model as a low-energy effective theory. It is only natural to introduce higher order operators as effective operators stemming from a UV complete theory.  $\eta$  receives order one corrections by the inclusion of such operators. That is why the hierarchy problem is more severe in an inflationary context. In this section we will review several models of inflation, and study how these deal with the  $\eta$ -problem.

### 1.5.1 Small field models

Small field models are models in which the inflation rolls over a sub-Planckian distance in field space during the last 60 e-folds of inflation. Inflation takes place around a local extremum  $V_0$  of the potential. In the first models [22, 23], such potentials arise from spontaneous symmetry breaking. In this class of models the  $\eta$ -problem appears when one adds for example a contribution of  $\delta V = \frac{V_0 \phi^2}{M_{\text{p}}^2}$  to the potential. While low-energy physics is not affected by such an extra contribution, the  $\eta$ -parameter gets an extra contribution of order one and inflation is spoiled. One needs to fine-tune the parameters in the problem again to get the desired  $\eta \lesssim 0.01$  at the point in field space where the inflaton passes 60 e-folds before the end of inflation (the pivot scale).

### 1.5.2 Large field models

Large field models typically use potentials of the “chaotic” type [24]. The chaotic initial conditions prescribe that the inflaton finds itself at a super-Planckian value in field space. Its subsequent rolling back to the origin creates inflation. Typical chaotic potentials are  $V(\phi) = \frac{1}{2}m^2\phi^2$  and  $V(\phi) = \frac{1}{4}\lambda\phi^4$ . In a way, the  $\eta$  problem is even worse now. As in the case of small field models, one has to tune  $m$  or  $\lambda$  to a sufficiently small value to get inflation going. Now however every higher order term in the potential of the type  $\delta V = \frac{\phi^{4+n}}{M_{\text{p}}^n}$  gives a large additional contribution to  $\eta$ . Including more and more non-renormalizable higher dimensional operators there is no end to the necessary tuning.

### 1.5.3 Hybrid models

Hybrid inflation [25] is two-field inflation. Next to the inflaton field  $\phi$  there are one or more so-called waterfall fields  $H$ , whose dynamics provide an elegant ending of inflation. During inflation, the waterfall fields are heavy and therefore stabilized in a local minimum. However, the rolling of the inflaton causes one of the waterfall fields to become unstable (tachyonic). When this waterfall field falls down the slow-roll conditions are no longer met and inflation stops.

### 1.5.4 Symmetries

In all these models, and in multifield models as well, we can invoke symmetries to get around the  $\eta$ -problem. We can for example work with a complex scalar field  $\Phi = \phi_R + i\phi_I$ . Now if the inflaton potential involves only powers of  $(\Phi - \bar{\Phi})$ , the field  $\phi_R$  will remain massless, whatever higher order operator we include. Now, however, the challenge is to break the symmetry just “softly” enough, such that a small tilt in the potential is created, for example from radiative corrections. In the next section we will see more examples of invoking symmetries to keep the inflaton potential flat.

### 1.5.5 Lyth’s bound

We conclude this section with the most characteristic phenomenological difference between small and large field inflation. Lyth has shown [26] that the length  $\Delta\phi$  of the inflaton’s path through field space during the last 60 e-folds is proportional to the tensor to scalar ratio  $r$ :

$$\frac{\Delta\phi}{M_{\text{p}}} = \mathcal{O}(1) \left( \frac{r}{0.01} \right)^{1/2}. \quad (1.65)$$

The detection of a primordial gravitational wave signal of order  $10^{-2}$  would therefore irrevocably point out that inflation is of the large field type.

## 1.6 Inflation in supergravity

In the Standard Model, the hierarchy is most often (partially) solved by imposing supersymmetry. Unbroken supersymmetry generates extra radiative corrections from the sparticle loops to the Higgs mass that cancel its dependence on  $\Lambda$ . Needless to say, solving the hierarchy problem comes at the cost of introducing many new degrees of freedom in the model. A lot of predictive power is lost. Moreover supersymmetry has to be broken at the TeV scale at least to explain why so many extremely intensive searches have not resulted in the detection of one single sparticle.

In this section we want to study inflation models in the context of local supersymmetry, supergravity, as a study of inflation cannot leave out gravity. The main advantage of working in supergravity is that we can now explicitly compute the coefficients of higher order operators, rather than guessing their form from general dimension analysis. Also, supergravity (sugra) is the low energy limit of string theory, so one could argue that sugra inflation models are compatible with quantum gravity.

A supergravity theory is defined by its Kähler potential  $K$  and scalar potential  $W$ , which are functions of the complex superfields present in the theory <sup>8</sup>.  $K$  contains information about the field space metric.  $W$  contains the superfield interactions. In this thesis we will often make use of the so-called Kähler function  $G$ , defined as

$$G \equiv K + \ln W. \quad (1.66)$$

In terms of  $G$  the F-term scalar potential reads

$$V_F = e^G [G_I G^{I\bar{J}} G_{\bar{J}} - 3], \quad (1.67)$$

where the sum is over all fields in the problem. In most of this thesis we will not consider the D-term contributions (from gauge interactions) to the scalar potential.

<sup>8</sup>In this introductory section we will take the gauge kinetic function  $f$  to be canonical.

The form of (1.67) shows that to get the positive energy density needed for inflation, we should for at least one of the superfields have  $G_I \neq 0$ , which means that this field has to break supersymmetry. This shows that, unlike the case for the Higgs field, supersymmetry alone can not protect the inflaton mass. It is also clear from (1.67) that all fields are coupled to each other. Therefore it seems even more challenging to have a light inflaton field, as its mass will typically get large corrections from interactions with the other fields. These have to be heavy to be stabilized during inflation. We will study this question in chapter 5. At the other hand, this could be a blessing as well. It is often argued that the coupling of the light inflaton field to heavy other fields can be used to probe Planck scale physics from the inflationary observables. For example, in scenarios in which the inflaton makes a sharp turn through field space heavy modes can get temporarily excited, leaving small but possibly detectable features in the power spectrum [27].

In a sugra context, the  $\eta$ -problem is still there. If we expand the Kähler potential around  $X_0$ , the inflaton field value during inflation, in  $\delta X = X - X_0$ , we get  $K = K_0 + K_{x\bar{x}}|_0 |\delta X|^2 + \dots = K_0 + |\Phi|^2 + \dots$ , with  $|\Phi|$  the canonically normalized complex field<sup>9</sup>. The scalar potential then gives

$$V_F = e^{|\Phi|^2} [V_0 + \dots]. \quad (1.68)$$

With the inflaton some linear combination of the real and imaginary parts of  $\Phi$ , it is clear that the exponent in (1.68) contributes order unity:  $\eta \approx 1 + \dots$ , which spoils inflation.

In small field sugra inflation models, the  $\eta$ -problem cannot be solved by introducing a symmetry that keeps the inflaton direction in field space flat. For example, when working with a Kähler potential  $K = K(\Phi - \bar{\Phi})$  one sees that after Taylor expanding around the extremum and performing a Kähler transformation with an arbitrary analytical function  $f$  (which leaves  $G$  and  $V$  invariant)

$$K \rightarrow K + 2 \operatorname{Re} f, \quad W \rightarrow W \operatorname{Exp}(-f), \quad (1.69)$$

the symmetry is lost. Therefore, we need to tune parameters again, just like in the non-supersymmetric case. We will see explicit examples of small field sugra inflation models in chapter 5.

In large field sugra inflation models, tuning parameters is not an option given the enormous length of the inflaton's trajectory. However, this is the perfect environment for keeping inflaton field directions flat by introducing shift symmetries (translation symmetries). Such models will be introduced in chapter 6.

Sugra hybrid inflation, first introduced in [28], can also circumvent the  $\eta$ -problem by invoking a shift symmetry in the Kähler potential. An explicit model of sugra hybrid inflation will be reviewed in chapter 7.

## 1.7 Higgs inflation

Recently there has been a lot of interest in models that employ the Standard Model Higgs field as the inflaton [29, 30]. The beauty of this model is its simplicity: to get inflation it suffices to add a non-minimal coupling between gravity and the Higgs field. The resulting ‘‘Jordan’’ frame action reads (in  $(+ - - -)$  metric, omitting the standard kinetic gauge terms)

$$S_J = \int d^4x \sqrt{-\hat{g}} \left[ - \left( \frac{M_{\text{p}}^2}{2} + \xi \mathcal{H}^\dagger \mathcal{H} \right) R(\hat{g}_{\mu\nu}) + \hat{g}^{\mu\nu} (D_\mu \mathcal{H})^\dagger (D_\nu \mathcal{H}) - \lambda \left( \mathcal{H}^\dagger \mathcal{H} - \frac{v^2}{2} \right)^2 \right], \quad (1.70)$$

---

<sup>9</sup>Note that we use the same notation for superfields and their component (scalar) fields.

where  $\mathcal{H}$  denotes the complex Higgs doublet. In this frame we have the standard Mexican hat potential. To get to the ‘‘Einstein frame’’ in which we have canonical gravity terms one performs a conformal transformation from the Jordan frame metric  $\hat{g}_{\mu\nu}$  to the Einstein frame metric  $g_{\mu\nu}$ :

$$\hat{g}_{\mu\nu} = \omega^2 g_{\mu\nu}. \quad (1.71)$$

After some algebra this gives

$$\begin{aligned} S_E = & \int d^4x \sqrt{-g} \left[ -\frac{M_{\text{p}}^2}{2} \left( 1 + \frac{2\xi \mathcal{H}^\dagger \mathcal{H}}{M_{\text{p}}^2} \right) (\omega^2 R(g_{\mu\nu}) - 6g^{\mu\nu} \omega \nabla_\mu \nabla_\nu \omega) \right. \\ & \left. + \omega^2 g^{\mu\nu} (D_\mu \mathcal{H})^\dagger (D_\nu \mathcal{H}) - \omega^4 \lambda (\mathcal{H}^\dagger \mathcal{H} - \frac{v^2}{2})^2 \right], \end{aligned} \quad (1.72)$$

with  $\nabla$  the covariant derivative based on the metric  $g_{\mu\nu}$ . Now we see how we should pick  $\omega$  in order to have a canonical gravitational term:

$$\omega^{-2} = 1 + \frac{2\xi \mathcal{H}^\dagger \mathcal{H}}{M_{\text{p}}^2}. \quad (1.73)$$

Some more algebra then gives

$$\begin{aligned} S_E = & \int d^4x \sqrt{-g} \left[ -\frac{M_{\text{p}}^2}{2} R(g_{\mu\nu}) + g^{\mu\nu} \left( 3\frac{\omega^4 \xi^2}{M_{\text{p}}^2} \partial_\mu (\mathcal{H}^\dagger \mathcal{H}) \partial_\nu (\mathcal{H}^\dagger \mathcal{H}) \right. \right. \\ & \left. \left. + \omega^2 (D_\mu \mathcal{H})^\dagger (D_\nu \mathcal{H}) \right) - \omega^4 \lambda (\mathcal{H}^\dagger \mathcal{H} - \frac{v^2}{2})^2 \right]. \end{aligned} \quad (1.74)$$

Indeed we are back to Einstein gravity. To check the form of the kinetic terms we put in

$$\mathcal{H} = \frac{1}{\sqrt{2}} \begin{pmatrix} \theta_1 + i\theta_2 \\ \phi_R + i\theta_3 \end{pmatrix}, \quad (1.75)$$

with  $\phi_R \equiv \phi + h$ . As before,  $\phi = \phi(t)$  is the background field, the quantum Higgs field is  $h(t, \vec{x})$ ,  $\theta_i(t, \vec{x})$  are the Goldstone bosons. For the kinetic terms we get

$$S_E^{(\text{kin})} = \int d^4x \sqrt{-g} \cdot \frac{1}{2} \cdot \left[ \omega^2 \delta_{ij} + 6\frac{\xi^2 \omega^4}{M_{\text{p}}^2} \chi_i \chi_j \right] \partial_\mu \chi_i \partial^\mu \chi_j, \quad (1.76)$$

with  $\chi_i = (\phi_R, \theta_i)$ . Now the last step is to transform to a field that has canonical kinetic terms. Considering only the background field  $\phi$  we want to transform to a field  $\tilde{\phi}$  defined via

$$\omega^2 \left[ \delta_{ij} + 6\frac{\xi^2 \omega^2}{M_{\text{p}}^2} \phi^2 \right] \partial_\mu \phi \partial^\mu \phi = \partial_\mu \tilde{\phi} \partial^\mu \tilde{\phi}. \quad (1.77)$$

In the small field regime  $\phi < M_{\text{p}}/\xi$  we get  $\tilde{\phi} \simeq \phi$  so the Mexican hat potential remains. In the mid field regime  $M_{\text{p}}/\xi < \phi < M_{\text{p}}/\sqrt{\xi}$  we find  $\tilde{\phi} \simeq \sqrt{\frac{3}{2}} \frac{\xi \phi^2}{M_{\text{p}}} + \frac{M_{\text{p}}}{\xi} \left( 1 - \sqrt{\frac{3}{2}} \right)$ . In the large field regime  $\phi > M_{\text{p}}/\sqrt{\xi}$ , where inflation should take place we get  $\tilde{\phi} \simeq M_{\text{p}} \left( \sqrt{6} \ln \left( \frac{\phi \sqrt{\xi}}{M_{\text{p}}} \right) + \sqrt{\frac{3}{2}} \right)$ . Then it follows that in this large field regime the potential written in terms of the canonically normalized field  $\tilde{\phi}$  is given by

$$V(\tilde{\phi}) = \frac{\lambda M_{\text{p}}^4}{4\xi^2} \left( 1 - \text{Exp} \left[ -\frac{2}{\sqrt{6}} \left( \frac{\tilde{\phi}}{M_{\text{p}}} - \sqrt{\frac{3}{2}} \right) \right] \right), \quad (1.78)$$

where we omitted the negligible the SM vev  $v$ . At the end of the day, the effect of the non-minimal coupling is an effective flattening of the Higgs potential. One finds that for  $\xi \approx 700 - 10^4$  the resulting potential can support inflation. For all these allowed values for  $\xi$ , the predictions  $n_s \approx 0.96$  and  $r \leq 0.01$  are in perfect agreement with the Planck results (1.51) and (1.52).

A drawback of the mechanism is, apart from the usual tuning needed in non-supersymmetric inflation models, that the Higgs mass found at the LHC seems to be just too light for Higgs inflation, which requires  $m_H \gtrsim 129$  GeV. However, this bound depends heavily on the top mass and might still shift in the future [31, 32]. Another problem is that in the regime  $M_p/\xi < \phi < M_p/\sqrt{\xi}$  the theory becomes for a short while explicitly dependent on its UV completion [30], which goes of course quite against the spirit of the model. To cure this problems it has been suggested to implement Higgs inflation in a supergravity framework [33, 34, 35]. However, now the appealing minimality of the model is lost. Finally a modification that includes a dilaton in the spectrum has been considered in [36]. Such a scenario has the power to explain both inflation and the late-time acceleration of the universe.

While more research on Higgs inflation is on its way, we will use the current framework as a motivation to compute in chapters 3 and 4 the effective action in models where the Higgs background field value changes in time.

## Chapter 2

# Effective field theory and the in-in formalism

In this chapter we review some basic concepts in out-of-equilibrium quantum field theory that we will use in the next part of this thesis. We will introduce the in-in formalism by comparing it to the more familiar in-out formalism. The in-in formalism is the right framework to compute expectation values in time dependent settings, and we will use it a lot in the next three chapters. We also review how one obtains the effective action from the classical action by taking quantum fluctuations into account. From the effective action we get to the effective equation of motion. We show that in the in-in formalism it is much more straightforward to compute the effective equation of motion and then obtain the effective action by integration, than computing the effective action right away.

Again, there is nothing new in this chapter. It is just an attempt to summarize the needed field theory in a convenient, compact but sufficient way. This chapter mostly follows [37, 38, 39, 40], which can be consulted for a much deeper treatment.

### 2.1 In-out formalism

In the standard in-out formalism one is ultimately interested in scattering amplitudes between a given in-state and a given out-state. In this section we write down expressions for scalar field propagators in the in-out formalism following from straightforward expansions of the quantum fields. After that we show how these can be derived from the path integral approach as well.

#### 2.1.1 Propagators and Wightman functions

Let us for now restrict ourselves to a free real scalar field  $\phi$  of mass  $m$ :

$$\mathcal{L} = \frac{1}{2} \partial_\mu \phi \partial^\mu \phi - \frac{1}{2} m^2 \phi^2. \quad (2.1)$$

Working in the usual Heisenberg picture it can be written as

$$\phi(x^\mu) = \int \frac{d^3k}{(2\pi)^3} \frac{1}{\sqrt{2E_{\vec{k}}}} \left[ a_{\vec{k}} e^{-ik \cdot x} + a_{\vec{k}}^\dagger e^{ik \cdot x} \right]_{k^0 = E_{\vec{k}}}. \quad (2.2)$$

Here we have  $E_{\vec{k}} \equiv \sqrt{m^2 + \vec{k} \cdot \vec{k}}$ . (In this work, inner products between three-vectors are always Euclidean.) The creation and annihilation operators  $a_{\vec{k}}^\dagger$  and  $a_{\vec{k}}$  satisfy

$$[a_{\vec{k}}, a_{\vec{l}}^\dagger] = (2\pi)^3 \delta(\vec{k} - \vec{l}), \quad [a_{\vec{k}}, a_{\vec{l}}] = 0, \quad [a_{\vec{k}}^\dagger, a_{\vec{l}}^\dagger] = 0. \quad (2.3)$$

The amplitude for a particle to propagate from  $y$  to  $x$  is given by the Wightman function  $D(x-y)$ , which is defined as

$$D(x-y) \equiv \langle 0 | \phi(x) \phi(y) | 0 \rangle. \quad (2.4)$$

Here the vacuum  $|0\rangle$  is defined via  $\langle 0 | a_{\vec{k}}^\dagger = a_{\vec{k}} | 0 \rangle = 0$ . Exploiting the properties of  $a_{\vec{k}}^\dagger$  and  $a_{\vec{k}}$  we get

$$D(x-y) = \int \frac{d^3k}{(2\pi)^3} \frac{1}{2E_{\vec{k}}} e^{-ik \cdot (x-y)}. \quad (2.5)$$

Wightman functions are on-shell:  $k^0$  is not free but equal to  $E_{\vec{k}}$ . Propagators are built out of Wightman functions, as we will now quickly review.

The propagator  $D^{(4)}(x-y)$  is defined as ( $i$  times) the Green's function of the kinetic operator in the equation of motion. In this case we therefore need

$$\left[ \partial_\mu^{(x)} \partial^{\mu(x)} + m^2 \right] D^{(4)}(x-y) = -i \delta^{(4)}(x-y). \quad (2.6)$$

This immediately gives

$$D^{(4)}(x-y) = \int \frac{d^4k}{(2\pi)^4} \frac{i}{k^2 - m^2} e^{-ik \cdot (x-y)}. \quad (2.7)$$

To get ready to describe time dependent problems later on, and to facilitate a better comparison with the in-in formalism in section 2.5 we want to perform the integral over  $k^0$ . There are four ways to close the contour around the poles at  $k^0 = \pm E_{\vec{k}}$ . Therefore there are in fact four different propagators.

The Feynman prescription passes under the pole at  $k^0 = -E_{\vec{k}}$  (along negative imaginary  $k^0$ ), and over the pole at  $k^0 = E_{\vec{k}}$ . This is often described by

$$D_F^{(4)}(x-y) \equiv \int \frac{d^4k}{(2\pi)^4} \frac{i}{k^2 - m^2 + i\epsilon} e^{-ik \cdot (x-y)}. \quad (2.8)$$

Straightforward contour integration gives

$$D_F(x-y) = \theta(x^0 - y^0) D(x-y) + \theta(y^0 - x^0) D(y-x) \equiv \langle 0 | T \phi(x) \phi(y) | 0 \rangle. \quad (2.9)$$

Here we have introduced the time-ordering operator  $T$ . It orders the expressions that it works on in time, with the "latest time" at the left.

The anti-Feynman, or Dyson, prescription passes the poles in the opposite way, which can be denoted as

$$D_{\bar{F}}^{(4)}(x-y) = \int \frac{d^4k}{(2\pi)^4} \frac{i}{k^2 - m^2 - i\epsilon} e^{-ik \cdot (x-y)}. \quad (2.10)$$

In this case one finds<sup>1</sup>

$$D_{\tilde{F}}(x-y) = -[\theta(x^0 - y^0)D(y-x) + \theta(y^0 - x^0)D(x-y)] \equiv -\langle 0|\tilde{T}\phi(x)\phi(y)|0\rangle. \quad (2.11)$$

$\tilde{T}$  stands for “anti-time-ordering”, which puts the latest time at the right.

Next we pass above both poles. When closing the contour in the lower half plane (for  $x^0 > y^0$ ), we get contributions from both poles. For  $x^0 < y^0$  we close the contour in the upper half plane without enclosing any pole. The integral gives zero. That is why this is the “retarded” propagator. We get

$$D_R(x-y) = \theta(x^0 - y^0)(D(x-y) - D(y-x)) = \theta(x^0 - y^0)\langle 0|[\phi(x), \phi(y)]|0\rangle. \quad (2.12)$$

Finally, the last option is to pass under both poles. There is only a contribution for  $x^0 < y^0$ , hence the name “advanced” propagator. The only difference with the retarded propagator is one overall minus sign caused by the fact the we run the contour counter clockwise:

$$D_A(x-y) = \theta(y^0 - x^0)(-D(x-y) + D(y-x)) = \theta(y^0 - x^0)\langle 0|[\phi(y), \phi(x)]|0\rangle. \quad (2.13)$$

### 2.1.2 Path integral method

To gain some intuition, we now briefly show how the same results can be deduced from the path integral method. The generating functional  $Z[J]$  for a theory described by a Lagrangian  $\mathcal{L}$  is given by

$$Z[J] = \int \mathcal{D}\phi \exp\left(i \int_{t_{\text{in}}}^{t_{\text{out}}} dt \int d^3x [\mathcal{L}[\phi] + J\phi]\right). \quad (2.14)$$

Following the superposition principle, the functional integration is over all possible field configurations  $\phi$ . The “in”-state is defined at  $t = t_{\text{in}}$ , the “out”-state at  $t = t_{\text{out}}$ .  $J$  is the source, needed to generate propagators and Wightman functions. To perform the functional integration one uses the identity

$$\int \mathcal{D}\phi \exp\left(i \left[ \int d^4x \frac{1}{2} \phi(x) A \phi(x) + J\phi(x) \right]\right) = c \exp\left(-\frac{i}{2} \int d^4x d^4y J(x) A^{-1}(x-y) J(y)\right). \quad (2.15)$$

Here  $c$  is an irrelevant constant.

For a scalar field we insert the free field Lagrangian (2.1) and get

$$Z[J] = c \exp\left(-\frac{1}{2} \int d^4x d^4y J(x) \Delta(x-y) J(y)\right) \quad \text{with} \quad \left(\partial_\mu^{(x)} \partial_\mu^{(x)} + m^2\right) \Delta(x-y) = -i\delta^{(4)}(x-y). \quad (2.16)$$

We recognise  $\Delta(x-y)$  as the sought for propagator of the free scalar field. At this point however it is not clear whether it is the general  $D^{(4)}(k)$  propagator, or whether there is already some pole prescription, that gives the Feynman, Dyson/anti-Feynman, retarded or advanced  $D^{(3)}(k)$  propagator.

We can now compute any n-point function from<sup>2</sup>

$$\langle 0|T\phi(x_1)\phi(x_2)\dots\phi(x_n)|0\rangle = (-i)^n \frac{\delta^n Z[J]}{\delta J(x_1)\delta J(x_2)\dots\delta J(x_n)} \Big|_{J=0}. \quad (2.17)$$

<sup>1</sup>One word of caution: many books define the anti-Feynman propagator as equal to  $\langle 0|\tilde{T}\phi(x)\phi(y)|0\rangle$ . This seems unfortunate, as now the defining equation for the anti-Feynman propagator differs a minus sign from the defining equation for the Feynman propagator.

<sup>2</sup>Here we are still working with a free scalar field. To compute n-point functions in an interacting theory, one adds an interaction Lagrangian to the free field Lagrangian and takes functional derivatives of  $W[J] \equiv -\log Z[J]$  rather than  $Z[J]$ .

For  $n = 2$  we should get the Feynman propagator itself. We find, only using that  $\frac{\delta J(x_2)}{\delta J(x_1)} = \delta(x_1 - x_2)$  and that  $\Delta(x_1 - x_2)$  is symmetric in  $x_1$  and  $x_2$ :

$$\langle 0|T\phi(x_1)\phi(x_2)|0\rangle = \Delta(x_1 - x_2). \quad (2.18)$$

So indeed  $\Delta(x - y)$  is the Feynman propagator. Still this is something that we impose ourselves. If we had chosen anti-time ordering in (2.17) we would have found that  $\Delta(x - y)$  is the anti-Feynman propagator. The literature ([40]) states: “as initial conditions are set in the distant past, we shift the mass to  $m^2 - i\epsilon$ .” That is indeed exactly the Feynman prescription.

## 2.2 Effective action for the real scalar field

In this section we are still working in the in-out formalism.

### 2.2.1 Quantum fluctuations modify the classical theory

Consider the action for a scalar field  $\phi$  moving in a potential  $V(\phi)$ :

$$S = \int d^4x \left[ \frac{1}{2} \partial_\mu \phi \partial^\mu \phi - V(\phi) \right]. \quad (2.19)$$

The effective action  $\Gamma$  is relevant when the background around which a quantum field is fluctuating is nonzero (a nonzero vev). We divide the field into a classical background value  $\phi_{\text{cl}}$  and a quantum perturbation on top of that, which we will call  $h$ . (In the next chapters  $h$  will be associated with the quantum Higgs field.) For now we take a constant background value: just like the Higgs field that is fluctuating around its vev of 246 GeV. So we set

$$\phi(x^\mu) = \phi_{\text{cl}} + h(x^\mu). \quad (2.20)$$

The classical action is simply<sup>3</sup>

$$S_{\text{cl}} = \int d^4x \left[ \frac{1}{2} \partial_\mu \phi_{\text{cl}} \partial^\mu \phi_{\text{cl}} - V(\phi_{\text{cl}}) \right]. \quad (2.21)$$

The effective action  $\Gamma$  is the action that one gets from taking the fluctuations  $h$  into account. It describes their backreaction on the dynamics of the background field  $\phi_{\text{cl}}$ , which can be calculated systematically in a loop expansion. Its variation yields the quantum corrected equation of motion. Formally one can compute the effective action by taking the Legendre transformation of  $W[J] = -i \ln(Z[J])$ . In this work we will instead derive it from a diagrammatic approach.

For the action we get (after a partial integration on the second term)

$$S = \int d^4x \left[ \frac{1}{2} \partial_\mu \phi_{\text{cl}} \partial^\mu \phi_{\text{cl}} - h \partial_\mu \partial^\mu \phi_{\text{cl}} + \frac{1}{2} \partial_\mu h \partial^\mu h - V(\phi_{\text{cl}}) - h \left. \frac{\partial V}{\partial \phi} \right|_{h=0} - \frac{1}{2} h^2 \left. \frac{\partial^2 V}{\partial \phi^2} \right|_{h=0} - \frac{1}{6} h^3 \left. \frac{\partial^3 V}{\partial \phi^3} \right|_{h=0} + \dots \right]. \quad (2.22)$$

<sup>3</sup>We have chosen this form because of its similarity with (2.19). In this context however  $\partial_\mu \phi_{\text{cl}} = 0$ .

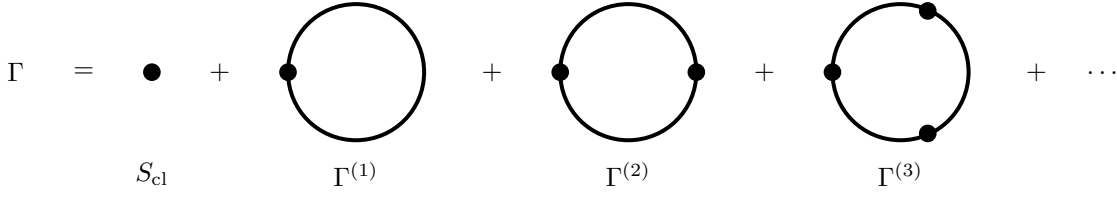


Figure 2.1: *Diagrammatic expansion of the effective action  $\Gamma$ . All drawn lines depict propagating  $h$ . The first “blob” denotes the classical action that is not corrected by any quantum behaviour.*

$$\begin{aligned}
 \text{---} \bullet &\equiv \lambda_h = -i \left( \partial_\mu \partial^\mu \phi_{\text{cl}} + \frac{\partial V}{\partial \phi} \Big|_{h=0} \right) \\
 \text{---} \bullet \text{---} &\equiv \lambda_{hh} = -i \frac{\partial^2 V}{\partial \phi^2} \Big|_{h=0} \\
 \text{---} \bullet \begin{array}{l} / \\ \backslash \end{array} &\equiv \lambda_{hhh} = -i \frac{\partial^3 V}{\partial \phi^3} \Big|_{h=0}
 \end{aligned}$$

Figure 2.2: *Feynman rules for the interactions of the quantum field  $h$ .*

With the two- and three-point interactions of the quantum field  $h$  that emerge in the last line we can make quantum loops. Actually the number of quantum loops acts as an order parameter: every quantum loop brings in a factor of  $\hbar$ . At leading order we only have the classical fields and interactions, so there are no quantum loops. At one-loop level we can draw more diagrams: see figure 2.1. In this work we will not consider two-loop effects.

The effective action  $\Gamma$  is the sum of all one-particle-irreducible vacuum diagrams:

$$\begin{aligned}
 \Gamma &= S_{\text{cl}} + \Gamma^{1\text{-loop}} + \dots \\
 &= S_{\text{cl}} + \Gamma^{(1)} + \Gamma^{(2)} + \Gamma^{(3)} + \dots
 \end{aligned} \tag{2.23}$$

where  $\Gamma^{(i)}$  denotes the contribution from the one-loop diagram with  $i$  vertices. We will soon see that only a limited number of diagrams contributes to the divergent parts of the effective action. In the other diagrams either the integrand vanishes in the UV, or it yields only finite contributions.

The Feynman rules for the new vertices that involve quantum fields  $h$  follow directly from the expansion (2.22) and are summarized in figure 2.2. From now on we will use the shorthand notation  $\frac{\partial V}{\partial \phi} \Big|_{h=0} \equiv V'(\phi_{\text{cl}})$  and likewise for higher derivatives.

### 2.2.2 Computation of $\Gamma$

So let us compute the contributions  $\Gamma^{(i)}$  to the effective action, shown in figure 2.1. In this work we will focus on the unrenormalized divergent contributions to the effective action.

Throughout this work we use a cutoff regularization scheme for the momentum integrals. For the goal of this work, this seems the most intuitive approach, since the momentum integrals are over three-momentum  $\vec{k}$ , and we cut off  $|\vec{k}| < \Lambda$ . Other regularization methods, such as for instance dimensional regularization, would give equivalent answers.

$$(\Gamma^{(1)} + \Gamma^{(2)})_{\text{in-out}} = \begin{array}{c} D_F(x-x) \\ \circlearrowleft \\ x \end{array} + \begin{array}{c} D_F(x-y) \\ \circlearrowleft \\ x \quad y \\ D_F(y-x) \end{array}$$

Figure 2.3: These are the two diagrams that give divergent corrections to the effective action. We work with Feynman propagators.

First of all, let us consider the “blob” in figure 2.1. This denotes the part of the action that does not involve any quantum fields  $h$ : the classical action.

Now for the loop diagrams, depicted again in figure 2.3. We will first work with massless propagators. Then the mass term  $\frac{1}{2}m^2\phi^2$  is treated as part of the interacting potential  $V(\phi)$ . In other words, rather than working with a massive free field we consider a massless interacting field. In the next section we will see that apart from the dependence on boundary terms there is no physical difference between these options. For  $\Gamma^{(1)}$  we get, using Feynman propagators that we defined in (2.9),

$$\begin{aligned} \Gamma_{\text{in-out}}^{(1)} &= -i \int d^4x \frac{1}{2} \lambda_{hh} D_F(x-x) \\ &= - \int d^4x \frac{V''(\phi_{\text{cl}})}{4} \int \frac{d^3k}{(2\pi)^3} \frac{1}{E_{\vec{k}}} \\ &= - \int d^4x \frac{V''(\phi_{\text{cl}})}{16\pi^2} \Lambda^2. \end{aligned} \quad (2.24)$$

Here we have taken a cut-off on the magnitude of the spatial three-momentum.  $\lambda_{hh}$  is the Feynman rule for the interaction between two quantum fields  $h$ , defined in figure 2.2. Note that now that we work with massless propagators, we have  $E_{\vec{k}}^2 = \vec{k} \cdot \vec{k}$ . The factor of  $\frac{1}{2}$  in the first line of (2.24) is a symmetry factor, coming from the reflection symmetry in the diagram.

Note that we could also have worked in terms of the  $D^{(4)}(k)$  propagator (2.7). That would have given

$$\begin{aligned} \Gamma_E^{(1)} &= -i \int d^4x \frac{1}{2} \lambda_{hh} \int \frac{d^4k}{(2\pi)^4} \frac{i}{k^2} e^{-ik \cdot (x-x)} = \frac{-i}{2} V''(\phi_{\text{cl}}) \int d^4x \int \frac{d^4k}{(2\pi)^4} \frac{1}{k^2} \\ &= - \int d^4x \frac{V''(\phi_{\text{cl}})}{32\pi^2} \Lambda_E^2. \end{aligned} \quad (2.25)$$

This is a different answer, but that was to be expected, as we now have a different cut-off: on Euclidean four-momentum. We will prefer to work with  $D^{(3)}(k)$  propagators because that generalizes easily to time dependent problems.

Now for  $\Gamma^{(2)}$ . The symmetry factor is  $\frac{1}{4}$ :  $\frac{1}{2}$  from the reflection symmetry and  $\frac{1}{2}$  from the rotation

symmetry between  $x$  and  $y$  that we have as well now. We get

$$\begin{aligned}
\Gamma_{\text{in-out}}^{(2)} &= -i \int d^4x \int d^4y \frac{1}{4} \lambda_{hh} D_F(x-y) \lambda_{hh} D_F(y-x) \\
&= i \frac{(V''(\phi_{\text{cl}}))^2}{4} \int d^4x \int d^4y \int \frac{d^3k}{(2\pi)^3} \int \frac{d^3l}{(2\pi)^3} \frac{1}{4E_{\vec{k}}E_{\vec{l}}} \\
&\quad \left[ \theta(x^0 - y^0) e^{-ik \cdot (x-y)} + \theta(y^0 - x^0) e^{-ik \cdot (y-x)} \right] \left[ \theta(y^0 - x^0) e^{-il \cdot (y-x)} + \theta(x^0 - y^0) e^{-il \cdot (x-y)} \right] \\
&= i \frac{(V''(\phi_{\text{cl}}))^2}{16} \int d^4x \int dy^0 \int \frac{d^3k}{(2\pi)^3} \frac{1}{(E_{\vec{k}})^2} \\
&\quad \left[ \theta(x^0 - y^0) e^{-2iE_{\vec{k}}(x^0 - y^0)} + \theta(y^0 - x^0) e^{-2iE_{\vec{k}}(y^0 - x^0)} \right].
\end{aligned} \tag{2.26}$$

Here we have used that the integration over  $\int d^3y$  gives  $\delta(\vec{k} + \vec{l})$  which sets  $\vec{k} = -\vec{l}$  and from there  $E_{\vec{k}} = E_{\vec{l}}$ . We continue:

$$\begin{aligned}
\Gamma_{\text{in-out}}^{(2)} &= i \frac{(V''(\phi_{\text{cl}}))^2}{16} \int d^4x \int \frac{d^3k}{(2\pi)^3} \frac{1}{(E_{\vec{k}})^2} \left[ \frac{e^{-2iE_{\vec{k}}(x^0 - y^0)}}{2iE_{\vec{k}}} \Big|_{y^0=-\infty}^{y^0=x^0} + \frac{e^{-2iE_{\vec{k}}(y^0 - x^0)}}{-2iE_{\vec{k}}} \Big|_{y^0=x^0}^{y^0=\infty} \right] \\
&= \frac{(V''(\phi_{\text{cl}}))^2}{32} \int d^4x \int \frac{d^3k}{(2\pi)^3} \frac{1}{(E_{\vec{k}})^3} \left[ (1 - e^{-i\infty}) - (e^{-i\infty} - 1) \right] \\
&= \int d^4x \frac{(V''(\phi_{\text{cl}}))^2}{32\pi^2} \ln \left( \frac{\Lambda}{m} \right).
\end{aligned} \tag{2.27}$$

The mass that shows up in the argument of the logarithm is just meant to render it dimensionless. Given that we do not care about the finite terms, we can always insert such an arbitrary mass scale.

At this point we have just dropped the (complex) exponentials in the one-to-the-last line in (2.27). Note also that these depend both the initial and the ‘‘final’’ boundary conditions, which will be problematic when we want to compute expectation values in time dependent backgrounds. This will improve once we go to the in-in computation. For now we state the final in-out answer

$$\begin{aligned}
\Gamma_{\text{in-out}} &= S_{\text{cl}} + \Gamma_{\text{in-out}}^{(1)} + \Gamma_{\text{in-out}}^{(2)} + \dots \\
&= \int d^4x \left[ \frac{1}{2} \partial_\mu \phi_{\text{cl}} \partial^\mu \phi_{\text{cl}} - V(\phi_{\text{cl}}) - \frac{V''(\phi_{\text{cl}})}{16\pi^2} \Lambda^2 + \frac{(V''(\phi_{\text{cl}}))^2}{32\pi^2} \ln \left( \frac{\Lambda}{m} \right) + \text{finite} \right].
\end{aligned} \tag{2.28}$$

In this time independent context one often writes the so-called Coleman-Weinberg potential

$$\begin{aligned}
\Gamma &= \int d^4x \left[ \frac{1}{2} \partial_\mu \phi_{\text{cl}} \partial^\mu \phi_{\text{cl}} - \left( V(\phi_{\text{cl}}) + V_{CW}(\phi_{\text{cl}}) \right) \right] \\
V_{CW}(\phi_{\text{cl}}) &= \frac{V''(\phi_{\text{cl}})}{16\pi^2} \Lambda^2 - \frac{(V''(\phi_{\text{cl}}))^2}{32\pi^2} \ln \left( \frac{\Lambda}{m} \right) + \text{finite}.
\end{aligned} \tag{2.29}$$

## 2.3 Free mass split

In the seminal work by Coleman and Weinberg [41] it was already stated that the loop expansion is independent of the split of the two-point terms into a free and interacting part. Therefore, let us show

the freedom to view the mass as a part of the propagator, or as a part of the interaction. For simplicity we take  $V = \frac{1}{2} (m^2 + \delta m^2) \phi^2$ . We will use this freedom in the next chapters. This exercise will also give some more intuition for the meaning of the effective potential.

If we work with massless propagators, as we did before, we get for the correction terms, from (2.28),

$$\Gamma^{(\text{corr})} \equiv \Gamma^{(1)} + \Gamma^{(2)} = - \int d^4x \left[ \frac{\Lambda^2}{16\pi^2} (m^2 + \delta m^2) - \frac{\ln(\Lambda/m)}{32\pi^2} (m^2 + \delta m^2)^2 \right]. \quad (2.30)$$

Now we put the factor of  $m^2$  in the propagator. The factor of  $\delta m^2$  is used in the explicit two-point interactions. For  $\Gamma^{(1)}$  we then get (begin from (2.24))

$$\Gamma^{(1)} = - \int d^4x \frac{\delta m^2}{4} \int \frac{d^3k}{(2\pi)^3} \frac{1}{E_{\vec{k}}} = - \int d^4x \frac{\delta m^2}{16\pi^2} \left[ \Lambda^2 - m^2 \ln \left( \frac{\Lambda}{m} \right) + \dots \right], \quad (2.31)$$

where we did a Taylor expansion of  $E_{\vec{k}} = \sqrt{m^2 + \vec{k} \cdot \vec{k}}$ .

For  $\Gamma^{(2)}$  we get (begin from (2.27))

$$\begin{aligned} \Gamma^{(2)} &= \frac{(\delta m^2)^2}{16} \int d^4x \int \frac{d^3k}{(2\pi)^3} \frac{1}{(E_{\vec{k}})^3} = \frac{(\delta m^2)^2}{16} \int d^4x \int \frac{d^3k}{(2\pi)^3} \frac{1}{(k^2 + m^2)^{3/2}} \\ &= \frac{(\delta m^2)^2}{16} \int d^4x \frac{1}{(2\pi)^3} 4\pi \int_0^\Lambda dk \frac{k^2}{k^3 (1 + \frac{m^2}{k^2})^{3/2}} \\ &= \int d^4x \frac{(\delta m^2)^2}{32\pi^2} \ln \left( \frac{\Lambda}{m} \right) + \dots \end{aligned} \quad (2.32)$$

So if we omit the finite terms on the dots we now get for the divergent correction terms

$$\Gamma^{(\text{corr})} = - \int d^4x \left[ \frac{\Lambda^2}{16\pi^2} \delta m^2 - \frac{\ln \Lambda}{32\pi^2} (2m^2 \delta m^2 + \delta m^4) \right]. \quad (2.33)$$

The difference with (2.30) is

$$- \int d^4x \left[ \frac{\Lambda^2}{16\pi^2} m^2 - \frac{\ln(\Lambda/m)}{32\pi^2} m^4 \right]. \quad (2.34)$$

Now, as long as gravity is not taken into account, one is always free to add or subtract constants to the effective action. Therefore, as long as there is not any spacetime dependence in  $m^2$ , both answers (2.30) and (2.33) are physically equal, as they should be. In the end, both answers lead to the same equation of motion.

So what happens when we put all mass terms we have in the propagator? Then we have no explicit two-point interactions left. We can make no diagrams. However, we can still compute the effective action. The quantum contributions to the classical theory can be derived from filling spacetime with harmonic oscillators of all possible frequencies  $\omega$ , with their ground state energy of  $\frac{1}{2} \hbar \omega$ . That gives for the correction to the classical action

$$\begin{aligned} \Gamma^{(\text{corr})} &= - \int d^4x \int \frac{d^3k}{(2\pi)^3} \frac{1}{2} E_{\vec{k}} = - \int d^4x \int \frac{d^3k}{(2\pi)^3} \frac{1}{2} \sqrt{k^2 + (m^2 + \delta m^2)} \\ &= - \int d^4x \left[ \frac{\Lambda^4}{16\pi^2} + \frac{\Lambda^2 (m^2 + \delta m^2)}{16\pi^2} - \frac{\ln(\Lambda/m) (m^2 + \delta m^2)^2}{32\pi^2} + \dots \right]. \end{aligned} \quad (2.35)$$

The first term is again an unphysical constant that we can renormalize away. The two next terms agree with (2.30).

We conclude that indeed we can freely divide mass terms over the propagator and the explicit interactions. However, the boundary conditions can suggest a preferred mass split. This will become more clear in the next chapter.

## 2.4 Effective equation of motion for the real scalar field

Instead of working with the action  $\int d^4x [\partial_\mu \phi \partial^\mu \phi - V(\phi)]$ , we can also work in terms of the equation of motion. Now we try to find quantum corrections to the classical equation of motion  $\partial_\mu \partial^\mu \phi + \frac{\partial V}{\partial \phi} = 0$ .

The equation of motion follows from performing Euler-Lagrange on the action. Or, after the usual partial integration on the kinetic term, simply from taking the functional derivative of the effective action with respect to  $\phi$  and equating to zero:

$$\frac{\delta \Gamma}{\delta \phi} = 0. \quad (2.36)$$

Therefore, we can just insert the final result<sup>4</sup> (2.28) to obtain the effective equation of motion:

$$\partial_\mu \partial^\mu \phi_{\text{cl}} + V'(\phi_{\text{cl}}) + \frac{V'''(\phi_{\text{cl}})}{16\pi^2} \Lambda^2 - \frac{V'''(\phi_{\text{cl}}) V''(\phi_{\text{cl}})}{16\pi^2} \ln \left( \frac{\Lambda}{m} \right) = 0. \quad (2.37)$$

Now, there is another, diagrammatic, way to obtain this same equation of motion, due to Weinberg [42, 43]. This “tadpole” method states that the equation of motion follows from setting

$$\langle h \rangle = 0, \quad (2.38)$$

where  $h$  is still the quantum field fluctuating on top of the background field  $\phi_{\text{cl}}$ , see (2.20). Therefore we have to compute the same Feynman diagrams we needed to get the effective action, but with one added quantum line sticking out. Since this approach generalizes much better to the in-in formalism, we will use it a lot in the next chapters. In this section, where we know the effective action, we will compute Weinberg’s tadpole diagrams, depicted in figure 2.4, and check that equating their sum  $\mathcal{A}$  to zero indeed returns (2.37).

First we take the diagram depicted by  $\mathcal{A}_{\text{cl}}$ . Taking the “blob” at spacetime point  $x$  and the external field  $h$  coming in from spacetime point  $x'$  we should write

$$\tilde{\mathcal{A}}_{\text{cl}} = -i \int d^4x D_F(x - x') \lambda_h. \quad (2.39)$$

However, since we will in the end equate the sum of these diagrams to zero, we might as well truncate the part that all diagrams have in common. The convention (chosen such that setting  $\mathcal{A} = 0$  indeed returns the equation of motion) is to leave out the Feynman propagator for the external line, the integration over the interaction point  $x$ , and one minus sign. So we have

$$\mathcal{A}_{\text{cl}} = i \lambda_h = \partial_\mu \partial^\mu \phi_{\text{cl}} + V'(\phi_{\text{cl}}), \quad (2.40)$$

which yields the classical part of (2.37).

<sup>4</sup>We used the freedom to negate the equation of motion to write it in a more familiar form.

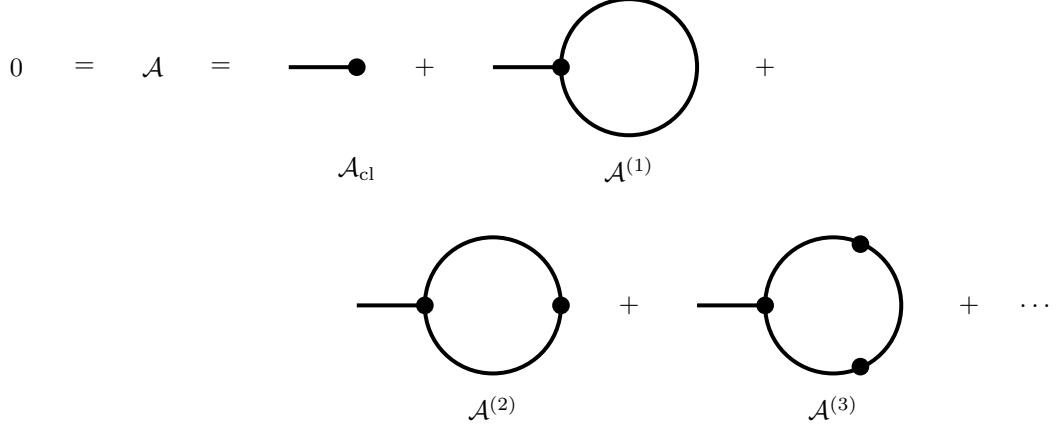


Figure 2.4: Diagrammatic expansion of the effective equation of motion  $\mathcal{A} = 0$ . Classical lines (propagating  $\phi$ ) have been suppressed, all drawn lines depict propagating  $h$ . The first “tadpole” denotes the classical equation of motion that is not corrected by any quantum behaviour.

Now for  $\mathcal{A}^{(1)}$ . Let us again first work with massless propagators. The only difference with  $\Gamma^{(1)}$ , computed in (2.24), is that there is a three-point interaction at the spacetime point  $x$  now. (There is also a minus sign difference coming from the convention defined above (2.40).)

$$\begin{aligned}
 \mathcal{A}^{(1)} &= i \times \frac{1}{2} \lambda_{hhh} D_F(x-x) \\
 &= \dots \\
 &= \frac{V'''(\phi_{\text{cl}})}{16\pi^2} \Lambda^2.
 \end{aligned} \tag{2.41}$$

We have found the first divergent term of (2.37).

We continue with  $\mathcal{A}^{(2)}$ . Now there is one extra difference with respect to the corresponding diagram  $\Gamma^{(2)}$ , computed in (2.26)-(2.27). Apart from the three point interaction at spacetime point  $x$ , there is a different symmetry factor as well. For  $\Gamma^{(2)}$ , the reflection symmetry and the rotations symmetry gave a symmetry factor of  $1/2 \times 1/2 = 1/4$ . For  $\mathcal{A}^{(2)}$ , there is no more rotation symmetry since the interactions at the spacetime points  $x$  and  $y$  are no longer the same. The reflection symmetry is still there. In short, we lose one factor of  $1/2$ . Therefore, we get

$$\begin{aligned}
 \mathcal{A}^{(2)} &= i \int d^4y \frac{1}{2} \lambda_{hhh} D_F(x-y) \lambda_{hh} D_F(y-x) \\
 &= -i \frac{V''(\phi_{\text{cl}})V'''(\phi_{\text{cl}})}{8} \int dy^0 \int \frac{d^3k}{(2\pi)^3} \frac{1}{(E_{\vec{k}})^2} \left[ \theta(x^0 - y^0) e^{-2iE_{\vec{k}}(x^0 - y^0)} + \theta(y^0 - x^0) e^{-2iE_{\vec{k}}(y^0 - x^0)} \right] \\
 &= -\frac{V'''(\phi_{\text{cl}})V''(\phi_{\text{cl}})}{16\pi^2} \ln\left(\frac{\Lambda}{m}\right).
 \end{aligned} \tag{2.42}$$

Indeed, computing Weinberg’s tadpole diagrams has produced the effective equation of motion in a diagrammatic way.

Now it will not come as a surprise that again we are free to shift the two-point interactions between the free part and the interacting part of the theory. We will not bother explicitly writing down the

analogues to the equations (2.31)-(2.34), but it is interesting to see what happens when we shift all the interactions in the propagators, as we did for  $\Gamma$  in (2.35). As all two point interactions disappear, the quantum corrections follow from the only diagram we can still draw:  $\mathcal{A}^{(1)}$  with massive propagators. We get

$$\begin{aligned}\mathcal{A}^{\text{corr}} &= i \times \frac{1}{2} \lambda_{hhh} D_F(x-x) \\ &= \frac{1}{2} V'''(\phi_{\text{cl}}) \int \frac{d^3k}{(2\pi)^3} \frac{1}{2E_{\vec{k}}} e^{-ik \cdot (x-x)} \\ &= \frac{V'''(\phi_{\text{cl}})}{16\pi^2} \left[ \Lambda^2 - V''(\phi_{\text{cl}}) \ln \left( \frac{\Lambda}{m} \right) \right].\end{aligned}\quad (2.43)$$

Here we have made a Taylor expansion of  $E_{\vec{k}} = \sqrt{\vec{k} \cdot \vec{k} + m^2}$ . The result agrees with what we found in (2.41) and (2.42).

## 2.5 In-in formalism

The in-in (or Closed Time Path (CTP), or Schwinger/Keldysh) formalism [40, 44, 45, 46, 47, 48, 49, 50] is a generalization of the path integral formalism. It gives manifestly real results. Before we were working in the in-out formalism: we were computing probabilities of transitions between a given in-state and a given out-state. In non-equilibrium QFT we are rather interested in expectation values at one given point in time, our in-state, while we are not interested in (and/or ignorant of) the out-state. Therefore we use a trick: we double the number of fields and sources. We use one set of fields  $\phi_+$  and sources  $J_+$  to go from our known in-state to an arbitrary out-state, and then use a second set of fields  $\phi_-$  and  $J_-$  to get back from that out-state to our original in-state. We integrate over all possible out-states. In the end we set  $\phi_+ = \phi_- = \phi$ .

In the in-in formalism (2.14) is generalized to

$$\begin{aligned}Z[J] &= \int \mathcal{D}\phi_+ \mathcal{D}\phi_- \exp \left( i \int_{t_{\text{in}}}^{t_{\text{out}}} \int d^3x [\mathcal{L}[\phi_+] + J_+ \phi_+] + i \int_{t_{\text{out}}}^{t_{\text{in}}} \int d^3x [\mathcal{L}[\phi_-] + J_- \phi_-] \right) \\ &= \int \mathcal{D}\phi_+ \mathcal{D}\phi_- \exp \left( i \int_{t_{\text{in}}}^{t_{\text{out}}} \int d^3x [\mathcal{L}[\phi_+] - \mathcal{L}[\phi_-] + J_+ \phi_+ - J_- \phi_-] \right).\end{aligned}\quad (2.44)$$

For our scalar field we can again insert our free field Lagrangian which gives

$$\begin{aligned}Z[J] &= \int \mathcal{D}\phi_+ \int \mathcal{D}\phi_- \exp \left[ \frac{i}{2} \int d^4x \begin{pmatrix} \phi_+ & \phi_- \end{pmatrix} \begin{pmatrix} -(\partial^2 + m^2) & 0 \\ 0 & \partial^2 + m^2 \end{pmatrix} \begin{pmatrix} \phi_+ \\ \phi_- \end{pmatrix} \right. \\ &\quad \left. + i \begin{pmatrix} \phi_+ & \phi_- \end{pmatrix} \begin{pmatrix} J^+ \\ -J^- \end{pmatrix} \right] \\ &= c \exp \left[ -\frac{1}{2} \int d^4x \int d^4y \begin{pmatrix} J^+(x) & -J^-(x) \end{pmatrix} \begin{pmatrix} \Delta^{++}(x-y) & \Delta^{+-}(x-y) \\ \Delta^{-+}(x-y) & \Delta^{--}(x-y) \end{pmatrix} \begin{pmatrix} J^+(y) \\ -J^-(y) \end{pmatrix} \right]\end{aligned}$$

The propagators are now defined via

$$\begin{pmatrix} \partial^2 + m^2 & 0 \\ 0 & -(\partial^2 + m^2) \end{pmatrix} \begin{pmatrix} \Delta^{++}(x-y) & \Delta^{+-}(x-y) \\ \Delta^{-+}(x-y) & \Delta^{--}(x-y) \end{pmatrix} = -i\delta^{(4)}(x-y)\mathbf{1}.\quad (2.45)$$

We see that now we have four types of propagators. The propagator  $\Delta^{+-}(x-y)$ , for example, can be thought of as the correlation between a field  $\phi_+$  at  $x$  and a field  $\phi_-$  at  $y$ .

The four equations in (2.45) show that  $\Delta^{++}(x-y)$  is the Feynman / anti-Feynman propagator as before while  $\Delta^{--}(x-y)$  is minus the Feynman / anti-Feynman propagator. Again the imposed boundary conditions decide between the options. Along the “+”-branche we set, following [40], boundary conditions in the distant past, which means again shifting the mass squared to  $m^2 - i\epsilon$ . In other words: we take the Feynman propagator. Along the “-”-branche we set boundary conditions in the distant future, which shifts the mass in the other direction. So there we take the anti-Feynman propagator.

$\Delta^{+-}(x-y)$  and  $\Delta^{-+}(x-y)$  are obviously Wightman functions (up to a possible sign): acting with the Klein-Gordon operator on them gives zero.

Now let us again take functional derivatives to get  $n$ -point correlation functions (in the free theory, see footnote 2). (2.17) is now generalized to

$$\langle 0 | \left( \tilde{T}\phi(y_1)\dots\phi(y_m) \right) \left( T\phi(x_1)\dots\phi(x_n) \right) | 0 \rangle = (i)^m (-i)^n \frac{\delta^m}{\delta J_-(y_1)\dots\delta J_-(x_m)} \frac{\delta^n}{\delta J_+(x_1)\dots\delta J_+(x_n)} Z[J, J_+] \Big|_{J_+ = J_- = 0}. \quad (2.46)$$

For  $(m=0, n=2)$  we are exactly in the situation that we were before: the functional derivation is again going to give  $\Delta^{++}(x-y)$ , which therefore should be identified with the Feynman propagator:

$$\langle 0 | T\phi(x_1)\phi(x_2) | 0 \rangle = \Delta^{++}(x_1 - x_2). \quad (2.47)$$

For  $(m=2, n=0)$  we get  $(i)^2$  instead of  $(-i)^2$ , and two extra minus signs (because we have twice  $-J_-$  in the exponent), so in the end nothing changes. We find

$$\langle 0 | \tilde{T}\phi(y_1)\phi(y_2) | 0 \rangle = \Delta^{--}(y_1 - y_2). \quad (2.48)$$

As we had already found that  $D_{\tilde{F}}(x-y) = -\langle 0 | \tilde{T}\phi(x)\phi(y) | 0 \rangle$ , this confirms again that  $\Delta^{--}$  is minus the anti-Feynman propagator.<sup>5</sup>

For  $(n=m=1)$  we get

$$\langle 0 | \phi(y_1)\phi(x_1) | 0 \rangle = \Delta^{+-}(x_1 - y_1). \quad (2.49)$$

So indeed:  $\Delta^{+-}(x-y)$  is our Wightman function, but with inverse coordinates:  $D(y-x)$ . And we have the very important relation

$$\Delta^{+-}(x-y) = \Delta^{-+}(y-x). \quad (2.50)$$

Altogether we have

$$\begin{aligned} \Delta^{+-}(x-y) &= \langle 0 | \phi(y)\phi(x) | 0 \rangle \equiv D(y-x) \\ \Delta^{-+}(x-y) &= \langle 0 | \phi(x)\phi(y) | 0 \rangle \equiv D(x-y) \\ \Delta^{++}(x-y) &= \langle 0 | T\phi(x)\phi(y) | 0 \rangle = \theta(x^0 - y^0)\Delta^{-+}(x-y) + \theta(y^0 - x^0)\Delta^{+-}(x-y) = D_F(x-y) \\ \Delta^{--}(x-y) &= \langle 0 | \tilde{T}\phi(x)\phi(y) | 0 \rangle = \theta(x^0 - y^0)\Delta^{+-}(x-y) + \theta(y^0 - x^0)\Delta^{-+}(x-y) = -D_{\tilde{F}}(x-y). \end{aligned} \quad (2.51)$$

Finally, let us check how the Feynman rules defined in figure 2.2 are generalized in the in-in formalism. From (2.44) it is clear that where  $\phi_+$  behaves just as our general in-out field  $\phi$ , the field  $\phi_-$  comes with an

<sup>5</sup>However, many books define  $\langle 0 | \tilde{T}\phi(x)\phi(y) | 0 \rangle$  as the anti-Feynman propagator. If in doubt, the defining equations that everybody agrees on are (2.45), (2.47) and (2.48).

$$\begin{array}{lll}
\begin{array}{c} \oplus \\ \bullet \\ \text{---} \end{array} & \equiv & \lambda_h^+ = -i(\partial_\mu \partial^\mu \phi_{\text{cl}} + V'(\phi_{\text{cl}})) \\
\begin{array}{c} \oplus \\ \bullet \\ \text{---} \text{---} \end{array} & \equiv & \lambda_{hh}^+ = -iV''(\phi_{\text{cl}}) \\
\begin{array}{c} \oplus \\ \bullet \\ \text{---} \diagup \diagdown \end{array} & \equiv & \lambda_{hhh}^+ = -iV'''(\phi_{\text{cl}}) \\
\\
\begin{array}{c} \ominus \\ \bullet \\ \text{---} \end{array} & \equiv & \lambda_h^- = i(\partial_\mu \partial^\mu \phi_{\text{cl}} + V'(\phi_{\text{cl}})) \\
\begin{array}{c} \ominus \\ \bullet \\ \text{---} \text{---} \end{array} & \equiv & \lambda_{hh}^- = iV''(\phi_{\text{cl}}) \\
\begin{array}{c} \ominus \\ \bullet \\ \text{---} \diagup \diagdown \end{array} & \equiv & \lambda_{hhh}^- = iV'''(\phi_{\text{cl}})
\end{array}$$

Figure 2.5: Feynman rules for the interactions of the quantum field  $h_+$  (above) and  $h_-$  (below).

extra minus sign in the generating functional. In our computation, therefore, we have that the Feynman rules for the interactions of the field  $h_+$  are equal to the Feynman rules we had for  $h$ . The Feynman rules for  $h_-$  all come with an extra minus sign. See figure 2.5.

## 2.6 Effective equation of motion in the in-in formalism

At this point the logical next step might seem to compute the effective action  $\Gamma$  in this in-in formalism. However, this is a messy computation, since we still have our two sets of fields  $\phi_+$  and  $\phi_-$  around. Only when we take the variational derivative to get to the equation of motion we are allowed to set these fields equal to each other:

$$\left. \frac{\delta \Gamma}{\delta \phi_+} \right|_{\phi_+ = \phi_- = \phi} = 0 \quad \text{or} \quad \left. \frac{\delta \Gamma}{\delta \phi_-} \right|_{\phi_+ = \phi_- = \phi} = 0. \tag{2.52}$$

Therefore, it is much better to recover the effective equation of motion directly from Weinberg's tadpole method. Once we have the equation of motion, we can integrate back to obtain an effective action whose variation yields that equation of motion. We will do so in the next subsection.

Figure 2.6 shows the correction diagrams  $\mathcal{A}^{(1)}$  and  $\mathcal{A}^{(2)}$ . Without losing generality we can choose the spacetime point  $x$  to be on the  $+$ -branche (in other words: we have an interaction between  $h_+$  fields at  $x$ , we compute the equation of motion from setting  $\langle h_+ \rangle = 0$ ). Now  $y$  can still be on both branches, which gives one extra diagram to compute. The truncation convention works just as before (technically we now factor out  $-\int d^4x [\Delta^{++}(x-x') + \Delta^{-+}(x-x')]$ ).

Since we already identified the  $\Delta^{++}$  propagator with the Feynman propagator, and since we have seen that the Feynman rules for the interactions of  $h_+$  are equal to those for  $h$  in the in-out computation, we



### 2.6.1 Effective action in the in-in formalism

Finally we can integrate the equation of motion  $\mathcal{A} = 0$  just found to get an effective action  $\Gamma$ , since we have

$$\mathcal{A} = -\frac{\delta\Gamma}{\delta\phi_{\text{cl}}}. \quad (2.55)$$

As the in-in equation of motion is equal to the in-out one, this will of course return the in-out effective action that we found in (2.28). Now that we have not computed the effective action directly, it does not contain any more physical information than the effective equation of motion. Technically, it is not even the true effective action, since only at the level of the equation of motion we can set  $h_+ = h_- = h$ . Still we do not want to drop the effective action altogether. In later chapters we will encounter some manipulations that only work on the level of the effective action.

## 2.7 Scalar field with time dependent mass

Now we want to generalize our computation of the effective equation of motion to the case in which the (free) scalar field has a mass that changes in time. The classical equation of motion of the scalar field is now

$$[\partial_\mu\partial^\mu + m^2(t)]\phi = 0. \quad (2.56)$$

We divide the mass squared of the quantum field in a time independent “background” value plus a time dependent part on top of that:

$$m^2(t) = \bar{m}^2 + \delta m^2(t). \quad (2.57)$$

(We could as well have worked with general  $V(\phi)$ , the mass  $m^2(t)$  can really be seen as a notational shorthand for  $\frac{\partial^2 V(\phi_{\text{cl}}(t))}{\partial\phi^2}$ .) As boundary condition we take  $\delta m^2(t=0) = 0$ .

We will compute the effective equation of motion for two different mass splits.

### 2.7.1 Perturbative approach

By “perturbative” we mean: the time independent “background” masses  $\bar{m}^2$  are in the propagators, the time dependent corrections  $\delta m^2(t)$  are in the interactions. The propagators will now involve factors of  $\bar{E}_{\vec{k}} \equiv \sqrt{\vec{k} \cdot \vec{k} + \bar{m}^2}$ . The Feynman rules for the interactions are as in figure 2.5, but now with potential  $V = \frac{1}{2}\delta m^2(t)\phi^2$ . Following the tadpole method, we again have to compute the three diagrams in figure 2.6. These diagrams effectively make up a perturbation expansion in  $\delta m^2/\bar{E}_{\vec{k}}^2$ . Note however that the result found for the divergent terms is exact.

For  $\mathcal{A}^{(1)}$ , there are no new conceptual problems. The interaction at spacetime point  $x$  is now time ( $x^0$ ) dependent, but since we do not integrate over  $x$ , that is no problem. We can follow the computation in (2.41), replacing the massless propagators with propagators  $\bar{\Delta}$  for a field of mass squared  $\bar{m}^2$ . Working again on the  $+$  - branche, and following the same conventions as before, we get

$$\begin{aligned}
\mathcal{A}^{(1)} &= i \frac{1}{2} \lambda_{hhh}^+(x^0) \bar{\Delta}^{++}(x-x) \\
&= \frac{\delta m^2(x^0)'}{4} \int \frac{d^3 k}{(2\pi)^3} \frac{1}{\sqrt{k^2 + \bar{m}^2}} \\
&= \frac{\delta m^2(x^0)'}{16\pi^2} \left[ \Lambda^2 - \bar{m}^2 \ln \left( \frac{\Lambda}{\bar{m}} \right) + \dots \right], \tag{2.58}
\end{aligned}$$

in accordance with (2.31). (The derivative on  $\delta m^2(x^0)$  is still with respect to the field  $\phi_{\text{cl}}$ .)

For  $\mathcal{A}^{(2)}$ , the computation initially follows the one in (2.54) and before. However, the big difference is now that the insertion at spacetime point  $y$  is time dependent ( $y^0$ -dependent), so it can not be taken outside the integral over  $y^0$ . So we get

$$\begin{aligned}
\mathcal{A}^{(2)} &= \mathcal{A}_{++}^{(2)} + \mathcal{A}_{+-}^{(2)} \\
&= i \int d^4 y \frac{1}{2} \lambda_{hhh}^+(x^0) \left[ \bar{\Delta}^{++}(x-y) \lambda_{hh}^+(y^0) \bar{\Delta}^{++}(y-x) \right. \\
&\quad \left. + \bar{\Delta}^{+-}(x-y) \lambda_{hh}^-(y^0) \bar{\Delta}^{-+}(y-x) \right] \\
&= \dots \\
&= -\frac{\delta m^2(x^0)'}{4} \int \frac{d^3 k}{(2\pi)^3} \frac{1}{(\bar{E}_{\vec{k}})^2} \int_0^{x^0} dy^0 \delta m^2(y^0) \sin 2\bar{E}_{\vec{k}}(x^0 - y^0) \\
&= -\frac{\delta m^2(x^0)'}{4} \int \frac{d^3 k}{(2\pi)^3} \frac{1}{(\bar{E}_{\vec{k}})^2} \left[ \delta m^2(y^0) \frac{\cos 2\bar{E}_{\vec{k}}(x^0 - y^0)}{2\bar{E}_{\vec{k}}} \Big|_{y^0=0}^{y^0=x^0} \right. \\
&\quad \left. - \int_0^{x^0} dy^0 (\partial_{y^0} \delta m^2(y^0)) \frac{\cos 2\bar{E}_{\vec{k}}(x^0 - y^0)}{2\bar{E}_{\vec{k}}} + \dots \right] \\
&= -\frac{\delta m^2(x^0)'}{8} \int \frac{d^3 k}{(2\pi)^3} \frac{1}{(\bar{E}_{\vec{k}})^3} \left[ \delta m^2(x^0) - \delta m^2(0) \cos 0 \right] \\
&= -\frac{\delta m^2(x^0)' \delta m^2(x^0)}{16\pi^2} \ln \left( \frac{\Lambda}{\bar{m}} \right) + \dots \tag{2.59}
\end{aligned}$$

Note how we isolate the divergent terms by a partial integration. Note as well that the boundary condition  $\delta m^2(0) = 0$  now gives a reason to drop the unwanted term.

Now we can again (see (2.34)) add some spacetime independent terms for free. Reinstalling a general potential  $V(\phi)$  we find the effective equation of motion as a straightforward generalization of (2.37):

$$\mathcal{A} = 0 \quad \leftrightarrow \quad \partial_\mu \partial^\mu \phi_{\text{cl}} + V'(\phi_{\text{cl}}(t)) + \frac{V'''(\phi_{\text{cl}}(t))}{16\pi^2} \Lambda^2 - \frac{V'''(\phi_{\text{cl}}(t))V''(\phi_{\text{cl}}(t))}{16\pi^2} \ln \left( \frac{\Lambda}{\bar{m}} \right) + \text{finite} = 0. \tag{2.60}$$

## 2.7.2 Non-perturbative approach

By ‘‘non-perturbative’’ we mean: we put all masses  $m^2(t) = \bar{m}^2 + \delta m^2(t)$  in the propagator. This approach yields a better basis to study the equation of motion in a numerical way, but we will only use it

as a consistency check. We follow the analysis in [51]. The difficulty is now in finding a propagator that takes the time dependent mass into account. Once we have that, we only need to compute one diagram, just like the computation we did in (2.43). (Note that since there is only one interaction point in the diagram, there will be no difference between the in-in and the in-out answer.)

To find the propagator, we have to generalize the expansion (2.2) of the quantum field  $\phi$  to the case in which its mass is time dependent. In (2.2), the quantum field is built out of mode functions  $e^{-ik \cdot x}$  that satisfy the equation of motion  $[\partial_\mu \partial^\mu + m^2] \phi = 0$ . Now we have to take mode functions  $f_{\vec{k}}(x^\mu)$  that satisfy  $[\partial_\mu \partial^\mu + m^2(t)] \phi = 0$ . As an Ansatz for these mode functions we propose to take  $f_{\vec{k}}(x^\mu) = U_{\vec{k}}(t) e^{i\vec{k} \cdot \vec{x}}$ . The whole quantum field is now given by (compare to (2.2))

$$\phi(x) = \int \frac{d^3k}{(2\pi)^3} \frac{1}{\sqrt{2\bar{E}_{\vec{k}}}} \left[ a_{\vec{k}} U_{\vec{k}}(t) e^{i\vec{k} \cdot \vec{x}} + a_{\vec{k}}^\dagger U_{\vec{k}}^*(t) e^{-i\vec{k} \cdot \vec{x}} \right]. \quad (2.61)$$

For the full time dependent propagator, closing in on itself, that we need we then get

$$\Delta^{++}(x-x) = D_F(x-x) = \langle 0 | \phi(x) \phi(x) | 0 \rangle = \int \frac{d^3k}{(2\pi)^3} \frac{1}{2\bar{E}_{\vec{k}}} U_{\vec{k}}(x^0) U_{\vec{k}}^*(x^0) e^{i\vec{k} \cdot (\vec{x} - \vec{x})}. \quad (2.62)$$

The first two steps follow from the standard propagator prescription (2.51). In the third step we have used the expansion for an explicitly time-dependent scalar field (2.61), and the standard manipulations with the creation and annihilation operators.

Solving the equation of motion will give  $U_{\vec{k}}(t)$ , and that is what we will do now. We have

$$[\partial_\mu \partial^\mu + m^2(t)] f_{\vec{k}}(x^\mu) = [\partial_\mu \partial^\mu + m^2(t)] U_{\vec{k}}(t) e^{i\vec{k} \cdot \vec{x}} = 0, \quad (2.63)$$

which gives

$$\left[ \ddot{U}_{\vec{k}} + (\vec{k}^2 + m^2(t)) U_{\vec{k}} \right] e^{i\vec{k} \cdot \vec{x}} = 0, \quad \rightarrow \quad \ddot{U}_{\vec{k}} + E_{\vec{k}}^2(t) U_{\vec{k}} = 0. \quad (2.64)$$

We now propose to write  $U(t)$  as

$$U_{\vec{k}}(t) = e^{-i\bar{E}_{\vec{k}} t} [1 + g_{\vec{k}}(t)]. \quad (2.65)$$

If we again impose that at  $t = 0$  we have  $\delta m^2 = 0$ , it directly follows that we need

$$\left( U(0) = e^{-i\bar{E}_{\vec{k}} t} \Big|_{t=0} = 1, \quad \dot{U}(0) = -i\bar{E}_{\vec{k}} \right) \quad \rightarrow \quad (g(0) = 0, \quad \dot{g}(0) = 0). \quad (2.66)$$

So let us write the equation of motion (2.64) as an equation for  $g_{\vec{k}}(t)$ . As we have

$$\partial_t^2 \left[ e^{-i\bar{E}_{\vec{k}} t} (1 + g_{\vec{k}}(t)) \right] = \left( -\bar{E}_{\vec{k}}^2 - 2i\bar{E}_{\vec{k}} \frac{\dot{g}_{\vec{k}}}{1 + g_{\vec{k}}} + \frac{\ddot{g}_{\vec{k}}}{1 + g_{\vec{k}}} \right) e^{-i\bar{E}_{\vec{k}} t} [1 + g_{\vec{k}}(t)] \quad (2.67)$$

we get

$$\ddot{g}_{\vec{k}} - 2i\bar{E}_{\vec{k}} \dot{g}_{\vec{k}} = -\delta m^2(t) (1 + g_{\vec{k}}). \quad (2.68)$$

Note that until here, no expansion has been made: this is still the exact equation of motion. In appendix A we show that the solution of equation (2.68) is given by

$$|U_{\vec{k}}(t)|^2 = |1 + g_{\vec{k}}(t)|^2 = 1 - \frac{\delta m^2(t)}{2\bar{E}_{\vec{k}}^2} + \mathcal{O}(\bar{E}_{\vec{k}}^{-3}). \quad (2.69)$$

Putting everything together we get for the time dependent generalization of the computation in (2.43)

$$\begin{aligned}
\mathcal{A}^{(\text{corr})} &= i \frac{1}{2} \lambda_{hhh}(x^0) \Delta^{++}(x-x) \\
&= \frac{1}{2} (\partial_{\phi_{\text{cl}}} m^2(x^0)) \int \frac{d^3k}{(2\pi)^3} \frac{1}{2\bar{E}_{\vec{k}}} U_{\vec{k}}(x^0) U_{\vec{k}}^*(x^0) e^{i\vec{k}\cdot(\vec{x}-\vec{x})} \\
&= \frac{1}{2} (\partial_{\phi_{\text{cl}}} m^2(x^0)) \int \frac{d^3k}{(2\pi)^3} \frac{1}{2\bar{E}_{\vec{k}}} \left( 1 - \frac{\delta m^2(x^0)}{2\bar{E}_{\vec{k}}^2} \right) \\
&= \frac{\partial_{\phi_{\text{cl}}} m^2(x^0)}{16\pi^2} \left[ \Lambda^2 - m^2(x^0) \ln \left( \frac{\Lambda}{\bar{m}} \right) \right]. \tag{2.70}
\end{aligned}$$

This agrees with the perturbative answer (2.60).

### 2.7.3 Effective action

We already mentioned that computing the effective action in the in-in formalism is not very straightforward, as we still have both sets of field  $h_+$  and  $h_-$  around. Only at the level of the effective equation of motion these can be set equal. Now that we have found the equation of motion (2.60) from the tadpole method, we can follow (2.55) and simply write down an action whose variation gives (2.60):

$$\Gamma = \int d^4x \left[ \frac{1}{2} \partial_\mu \phi_{\text{cl}} \partial^\mu \phi_{\text{cl}} - V(\phi_{\text{cl}}(t)) - \frac{V''(\phi_{\text{cl}}(t))}{16\pi^2} \Lambda^2 + \frac{(V''(\phi_{\text{cl}}(t)))^2}{32\pi^2} \ln \left( \frac{\Lambda}{\bar{m}} \right) + \text{finite} \right]. \tag{2.71}$$

This effective action is a direct time dependent generalization of (2.28). Note that we could have found it as well from the harmonic oscillator approach in (2.35). That computation generalizes directly to a time dependent context, the fact that  $\phi_{\text{cl}}$  is now time dependent does not change anything. We get

$$\begin{aligned}
\Gamma^{(\text{corr})} &= - \int d^4x \int \frac{d^3k}{(2\pi)^3} \frac{1}{2} E_{\vec{k}}(t) \\
&= - \int d^4x \int \frac{d^3k}{(2\pi)^3} \frac{1}{2} \sqrt{k^2 + (\bar{m}^2 + \delta m^2(t))} \\
&= - \int d^4x \left[ \frac{\Lambda^4}{16\pi^2} + \frac{\Lambda^2(\bar{m}^2 + \delta m^2(t))}{16\pi^2} - \frac{\ln(\Lambda/\bar{m})(\bar{m}^2 + \delta m^2(t))^2}{32\pi^2} + \text{finite} \right], \tag{2.72}
\end{aligned}$$

which is up to unphysical terms (terms that can be renormalized away) equivalent to the result (2.71).

**Part II**

**Rolling fields**



## Chapter 3

# Effective action for the U(1) Abelian Higgs model

### 3.1 Motivation: Goldstone bosons in a rolling background

In the Standard Model, the background Higgs field  $\phi_{\text{cl}}$  resides (after spontaneous symmetry breaking) in the minimum of its famous “Mexican hat” potential. The Higgs quantum field  $h$  and the related Goldstone bosons  $\theta_i$  fluctuate around this minimum. We can write

$$H = \frac{1}{\sqrt{2}} \begin{pmatrix} \theta_1 + i\theta_2 \\ \phi_{\text{cl}} + h + i\theta_3 \end{pmatrix}. \quad (3.1)$$

With  $\phi_{\text{cl}}$  constant in time the Goldstone bosons are massless, due to the Goldstone theorem [52, 53]. Therefore they do not contribute to the Coleman-Weinberg potential (2.29). Actually, when one chooses to work in unitary gauge, they disappear from the theory. This is why, in the broken phase (Higgs field fluctuating around  $\phi_{\text{cl}} \neq 0$ ), the Goldstone bosons are considered unphysical. They do not represent true degrees of freedom. To understand the situation one has to take the vector bosons into account that are associated with the gauge symmetry of the Higgs field. In the unbroken phase (Higgs field fluctuating around  $\phi_{\text{cl}} = 0$ ) the Goldstone bosons are physical degrees of freedom while these vector bosons are massless. In the broken phase the Goldstone bosons are unphysical, so we lose three degrees of freedom. However, three of the vector bosons have acquired a mass now, and have therefore each won a degree of freedom.

We have seen in section 1.7 that this situation is different in Higgs inflation. The Higgs field plays the role of the inflaton now. During inflation, therefore, the background Higgs field slowly rolls down the potential. Its vev  $\phi_{\text{cl}}$  is not constant in time, as it does not extremize the potential anymore. As a result, we find that the second derivatives of the potential with respect to the Goldstone fields do not vanish anymore (see the subsection below). Since the Goldstone bosons still have canonical kinetic terms, it seems that their masses are nonzero. Therefore, they do contribute to the effective Coleman-Weinberg potential. Are these contributions physical? From the fact that we can still remove all dependence on the Goldstone fields by going to unitary gauge, one would be tempted to state that they are not. However, that would lead to new complications. When the background field moves an infinitesimal distance from  $\phi_{\text{cl}} = 0$  to, say,  $\phi_{\text{cl}} = \epsilon$ , (when we go from the unbroken to the broken phase) the Goldstone bosons would instantly become unphysical. Their nonzero masses would instantly cease to contribute to the effective

potential. That would give a discontinuity in the effective potential, which seems unacceptable. (Of course the masses of the associated vector bosons are turned on once we leave the unbroken phase, but these masses are proportional to  $\phi_{\text{cl}}$  and can therefore never cure this discontinuity.) In addition, removing the Goldstone dependence by hand would have disastrous consequences for supersymmetric Higgs inflation [33, 34, 35]. In these set-ups all masses conspire together to make quadratic divergences in the effective action cancel. Taking out some nonzero masses obviously brings back these quadratic divergences.

In short, both possible answers to the question whether the Goldstone contributions to the effective potential are physical or not seem to be problematic. In this chapter we therefore want to compute the effective potential for a time-dependent background from scratch, and then comment on the result. Instead of treating the full framework of Higgs inflation, we will strip off the parts that are not relevant for this question (the non-Abelian symmetry and the non-minimal coupling) and study the Abelian Higgs model. Mostly following the computations in [54, 55, 56, 57] we will compute the unrenormalized divergent parts of the effective action. The novelty in our computation is that it applies to a time dependent background, it is gauge invariant and works for any arbitrary potential, three ingredients that were not simultaneously combined before. This chapter is based on our work [2].

### 3.1.1 Goldstone's theorem

In this subsection we show how Goldstone's theorem predicts that Goldstone bosons are no longer massless when the classical background field becomes time dependent.

Consider a theory with a complex scalar field  $\Phi$ , which we will refer to as the Higgs field. It is invariant under a global  $U(1)$  transformation. The field has a time dependent expectation value  $\Phi_{\text{cl}} = (\phi_R(t) + i\phi_I(t))/\sqrt{2}$ ; without loss of generality we can align this with the real direction and set  $\phi_I = 0$ . Goldstone showed that in the broken phase  $\phi_R \neq 0$  there is a massless excitation in the spectrum, provided the potential is extremized. Here we repeat his argument for a (time dependent) classical background field which is displaced from its minimum  $\partial_{\phi_R} V|_{\text{cl}} \neq 0$ .

Under an infinitesimal global  $U(1)$  transformation  $\Phi \rightarrow e^{i\alpha}\Phi$  the invariant potential  $V(\Phi\Phi^\dagger)$  transforms as

$$\delta_\alpha V = \frac{\partial V}{\partial \phi_i} \delta_\alpha \phi_i = 0, \quad (3.2)$$

with  $i = \{R, I\}$ . Written out in terms of real fields the change under a gauge transformation is  $\delta_\alpha \phi_R = -\alpha \phi_I$  and  $\delta_\alpha \phi_I = \alpha \phi_R$ . Differentiating (3.2) with respect to  $\phi_k$ , the equation for  $k = R$  is trivially satisfied. For  $k = I$  evaluated on the classical background configuration it yields, however,

$$\frac{\partial^2 V}{\partial \phi_I \partial \phi_I} \phi_R - \frac{\partial V}{\partial \phi_R} \Big|_{\text{cl}} = 0. \quad (3.3)$$

If the Higgs extremizes the potential, the second term in the equation above vanishes. One concludes that the spectrum contains a massless Goldstone boson. However, with the Higgs displaced from its minimum — as is the case during Higgs inflation — the first derivative of the potential no longer vanishes. Therefore the Goldstone boson mass is apparently non-zero:

$$m_I^2 \equiv \frac{\partial^2 V}{\partial \phi_I^2} \Big|_{\text{cl}} = \frac{1}{\phi_R} \frac{\partial V}{\partial \phi_R} \Big|_{\text{cl}} = -\frac{\ddot{\phi}_R}{\phi_R} \Big|_{\text{cl}}. \quad (3.4)$$

Note that the last equality is only valid on-shell, as we used that the evolution of the classical background  $\phi_R(t)$  is governed by the Klein-Gordon equation, which in a Minkowski universe reads  $\ddot{\phi}_R + \partial_{\phi_R} V = 0$ .

## 3.2 Lagrangian

The Lagrangian of the  $U(1)$  Abelian Higgs model is, in  $R_\xi$ -gauge,

$$\begin{aligned}\mathcal{L} &= \mathcal{L}_{\text{gauge-kin}} + \mathcal{L}_{\text{higgs-kin}} + \mathcal{L}_{\text{pot}} + \mathcal{L}_{\text{gaugefixing}} + \mathcal{L}_{\text{ghost}} \\ &= -\frac{1}{4}F_{\mu\nu}F^{\mu\nu} + D_\mu\Phi(D^\mu\Phi)^\dagger - V(\Phi\Phi^\dagger) - \frac{1}{2\xi}G^2 + \bar{\eta}g\frac{\delta G}{\delta\alpha}\eta.\end{aligned}\quad (3.5)$$

Here the complex Higgs singlet can be decomposed in a real background, that is now time dependent, plus two quantum fields  $h(x^\mu)$  and  $\theta(x^\mu)$  (Higgs quantum field and Goldstone quantum field) fluctuating on top of that:

$$\Phi(x^\mu) = \frac{1}{\sqrt{2}}[\phi_{\text{cl}}(t) + h(x^\mu) + i\theta(x^\mu)].\quad (3.6)$$

The  $U(1)$  covariant derivative acts as  $D_\mu = \partial_\mu + igA_\mu$  on the  $U(1)$ -charged field  $\Phi$ . Under a  $U(1)$  gauge transformation specified by the infinitesimal gauge parameter  $\alpha$  the fields transform as

$$\Phi \rightarrow e^{i\alpha}\Phi, \quad A_\mu \rightarrow A_\mu - \frac{1}{g}\partial_\mu\alpha.\quad (3.7)$$

$G$  stands for the gauge-fixing function  $G = \partial_\mu A^\mu - \xi g[\phi_{\text{cl}} + h]\theta$ . The parameter  $\xi$  specifies the gauge.  $\xi = 0$  corresponds to Landau gauge, unitary gauge is achieved in the limit  $\xi \rightarrow \infty$ .  $\eta$  denotes the ghost field.

We work out these terms in turn. The gauge kinetic terms gives the standard result

$$\mathcal{L}_{\text{gauge-kin}} = \frac{1}{2}A_\mu[\eta^{\alpha\beta}\partial_\alpha\partial_\beta\eta^{\mu\nu} - \partial^\mu\partial^\nu]A_\nu.\quad (3.8)$$

For the Higgs kinetic terms we get

$$\begin{aligned}\mathcal{L}_{\text{higgs-kin}} &= \frac{1}{2}\left[\partial_\mu h\partial^\mu h + \partial_\mu\theta\partial^\mu\theta + g^2\phi_{\text{cl}}^2 A_\mu A^\mu\right] \\ &\quad + g\phi_{\text{cl}}A^\mu\partial_\mu\theta - g\dot{\phi}_{\text{cl}}A_0\theta + \dot{h}\dot{\phi}_{\text{cl}} - (\partial_i h)(\partial_i\phi_{\text{cl}}) + \frac{1}{2}\dot{\phi}_{\text{cl}}^2 \\ &\quad + g^2 h\phi_{\text{cl}}A_\mu A^\mu + \frac{1}{2}g^2 h^2 A_\mu A^\mu + \frac{1}{2}g^2\theta^2 A_\mu A^\mu + \partial_\mu\theta gA^\mu h - \partial_\mu h gA^\mu\theta.\end{aligned}\quad (3.9)$$

The first line contains kinetic and mass terms. The first term in the second line is familiar from the time independent case. It disappears in unitary gauge, and so does the kinetic term for the Goldstone boson  $\theta$ . The last four terms in the second line are caused by the rolling of the Higgs background field. The third line contains terms with three or more quantum fields.

The potential term can be expanded as

$$\mathcal{L}_{\text{pot}} = -V(\phi_{\text{cl}}) - V_{\phi_{\text{cl}}}(\phi_{\text{cl}})h - \frac{1}{2}V_{hh}(\phi_{\text{cl}})h^2 - \frac{1}{2}V_{\theta\theta}(\phi_{\text{cl}})\theta^2 - \frac{1}{6}V_{\phi_{\text{cl}}hh}(\phi_{\text{cl}})h^3 - \frac{1}{2}V_{\phi_{\text{cl}}\theta\theta}(\phi_{\text{cl}})h\theta^2 + \dots\quad (3.10)$$

We have used that given the  $U(1)$  symmetry in the model, we have  $V_\theta = 0^1$ . Note also that  $V_h = V_{\phi_{\text{cl}}}$ : when we insert  $\Phi = (\phi_{\text{cl}} + h + i\theta)/\sqrt{2}$  the situation is symmetric in  $\phi_{\text{cl}}$  and  $h$ .

<sup>1</sup>Indeed, the potential is a function of  $\Phi\Phi^\dagger = ((\phi_{\text{cl}} + h)^2 + \theta^2)/2$ , so there is no term linear in  $\theta$  when we expand around  $\theta = 0$ .

The gauge-fixing term gives

$$\begin{aligned} \mathcal{L}_{\text{gauge-fixing}} = & \frac{1}{2\xi} A_\mu \partial^\mu \partial^\nu A_\nu - g A^\mu \partial_\mu [\phi_{\text{cl}} + h] \theta - g A^\mu [\phi_{\text{cl}} + h] \partial_\mu \theta - \frac{1}{2} \xi g^2 \phi_{\text{cl}}^2 \theta^2 \\ & - \xi g^2 \phi_{\text{cl}} h \theta^2 - \frac{1}{2} \xi g^2 h^2 \theta^2. \end{aligned} \quad (3.11)$$

For the ghost term (Faddeev-Popov term) we first use that the working of a gauge transformation on the gauge fixing function  $G$  is given by

$$G \rightarrow \partial_\mu \left( A^\mu - \frac{1}{g} \partial^\mu \alpha \right) - \xi g (\phi_{\text{cl}} + h - \alpha \theta) (\theta + \alpha \phi_{\text{cl}} + \alpha h). \quad (3.12)$$

Therefore we have

$$\frac{\delta G}{\delta \alpha} = \frac{1}{g} \left[ -\partial_\mu \partial^\mu - \xi g^2 (\phi_{\text{cl}} + h)^2 + \xi g^2 \theta^2 \right], \quad (3.13)$$

which gives

$$\mathcal{L}_{\text{ghost}} = \bar{\eta} g \frac{\delta G}{\delta \alpha} \eta = -\bar{\eta} \partial_\mu \partial^\mu \eta - \xi g^2 (\phi_{\text{cl}} + h)^2 \bar{\eta} \eta + \xi g^2 \theta^2 \bar{\eta} \eta. \quad (3.14)$$

Now we take these five contributions together. We split the result in a classical part, a free (quadratic) part from which we can derive propagators and an interaction part:

$$\begin{aligned} \mathcal{L}_{\text{class}} &= \frac{1}{2} \partial_\mu \phi_{\text{cl}} \partial^\mu \phi_{\text{cl}} - V(\phi_{\text{cl}}) \\ \mathcal{L}_{\text{free}} &= -\frac{1}{2} A_\mu \left[ -\eta^{\mu\nu} (\eta^{\alpha\beta} \partial_\alpha \partial_\beta + g^2 \phi_{\text{cl}}^2) + \left( 1 - \frac{1}{\xi} \right) \partial^\mu \partial^\nu \right] A_\nu \\ &\quad - \bar{\eta} [\partial_\mu \partial^\mu + \xi g^2 \phi_{\text{cl}}^2] \eta \\ &\quad - \frac{1}{2} h [\partial_\mu \partial^\mu + V_{hh}(\phi_{\text{cl}})] h \\ &\quad - \frac{1}{2} \theta [\partial_\mu \partial^\mu + V_{\theta\theta}(\phi_{\text{cl}}) + \xi g^2 \phi_{\text{cl}}^2] \theta \\ \mathcal{L}_{\text{int}} &= \dot{h} \dot{\phi}_{\text{cl}} - (\partial_i h) (\partial_i \phi_{\text{cl}}) - V_{\phi_{\text{cl}}} h \\ &\quad - \frac{1}{6} V_{\phi_{\text{cl}} hh}(\phi_{\text{cl}}) h^3 - 2\xi g^2 \phi_{\text{cl}} h \eta \bar{\eta} - \frac{1}{2} V_{\phi_{\text{cl}} \theta\theta}(\phi_{\text{cl}}) h \theta \theta - \xi g^2 \phi_{\text{cl}} h \theta \theta + g^2 h \phi_{\text{cl}} A_\mu A^\mu \\ &\quad - 2g \dot{\phi}_{\text{cl}} A_0 \theta - 2g \dot{h} A_0 \theta + \dots \end{aligned} \quad (3.15)$$

Note that in the last line there is a new two point interaction between the Goldstone boson  $\theta$  and the temporal component of the gauge field, induced by the rolling of the background field. This is the key to the solution of the problem brought up in the previous section. We will comment more at the end of this chapter, but here it is clear already that  $V_{\theta\theta}$  can not be identified with the mass of the Goldstone boson  $\theta$ . The true Goldstone boson is a linear combination of  $\theta$  and  $A_0$  (and the spatial components of  $A_\mu$  as well, as these couple in their kinetic terms to  $A_0$ , unless  $\xi = 1$ ). Therefore,  $V_{\theta\theta}$  is not a mass eigenvalue, and finding  $V_{\theta\theta} \neq 0$  does not mean that the Goldstone boson mass is nonzero.

From the Lagrangian we can define the following masses

$$\begin{aligned} m_h^2 &= V_{hh} \\ m_\theta^2 &= V_{\theta\theta} + \xi g^2 \phi_{\text{cl}}^2 \\ m_\eta^2 &= \xi g^2 \phi_{\text{cl}}^2 \\ m_{A_\mu A_\nu}^2 &= -\eta^{\mu\nu} g^2 \phi_{\text{cl}} \equiv -\eta^{\mu\nu} m_A^2. \end{aligned} \quad (3.16)$$

Since we have  $\phi_{\text{cl}} = \phi_{\text{cl}}(t)$  all interactions are time dependent ( $V_{hh}$  and  $V_{\theta\theta}$  change in time as well). If we formally write

$$\phi_{\text{cl}}^2(t) = \phi_{\text{cl}}^2(0) + (\phi_{\text{cl}}^2(t) - \phi_{\text{cl}}^2(0)) \quad (3.17)$$

and the same for  $V_{hh}$  and  $V_{\theta\theta}$ , we can again split all masses in a time independent “background” part and a time dependent contribution on top of that. The boundary condition is that the time dependent part vanishes at  $t = 0$ . Every mass can then be written as

$$m^2(t) = \bar{m}^2 + \delta m^2(t), \quad (3.18)$$

just like the case of the real scalar field described in section 2.7. In the next two sections we will compute the effective equation of motion (and from there the effective action) following the two approaches proposed there.

The Lagrangian (3.15) contains one more two point interaction, between  $A_0$  and  $\theta$ . As we just discussed, this one disappears in the time independent limit. It seems natural to define

$$\delta m_{A_0\theta}^2 = 2g\dot{\phi}_{\text{cl}}. \quad (3.19)$$

Now we can deduce Feynman rules for all one-, two- and three point interactions needed in further computations. We will put the time independent parts  $\bar{m}^2$  of the masses defined in (3.16) in the propagators. Therefore the two point interactions contain time dependent factors of  $\delta m^2$ .

Since we want to work in the in-in formalism, we first formally double our fields. The resulting vertices on the positive branche are in figure 3.1. The vertices on the negative branche differ one minus sign from their positive counterparts.

To get the Feynman rule for the  $\lambda_{hA_0\theta}$ -vertex we did a partial integration to let the time derivative work on the rest of the diagram rather than on  $h(x)$ . When  $h(x)$  is free of time derivatives we can again formally factor out the propagator  $D_F(x - x')$ , as we discussed above (2.40).

### 3.3 Perturbative computation (in arbitrary gauge)

Here we follow the approach proposed in subsection 2.7.1. We need to compute the same diagrams, with a  $h_+$  field sticking out, but sum over all possible fields  $\alpha = \{h, \eta, \theta, A_\mu\}$  running in the loop:

$$\mathcal{A} = \mathcal{A}_{\text{cl}} + \sum_{\alpha} \left[ \mathcal{A}_{\alpha}^{(1)} + \mathcal{A}_{\alpha}^{(2)} \right]. \quad (3.20)$$

(Here the superscripts (1) and (2) denote the number of interactions in the graphs. We still work at the one-loop level.)

#### Classical contribution

The classical contribution to the effective equation of motion follows as before from the term linear in  $h$  in (3.15), and yields (again)

$$\mathcal{A}_{\text{cl}} = \partial_\mu \partial^\mu \phi_{\text{cl}} + V'(\phi_{\text{cl}}). \quad (3.21)$$

#### First order

$$\begin{array}{ll}
h_+ \text{---} \oplus \bullet & \equiv \lambda_h^+ = -i(\partial_\mu \partial^\mu \phi_{\text{cl}} + V'(\phi_{\text{cl}})) \\
\\
h_+ \text{---} \oplus \bullet \text{---} h_+ & \equiv \lambda_{hh}^+ = -i\delta m_h^2 & \begin{array}{l} h_+ \text{---} \oplus \bullet \begin{array}{l} / h_+ \\ \backslash h_+ \end{array} \\ \equiv \lambda_{hhh}^+ = -iV_{\phi_{\text{cl}}hh} = -i\partial_{\phi_{\text{cl}}} m_h^2 \end{array} \\
\\
\theta_+ \text{---} \oplus \bullet \text{---} \theta_+ & \equiv \lambda_{\theta\theta}^+ = -i\delta m_\theta^2 & \begin{array}{l} h_+ \text{---} \oplus \bullet \begin{array}{l} / \theta_+ \\ \backslash \theta_+ \end{array} \\ \equiv \lambda_{h\theta\theta}^+ = -i(V_{\phi_{\text{cl}}\theta\theta} + 2g^2\phi_{\text{cl}}) \\ = -i\partial_{\phi_{\text{cl}}} m_\theta^2 \end{array} \\
\\
\eta_+ \text{---} \oplus \bullet \text{---} \bar{\eta}_+ & \equiv \lambda_{\eta\bar{\eta}}^+ = -i\delta m_\eta^2 & \begin{array}{l} h_+ \text{---} \oplus \bullet \begin{array}{l} / \eta_+ \\ \backslash \bar{\eta}_+ \end{array} \\ \equiv \lambda_{h\eta\bar{\eta}}^+ = -2i\xi g^2 \phi_{\text{cl}} = -i\partial_{\phi_{\text{cl}}} m_\eta^2 \end{array} \\
\\
A_{\mu+} \text{---} \oplus \bullet \text{---} A_{\nu+} & \equiv \lambda_{A_\mu A_\nu}^+ = i\eta^{\mu\nu} \delta m_A^2 & \begin{array}{l} h_+ \text{---} \oplus \bullet \begin{array}{l} / A_{\mu+} \\ \backslash A_{\nu+} \end{array} \\ \equiv \lambda_{hA_\mu A_\nu}^+ = 2i\eta^{\mu\nu} g^2 \phi_{\text{cl}} \\ = i\eta^{\mu\nu} \partial_{\phi_{\text{cl}}} m_A^2 \end{array} \\
\\
A_{0+} \text{---} \oplus \bullet \text{---} \theta_+ & \equiv \lambda_{A_0\theta}^+ = -i\delta m_{A_0\theta}^2 & \begin{array}{l} h_+ \text{---} \oplus \bullet \begin{array}{l} / A_{0+} \\ \backslash \theta_+ \end{array} \\ \equiv \lambda_{hA_0\theta}^+ = 2ig\partial_t \end{array}
\end{array}$$

Figure 3.1: Feynman rules for all needed interactions on the positive branche, derived from the Lagrangian (3.15). The extra coupling between  $A_0$  and  $\theta$ , induced by the time dependence of the background field  $\phi_{\text{cl}}$ , is in the last line.

For the fields  $h$ ,  $\eta$  and  $\theta$  we can use the result (2.58). We have to take into account that the ghost field  $\eta$  carries two degrees of freedom. Moreover it gets an extra minus sign from its anticommuting nature. We get

$$\begin{aligned}
\mathcal{A}_{\{h,\eta,\theta\}}^{(1)} &= i \frac{1}{2} \left[ \lambda_{hhh}^+(x^0) \bar{\Delta}_{hh}^{++}(x-x) - 2 \lambda_{h\eta\bar{\eta}}^+(x^0) \bar{\Delta}_{\eta\bar{\eta}}^{++}(x-x) + \lambda_{h\theta\theta}^+(x^0) \bar{\Delta}_{\theta\theta}^{++}(x-x) \right] \\
&= \frac{\partial_{\phi_{\text{cl}}} m_h^2(x^0)}{16\pi^2} \left[ \Lambda^2 - \bar{m}_h^2 \ln \left( \frac{\Lambda}{\bar{m}} \right) \right] - 2 \frac{\partial_{\phi_{\text{cl}}} m_\eta^2(x^0)}{16\pi^2} \left[ \Lambda^2 - \bar{m}_\eta^2 \ln \left( \frac{\Lambda}{\bar{m}} \right) \right] \\
&\quad + \frac{\partial_{\phi_{\text{cl}}} m_\theta^2(x^0)}{16\pi^2} \left[ \Lambda^2 - \bar{m}_\theta^2 \ln \left( \frac{\Lambda}{\bar{m}} \right) \right]. \tag{3.22}
\end{aligned}$$

The bar on the propagator is to remind that it contains only time independent background masses. We also explicitly indicated the time dependence of the three point interactions.

For the gauge field, with its mixing degrees of freedom, we need

$$\mathcal{A}_{A_\mu}^{(1)} = i \frac{1}{2} \lambda_{hA_\mu A_\nu}^+(x^0) \bar{\Delta}_{A_\mu A_\nu}^{++}(x-x) = -\frac{1}{2} (\partial_{\phi_{\text{cl}}} m_A^2) \eta^{\mu\nu} \bar{\Delta}_{A_\mu A_\nu}^{++}(0). \quad (3.23)$$

Now we can use (C.3):

$$\eta^{\mu\nu} \bar{\Delta}_{A_\mu A_\nu}^{++}(0) = -3\bar{\Delta}_A^{++}(0) - \xi \bar{\Delta}_\xi^{++}(0). \quad (3.24)$$

Here  $\bar{\Delta}_A^{++}$  denotes the Feynman propagator for a field with mass squared  $m_A^2$  and  $\bar{\Delta}_\xi^{++}$  denotes the Feynman propagator for a field with mass squared  $m_\xi^2 \equiv \xi m_A^2$ .

So effectively we only have scalars left, and we know how to treat them. We get (defining as well  $\delta m_\xi^2 \equiv \xi \delta m_A^2$ )

$$\mathcal{A}_{A_\mu}^{(1)} = 3 \times \frac{\partial_{\phi_{\text{cl}}} m_A^2(x^0)}{16\pi^2} \left[ \Lambda^2 - \bar{m}_A^2 \ln \left( \frac{\Lambda}{\bar{m}} \right) \right] + \frac{\partial_{\phi_{\text{cl}}} m_\xi^2(x^0)}{16\pi^2} \left[ \Lambda^2 - \bar{m}_\xi^2 \ln \left( \frac{\Lambda}{\bar{m}} \right) \right]. \quad (3.25)$$

### Second order

For the fields  $h$ ,  $\eta$  and  $\theta$  we can again copy the time dependent scalar result (2.59) with the appropriate numerical factors of 1, -2, 1:

$$\begin{aligned} \mathcal{A}_{\{h,\eta,\theta\}}^{(2)} = & - \left[ \frac{\delta m_h^2(x^0) \partial_{\phi_{\text{cl}}} m_h^2(x^0)}{16\pi^2} \ln \left( \frac{\Lambda}{\bar{m}} \right) - 2 \frac{\delta m_\eta^2(x^0) \partial_{\phi_{\text{cl}}} m_\eta^2(x^0)}{16\pi^2} \ln \left( \frac{\Lambda}{\bar{m}} \right) \right. \\ & \left. + \frac{\delta m_\theta^2(x^0) \partial_{\phi_{\text{cl}}} m_\theta^2(x^0)}{16\pi^2} \ln \left( \frac{\Lambda}{\bar{m}} \right) \right]. \end{aligned} \quad (3.26)$$

Now we put the gauge field in the loop. We need to write the vector analogue of (2.59):

$$\begin{aligned} \mathcal{A}_{A_\mu}^{(2)} = & i \int d^4 y \frac{1}{2} \lambda_{hA_\mu A_\nu}^+(x^0) \left[ \bar{\Delta}_{A_\nu A_\rho}^{++}(x-y) \lambda_{A_\rho A_\sigma}^+(y^0) \bar{\Delta}_{A_\sigma A_\mu}^{++}(y-x) \right. \\ & \left. + \bar{\Delta}_{A_\nu A_\rho}^{+-}(x-y) \lambda_{A_\rho A_\sigma}^-(y^0) \bar{\Delta}_{A_\sigma A_\mu}^{-+}(y-x) \right]. \end{aligned} \quad (3.27)$$

Using (2.51) we can again write the Feynman propagators in terms of Wightman functions. Upon using the identity  $1 = \theta(x^0 - y^0) + \theta(y^0 - x^0)$  in the second line the terms multiplying  $\theta(y^0 - x^0)$  will then cancel, just as we saw before, when we combined (2.42) and (2.53) to get (2.54). In appendix C.1 we show that in the end we get

$$\mathcal{A}_{A_\mu}^{(2)} = -\frac{1}{4} (\partial_{\phi_{\text{cl}}} m_A^2(x^0)) \delta m_A^2(x^0) \times \left( 3 \int \frac{d^3 k}{(2\pi)^3} \frac{1}{2 \left( \bar{E}_{\vec{k}}^{(A)} \right)^3} + \xi^2 \int \frac{d^3 k}{(2\pi)^3} \frac{1}{2 \left( \bar{E}_{\vec{k}}^{(\xi)} \right)^3} \right). \quad (3.28)$$

These are two separate scalar computations that we already did before. From (2.59) it is easy to see that we will get

$$\mathcal{A}_{A_\mu}^{(2)} = - \left[ \frac{3 (m_A^2(x^0))' \delta m_A^2(x^0)}{16\pi^2} \ln \left( \frac{\Lambda}{\bar{m}} \right) + \frac{(m_\xi^2(x^0))' \delta m_\xi^2(x^0)}{16\pi^2} \ln \left( \frac{\Lambda}{\bar{m}} \right) \right]. \quad (3.29)$$

$$\begin{aligned}
0 = \mathcal{A} &= h^+ \text{---} \bullet \\
&\oplus \\
&+ \sum_{\alpha} h^+ \text{---} \bullet \text{---} \bigcirc \text{---} \bullet \\
&\oplus \quad \bar{\Delta}_{\alpha\alpha}^{++}(x-x) \quad \oplus \quad \bar{\Delta}_{\alpha\alpha}^{++}(x-y) \quad \oplus \quad \bar{\Delta}_{\alpha\alpha}^{+-}(x-y) \\
&\oplus \quad \bar{\Delta}_{\alpha\alpha}^{++}(y-x) \quad \oplus \quad \bar{\Delta}_{\alpha\alpha}^{-+}(y-x) \\
&+ \quad h^+ \text{---} \bullet \text{---} \bigcirc \text{---} \bullet \quad + \quad h^+ \text{---} \bullet \text{---} \bigcirc \text{---} \bullet \\
&\oplus \quad \bar{\Delta}_{A_0 A_0}^{++}(x-y) \quad \oplus \quad \bar{\Delta}_{A_0 A_0}^{+-}(x-y) \\
&\oplus \quad \bar{\Delta}_{\theta\theta}^{++}(y-x) \quad \oplus \quad \bar{\Delta}_{\theta\theta}^{-+}(y-x)
\end{aligned}$$

Figure 3.2: Diagrammatic expansion of the effective equation of motion  $\mathcal{A} = 0$  in the perturbative computation. The left interaction is at spacetime point  $x$ , the right interaction is at spacetime point  $y$ . The sum in the second line is over  $\alpha = \{h, \eta, \theta, A_{\mu}\}$ . Note the extra diagrams with the mixed  $A_0 - \theta$  loop.

Here we have again used the notation  $m_{\xi}^2 \equiv \xi m_A^2$ .

Finally we can also make a mixed second order diagram with an  $A_0$  going from  $x$  to  $y$  and a  $\theta$  going back, and vice versa. We have to drop the factor of  $1/2$ , as there is no reflection symmetry left. We get

$$\begin{aligned}
\mathcal{A}_{A_0\theta}^{(2)} &= i \int d^4y \lambda_{hA_0\theta}^+(x^0) \left[ \bar{\Delta}_{00}^{++}(x-y) \lambda_{A_0\theta}^+(y^0) \bar{\Delta}_{\theta}^{++}(y-x) \right. \\
&\quad \left. + \bar{\Delta}_{00}^{+-}(x-y) \lambda_{A_0\theta}^-(y^0) \bar{\Delta}_{\theta}^{-+}(y-x) \right] \\
&= -i \int d^4y (2g\partial_{x^0}) \delta m_{A_0\theta}^2(y^0) \times \\
&\quad \left( \left[ \left( 1 - \frac{\bar{E}_A^2}{\bar{m}_A^2} \right) \bar{\Delta}_A^{++}(x-y) + \xi \frac{\bar{E}_{\xi}^2}{\bar{m}_{\xi}^2} \bar{\Delta}_{\xi}^{++}(x-y) \right] \bar{\Delta}_{\theta}^{++}(y-x) \right. \\
&\quad \left. - \left[ \left( 1 - \frac{\bar{E}_A^2}{\bar{m}_A^2} \right) \bar{\Delta}_A^{+-}(x-y) + \xi \frac{\bar{E}_{\xi}^2}{\bar{m}_{\xi}^2} \bar{\Delta}_{\xi}^{+-}(x-y) \right] \bar{\Delta}_{\theta}^{-+}(y-x) \right). \quad (3.30)
\end{aligned}$$

Here  $\Delta_{00}$  is shorthand for  $\Delta_{A_0 A_0}$ . We have used (C.5) to rewrite the vector propagator. We have  $\bar{E}_A^2 = \vec{k} \cdot \vec{k} + \bar{m}_A^2$  and  $\bar{E}_{\xi}^2 = \vec{k} \cdot \vec{k} + \bar{m}_{\xi}^2$ .

Now if we had  $\bar{E}_A^2 = \bar{E}_{\xi}^2 \equiv \bar{E}^2$  we would get (see for example (2.59))

$$\begin{aligned}
&-i \int d^4y (2g\partial_{x^0}) (\delta m^2(y^0)) \left( \bar{\Delta}^{++}(x-y) \bar{\Delta}^{++}(y-x) - \bar{\Delta}^{+-}(x-y) \bar{\Delta}^{-+}(y-x) \right) \\
&= -\frac{1}{4} (2g\partial_{x^0}) \delta m^2(x^0) \int \frac{d^3k}{(2\pi)^3} \frac{1}{\bar{E}^3}. \quad (3.31)
\end{aligned}$$

In case there are two different energies  $E_1$  and  $E_2$  in the two parts of the loop we should substitute (follows for example from (2.54) and the computations just before that)

$$\frac{1}{\bar{E}^3} \rightarrow \frac{2}{\bar{E}_1 \bar{E}_2 (\bar{E}_1 + \bar{E}_2)}. \quad (3.32)$$

That gives for our computation:

$$\begin{aligned} \mathcal{A}_{A_0\theta}^{(2)} &= \\ & -\frac{1}{4} (2g\partial_{x^0}) \delta m_{A_0\theta}^2(x^0) \int \frac{d^3k}{(2\pi)^3} \left[ \frac{2}{\bar{E}_A \bar{E}_\theta (\bar{E}_A + \bar{E}_\theta)} \left( 1 - \frac{\bar{E}_A^2}{\bar{m}_A^2} \right) + \frac{2}{\bar{E}_\xi \bar{E}_\theta (\bar{E}_\xi + \bar{E}_\theta)} \xi \frac{\bar{E}_\xi^2}{\bar{m}_\xi^2} \right] \\ & = -\frac{1}{8\pi^2} (2g\partial_{x^0}) \delta m_{A_0\theta}^2(x^0) \int dk \left[ \frac{\xi}{k} - \frac{k}{\bar{m}_A^2} + \frac{\xi k}{\bar{m}_\xi^2} + \frac{3(\bar{m}_A^2 + \bar{m}_\theta^2)}{4k\bar{m}_A^2} - \frac{3\xi(\bar{m}_\xi^2 + \bar{m}_\theta^2)}{4k\bar{m}_\xi^2} \right. \\ & \quad \left. - \frac{3\xi(\bar{m}_\xi^2 + \bar{m}_\theta^2)}{4k^3} \right] \\ & = -\frac{3+\xi}{32\pi^2} (2g\partial_{x^0}) \delta m_{A_0\theta}^2(x^0) \ln \left( \frac{\Lambda}{\bar{m}} \right). \end{aligned} \quad (3.33)$$

Now we put the contributions  $\mathcal{A}_{\text{cl}}$ ,  $\mathcal{A}_{\{h,\eta,\theta\}}^{(1)}$ ,  $\mathcal{A}_{A_\mu}^{(1)}$ ,  $\mathcal{A}_{\{h,\eta,\theta\}}^{(2)}$ ,  $\mathcal{A}_{A_\mu}^{(2)}$  and  $\mathcal{A}_{A_0\theta}^{(2)}$  all together and get

$$\begin{aligned} \mathcal{A} &= \partial_\mu \partial^\mu \phi_{\text{cl}} + \frac{\partial V}{\partial \phi_{\text{cl}}} \\ & + \frac{\Lambda^2}{16\pi^2} \left( \partial_{\phi_{\text{cl}}} m_h^2(t) - 2\partial_{\phi_{\text{cl}}} m_\eta^2(t) + \partial_{\phi_{\text{cl}}} m_\theta^2(t) + 3\partial_{\phi_{\text{cl}}} m_A^2(t) + \partial_{\phi_{\text{cl}}} m_\xi^2(t) \right) \\ & - \frac{\ln(\Lambda/\bar{m})}{16\pi^2} \left( m_h^2(t) \partial_{\phi_{\text{cl}}} m_h^2(t) - 2m_\eta^2(t) \partial_{\phi_{\text{cl}}} m_\eta^2(t) + m_\theta^2(t) \partial_{\phi_{\text{cl}}} m_\theta^2(t) \right. \\ & \quad \left. + 3m_A^2(t) \partial_{\phi_{\text{cl}}} m_A^2(t) + m_\xi^2(t) \partial_{\phi_{\text{cl}}} m_\xi^2(t) + (6+2\xi) g^2 \ddot{\phi}_{\text{cl}}(t) \right). \end{aligned} \quad (3.34)$$

To extract an effective action  $\Gamma$  out of  $\mathcal{A}$  we use the Euler-Lagrange prescription

$$\mathcal{A} = \partial_t \frac{\delta \Gamma}{\delta \dot{\phi}_{\text{cl}}} - \frac{\delta \Gamma}{\delta \phi_{\text{cl}}}. \quad (3.35)$$

Note that here we had to generalize (2.55) since there is a term in  $\ddot{\phi}_{\text{cl}}$  as well now. For the last term in particular we write

$$g^2 \ddot{\phi}_{\text{cl}} = \partial_t \frac{\delta}{\delta \dot{\phi}_{\text{cl}}} \left[ \frac{1}{2} g^2 \dot{\phi}_{\text{cl}}^2 \right] = \partial_t \frac{\delta}{\delta \dot{\phi}_{\text{cl}}} \left[ \frac{\delta m_{A_0\theta}^4}{8} \right]. \quad (3.36)$$

That gives

$$\begin{aligned} \Gamma = & \int d^4x \left[ \frac{1}{2} \partial_\mu \phi_{\text{cl}} \partial^\mu \phi_{\text{cl}} - V(\phi_{\text{cl}}) \right. \\ & - \frac{\Lambda^2}{16\pi^2} \left( m_h^2(t) - 2m_\eta^2(t) + m_\theta^2(t) + 3m_A^2(t) + m_\xi^2(t) \right) \\ & \left. + \frac{\ln(\Lambda/\bar{m})}{32\pi^2} \left( m_h^4(t) - 2m_\eta^4(t) + m_\theta^4(t) + 3m_A^4(t) + m_\xi^4(t) - (6 + 2\xi) m_A^2(t) V_{\theta\theta}(t) \right) \right]. \end{aligned} \quad (3.37)$$

Here we have used the zeroth order background equation of motion and the  $U(1)$  gauge invariance discussed around (3.4) ( $V_{\phi_{\text{cl}}} = \phi_{\text{cl}} V_{\theta\theta}$ ) to write

$$\int dt \delta m_{A_0\theta}^4 = 4g^2 \int dt \dot{\phi}_{\text{cl}}^2 = -4g^2 \int dt \phi_{\text{cl}} \ddot{\phi}_{\text{cl}} = 4g^2 \int dt \phi_{\text{cl}} V_{\phi_{\text{cl}}} = 4 \int dt m_A^2 V_{\theta\theta} \quad (3.38)$$

up to higher loop corrections. Note that this manipulation does not work on the level of the equation of motion, where there is no integration over  $t$ .

Plugging in the masses gives, finally,

$$\begin{aligned} \Gamma = & \int d^4x \left[ \frac{1}{2} \partial_\mu \phi_{\text{cl}} \partial^\mu \phi_{\text{cl}} - V(\phi_{\text{cl}}) \right. \\ & - \frac{\Lambda^2}{16\pi^2} \left( V_{hh}(t) + V_{\theta\theta}(t) + 3g^2 \phi_{\text{cl}}(t)^2 \right) \\ & \left. + \frac{\ln(\Lambda/\bar{m})}{32\pi^2} \left( V_{hh}^2(t) + V_{\theta\theta}^2(t) + 3g^4 \phi_{\text{cl}}(t)^4 - 6g^2 \phi_{\text{cl}}(t)^2 V_{\theta\theta}(t) \right) \right]. \end{aligned} \quad (3.39)$$

With this last substitution the final expression is in terms of explicitly gauge independent quantities. As a result the *on-shell* one loop effective potential is gauge invariant. In the static limit ( $V_{\theta\theta} \rightarrow 0$  and all other masses time independent) our results reproduce the standard Coleman-Weinberg potential.

### 3.4 Non-perturbative computation (in the gauge $\xi = 1$ )

In this second approach to get to the effective equation of motion of the Abelian Higgs model, we put all masses  $m^2(t) = \bar{m}^2 + \delta m^2(t)$  in the propagator, as we did for the real scalar field in subsection 2.7.2. Therefore, the two point interactions  $\lambda_{hh}$ ,  $\lambda_{\eta\bar{\eta}}$ ,  $\lambda_{\theta\theta}$  and  $\lambda_{A_\mu A_\nu}$  all disappear, and the computation basically follows the one we did around (2.70). The two point interaction  $\lambda_{A_0\theta}$  is accounted for in a mixed  $A_0 - \theta$  propagator. The technical challenge now is in computing the diagrams involving this propagator. See figure 3.3.

We will work in the  $\xi = 1$  gauge. The equation of motion is

$$\mathcal{A} = \mathcal{A}_{\text{cl}} + \mathcal{A}^{(\text{corr})} = 0, \quad (3.40)$$

with  $\mathcal{A}_{\text{cl}}$  given by (3.21).  $\mathcal{A}^{(\text{corr})}$  follows as before from a closed Feynman propagator:

$$\mathcal{A}^{(\text{corr})} = i \frac{1}{2} \sum \lambda_{h\alpha\beta}^+ \Delta_{\alpha\beta}^{++}(0). \quad (3.41)$$

$$\begin{aligned}
0 = \mathcal{A} = & \begin{array}{c} h^+ \\ \oplus \end{array} \bullet + \begin{array}{c} h^+ \\ \oplus \end{array} \bullet \bigcirc^{\Delta_{hh}^{++}(x-x)} - 2 \begin{array}{c} h^+ \\ \oplus \end{array} \bullet \bigcirc^{\Delta_{\eta\eta}^{++}(x-x)} \\
& + 3 \begin{array}{c} h^+ \\ \oplus \end{array} \bullet \bigcirc^{\Delta_{A_i A_i}^{++}(x-x)} + \begin{array}{c} h^+ \\ \oplus \end{array} \bullet \bigcirc^{\Delta_{A_0 A_0}^{++}(x-x)} \\
& + \begin{array}{c} h^+ \\ \oplus \end{array} \bullet \bigcirc^{\Delta_{\theta\theta}^{++}(x-x)} + \begin{array}{c} h^+ \\ \oplus \end{array} \bullet \bigcirc^{\Delta_{A_0\theta}^{++}(x-x)}
\end{aligned}$$

Figure 3.3: Diagrammatic expansion of the effective equation of motion  $\mathcal{A} = 0$  in (3.40). The interaction is at spacetime point  $x$ . We have reinstated the in-in indices. Note the extra diagram with the  $A_0 - \theta$  propagator, caused by the time dependence of the background field.

Let us begin with the easy part: the fields  $h$ ,  $\eta$  and  $A_i$  that act like independent scalar fields (the spatial  $A_i$  fields decouple in this gauge, see (3.15)). For these we can directly use the result (2.70). Taking into account the number of degrees of freedom in each field (discussed above (3.22)) we get

$$\begin{aligned}
\sum_{\alpha=\{h,\eta,A_i\}} \mathcal{A}_\alpha^{(\text{corr})} = & \frac{1}{16\pi^2} \left[ \begin{array}{l} (\partial_{\phi_{\text{cl}}} m_h^2) \left( \Lambda^2 - m_h^2 \ln \left( \frac{\Lambda}{\bar{m}} \right) \right) \\ -2 (\partial_{\phi_{\text{cl}}} m_\eta^2) \left( \Lambda^2 - m_\eta^2 \ln \left( \frac{\Lambda}{\bar{m}} \right) \right) \\ +3 (\partial_{\phi_{\text{cl}}} m_A^2) \left( \Lambda^2 - m_A^2 \ln \left( \frac{\Lambda}{\bar{m}} \right) \right) \end{array} \right]. \quad (3.42)
\end{aligned}$$

Now let us compose the  $A_0 - \theta$  propagator. The coupled equations of motion for  $A_0$  and  $\theta$  follow from the Lagrangian (3.15) and read

$$\left[ \begin{pmatrix} -(\partial_t^2 + \bar{E}_A^2) & 0 \\ 0 & \partial_t^2 + \bar{E}_\theta^2 \end{pmatrix} + \begin{pmatrix} -\delta m_A^2 & \delta m_{A_0\theta}^2 \\ \delta m_{A_0\theta}^2 & \delta m_\theta^2 \end{pmatrix} \right] \begin{pmatrix} A_0 \\ \theta \end{pmatrix} = 0. \quad (3.43)$$

Here we already used that the  $\partial_t^2$  on the exponent gives  $-\vec{k} \cdot \vec{k}$  that has been absorbed into  $\bar{E}^2$ . We have dropped the  $\vec{k}$ -index. We have

$$\begin{aligned}
E_{A_0}^2 &= \vec{k} \cdot \vec{k} + m_A^2 = \vec{k} \cdot \vec{k} + \bar{m}_A^2 + \delta m_A^2 = \bar{E}_{A_0}^2 + \delta m_A^2 \\
E_\theta^2 &= \vec{k} \cdot \vec{k} + m_\theta^2 = \vec{k} \cdot \vec{k} + \bar{m}_\theta^2 + \delta m_\theta^2 = \bar{E}_\theta^2 + \delta m_\theta^2.
\end{aligned} \quad (3.44)$$

Now the idea is to write two sets of mode functions for both fields: so we will have  $U_{A_0}^1$  and  $U_{A_0}^2$ ,  $U_\theta^1$  and  $U_\theta^2$ . This is a straightforward generalization of the one-field set-up used in (2.66). Both sets have to

satisfy the equation of motion independently:

$$\left[ \begin{pmatrix} -(\partial_t^2 + \bar{E}_{A_0}^2) & 0 \\ 0 & \partial_t^2 + \bar{E}_\theta^2 \end{pmatrix} + \begin{pmatrix} -\delta m_A^2 & \delta m_{A_0\theta}^2 \\ \delta m_{A_0\theta}^2 & \delta m_\theta^2 \end{pmatrix} \right] \begin{pmatrix} U_{A_0}^\alpha \\ U_\theta^\alpha \end{pmatrix} = 0, \quad (3.45)$$

with

$$U_m^\alpha(0) = \delta_m^\alpha, \quad \dot{U}_m^\alpha(0) = -i\bar{E}_m \delta_m^\alpha. \quad (3.46)$$

The  $\alpha = 1$  mode is the ‘‘mostly gauge boson’’ mode, and  $\alpha = 2$  is the ‘‘mostly Goldstone boson’’ mode. The modes do not decouple because of the off-diagonal  $\delta m_{A_0\theta}^2$  term.

We want to write the  $2 \times 2$  Feynman propagator  $\Delta^{++}(x-y)$  for this coupled situation. Its defining equation is

$$\begin{pmatrix} -(\partial_{(x)}^\mu \partial_{(x)}^\mu + m_A^2) & \delta m_{A_0\theta}^2 \\ \delta m_{A_0\theta}^2 & \partial_{(x)}^\mu \partial_{(x)}^\mu + m_\theta^2 \end{pmatrix} \begin{pmatrix} \Delta_{A_0 A_0}^{++}(x-y) & \Delta_{A_0\theta}^{++}(x-y) \\ \Delta_{\theta A_0}^{++}(x-y) & \Delta_{\theta\theta}^{++}(x-y) \end{pmatrix} = -i\delta^{(4)}(x-y) \begin{pmatrix} 1 & 0 \\ 0 & 1 \end{pmatrix}. \quad (3.47)$$

(The kinetic operator at the left hand side is just the same as the one in (3.45).) In appendix B.1 we show that this equation is solved by

$$\begin{aligned} \Delta_{kn}^{++}(x-y) &= \theta(x^0 - y^0) \int \frac{d^3k}{(2\pi)^3} \left[ -\frac{1}{2\bar{E}_{A_0}} U_k^1(x^0) U_n^{1*}(y^0) + \frac{1}{2\bar{E}_\theta} U_k^2(x^0) U_n^{2*}(y^0) \right] e^{i\vec{k}\cdot(\vec{x}-\vec{y})} \\ &+ \theta(y^0 - x^0) \int \frac{d^3k}{(2\pi)^3} \left[ -\frac{1}{2\bar{E}_{A_0}} U_k^{1*}(x^0) U_n^1(y^0) + \frac{1}{2\bar{E}_\theta} U_k^{2*}(x^0) U_n^2(y^0) \right] e^{-i\vec{k}\cdot(\vec{x}-\vec{y})}. \end{aligned} \quad (3.48)$$

Therefore we get

$$\begin{aligned} \mathcal{A}_{\{A_0, \theta\}}^{\text{(corr)}} &= i \frac{1}{2} [\lambda_{hA_0 A_0}^+ \Delta_{A_0 A_0}^{++}(0) + \lambda_{h\theta\theta}^+ \Delta_{\theta\theta}^{++}(0) + 2\lambda_{hA_0\theta}^+ \Delta_{A_0\theta}^{++}(0)] \\ &= \frac{1}{2} \int \frac{d^3k}{(2\pi)^3} \left[ \partial_{\phi_{\text{cl}}} m_A^2 \left( \frac{1}{2\bar{E}_{A_0}} |U_{A_0}^1|^2 - \frac{1}{2\bar{E}_\theta} |U_{A_0}^2|^2 \right) \right. \\ &\quad \left. + \partial_{\phi_{\text{cl}}} m_\theta^2 \left( -\frac{1}{2\bar{E}_{A_0}} |U_\theta^1|^2 + \frac{1}{2\bar{E}_\theta} |U_\theta^2|^2 \right) \right. \\ &\quad \left. - (4g\partial_t) \left( -\frac{1}{2\bar{E}_{A_0}} (U_{A_0}^1 U_\theta^{1*} + U_{A_0}^{1*} U_\theta^1) + \frac{1}{2\bar{E}_\theta} (U_{A_0}^2 U_\theta^{2*} + U_{A_0}^{2*} U_\theta^2) \right) \right]. \end{aligned} \quad (3.50)$$

To solve for the mode functions we make the Ansatz which is consistent with the boundary conditions if we again choose  $f(0) = \dot{f}(0) = 0$ :

$$\begin{aligned} U_{A_0}^1 &= e^{-i\bar{E}_{A_0}t} (1 + f_{A_0}^1), & U_\theta^1 &= e^{-i\bar{E}_\theta t} f_\theta^1, \\ U_{A_0}^2 &= e^{-i\bar{E}_{A_0}t} (1 + f_{A_0}^2), & U_\theta^2 &= e^{-i\bar{E}_{A_0}t} f_{A_0}^2. \end{aligned} \quad (3.51)$$

We can again solve iteratively, and define an expansion in terms of mass term insertions  $f_m^\alpha = f_m^{\alpha(1)} + f_m^{\alpha(2)} \dots$ . To isolate the divergent part of the one-loop potential we again only need the first order result.

Plugging the Ansatz (3.51) in the mode equations (3.45) gives

$$\begin{aligned}
\ddot{f}_{A_0}^1 - 2i\bar{E}_{A_0}\dot{f}_{A_0}^1 &= -\delta m_A^2 (1 + f_{A_0}^1) + \delta m_{A_0\theta}^2 e^{i(\bar{E}_{A_0} - \bar{E}_\theta)t} f_\theta^1 \\
\ddot{f}_{A_0}^2 - 2i\bar{E}_{A_0}\dot{f}_{A_0}^2 &= -\delta m_A^2 f_{A_0}^2 + \delta m_{A_0\theta}^2 e^{i(\bar{E}_{A_0} - \bar{E}_\theta)t} (1 + f_\theta^2) \\
\ddot{f}_\theta^1 - 2i\bar{E}_\theta\dot{f}_\theta^1 &= -\delta m_\theta^2 f_\theta^1 - \delta m_{A_0\theta}^2 e^{-i(\bar{E}_{A_0} - \bar{E}_\theta)t} (1 + f_{A_0}^1) \\
\ddot{f}_\theta^2 - 2i\bar{E}_\theta\dot{f}_\theta^2 &= -\delta m_\theta^2 (1 + f_\theta^2) - \delta m_{A_0\theta}^2 e^{-i(\bar{E}_{A_0} - \bar{E}_\theta)t} f_{A_0}^2.
\end{aligned} \tag{3.52}$$

Appendix (B.2) shows that solving these equations gives (upon setting  $\delta m_A^2(0) = \delta m_\theta^2(0) = \delta m_{A_0\theta}^2(0) = 0$ )

$$\begin{aligned}
|U_{A_0}^1|^2 &= 1 - \frac{\delta m_A^2(t)}{2\bar{E}_{A_0}^2} + \mathcal{O}(\bar{E}_{A_0}^{-3}) \\
|U_{A_0}^2|^2 &= \mathcal{O}(\bar{E}_{A_0}^{-4}) \\
|U_\theta^1|^2 &= \mathcal{O}(\bar{E}_\theta^{-4}) \\
|U_\theta^2|^2 &= 1 - \frac{\delta m_\theta^2(t)}{2\bar{E}_\theta^2} + \mathcal{O}(\bar{E}_\theta^{-3}) \\
U_{A_0}^1 U_\theta^{1*} &= U_{A_0}^{1*} U_\theta^1 = \delta m_{A_0\theta}^2 \left( \frac{1}{2\bar{E}_\theta (\bar{E}_{A_0} - \bar{E}_\theta)} - \frac{1}{4\bar{E}_\theta^2} \right) + \mathcal{O}(\bar{E}^{-3}) \\
U_{A_0}^2 U_\theta^{2*} &= U_{A_0}^{2*} U_\theta^2 = \delta m_{A_0\theta}^2 \left( \frac{1}{2\bar{E}_{A_0} (\bar{E}_{A_0} - \bar{E}_\theta)} + \frac{1}{4\bar{E}_{A_0}^2} \right) + \mathcal{O}(\bar{E}^{-3}).
\end{aligned} \tag{3.53}$$

Now we can insert everything in (3.50). The first line gives, just like the scalar field computation in (2.70)

$$\mathcal{A}_{A_0}^{(\text{corr})} = \frac{1}{2} \partial_{\phi_{\text{cl}}} m_A^2 \int \frac{d^3 k}{(2\pi)^3} \frac{1}{2\bar{E}_{A_0}} |U_{A_0}^1|^2 = \frac{\partial_{\phi_{\text{cl}}} m_A^2(x^0)}{16\pi^2} \left[ \Lambda^2 - m_A^2(x^0) \ln \left( \frac{\Lambda}{\bar{m}} \right) \right]. \tag{3.54}$$

The second line gives

$$\mathcal{A}_\theta^{(\text{corr})} = \frac{1}{2} \partial_\phi m_\theta^2 \int \frac{d^3 k}{(2\pi)^3} \frac{1}{2\bar{E}_\theta} |U_\theta^2|^2 = \frac{\partial_{\phi_{\text{cl}}} m_\theta^2(x^0)}{16\pi^2} \left[ \Lambda^2 - m_\theta^2(x^0) \ln \left( \frac{\Lambda}{\bar{m}} \right) \right]. \tag{3.55}$$

The third line gives

$$\begin{aligned}
\mathcal{A}_{A_0\theta}^{(\text{corr})} &= -2g\partial_t \int \frac{d^3 k}{(2\pi)^3} \left[ -\frac{1}{4\bar{E}_{A_0}} \delta m_{A_0\theta}^2 \left( \frac{1}{\bar{E}_\theta (\bar{E}_{A_0} - \bar{E}_\theta)} - \frac{1}{2\bar{E}_\theta^2} \right) \right. \\
&\quad \left. + \frac{1}{4\bar{E}_\theta} \delta m_{A_0\theta}^2 \left( \frac{1}{\bar{E}_{A_0} (\bar{E}_{A_0} - \bar{E}_\theta)} + \frac{1}{2\bar{E}_{A_0}^2} \right) \right] \\
&= -\frac{g\partial_t \delta m_{A_0\theta}^2}{4} \int \frac{d^3 k}{(2\pi)^3} \frac{1}{\bar{E}_{A_0} \bar{E}_\theta} \left( \frac{1}{\bar{E}_{A_0}} + \frac{1}{\bar{E}_\theta} \right) \\
&= -\frac{g^2 \ddot{\phi}}{2\pi^2} \ln \left( \frac{\Lambda}{\bar{m}} \right).
\end{aligned} \tag{3.56}$$

Adding it all up, the one-loop equation of motion  $\mathcal{A} = 0$  becomes

$$0 = \partial_\mu \partial^\mu \phi_{\text{cl}} + V_{\phi_{\text{cl}}} + \sum_{\{h,\eta,A_i,A_0,\theta\}} \frac{S_i}{16\pi^2} \partial_{\phi_{\text{cl}}} m_i^2 \left( \Lambda^2 - m_i^2 \ln \left( \frac{\Lambda}{\bar{m}} \right) \right) - \frac{g^2 \ddot{\phi}}{2\pi^2} \ln \left( \frac{\Lambda}{\bar{m}} \right) \tag{3.57}$$

with  $S_i = \{1, -2, 3, 1, 1\}$  for  $i = \{\phi, \eta, A_i, \theta, A_0\}$  counting the degrees of freedom. It is equal to the perturbative result (3.34) (in the gauge  $\xi = 1$ ).

### 3.5 Discussion: on-shell gauge invariance and the trouble of unitary gauge

We have reached our final expression (3.39) for the divergent contributions to the unrenormalized effective action for the  $U(1)$  Abelian Higgs model in two different ways. Let us now try to interpret this result.

First of all, we clearly see that the contributions to the effective potential induced by the Goldstone field  $\theta$  are real and can not be discarded. This result ensures that the effective potential is continuous when moving from the symmetric to the broken phase, and that supersymmetric Higgs inflation is free of quadratic divergences.

At first glance, it may seem counterintuitive that the field  $\theta$  apparently does carry a physical degree of freedom. After all, when working in unitary gauge, all reference to this field can be discarded, even in the time dependent setting that we have considered in this chapter.

The resolution to this paradox is twofold. First, we have seen from the Lagrangian (3.15) that when  $\phi_{\text{cl}} \neq 0$ , the field  $\theta$  couples to the temporal component of the gauge field,  $A_0$ . Moreover, in all gauges with  $\xi \neq 1$ , there are additional kinetic couplings between the components of the gauge field. Therefore,  $V_{\theta\theta}$  cannot be identified with the mass squared of the Goldstone field. To find the true masses of the fields  $\{A_\mu, \theta\}$ , one should transform to a new set of fields that have canonical kinetic terms and diagonal mass terms. Given the implicit gauge and time dependence, this seems a very nontrivial thing to do. We had better stick to the approach followed here, in which we can compute propagators and vertices, rendering a physical, gauge invariant expression even if we do not know what combination of fields represents the true Goldstone boson.

Second, we should acknowledge that in this time dependent setting, the unitary gauge is simply not suitable to work in. The reason is that unitary gauge is a singular limit. It corresponds to taking the limit  $\xi \rightarrow \infty$  such that the  $\theta$  propagator vanishes. This procedure, however, does not commute with the  $k \rightarrow \infty$  limit taken in the momentum integrals to isolate the divergent terms. That unitary gauge gives an incorrect result has been noted before [58, 59, 60, 61]. In this gauge higher order loop corrections affect the leading term and must be taken into account [62].

At this point, it might seem much more straightforward to solve our problem with a  $U(1)$  symmetry using polar coordinates respecting that symmetry, rather than the Cartesian coordinates that we have employed. This point of view was for example advocated in [63]. Rather than using our decomposition (3.6) we should write

$$H = (\phi_{\text{cl}}(t) + \rho(x, t)) e^{i\psi(x, t)}. \quad (3.58)$$

However, this leads to a non-canonical term for the Goldstone field  $\psi$ : the kinetic part of the Lagrangian will contain a term  $\phi_{\text{cl}}^2 \psi^2$ . Therefore the kinetic terms contain time dependent interactions. Again, performing a one loop analysis will miss terms that are of the same order as the ones that we do find. Therefore, it might indeed seem more natural to work with polar coordinates, but the road to the final answer (3.39) will be a lot more complicated.

Furthermore we have seen that the final, gauge invariant result could only be achieved after using the equations of motion. We had to go on-shell to get rid of the gauge parameter  $\xi$  in the final answer. This is in line with the so-called Nielsen identity [64, 65, 66], which states that in a time independent background

### 3.5. DISCUSSION: ON-SHELL GAUGE INVARIANCE AND THE TROUBLE OF UNITARY GAUGE 67

we have

$$\frac{\partial V_{\text{eff}}}{\partial \xi} + \frac{\partial \phi_{\text{cl}}}{\partial \xi} \frac{\partial V_{\text{eff}}}{\partial \phi_{\text{cl}}} = 0. \quad (3.59)$$

In other words: the effective potential is physical ( $\xi$  independent) only at its extrema. Indeed, computing the Coleman-Weinberg effective action for the Abelian Higgs model with a time independent background initially yields the unphysical (gauge dependent) answer

$$V_{CW} = \frac{\Lambda}{16\pi^2} (V_{hh} + V_{\theta\theta} + 3g^2\phi_{\text{cl}}^2) - \frac{\ln(\Lambda/m)}{32\pi^2} (V_{hh}^2 + V_{\theta\theta}^2 + 3g^4\phi_{\text{cl}}^4 + 2V_{\theta\theta}^2\xi g^2\phi_{\text{cl}}^2). \quad (3.60)$$

To get a physical answer one needs to exploit the  $U(1)$  invariance in the problem via (3.3) and its classical equation of motion to find

$$V_{\theta\theta} = \frac{1}{\phi_{\text{cl}}} \frac{\partial V}{\partial \phi_{\text{cl}}} = 0. \quad (3.61)$$

(Of course one could also get rid of the  $V_{\theta\theta}$  term by going to unitary gauge, which is fine in this time independent case, but the aim here is to find a physical, gauge independent answer.)

Now, in the model we have studied in this chapter we have in fact found a time dependent generalization of the Nielsen identity. We have shown that once we go on-shell, so once the equation of motion of the system is satisfied (once we extremize the action) we find a physical, gauge independent answer. We could rewrite (3.59) as

$$\frac{\partial V_{\text{eff}}}{\partial \xi} + \frac{\partial \phi_{\text{cl}}}{\partial \xi} \left[ \frac{\partial V_{\text{eff}}}{\partial \phi_{\text{cl}}} + \ddot{\phi}_{\text{cl}} \right] = 0. \quad (3.62)$$

Let us also comment on what we have won by allowing the Higgs background field to be time dependent. In the case of a real scalar field, the time dependent effective action (2.71) is a straightforward generalization of the time independent result (2.28). In the time dependent effective action of the Abelian Higgs model, however, there is a new term (compared to the time independent result). It follows from the coupling between  $\theta$  and  $A_0$  that is induced by the time dependence of the background field.



# Chapter 4

## Extension to FLRW

All results obtained in the previous chapter assumed a Minkowski flat spacetime. As cosmologists, we should consider an expanding Friedmann-Lemaître-Robertson-Walker universe, and see how the expansion of the universe affects the effective action just obtained. That will be the purpose of this chapter, which is based on our work [4].

We now work in a FLRW background:

$$g_{\mu\nu} = a^2(\tau)\text{Diag}(1, -1, -1, -1) = a^2(\tau)\eta_{\mu\nu}. \quad (4.1)$$

We work with conformal time  $\tau$ , which is related to cosmic time  $t$  via  $d\tau \equiv \frac{dt}{a}$ , as was already discussed in the introduction.

### 4.1 Real scalar field

Let us, again, consider the case of a real scalar field first, to warm up for the  $U(1)$  Abelian Higgs model. The action for a scalar field in a potential  $V = \frac{1}{2}m^2\phi^2$  in arbitrary metric  $g_{\mu\nu}$  is

$$S = \int d^4x \sqrt{-g} \left[ \frac{1}{2} \partial_\mu \phi g^{\mu\nu} \partial_\nu \phi - \frac{1}{2} m^2 \phi^2 \right]. \quad (4.2)$$

In conformal FLRW this becomes

$$S = \int d^4x (-a^2) \cdot \frac{1}{2} \phi \left[ \eta^{\mu\nu} \partial_\mu \partial_\nu + 2\mathcal{H} \partial_\eta + m^2 a^2 \right] \phi. \quad (4.3)$$

Here we have done a partial integration and dropped the surface term:

$$\int d^4x \sqrt{-g} (\partial_\mu \phi) g^{\mu\nu} \partial_\nu \phi = - \int d^4x \phi \partial_\mu (\sqrt{-g} g^{\mu\nu} \partial_\nu \phi). \quad (4.4)$$

In cosmic FLRW,  $g_{\mu\nu} = \text{Diag}(1, -a^2(t), -a^2(t), -a^2(t))$ , we would have found

$$S = \int d^4x (-a^3) \cdot \frac{1}{2} \phi \left[ \partial_t^2 - \frac{\nabla^2}{a^2} + 3H \partial_t + m^2 \right] \phi. \quad (4.5)$$

The equation of motion for the scalar field in conformal or cosmic FLRW follows directly from the two equations above.

We stick to the conformal FLRW metric and define  $\tilde{\phi} \equiv a\phi$ .

$$\mathcal{L} = -\frac{1}{2}\tilde{\phi}\left[\eta^{\mu\nu}\partial_\mu\partial_\nu + m^2a^2 - \frac{a''}{a}\right]\tilde{\phi}, \quad (4.6)$$

with  $a' \equiv \partial_\tau a$ .

In this ‘‘conformal frame’’ the Lagrangian looks very familiar, it is a scalar field with a time dependent shift in its mass. Therefore its effective action  $\Gamma$  follows straight from, for example, (2.71):

$$\Gamma = \int d^4x \left[ -\frac{1}{2}\tilde{\phi}\left[\eta^{\mu\nu}\partial_\mu\partial_\nu + m^2a^2 - \frac{a''}{a}\right]\tilde{\phi} - \frac{m^2a^2 - \frac{a''}{a}}{16\pi^2}\tilde{\Lambda}^2 + \frac{(m^2a^2 - \frac{a''}{a})^2}{32\pi^2} \ln\left(\frac{\tilde{\Lambda}}{\bar{m}}\right) \right]. \quad (4.7)$$

In this expression the cut-off  $\tilde{\Lambda}$  has been taken on the magnitude of the spatial three-momentum  $\vec{k}$ , for which we have

$$\omega_{\vec{k}}^2 - \vec{k} \cdot \vec{k} = m^2a^2 - \frac{a''}{a}. \quad (4.8)$$

However: what are these  $\vec{k}$ ? They are comoving momenta, just because they have been defined as conjugated to the conformal  $\vec{x}$ . To see this in a better way, we divide the previous equation by  $a^2$ :

$$\left(\frac{\omega_{\vec{k}}}{a}\right)^2 - \frac{\vec{k}}{a} \cdot \frac{\vec{k}}{a} = m^2 - \frac{a''}{a^3}. \quad (4.9)$$

On the left hand side are now physical quantities, that have the usual norm  $m^2$  plus a correction term. In short, we want to set the cut off at

$$\Lambda = \frac{|\vec{k}|}{a} \quad (4.10)$$

which means that (as  $\tilde{\Lambda}$  was a cut-off on  $|\vec{k}|$ ) we have to set  $\tilde{\Lambda} = a\Lambda$ . (Or in other words: the physical quantity is  $k/a$ , so we integrate  $k$  up to  $a\Lambda$ .) Going back to the physical frame by reinserting  $\phi$  we get

$$\begin{aligned} \Gamma &= \int d\tau d^3x \left[ -a^2\frac{1}{2}\phi\left[\eta^{\mu\nu}\partial_\mu\partial_\nu + 2\mathcal{H}\partial_\eta + m^2a^2\right]\phi - a^4\left[\frac{m^2 - \frac{a''}{a^3}}{16\pi^2}\Lambda^2 - \frac{(m^2 - \frac{a''}{a^3})^2}{16\pi^2} \ln\left(\frac{a\Lambda}{\bar{m}}\right)\right] \right] \\ &= \int dt d^3x \sqrt{-g} \left[ \frac{1}{2}\partial_\mu\phi g^{\mu\nu}\partial_\nu\phi - \frac{1}{2}m^2\phi^2 - \frac{m^2 - \frac{a''}{a^3}}{16\pi^2}\Lambda^2 + \frac{(m^2 - \frac{a''}{a^3})^2}{16\pi^2} \ln\left(\frac{a\Lambda}{\bar{m}}\right) \right]. \end{aligned} \quad (4.11)$$

This result has been known for a long time [67, 68, 69, 70]. If the scalar is coupled to other scalars or to fermions via e.g. a Yukawa interaction, additional scalar and fermion loops contribute [68, 71, 72]. In this chapter we extend these results by including a coupling to a gauge field.

N.B. Working in cosmic time, one can rewrite the action (4.5) in terms of  $\tilde{\phi} \equiv a^{3/2}\phi$ , which yields

$$\mathcal{L} = -\frac{1}{2}\tilde{\phi}\left[\partial_t^2 - \frac{\nabla^2}{a^2} + m^2 - \frac{3}{2}\frac{a''}{a} - \frac{3}{4}\left(\frac{\dot{a}}{a}\right)^2\right]\tilde{\phi}. \quad (4.12)$$

Now the shift in the mass is different. However, this field  $\tilde{\phi}$  does not have canonically normalized kinetic terms. It is only in conformal FLRW where the action resembles the Minkowski action, and where the results of the previous chapter can be applied directly, as we did in (4.7).

## 4.2 Action

In section 3.2 we have computed the Lagrangian of the  $U(1)$  Abelian Higgs model in a Minkowski background. In this section we generalize the result (3.15) to FLRW. Following the previous section, we will work in conformal coordinates.

Using the conformal FLRW metric (4.1), we get for the nonzero connections

$$\Gamma_{i0}^i = \Gamma_{0i}^i = \Gamma_{00}^0 = \Gamma_{ii}^0 = \mathcal{H}. \quad (4.13)$$

Here we defined  $\mathcal{H} = a'/a$ , analogous to the usual definition in coordinate time  $H = \dot{a}/a$ . We can again decompose the charged scalar field into a real and imaginary part,

$$\Phi(x^\mu) = \frac{1}{\sqrt{2}}(\phi_{\text{cl}}(\tau) + h(\tau, \vec{x}) + i\theta(\tau, \vec{x})), \quad (4.14)$$

with  $\phi_{\text{cl}}(\tau)$  the time dependent classical background field.

For the action we can directly generalize (3.5):

$$\begin{aligned} S &= \int d^4x \mathcal{L} \\ \mathcal{L} &= \mathcal{L}_{\text{gauge-kin}} + \mathcal{L}_{\text{higgs-kin}} + \mathcal{L}_{\text{pot}} + \mathcal{L}_{\text{gaugefixing}} + \mathcal{L}_{\text{ghost}} \\ &= -\frac{1}{4}g^{\mu\alpha}g^{\nu\beta}F_{\mu\nu}F_{\alpha\beta} + g^{\mu\nu}D_\mu\Phi(D_\nu\Phi)^\dagger - V(\Phi\Phi^\dagger) - \frac{1}{2\xi}G^2 + \eta\bar{g}\frac{\delta G}{\delta\alpha}\eta. \end{aligned} \quad (4.15)$$

The gauge-fixing function  $G$  is now given by  $G = G = g^{\mu\nu}\nabla_\mu A_\nu - \xi g(\phi_{\text{cl}} + h)\theta$ . Note that  $\nabla_\mu g^{\mu\nu} = 0$  (because of metric compatibility), and thus  $g^{\mu\nu}\nabla_\mu A_\nu = \nabla_\mu g^{\mu\nu}A_\nu$  and there is no ambiguity.

To make explicit all factors of the scale factor we now write  $g^{\mu\nu} = a^{-2}\eta^{\mu\nu}$  with  $\eta^{\mu\nu}$  the Minkowski metric. If we again rescale fields as we did in the previous section, we get to the conformal frame, in which the metric is Minkowski. Before we needed  $\tilde{\phi} \equiv a\phi$ , now we define

$$\hat{\phi}_\alpha = a\phi_\alpha, \quad \hat{V} = a^4V(\hat{\phi}), \quad (4.16)$$

with  $\phi_\alpha = \{\phi_{\text{cl}}, h, \theta, \eta\}$  the scalars in the theory. We denote all mass scales in these comoving coordinates with a hat.

The hatted fields are canonically normalized in the comoving frame, just as the field  $\tilde{\phi}$  in the previous section. Since the gauge field kinetic terms are conformally invariant, there is no rescaling of the gauge field. The comoving fields feel a potential  $\hat{V}$ . All the comoving quantities map directly to the equivalent set-up in Minkowski, and we can use the usual Minkowski machinery to calculate Feynman diagrams, as we showed in the previous section for the case of a real scalar field. In the expressions below, all indices are raised and lowered using the Minkowski metric.

The action (4.15) is expanded in quantum fluctuations around the background. Here we state the results at each order; for details see appendix D. The classical action that contains no quantum fields reads now (D.11)

$$S^{(0)} = \int d^4x \left\{ \frac{1}{2}(\hat{\phi}'_{\text{cl}})^2 - \frac{1}{2}(\partial_i \hat{\phi}_{\text{cl}})^2 + \frac{1}{2} \frac{a''}{a} \hat{\phi}_{\text{cl}}^2 - a^4 V \right\}. \quad (4.17)$$

At first order in the quantum field we get (D.12)

$$S^{(1)} = \int d^4x \left\{ -\hat{h} \left( (\partial^2 - \frac{a''}{a}) \hat{\phi}_{\text{cl}} + a^3 V_{\phi_{\text{cl}}} \right) \right\}. \quad (4.18)$$

The second order action, from which we will derive the propagators (plus some explicit two point interactions), is given by (D.13)

$$\begin{aligned}
S^{(2)} = & \frac{1}{2} \int d^4x \left\{ A_\mu \left[ (\partial_\rho \partial^\rho + g^2 \hat{\phi}_{\text{cl}}^2) \eta^{\mu\nu} - \left(1 - \frac{1}{\xi}\right) \partial^\mu \partial^\nu \right] A_\nu \right. \\
& + \frac{2}{\xi} [A_0 (\mathcal{H}' - 2\mathcal{H}^2) A_0 - A_0 2\mathcal{H} \partial^i A_i] \\
& - \hat{\theta} \left( \partial^2 - \frac{a''}{a} + a^2 V_{\theta\theta} + \xi g^2 \hat{\phi}_{\text{cl}}^2 \right) \hat{\theta} - 4g A_0 \hat{\theta} \left( \partial_\tau - \frac{a'}{a} \right) \hat{\phi}_{\text{cl}} \\
& \left. - \hat{h} \left( \partial^2 - \frac{a''}{a} + a^2 V_{hh} \right) \hat{h} - 2\hat{\eta} \left[ \partial^2 - \frac{a''}{a} + \xi g^2 \hat{\phi}_{\text{cl}}^2 \right] \hat{\eta} \right\}. \quad (4.19)
\end{aligned}$$

Here we see that the expansion of the universe does not only shift all masses. It also creates a degeneracy between the masses of  $A_0$  and  $A_i$ , and moreover it introduces a new interaction between  $A_0$  and  $A_i$ .

For the third order action we get (D.14)

$$S^{(3)} = \int d^4x \left\{ -S_{\alpha\beta\gamma} a V_{\alpha\beta\gamma} \hat{\varphi}_\alpha \hat{\varphi}_\beta \hat{\varphi}_\gamma - 2g A^\mu \hat{\theta} \left( \partial_\mu - \frac{a'}{a} \delta_\mu^0 \right) \hat{h} + g^2 (A^2 - \xi \hat{\theta}^2 - 2\xi \hat{\eta} \hat{\eta}) \hat{\phi}_{\text{cl}} \hat{h} \right\}, \quad (4.20)$$

with  $\varphi_\alpha = \{h, \theta\}$ , and  $S_{\alpha\beta\gamma(\delta)}$  symmetry factors following from a Taylor expansion of  $V(\Phi^\dagger \Phi)$  around  $\Phi = \phi_{\text{cl}}$ .

Note that in the Minkowski limit (where the conformal frame reduces to Minkowski spacetime) the results (4.17), (4.18), (4.19) and (4.20) reduce to what we found in (3.15).

The Feynman rules that follow from this action are in figure 4.1.

The one point vertex  $\hat{\lambda}_h^+$  in figure 4.1 follows directly from (4.18):

$$\hat{\lambda}_h^+ = -i \left[ \left( \partial_\tau^2 - \nabla^2 - (\mathcal{H}' + \mathcal{H}^2) \right) \hat{\phi}_{\text{cl}} + \hat{V}_{\hat{\phi}_{\text{cl}}} \right] = -i \left[ a^3 \left( \ddot{\phi}_{\text{cl}} - \frac{\nabla^2}{a^2} + 3H \dot{\phi}_{\text{cl}} + V_{\phi_{\text{cl}}} \right) \right]. \quad (4.21)$$

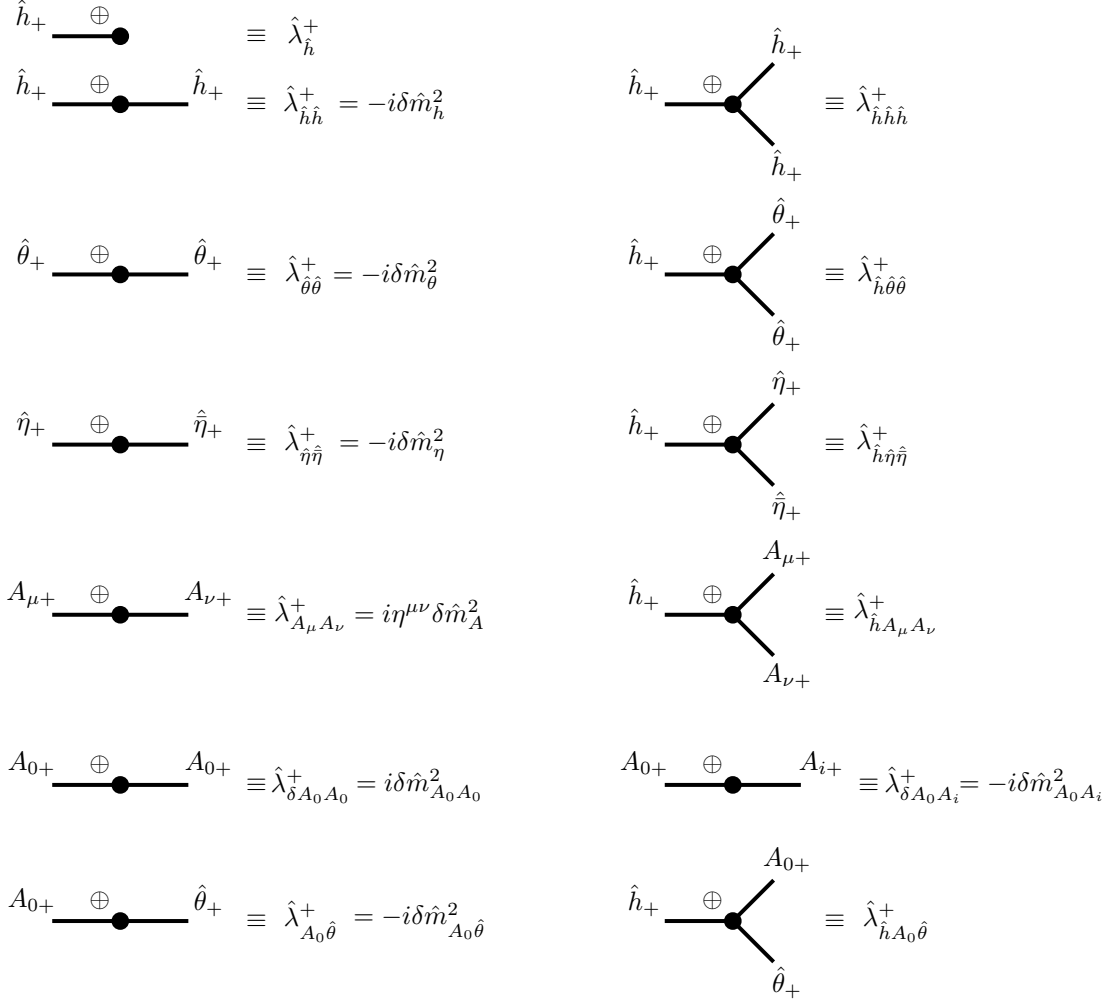
(Note that  $\mathcal{H}' + \mathcal{H}^2 = \frac{a''}{a}$ .)

To write the next four two point vertices in figure 4.1 we first read off the time dependent masses from (4.19)

$$\begin{aligned}
\hat{m}_h^2 &= \hat{V}_{\hat{h}\hat{h}} - (\mathcal{H}' + \mathcal{H}^2) = a^2 \left[ V_{hh} - (\dot{H} + 2H^2) \right], \\
\hat{m}_\theta^2 &= \hat{V}_{\hat{\theta}\hat{\theta}} + \xi g^2 \hat{\phi}_{\text{cl}}^2 - (\mathcal{H}' + \mathcal{H}^2) = a^2 \left[ V_{\theta\theta} + \xi g^2 \hat{\phi}_{\text{cl}}^2 - (\dot{H} + 2H^2) \right], \\
\hat{m}_\eta^2 &= \xi g^2 \hat{\phi}_{\text{cl}}^2 - (\mathcal{H}' + \mathcal{H}^2) = a^2 \left[ \xi g^2 \hat{\phi}_{\text{cl}}^2 - (\dot{H} + 2H^2) \right], \\
\hat{m}_{A_\mu A_\nu}^2 &= -\eta^{\mu\nu} g^2 \hat{\phi}_{\text{cl}}^2 \equiv -\eta^{\mu\nu} \hat{m}_A^2 = -\eta^{\mu\nu} a^2 \left[ g^2 \hat{\phi}_{\text{cl}}^2 \right] \equiv -\eta^{\mu\nu} a^2 m_A^2, \quad (4.22)
\end{aligned}$$

where we used  $\mathcal{H}^2 = a^2 H^2$  and  $\mathcal{H}' = a^2 (\dot{H} + H^2)$ . These masses we will again split up in a time independent background part, which is used to construct the propagators, and a time dependent part that shows up in the interactions in figure 4.1:

$$\hat{m}^2(\tau) = \hat{m}^2 + \delta \hat{m}^2(\tau). \quad (4.23)$$

Figure 4.1: *Feynman rules for the Abelian Higgs model in FLRW (in the conformal frame).*

The split is again defined by requiring the interaction to vanish at the initial time, which we choose without loss of generality to be at  $t_0 = 0$ :

$$\delta m^2(0) = 0. \quad (4.24)$$

We will comment further on this split, and the resulting initial conditions, in subsection 4.4.2.

The corresponding three point vertices follow directly from (4.20) and read

$$\begin{aligned}
\hat{\lambda}_{\hat{h}\hat{h}\hat{h}}^+ &= -i\hat{V}_{\hat{\phi}_{\text{cl}}\hat{h}\hat{h}} = -i\partial_{\hat{\phi}_{\text{cl}}}\hat{m}_{\hat{h}}^2, \\
\hat{\lambda}_{\hat{h}\hat{\theta}\hat{\theta}}^+ &= -i\left(\hat{V}_{\hat{\phi}_{\text{cl}}\hat{\theta}\hat{\theta}} + 2\xi g^2\hat{\phi}_{\text{cl}}\right) = -i\partial_{\hat{\phi}_{\text{cl}}}\hat{m}_{\hat{\theta}}^2, \\
\hat{\lambda}_{\hat{h}\hat{\eta}\hat{\eta}}^+ &= -2i\xi g^2\hat{\phi}_{\text{cl}} = -i\partial_{\hat{\phi}_{\text{cl}}}\hat{m}_{\hat{\eta}}^2, \\
\hat{\lambda}_{\hat{h}A_{\mu}A_{\nu}}^+ &= 2i\eta^{\mu\nu}g^2\hat{\phi}_{\text{cl}} = i\eta^{\mu\nu}\partial_{\hat{\phi}_{\text{cl}}}\hat{m}_A^2.
\end{aligned} \quad (4.25)$$

Next are the extra interactions between the gauge fields, that we call  $\hat{\lambda}_{\delta A_0 A_0}^+$  and  $\hat{\lambda}_{\delta A_0 A_i}^+$ , that are absent in Minkowski. From (D.13) we get

$$\delta \hat{m}_{A_0 A_0}^2 = \frac{2}{\xi} (\mathcal{H}' - 2\mathcal{H}^2) \quad (4.26)$$

$$\delta \hat{m}_{A_0 A_i}^2 = \frac{2}{\xi} \mathcal{H} \partial^i. \quad (4.27)$$

Finally we have the interactions between  $A_0$  and  $\theta$ , caused by the rolling of the background field and therefore also present in Minkowski. From (4.19) and (4.20) we get

$$\begin{aligned} \delta \hat{m}_{A_0 \hat{\theta}}^2 &= 2g(\partial_\tau - \mathcal{H}) \hat{\phi}_{\text{cl}} = a^2 [2g \dot{\phi}_{\text{cl}}], \\ \hat{\lambda}_{\hat{h} A_0 \hat{\theta}}^+ &= 2ig(\partial_\tau + \mathcal{H}), \end{aligned} \quad (4.28)$$

where we did the same partial integration as described at the very end of section 3.2.

Equation (4.20) also contains a term  $-2gA^i \hat{\theta} \partial_i \hat{h}$ . Since the final expression of each tadpole graph is independent of the spatial coordinates, this three point interaction does not contribute to the overall result. We have checked this by explicit computation.

### 4.3 Effective equation of motion

We again choose to perform the computation on the level of the effective equation of motion  $\mathcal{A}$ , so we will be computing corrections to the classical equation of motion (Weinberg's tadpole method, we now compute  $\langle h^+ \rangle$ ). We want to organize the computation in the ‘‘perturbative’’ way that we also employed in sections 2.7.1 and 3.3: time independent part of the masses in the propagators, time dependent part in the interactions. In the next section we will integrate the result to get to the effective action, just like we did at the end of section 3.3. This action is then transformed from the comoving to the physical frame, thereby obtaining the effective action.

The calculation is done in the conformal frame, in terms of hatted fields and mass scales, conformal time and momenta. For notational convenience, in this section we drop the hat on all quantities; it shall be reinstated at the end when we give the results.

The calculation is analogous to the one for a Minkowski background done in the previous chapter, but with two-point interactions (4.22) that now depend on the FLRW scale factor. This is straightforward to incorporate for the diagrams with a scalar running in the loop. There are however some new technical difficulties that come in with the gauge boson loops:

1. The mass of the temporal gauge boson gets FLRW corrections (described by the vertex  $\lambda_{\delta A_0 A_0}$ ) but the mass of the spatial components does not. This is possible because Lorentz symmetry is broken by the time dependent background. Consequently the diagrams with  $A_0$  and  $A_i$  contribute differently.
2. The off-diagonal gauge boson two point interaction is non-zero, which results in the vertex  $\lambda_{\delta A_0 A_i}$ . Moreover, it contains an extra spatial derivative. This leads to new diagrams with both two and three two point insertions.

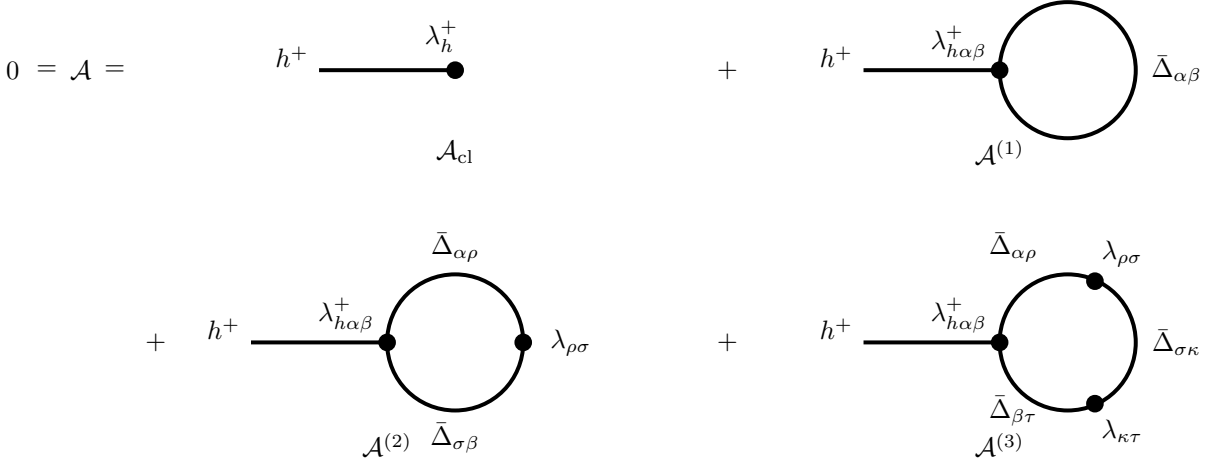


Figure 4.2: Tree level tadpole giving the classical equation of motion and the first, second and third order diagrams respectively. The summation is over all fields, for the gauge bosons also over Lorentz indices, and over  $\pm$  at the two point vertices.

3. The formalism is set up in such a way that the two point interactions vanish at the initial time (4.24). This avoids divergences that depend on the initial conditions. We will argue in subsection 4.4.2 that this is always an allowed choice, for arbitrary initial conditions, provided the initial vacuum is chosen accordingly.

We will again extract the one-loop equation of motion from the series of tadpole diagrams with one external  $h^+$  leg depicted in figure 4.2. So we have

$$0 = \mathcal{A} = \mathcal{A}_{\text{cl}} + \mathcal{A}^{(1)} + \mathcal{A}^{(2)} + \mathcal{A}^{(3)} + \text{finite} \quad (4.29)$$

where  $\mathcal{A}_{\text{cl}}$  denotes the first tadpole diagram, without a quantum loop, that gives the classical equation of motion, and  $\mathcal{A}^{(i)}$  stands for the tadpole diagram with  $i$  vertices.

So let us begin at the classical level. From (4.21) we find directly (remember we dropped the hat for conformal coordinates and scales):

$$\mathcal{A}_{\text{cl}} = i\lambda_h^+ = \partial_\mu \partial^\mu \phi_{\text{cl}} - (\mathcal{H}' + \mathcal{H}^2)\phi_{\text{cl}} + V_{\phi_{\text{cl}}}, \quad (4.30)$$

and setting  $\mathcal{A}_{\text{cl}} = 0$  yields the classical equation of motion. Note that we are still working with the conventions defined above (2.40).

Now for the correction diagrams. We divide the calculation based on the order of the contributing graphs, which is the number of vertices in the loop of the tadpole. As discussed above, we must work to third order. Independent of this, we can distinguish three classes of diagrams depending on how they contribute to the answer. First there is the contribution that is fully analogous to the Minkowski calculation  $\mathcal{A}_{\text{Mink}} = \mathcal{A}_{\text{Mink}}^{(1)} + \mathcal{A}_{\text{Mink}}^{(2)}$ , the only difference is that the mass term of the scalars now depends on the scale factor. Second is  $\mathcal{A}_{\text{mass}} = \mathcal{A}_{\text{mass}}^{(2)}$ , which arises from the extra Feynman diagrams due to the FLRW mass correction of the temporal gauge field  $\delta m_{A_0 A_0}^2$ ; see (4.26). And finally there is  $\mathcal{A}_{\text{mix}} = \mathcal{A}_{\text{mix}}^{(2)} + \mathcal{A}_{\text{mix}}^{(3)}$ , the diagrams with one and two off-diagonal vertices  $\delta m_{A_0 A_i}^2$  connecting the temporal and spatial gauge fields (see (4.27)), also absent in Minkowski.

### 4.3.1 First order contribution $\mathcal{A}^{(1)}$

The calculation of the first order diagrams proceeds analogously to the equivalent calculation in Minkowski, done in the previous section. At first order, four diagrams contribute, with  $\psi_\alpha = \{h, \theta, \eta, A^\mu\}$  running in the loop. The result only depends on the time independent part of the two point interaction, as there is no vertex insertion. For each diagram the result has the same structure, given by (compare to (2.41) and (3.22))

$$(\mathcal{A}_{\text{Mink}}^{(1)})_\alpha = i \frac{1}{2} \lambda_{h\alpha\alpha}^+ \bar{\Delta}_\alpha^{++}(x-x). \quad (4.31)$$

Just as in Minkowski the gauge loop can be expressed in terms of scalar propagators (C.3) via

$$\eta^{\mu\nu} \bar{\Delta}_{A_\mu A_\nu}^{++}(0) = -3\bar{\Delta}_A^{++}(0) - \xi \bar{\Delta}_\xi^{++}(0). \quad (4.32)$$

The sum of all first order diagrams is, just as in the Minkowski case in (3.22) and (3.25)

$$\begin{aligned} \mathcal{A}_{\text{Mink}}^{(1)} &= \frac{1}{2} \sum_\alpha S_\alpha(\partial_{\phi_{\text{cl}}} m_\alpha^2) \frac{1}{4\pi^2} \int_0^\Lambda k^2 dk \left[ \frac{1}{k} - \frac{1}{2} \frac{\bar{m}_\alpha^2}{k^3} + \dots \right] \\ &= \frac{1}{16\pi^2} \sum_\alpha S_\alpha(\partial_{\phi_{\text{cl}}} m_\alpha^2) [\Lambda^2 - \bar{m}_\alpha^2 \ln(\Lambda/\bar{m}) + \text{finite}]. \end{aligned} \quad (4.33)$$

In the momentum integrals here and below, the variable  $k$  is the comoving momentum,  $\Lambda$  is a comoving cutoff, and we have  $k < \Lambda$ . (Recall that graphs in this section in the comoving frame, and all quantities are actually hatted quantities. The cutoff regularisation we apply here is equivalent to a physical cutoff on physical momentum.) The sum is over  $\alpha = \{h, \theta, \eta, A, \xi\}$ , and  $S_\alpha = \{1, 1, -2, 3, 1\}$  counting the real degrees of freedom (with a minus sign for the anticommuting ghost). Note that the factor  $\partial_{\phi_{\text{cl}}} m_\alpha^2$  is time dependent, and evaluated at  $\tau$ ; hence  $A_1^{\text{Mink}}$  is a function of  $\tau$ . The finite terms that we have neglected remain finite as  $\Lambda \rightarrow \infty$ .

### 4.3.2 Second order contribution $\mathcal{A}^{(2)}$

$\mathcal{A}_{\text{Mink}}^{(2)}$

Here we can straightaway translate the Minkowski result we found in (3.26), (3.29) and (3.33). Once we are in the conformal frame there is nothing new in the computations, we just have some shifted masses to insert. We get

$$\mathcal{A}_{\text{Mink}}^{(2)} = -\frac{1}{16\pi^2} \sum_\alpha S_\alpha(\partial_\phi m_\alpha^2) \delta m_\alpha^2 \ln(\Lambda/\bar{m}) - \frac{(3+\xi)}{32\pi^2} (-i\lambda_{hA_0\theta}^+) \delta m_{A_0\theta}^2 \ln(\Lambda/\bar{m}) + \text{finite}. \quad (4.34)$$

As before: the sum is over  $\alpha = \{h, \theta, \eta, A, \xi\}$ , and  $S_\alpha = \{1, 1, -2, 3, 1\}$ .

$\mathcal{A}_{\text{mass}}^{(2)}$  and  $A_{\text{mix}}^{(2)}$

The loop with  $\lambda_{\delta A_0 A_0}$  proceeds analogously to the gauge loop computed in section 3.3. We need to set  $\rho = \sigma = 0$  in (3.27). When doing the computation, sketched in appendix C.2.1, one finds that now that

the field running in the loop can only be the temporal component of the gauge field, there is an additional factor of  $\frac{1}{4}$  in the final answer (compare to (3.29)). We get

$$\begin{aligned}
\mathcal{A}_{\text{mass}}^{(2)} &= i \int d^4 y \frac{1}{2} \lambda_{hA_\mu A_\nu}^+(x^0) \left[ \bar{\Delta}_{A_\nu A_0}^{++}(x-y) \lambda_{\delta A_0 A_0}^+(y^0) \bar{\Delta}_{A_0 A_\mu}^{++}(y-x) \right. \\
&\quad \left. + \bar{\Delta}_{A_\nu A_0}^{+-}(x-y) \lambda_{\delta A_0 A_0}^-(y^0) \bar{\Delta}_{A_0 A_\mu}^{-+}(y-x) \right] \\
&= \dots \\
&= -(\partial_{\phi_{\text{cl}}} m_A^2(\tau)) \delta m_{A_0 A_0}^2(\tau) \frac{(3 + \xi^2)}{64\pi^2} \ln(\Lambda/\bar{m}) + \text{finite}. \tag{4.35}
\end{aligned}$$

The off-diagonal interaction  $\lambda_{\delta A_0 A_i}$  contains a spatial derivative, and brings down a factor of the momentum. Since the insertion is asymmetrical, there is no more reflection symmetry, so we lose the factor of  $1/2$  that we had in (4.35). In appendix C.2.2 we show that the diagram is given by

$$\begin{aligned}
\mathcal{A}_{\text{mix}}^{(2)} &= i \int d^4 y \lambda_{hA_\mu A_\nu}^+(x^0) \left[ \bar{\Delta}_{A_\nu A_0}^{++}(x-y) \lambda_{\delta A_0 A_i}^+(y^0) \bar{\Delta}_{A_i A_\mu}^{++}(y-x) \right. \\
&\quad \left. + \bar{\Delta}_{A_\nu A_0}^{+-}(x-y) \lambda_{\delta A_0 A_i}^-(y^0) \bar{\Delta}_{A_i A_\mu}^{-+}(y-x) \right] \\
&= \dots \\
&= (\partial_{\phi_{\text{cl}}} m_A^2(\tau)) \frac{3\mathcal{H}'(\tau)(1-\xi)^2}{32\pi^2\xi} \ln(\Lambda/\bar{m}) + \text{finite}. \tag{4.36}
\end{aligned}$$

### 4.3.3 Third order contribution $\mathcal{A}^{(3)}$

The third order diagrams with two two point insertions are UV finite, which can be easily checked by power counting. The only exception to this is the diagram with two off-diagonal  $\lambda_{\delta A_0 A_i}$  insertions, because each insertion contains a spatial derivative, and thus brings down a power of momentum. We thus consider the third order diagram with two mixed-interaction insertions:

$$\begin{aligned}
\mathcal{A}_{\text{mix}}^{(3)} &= i \int d^4 y \int d^4 z \frac{1}{2} \lambda_{hA_\mu A_\nu}^+(x^0) \times \\
&\quad \sum \bar{\Delta}_{A_\nu A_\rho}^{+a}(x-y) \lambda_{\delta A_\rho A_\sigma}^a(y^0) \bar{\Delta}_{A_\sigma A_\kappa}^{ab}(y-z) \lambda_{\delta A_\kappa A_\tau}^b(z^0) \bar{\Delta}_{A_\tau A_\mu}^{b+}(z-x) \\
&= i \int d^4 y \int d^4 z \frac{1}{2} i\eta^{\mu\nu} (\partial_{\phi_{\text{cl}}} m_A^2(x^0)) \times \\
&\quad \sum \bar{\Delta}_{A_\nu A_\rho}^{+a}(x-y) \left( -is(a)\delta m_{A_\rho A_\sigma}^2(y^0) \right) \bar{\Delta}_{A_\sigma A_\kappa}^{ab}(y-z) \times \\
&\quad \left( -is(b)\delta m_{A_\kappa A_\tau}^2(z^0) \right) \bar{\Delta}_{A_\tau A_\mu}^{b+}(z-x). \tag{4.37}
\end{aligned}$$

Here the factor of  $1/2$  comes from the reflection symmetry between the spacetime points  $x$  and  $y$ . As we want to have two  $\delta m_{A_0 A_i}^2$  insertions, the sum is over the four possibilities for the Lorentz indices:

$$(\rho, \sigma, \kappa, \tau) = (i, 0, j, 0), (0, i, 0, j), (0, i, j, 0), (i, 0, 0, j). \tag{4.38}$$

Working in the in-in formalism, the spacetime points  $y$  and  $z$  can be on the positive or on the negative branch, which gives four possibilities that we should sum over as well (spacetime point  $x$  is always taken

on the positive branche):

$$(a, b) = (++) , (-+) , (+-) , (---). \quad (4.39)$$

Of course, the choice of the branche has consequences for the sign of the Feynman rule. Therefore we used the sign function  $s(a)$  which we define as  $s(+)=1$ ,  $s(-)=-1$ .

In appendix C.2.3 we show that in the end this diagram yields

$$\mathcal{A}_{\text{mix}}^{(3)} = (\partial_{\phi_{\text{cl}}} m_A^2(\tau)) \mathcal{H}^2(\tau) \frac{-6(1+\xi)}{32\pi^2\xi} \ln(\Lambda/\bar{m}) + \text{finite}. \quad (4.40)$$

#### 4.3.4 Summary of graphs

In the previous subsections we have computed all quadratically and logarithmically divergent contributions to the one loop equation of motion. Here we collect and summarize the results, putting the hats back on the relevant variables to indicate that we are still in the conformal frame.

The first order graphs are given by (4.33). The second order contributions are (4.34), (4.35) and (4.36), and are summarized in figure 4.3. At third order there is only one piece, given by (4.40). We now collect these terms into the three groups  $\hat{\mathcal{A}}_{\text{Mink}}$ ,  $\hat{\mathcal{A}}_{\text{mass}}$  and  $\hat{\mathcal{A}}_{\text{mix}}$ .

The first and second order combined  $\hat{\mathcal{A}}_{\text{Mink}} = \hat{\mathcal{A}}_{\text{Mink}}^{(1)} + \hat{\mathcal{A}}_{\text{Mink}}^{(2)}$  is

$$\hat{\mathcal{A}}_{\text{Mink}} = \frac{1}{16\pi^2} \sum_{\alpha} S_{\alpha} \left( \partial_{\phi_{\text{cl}}} \hat{m}_{\alpha}^2(\tau) \right) \left[ \hat{\Lambda}^2 - \hat{m}_{\alpha}^2 \ln \left( \hat{\Lambda}/\hat{m} \right) \right] - \frac{(3+\xi)}{32\pi^2} (-i\hat{\lambda}_{hA_0\hat{\theta}}^+) \delta\hat{m}_{A_0\hat{\theta}}^2 \ln(\hat{\Lambda}/\hat{m}). \quad (4.41)$$

This agrees with the result (3.34) found in the previous chapter. As expected, this is independent of how the two point interaction is split into a free and interacting term, since the first and second order pieces combine in the sum  $\hat{m}_{\alpha}^2 = \hat{m}_{\alpha}^2 + \delta\hat{m}_{\alpha}^2$ . For  $A_0$  mass insertions we have the second order piece (4.35)

$$\hat{\mathcal{A}}_{\text{mass}} = - (\partial_{\phi_{\text{cl}}} m_A^2(\tau)) \delta m_{A_0 A_0}^2(\tau) \frac{(3+\xi^2)}{64\pi^2} \ln(\Lambda/\bar{m}) + \text{finite}. \quad (4.42)$$

For the mixed piece we have contributions from second order (4.36) and third order (4.40), giving a total

$$\hat{\mathcal{A}}_{\text{mix}} = \left( \partial_{\phi_{\text{cl}}} \hat{m}_A^2(\tau) \right) \left( \frac{3\mathcal{H}'(1-\xi)^2}{\xi} - \frac{6\mathcal{H}^2(1+\xi)}{\xi} \right) \frac{1}{32\pi^2} \ln(\hat{\Lambda}/\hat{m}). \quad (4.43)$$

All factors in ((4.41), (4.42), (4.43)) that are time dependent — being the  $\hat{m}^2$ 's,  $\hat{\lambda}_{hA_0\hat{\theta}}^+$  and  $\mathcal{H}$  — are understood to be evaluated at  $\tau$ .

## 4.4 Effective action

The previous section found the effective one loop equation of motion. Now we want to extract an effective action from that (even if we know that formally we can set  $\varphi^+ = \varphi^-$ , for any quantum field  $\varphi$ , only at the level of the equation of motion). As we did around (3.35), we will find the effective action  $\Gamma$  from the Euler-Lagrange prescription, which now reads

$$\mathcal{A} = \partial_{\tau} \frac{\delta\Gamma}{\delta\partial_{\tau}\phi_{\text{cl}}} - \frac{\delta\Gamma}{\delta\phi_{\text{cl}}}. \quad (4.44)$$

$$\begin{aligned}
\sum \mathcal{A}_i^{(2)} = & \left[ \begin{array}{c} \text{Diagram 1: Circle with left vertex, top label } \bar{\Delta}_{\hat{h}\hat{h}}^{\alpha+}, \text{ bottom label } \bar{\Delta}_{\hat{h}\hat{h}}^{\alpha+} \\ \partial_{\phi_{\text{cl}}} \hat{m}_h^2 \delta \hat{m}_h^2 \end{array} \right. \\
& + \begin{array}{c} \text{Diagram 2: Circle with left vertex, top label } \bar{\Delta}_{\hat{\theta}\hat{\theta}}^{\alpha+}, \text{ bottom label } \bar{\Delta}_{\hat{\theta}\hat{\theta}}^{\alpha+} \\ \partial_{\phi_{\text{cl}}} \hat{m}_\theta^2 \delta \hat{m}_\theta^2 \end{array} \\
& + \begin{array}{c} \text{Diagram 3: Circle with left vertex, top label } \bar{\Delta}_{\hat{\eta}\hat{\eta}}^{\alpha+}, \text{ bottom label } \bar{\Delta}_{\hat{\eta}\hat{\eta}}^{\alpha+} \\ -2 \partial_{\phi_{\text{cl}}} \hat{m}_\eta^2 \delta \hat{m}_\eta^2 \end{array} \\
& + \begin{array}{c} \text{Diagram 4: Circle with left vertex, top label } \bar{\Delta}_{A_\mu A_\nu}^{\alpha+}, \text{ bottom label } \bar{\Delta}_{A_\mu A_\nu}^{\alpha+} \\ \partial_{\phi_{\text{cl}}} \hat{m}_A^2 \delta \hat{m}_A^2 (3 + \xi^2) \end{array} \\
& + \begin{array}{c} \text{Diagram 5: Circle with left vertex, top label } \bar{\Delta}_{A_0 A_\mu}^{\alpha+}, \text{ bottom label } \bar{\Delta}_{A_0 A_\nu}^{\alpha+} \\ \partial_{\phi_{\text{cl}}} \hat{m}_A^2 \delta \hat{m}_{A_0 A_0}^2 \frac{3+\xi^2}{4} \end{array} \\
& + \begin{array}{c} \text{Diagram 6: Circle with left vertex, top label } \bar{\Delta}_{A_0 A_\mu}^{\alpha+}, \text{ bottom label } \bar{\Delta}_{A_i A_\nu}^{\alpha+} \\ -\partial_{\phi_{\text{cl}}} \hat{m}_A^2 \frac{3\mathcal{H}'(\xi-1)^2}{2\xi} \end{array} \\
& \left. + \begin{array}{c} \text{Diagram 7: Circle with left vertex, top label } \bar{\Delta}_{A_0 A_0}^{\alpha+}, \text{ bottom label } \bar{\Delta}_{\hat{\theta}\hat{\theta}}^{\alpha+} \\ -i \hat{\lambda}_{h A_0 \hat{\theta}}^+ \delta \hat{m}_{A_0 \hat{\theta}}^2 \frac{3+\xi}{2} \end{array} \right] \times \frac{-1}{16\pi^2} \log(\Lambda/\bar{m})
\end{aligned}$$

Figure 4.3: The second order tadpole diagrams and their corresponding mathematical expression (below each graph). These Feynman diagrams are in (conformal) coordinate space, with the left and right vertices at  $x$  and  $y$  respectively.  $x$  is always on the plus-branch,  $y$  can be on both branches, so we sum over  $\alpha = \{+, -\}$ . The argument of each of the propagators is  $(y-x)$  (we used that  $\bar{\Delta}^{+-}(x-y) = \bar{\Delta}^{-+}(y-x)$ ). All time-dependent quantities are evaluated at  $x^0 = \tau$ .

So let us again begin at the classical level. We found  $\mathcal{A}_{\text{cl}}$  in (4.30). Reinstating the hats (we were working in the conformal frame) we find the classical action:

$$\begin{aligned}
\Gamma_{\text{cl}} &= \int d^3x d\tau \left[ -\frac{1}{2} \hat{\phi}_{\text{cl}} \left( \partial_\tau^2 - \nabla^2 - \frac{a''}{a} \right) \hat{\phi}_{\text{cl}} - \hat{V} \right] \\
&= \int d^3x d\tau \sqrt{-g_{\text{conf}}} \left[ -\frac{1}{2a^2} \phi_{\text{cl}} \left( \partial_\tau^2 - \nabla^2 + 2\frac{a'}{a} \partial_\tau \right) \phi_{\text{cl}} - V \right] \\
&= \int d^3x dt \sqrt{-g_{\text{phys}}} \left[ -\frac{1}{2} \phi_{\text{cl}} \left( \partial_t^2 - \frac{\nabla^2}{a^2} + 3H \partial_t \right) \phi_{\text{cl}} - V \right], \tag{4.45}
\end{aligned}$$

where we used that  $\mathcal{H}' + \mathcal{H}^2 = a''/a$ , and  $H = \dot{a}/a$ . In the second line we went to unhatted quantities, and in the third we changed to physical time. The measure in conformal coordinates is  $\sqrt{-g_{\text{conf}}} = a^4$ , and in physical coordinates  $\sqrt{-g_{\text{phys}}} = a^3$ . These results we had already found in (4.5) and (4.6). We can

of course also write

$$\Gamma_{\text{cl}} = \int d^4x \sqrt{-g} \left[ \frac{1}{2} \partial_\mu \phi_{\text{cl}} \partial^\mu \phi_{\text{cl}} - V(\phi_{\text{cl}}) \right]. \quad (4.46)$$

Now for the quantum corrections to the classical action. The relevant terms at the level of the equations of motion are summarized in section 4.3.4, and the one loop correction to the effective action is defined as

$$\Gamma^{1\text{-loop}} = \int d^3x d\tau (\hat{\mathcal{L}}_{\text{Mink}} + \hat{\mathcal{L}}_{\text{mass}} + \hat{\mathcal{L}}_{\text{mix}} + \text{finite}). \quad (4.47)$$

All but one term in  $\hat{\mathcal{A}}_{\text{Mink}}$  are polynomial, the exception being the  $\hat{\lambda}_{\hat{h}A_0\hat{\theta}}^+$  term. For this term, the  $\hat{\phi}_{\text{cl}}$  dependent factors are

$$-i\hat{\lambda}_{\hat{h}A_0\hat{\theta}} \delta \hat{m}_{A_0\hat{\theta}}^2 = 4g^2 \left( \hat{\phi}_{\text{cl}}'' - \mathcal{H}' \hat{\phi}_{\text{cl}} - \mathcal{H}^2 \hat{\phi}_{\text{cl}} \right). \quad (4.48)$$

This expression follows from performing Euler-Lagrange on a Lagrangian

$$\mathcal{L} = 2g^2 \left( \hat{\phi}_{\text{cl}}'^2 - 2\mathcal{H} \hat{\phi}_{\text{cl}} \hat{\phi}_{\text{cl}}' + \mathcal{H}^2 \hat{\phi}_{\text{cl}}^2 \right) = \frac{1}{2} \delta \hat{m}_{A_0\hat{\theta}}^4. \quad (4.49)$$

For the rest of the terms in  $\hat{\mathcal{A}}_{\text{Mink}}$ , which are polynomial in  $\hat{\phi}_{\text{cl}}$ , the corresponding action is found simply by integrating with respect to  $\hat{\phi}_{\text{cl}}$  and negating. All terms in  $\hat{\mathcal{A}}_{\text{mass}}$  and  $\hat{\mathcal{A}}_{\text{mix}}$  are also polynomial in  $\hat{\phi}_{\text{cl}}$ , so can be similarly integrated. Thus, from (4.41), (4.42) and (4.43), and using (4.49), we obtain

$$\begin{aligned} \hat{\mathcal{L}}_{\text{Mink}} &= -\frac{1}{16\pi^2} \sum_\alpha S_\alpha \left( \hat{m}_\alpha^2 \hat{\Lambda}^2 - \frac{1}{2} \hat{m}_\alpha^4 \ln(\hat{\Lambda}/\hat{m}) \right) - \frac{(3+\xi)}{64\pi^2} \delta \hat{m}_{A_0\hat{\theta}}^4 \ln(\hat{\Lambda}/\hat{m}), \\ \hat{\mathcal{L}}_{\text{mass}} &= -\frac{1}{32\pi^2} \hat{m}_A^2 \ln(\hat{\Lambda}/\hat{m}) \left( \frac{(3+\xi^2)}{\xi} (2\mathcal{H}^2 - \mathcal{H}') \right), \\ \hat{\mathcal{L}}_{\text{mix}} &= -\frac{1}{32\pi^2} \hat{m}_A^2 \ln(\hat{\Lambda}/\hat{m}) \left( \frac{3(1-\xi)^2}{\xi} \mathcal{H}' - \frac{6(1+\xi)}{\xi} \mathcal{H}^2 \right), \end{aligned} \quad (4.50)$$

with  $\alpha = \{h, \theta, \eta, A, \xi\}$  and  $S_\alpha = \{1, 1, -2, 3, 1\}$ .

Now write the hatted variables in terms of their unhatted counterparts to go back to the physical frame. Use that  $\mathcal{H}^2 = a^2 H^2$  and  $\mathcal{H}' = a^2 (\dot{H} + H^2)$ . We can factor four powers of the scale factor out of each term. One of them is used to change conformal time into cosmic time ( $dt = a d\tau$ ), the other three are swept into  $\sqrt{-g}$ . The result is

$$\Gamma^{1\text{-loop}} = \int d^3x dt \sqrt{-g} (\mathcal{L}_{\text{Mink}} + \mathcal{L}_{\text{mass}} + \mathcal{L}_{\text{mix}} + \text{finite}), \quad (4.51)$$

with

$$\mathcal{L}_{\text{Mink}} = -\frac{1}{16\pi^2} \sum_\alpha S_\alpha \left( m_\alpha^2 \Lambda^2 - \frac{1}{2} m_\alpha^4 \ln(\Lambda/\bar{m}) \right) - \frac{(3+\xi)}{64\pi^2} \delta m_{A_0\theta}^4 \ln(\Lambda/\bar{m}), \quad (4.52)$$

$$\mathcal{L}_{\text{mass}} = -\frac{1}{32\pi^2} m_A^2 \ln(\Lambda/\bar{m}) \left( \frac{(3+\xi^2)}{\xi} (H^2 - \dot{H}) \right), \quad (4.53)$$

$$\mathcal{L}_{\text{mix}} = -\frac{1}{32\pi^2} m_A^2 \ln(\Lambda/\bar{m}) \left( \frac{3(1-\xi)^2}{\xi} (\dot{H} + H^2) - \frac{6(1+\xi)}{\xi} H^2 \right). \quad (4.54)$$

Here we also used that whereas  $\hat{\Lambda}$  was a conformal cutoff on conformal three-momentum (equivalent to comoving momentum),  $\Lambda$  is now a physical cutoff on physical three-momentum. In other words:  $\tilde{\Lambda} = a\Lambda$ , just like in the discussion around (4.10).

When we now plug in the FLRW-corrected two point interactions (4.22), we find for the total one loop effective action (up to field independent terms)

$$\begin{aligned} \Gamma^{1\text{-loop}} = & \frac{-1}{16\pi^2} \int d^3x dt \sqrt{-g} \left[ (V_{hh} + V_{\theta\theta} + 3m_A^2) \Lambda^2 \right. \\ & - \left( (V_{hh} - \dot{H} - 2H^2)^2 + (V_{\theta\theta} - \dot{H} - 2H^2)^2 + 3m_A^4 \right. \\ & \left. \left. + 2\xi V_{\theta\theta} m_A^2 - (6 + 2\xi) g^2 \dot{\phi}_{\text{cl}}^2 + 6m_A^2 (\dot{H} + 2H^2) \right) \frac{\ln(\Lambda/\bar{m})}{2} \right]. \end{aligned} \quad (4.55)$$

Recall that  $m_A^2 = g^2 \phi_{\text{cl}}^2$ . This result is still gauge variant, which was to be expected. Gauge invariance is only achieved on-shell, as we already discussed in section 3.5. The FLRW analogue of (3.38) reads

$$\int d^4x \sqrt{-g} \delta m_{A\theta}^4 = \int d^4x 4g^2 a^3 \dot{\phi}_{\text{cl}}^2 = \int d^4x \sqrt{-g} 4g^2 \phi_{\text{cl}} V_{\phi_{\text{cl}}} = \int d^4x \sqrt{-g} 4m_A^2 V_{\theta\theta}. \quad (4.56)$$

We use this on the last term in (4.52) (or, in fact, on the second term in the third line of (4.55)). On-shell the result (4.55) takes the form

$$\begin{aligned} \Gamma^{1\text{-loop}} = & \frac{-1}{16\pi^2} \int d^3x dt \sqrt{-g} \left[ (V_{hh} + V_{\theta\theta} + 3m_A^2) \Lambda^2 \right. \\ & - \left( (V_{hh} - \dot{H} - 2H^2)^2 + (V_{\theta\theta} - \dot{H} - 2H^2)^2 + 3m_A^4 \right. \\ & \left. \left. - 6m_A^2 (V_{\theta\theta} - \dot{H} - 2H^2) \right) \frac{\ln(\Lambda/\bar{m})}{2} \right], \end{aligned} \quad (4.57)$$

which is gauge invariant, as it should be. Introducing the notation

$$\tilde{V}_{\alpha\alpha} \equiv V_{\alpha\alpha} - \dot{H} - 2H^2, \quad (4.58)$$

we rewrite the final result, up to field independent terms, as a straightforward generalization of (3.39):

$$\begin{aligned} \Gamma = & \int d^4x \left[ \frac{1}{2} \partial_\mu \phi_{\text{cl}} \partial^\mu \phi_{\text{cl}} - V(\phi_{\text{cl}}) \right. \\ & - \frac{\Lambda^2}{16\pi^2} \left( \tilde{V}_{hh}(t) + \tilde{V}_{\theta\theta}(t) + 3g^2 \phi_{\text{cl}}(t)^2 \right) \\ & \left. + \frac{\ln(\Lambda/\bar{m})}{32\pi^2} \left( \tilde{V}_{hh}^2(t) + \tilde{V}_{\theta\theta}^2(t) + 3g^4 \phi_{\text{cl}}(t)^4 - 6g^2 \phi_{\text{cl}}(t)^2 \tilde{V}_{\theta\theta}(t) \right) \right]. \end{aligned} \quad (4.59)$$

#### 4.4.1 Fermions and additional scalars

It is straightforward to add fermions and additional scalars to the calculation. If these fields are coupled to the Higgs field, and thus have a mass term dependent on  $\phi_{\text{cl}}$ , they will contribute to the effective equation of motion for the background Higgs field  $\phi_{\text{cl}}(t)$  and to the effective action.

We assume the extra scalars are in a basis with canonical kinetic terms and have diagonal masses, and do not mix with  $h$ . Similarly, we assume the extra fermions have diagonal masses. It is easy to relax these assumptions and generalize the results.

In terms of Feynman diagrams, there are extra tadpole graphs with the additional scalars and fermions running in the loop. The calculation for additional scalars is analogous to that of the Higgs fluctuations  $h$  already done, with a contribution at first and second order. The result is

$$\Gamma_{(\text{scalar})}^{1\text{-loop}} = -\frac{1}{16\pi^2} \int d^3x dt \sqrt{-g} \left[ V_{\chi\chi} \Lambda^2 - \left( V_{\chi\chi} - \dot{H} - 2H^2 \right)^2 \frac{\ln(\Lambda/\bar{m})}{2} \right], \quad (4.60)$$

where  $\chi$  is the additional real scalar and  $V(\chi, \phi)$  its potential.

Just as for the bosons, the tadpole diagrams with a fermion loop can be mapped to the calculation for Minkowski space, except that the ‘‘mass’’ terms now depend on the FLRW scale factor. To discuss fermions in curved spacetime, one has to use the vielbein formalism to transform to a local Lorentz frame, where Lorentz transformations and spin- $\frac{1}{2}$  particles are well defined. The vielbeins are defined via

$$g_{\mu\nu} = \epsilon_\mu^a \epsilon_\nu^b \eta_{ab}, \quad (4.61)$$

with  $\epsilon_\mu^a = a\delta_\mu^a$  for a conformal FLRW metric (4.1). The gamma matrices are  $\{\bar{\gamma}^\mu, \bar{\gamma}^\nu\} = 2g^{\mu\nu}$ , with  $\gamma^a = \epsilon_\mu^a \bar{\gamma}^\mu$  the usual Minkowski gamma matrices. In this notation the fermionic action is [71]

$$\mathcal{L}_f = \int d^4x \sqrt{-g} \bar{\psi} (\bar{\gamma}^\mu \nabla_\mu - m) \psi, \quad (4.62)$$

with the covariant derivative  $\nabla_\mu = \partial_\mu + \Omega_\mu$ , and  $\Omega_\mu = (1/4)\omega_{ab\mu} \gamma^a \gamma^b$ , with  $\Omega_i = (1/2)(a'/a)\gamma^i \gamma^0$  and  $\Omega_0 = 0$  for the conformal FLRW metric<sup>1</sup>. We rescale the fermion field  $\hat{\psi} = a^{3/2}\psi$  and mass  $\hat{m}_\psi = am_\psi$ . The Dirac equation then becomes

$$(i\gamma^\mu \partial_\mu - \hat{m}_\psi) \hat{\psi} = 0, \quad (4.63)$$

which is of the usual Minkowski form. Hence the end result is the Minkowski [72] result but with the replacement  $m_\psi \rightarrow \hat{m}_\psi = am_\psi$  [72] (we double checked this result using the non-perturbative approach, which requires to continue the computation in appendix A up to order  $E_k^{-3}$ ):

$$\begin{aligned} \Gamma_{(\text{fermion})}^{1\text{-loop}} &= \frac{1}{16\pi^2} \sum_f \int d^3x d\tau \left[ \hat{m}_\psi^2 \hat{\Lambda}^2 - \frac{1}{2} (\hat{m}_\psi^4 + \hat{m}_\psi'' \hat{m}_\psi) \ln(\hat{\Lambda}/\hat{m}) \right] \\ &= \frac{1}{16\pi^2} \sum_f \int d^3x dt \sqrt{-g} \left[ m_\psi^2 \Lambda^2 \right. \\ &\quad \left. - \frac{1}{2} \left( m_\psi^4 + m_\psi^2 \left( \frac{\ddot{m}_\psi + 3H\dot{m}_\psi}{m_\psi} + \dot{H} + 2H^2 \right) \right) \ln(\Lambda/\bar{m}) \right]. \end{aligned} \quad (4.64)$$

The sum is over all fermionic degrees of freedom, which are two (helicity) states for a Weyl fermion and four states for a Dirac fermion. The first line is the Minkowski result with the replacement  $m_\psi \rightarrow \hat{m}_\psi$ . In the second line we went to physical coordinates by factoring out an overall  $a^4$  factor, and rewriting the  $\hat{m}_\psi''$  in terms of derivatives with respect to physical time  $t$ . The first contribution to the logarithmic term incorporates the expansion of the universe. The second contribution to the logarithmic term is because the  $\phi_{\text{cl}}$  field is rolling, and is also present in Minkowski spacetime.

<sup>1</sup>If the fermions are charged under gauge groups, there will be an additional gauge connection. These extra terms do not affect the effective action for  $\phi_{\text{cl}}$ , and for simplicity we leave them out.

Again we can simplify this result by going on-shell. For a fermion mass  $m_\psi = \lambda\phi_{\text{cl}}$  that is linear in the Higgs field — which is the case for Yukawa interactions and also for gaugino masses in supersymmetric theories — this gives

$$\Gamma_{(\text{fermion})}^{1\text{-loop}} = \frac{1}{16\pi^2} \sum_f \int d^3x dt \sqrt{-g} \left[ m_\psi^2 \Lambda^2 - \frac{1}{2} \left( m_\psi^4 - m_\psi^2 \tilde{V}_{\theta\theta} \right) \ln(\Lambda/\bar{m}) \right]. \quad (4.65)$$

Here we have used, again, the background field equations and Goldstone's theorem.  $\tilde{V}_{\theta\theta}$  was defined in (4.58).

#### 4.4.2 Initial conditions

Finally, we want to comment on the initial conditions that we have chosen to compute the time dependent effective action. Physically they seem rather peculiar, but we want to argue here that this does not compromise our final result.

Our interactions are time dependent, and thus we needed to define the split between a time independent mass and a time dependent two point interaction (4.24)

$$m_{\alpha\beta}^2(t) = \bar{m}_{\alpha\beta}^2 + \delta m_{\alpha\beta}^2(t), \quad \delta m_{\alpha\beta}^2(0) = 0. \quad (4.66)$$

We furthermore chose initial conditions for  $\phi(t)$  and  $a(t)$  such that the off-diagonal and Lorentz violating two point interactions vanished completely at the initial time:

$$\delta\phi_{\text{cl}}(0) = \delta\phi'_{\text{cl}}(0) = \mathcal{H}(0) = \mathcal{H}'(0). \quad (4.67)$$

These choices ensured the simplicity of the propagators. They also ensured the vanishing of the  $t = 0$  boundary terms coming from integration by parts when evaluating the loop diagrams in section 4.3. If these boundary terms did not vanish, they would yield extra contributions to the final result, contributions that depend on the initial conditions, and that diverge as  $t \rightarrow 0$ .

Our chosen initial conditions are peculiar, and are not the ones to be used in a realistic situation. The problem in straightforwardly generalizing our calculation to arbitrary initial conditions are the two point interactions  $\delta m_{A_0 A_0}$ ,  $\delta m_{A_0 A_i}$  and  $\delta m_{A_0 \theta}^2$ . To simplify the structure of the free action, and use the standard expressions for the propagator, we have treated them as interactions. To satisfy (4.66) then requires the initial conditions (4.67).

However, in principle there is nothing to stop us from also splitting these two point interactions into a free and interacting part, as in (4.66). Technically, this is complicated, as Lorentz symmetry is broken, and the gauge fields and Goldstone bosons all mix at the initial time. Nevertheless, in principle we can expand all fields in mode functions, as we did for the Minkowski case in sections 2.7.2 and 3.4. The mode functions then satisfy the off-diagonal mode equations (diagonalizing the equations will result in a momentum dependent diagonalization). Then (4.66) is satisfied, all terms depending on the initial conditions vanish, and the results are the same as for our choice of initial conditions (4.67).

In slightly different words, we argue that the result is independent of the initial conditions as long as we choose the initial vacuum to be that of the free theory, which is defined by the split of the quadratic term into a time independent mass and a time dependent interaction term. That is, solve the mode equations derived from the free action with  $\bar{m}_{\alpha\beta}^2$ , and the corresponding annihilation operators annihilate the vacuum. The different vacua, corresponding to different initial conditions, are then related by a Bogoliubov transformation. For the scalar field theory this was shown by Baacke et al. [73] (see also [74]).

For a  $U(1)$  model we require a more general Bogoliubov transformation, with momentum and polarization dependent coefficients that mix the fields. In principle this should be straightforward, but we will not present any further details here.

In practice, choosing the initial conditions (4.67) simplifies the calculation of the free field mode functions and propagators, and eliminates boundary terms, which is why we choose it. We have argued that a full treatment of initial conditions would yield the same result, at least for the divergent corrections to the equation of motion.

## 4.5 Discussion

We conclude that in a FLRW universe the effective action depends in exactly the same way as in Minkowski on the masses of all scalar fields in the  $U(1)$  Abelian Higgs model. The only novelty is a universal mass shift:

$$m^2 \quad \rightarrow \quad m^2 - (\dot{H} + 2H^2) = m^2 - \frac{1}{a^2} (\mathcal{H}' + \mathcal{H}^2) = m^2 - \frac{a''}{a^3}. \quad (4.68)$$

We found the same shift in the scalar mass in the effective action when we considered only the real scalar field, in (4.11). This just reflects that a scalar field feels the expansion of the universe as an extra contribution to its effective mass, which was already shown in (4.6). Therefore, we might have guessed our final answer from directly shifting all scalar mass in the final Minkowski result (3.39), but it has taken this very non-trivial computation to convince ourselves.

The effective action for an Abelian gauge theory in de Sitter space-time has been calculated by [75, 76, 77] using the Landau gauge. More recently the calculation was done in the  $R_\xi$  gauge, showing gauge invariance of the effective action [78]. To obtain this result an adiabatic approximation was made which fails in the  $\xi \rightarrow 0$  limit. We have extended these results to a generic FLRW spacetime and allow for the possibility of time dependence of the background field, which in a cosmological set-up can be displaced from its potential minimum. For the first time, gauge invariance in general FLRW has been shown.

Our results agree with the expressions in the literature in the appropriate limit. In the limit of a static background field and a constant Hubble parameter our results agree with [78]. In the Minkowski limit we retrieve the effective action calculated in the previous chapter, and also the effective equations of motion found earlier in [51, 54, 55, 66]. Finally, taking both a static background field and a static background we get the familiar Coleman-Weinberg potential [41].

As already mentioned, we have only calculated the UV divergent terms, as these will generically give the dominant contribution. Using a renormalization prescription, these terms (together with the wavefunction renormalization of the gauge field) suffice to derive the renormalization group equations (RGE) and find the RG improved action. An additional task left for the future is to take into full account the backreaction of the scalar on spacetime. Essentially, one must allow for spin-0 fluctuations of the metric, determine their mixing with the scalar, diagonalize to a new basis, and use this basis as the starting point of the calculation. A further generalization is to include a non-minimal coupling to gravity, so as to describe models of Higgs inflation. Finally, one could also generalize the decomposition of  $\Phi$  (4.14) to allow for a time dependent classical background in the imaginary direction.

## Part III

# Inflation in supergravity



# Chapter 5

## Sgoldstino inflation

### 5.1 Introduction: single field sugra inflation

In the previous chapters we have carefully integrated out the quantum field oscillations in the context of the Abelian  $U(1)$  Higgs model, ending up with an effective theory in terms of the classical field  $\phi_{\text{cl}}$ . In this chapter we are again looking for such an effective description (but without inclusion of quantum corrections). Now we want to explore the possibilities of embedding a theory of single field inflation into a realistic sugra framework, i.e. one that leads to (at least) the MSSM. At first glance it seems a hopeless task to isolate an inflationary part of the theory from the remaining “matter” part of the theory. In section 1.6 we have seen that when we compute the scalar  $F$ -term potential in sugra, all fields couple in principle to each other. How can we ever be sure that we have not missed some heavy field whose dynamics interfere with the carefully constructed dynamics of the inflaton? In this chapter, based on our work [3], we argue that to have an inflationary sector that cannot be disturbed by any other field, we need to take the “sgoldstino” field, the scalar component of the superfield that breaks supersymmetry, as our inflaton.

There are good reasons why a single field description is desirable. In line with Ockham’s razor, it is the simplest model that fits the data. Multifield slow-roll inflation with several (real) light fields has been studied for over a decade [79, 80, 81, 82] (see [83, 84] and references therein), and is very constrained by the observations, in particular through the tight limits on isocurvature modes and non-Gaussianity [19]. On the other hand, however, it is technically challenging to obtain single field behavior in a full multifield set-up.

If the inflaton is the only light field in a multifield parent theory, integrating out the heavy fields should yield an effective single field description that is accurate up to terms  $\mathcal{O}(\partial^2/M^2)$ , with  $M$  the mass of the heavy field. Naively, if there is slow-roll and a large mass hierarchy, one would assume such terms can be ignored, but this expectation is premature<sup>1</sup>. In particular, if there are turns in the inflationary trajectory, derivative interactions between the inflaton and the heavy fields can become transiently strongly coupled. These lead to features and non-Gaussianity in the spectrum of primordial perturbations that would not be inferred from the naive effective field theory (EFT). If the heavy fields remain sufficiently massive,

---

<sup>1</sup>The caveats are due to other mass scales introduced by the changing background, whether in flat space or during slow-roll inflation [85]. This makes the details of decoupling during inflation different from particle phenomenology, where the effective field theory expansion is around a particular vacuum.

the turns result in a reduced speed of sound for the adiabatic perturbations but are otherwise completely consistent with slow-roll [27, 85, 86, 87, 88]. Careful integration of the heavy fields recovers the general low energy effective field theory of inflation including a variable speed of sound for the adiabatic perturbations [89, 90, 91, 92, 93] (see [94] for a detailed discussion).

These interactions are unavoidable whenever the potential “valley” provided by the multifield potential deviates from a geodesic of the multifield sigma model metric. A corollary from the point of view of inflationary model building is that, when it comes to precision cosmology, the field space geometry of the “spectator” heavy fields (that are supposed to sit at their adiabatic minima during slow-roll inflation) is as important as their masses and couplings inferred from the potential alone.

Among the many scalars in a supersymmetric theory, the sgoldstino field stands out. The sgoldstino is the scalar partner of the goldstino, and belongs to the chiral superfield whose nonzero F-term breaks supersymmetry<sup>2</sup>. It has the special property [95, 96, 85] that it decouples from all other fields in the theory<sup>3</sup>. This makes the sgoldstino an ideal inflaton candidate, for it allows for a description of inflation in terms of a single complex field. From the point of view of inflationary modeling this is still multifield inflation (with two real fields), but this two field model is not a toy model, it really is the correct effective description for the full multifield system.

If inflation is effectively driven by a single real scalar field, the inflaton, this can be identified with a suitable linear combination of the real and imaginary parts of the sgoldstino field. Meanwhile, the orthogonal combination is to remain stabilized at a local minimum of the potential during inflation. The effect of turns in the trajectory on the spectrum of primordial perturbations have to be taken into account when comparing to observations, but at least they can be calculated from the two field model (see [97, 27, 98, 99, 100] for recent discussions and references).

Needless to say, this does not mean that all other scalars in the theory (from the susy-preserving superfields) can be completely neglected, as they have to be stabilized in a minimum of the potential during inflation. Even though the sgoldstino decouples from these fields, vice versa this is not true: the masses and couplings of all other fields generically depend on the field value of the sgoldstino field. As during inflation the sgoldstino evolves along its inflationary trajectory, the masses of the scalars change. If the inflaton is the sgoldstino, they will remain at the critical points, but they may become light or even tachyonic, triggering a waterfall-type exit from inflation that is not seen in the two field model. Although it is still a complicated task to determine the minimum of the multifield potential along the inflationary trajectory, it is much simpler than the full multifield *dynamics* needed for a generic, non-sgoldstino, inflation model.

As we discussed already in section 1.6, the potential energy density driving inflation breaks susy spontaneously. For sgoldstino inflation there are two possibilities. First, the same superfield that drives inflation is also responsible for low energy susy breaking. This would be the ideal situation. Not only does inflation decouple from all other fields in the theory, it also links the scale of inflation to the scale of susy breaking. The second possibility is that the two sources of susy breaking are due to different fields. Both sources may be operative during inflation, or alternatively, it may be that only after inflation has ended, a phase transition takes place generating our present-day susy breaking. In both cases the present day sgoldstino field is not the sgoldstino during inflation.

---

<sup>2</sup>We will not consider D-term breaking in this work.

<sup>3</sup>More precisely, setting all other superfields at the minimum of their potential is a consistent truncation from the N=1 sugra multifield parent theory to an effective N=1 sugra with a single chiral superfield, the sgoldstino. In particular, the (real, two dimensional) sgoldstino plane is a geodesically generated surface of the Kähler metric in the parent theory, so there are no derivative interactions with the truncated heavy fields: all turns in the inflationary trajectory are entirely confined to the sgoldstino plane. The effects of the fluctuations of the heavy fields are suppressed by their mass squared exactly as one would expect from an EFT expansion.

If several sources of susy breaking are present during inflation, the inflaton can only be approximately identified with the sgoldstino, and only if the vacuum susy breaking scale is much below the inflationary scale. Care should be taken in this case because, as argued in [101], only if the lightest mass in the hidden sector responsible for vacuum susy breaking is much larger than the inflaton mass and if the inflaton mass is much larger than the scale of hidden sector susy breaking, is the effect of the hidden sector on the slow-roll dynamics of the inflaton negligible. This is far from trivial; for example, it has been proven extremely hard to combine a susy breaking moduli stabilization and inflation in a consistent way [102], even in a fine-tuned setting [103].

The decoupling of the sgoldstino from the other fields fits in with recent work on how to incorporate different fields, or sets of fields, in a sugra set-up minimizing the coupling between them [95, 104, 105, 106, 107, 108, 109, 110, 111, 112, 101, 113]. Quite commonly different sectors — e.g. the fields and couplings responsible for susy breaking, for inflation, for moduli stabilization, or making up the standard model — are combined by simply adding their respective Kähler- and superpotentials. However, following this procedure one cannot completely decouple these sectors. Even if the Kähler and superpotential do not contain direct interaction terms between fields in different sectors, the resulting scalar potential does. There are always at least Planck-suppressed interactions between the fields, and generically the mass matrix is not block diagonal in the different sectors. This complicates the analysis of the full model enormously. Sectors are affected by the presence of others, and although they work in isolation, they may no longer do so in the full set-up. Moreover, heavy fields generically cannot be integrated out in a consistent supersymmetric way<sup>4</sup>.

The cross-couplings between sectors can be minimized if instead of adding Kähler and superpotentials, one adds the Kähler invariant functions  $G = K + \ln |W|^2$  for the two sectors [114, 106]. This approach allows to integrate out fields in a susy preserving way [95]. In Ref. [106] the addition of sugra functions was used to couple a susy breaking moduli sector (fields  $X^i$ ) to a susy preserving sector, for example the standard model (fields  $z_i$ ):

$$G^{\text{tot}}(X^i, \bar{X}^i, z_i, \bar{z}_i) = g(X^i, \bar{X}^i) + G^{\text{other}}(z_i, \bar{z}_i). \quad (5.1)$$

In this chapter we want to use the same idea to couple a susy breaking inflationary sector (fields  $X^i$ ) to a susy preserving sector ( $z_k$ )<sup>5</sup>. For simplicity we restrict to effectively single field inflation, and models with a single inflaton field  $X$ . As susy is broken during inflation, the inflaton is then the sgoldstino. As it turns out, the ansatz (5.1) is actually too strict. We can allow for explicit couplings between the inflaton and the other fields, of the form

$$G(X, \bar{X}, z_k, \bar{z}_k) = g(X, \bar{X}) + \frac{1}{2} \sum_{i \geq j} \left[ \begin{aligned} &(z_i - (z_i)_0)(z_j - (z_j)_0) f^{(ij)}(X, \bar{X}, z_k, \bar{z}_k) \\ &+ (z_i - (z_i)_0)(\bar{z}_j - (\bar{z}_j)_0) h^{(ij)}(X, \bar{X}, z_k, \bar{z}_k) + \text{h.c.} \end{aligned} \right] \quad (5.2)$$

with  $f, h$  arbitrary functions of its arguments. As we will show, this is the most general ansatz consistent with  $X$  being the sgoldstino. The explicit  $X$ -dependence in the second term does not spoil the decoupling of the inflaton field, the mass matrix remains block diagonal in the two sectors, as long as the fields  $z_i$  sit at the susy critical point  $(z_i)_0$  during inflation. As we will show, during sgoldstino inflation the Kähler function  $G$  is well defined, maybe except from isolated points in field space.

<sup>4</sup>Here, once again, approximations that are justified for phenomenology applications where the background is static [112] fail during inflation [104, 105, 108, 85]

<sup>5</sup>In [115] the separable form (5.1) was used to combine hybrid inflation with a susy breaking moduli sector in a successful way. In this set-up the inflaton is not the goldstino.

We have seen in section 1.5 that single field inflation can be divided into three main classes: large field, small field and hybrid inflation. We discuss whether and how sgoldstino inflation might work in these three regimes.

Large field sgoldstino inflation does not work. As a consequence (invoking the Lyth bound [26, 116]), sgoldstino inflation predicts a tensor wave signal far too small to be observable by Planck. In other words, Planck could possibly rule out sgoldstino inflation, but so far it has not, see the results in (1.52).

Hybrid inflation provides the most natural embedding for sgoldstino inflation. Indeed, usual F-term hybrid inflation is an example of having a sgoldstino inflaton. In this set-up susy is restored in the vacuum, and there is no relation with low energy susy breaking. More complicated waterfall regimes may be devised, such that susy is broken in the minimum after inflation. However, such an analysis is multifield, and complicated multifield dynamics enters via the back door again.

Small field inflation offers the best possibility to link inflation to susy breaking. Naively all that is needed is finding and tuning a saddle or maximum in a single field potential with a susy breaking Minkowski minimum. We only find inflection points suitable for inflation rather than a maximum or saddle point. Inflection point inflation yields [117, 118] a low spectral index  $n_s \leq 0.92 - 0.93$  (for  $N = 50 - 60$  e-folds), which by now is actually ruled out by Planck, see (1.51). We will comment on possible resolutions. Interestingly enough, models in which susy is broken after inflation are much easier to embed in a multi-field set-up than models with a susy preserving vacuum. Finally, we comment on recent claims in the literature for small field sgoldstino inflation [119, 120] with no or very little fine-tuning. We will explain why these models cannot work.

## 5.2 Decoupling of the sgoldstino

In this section we will show the decoupling of the sgoldstino field explicitly. In the first subsection we derive the mass matrix, which is block diagonal along the sgoldstino inflation trajectory. We will argue in subsection 5.2.2 that the Kähler function for a dynamical sgoldstino field can always be put in the form (5.2). In subsection 5.2.3 we show that this sgoldstino trajectory is independent of the field values of all the other fields. Vice versa that is not the case: the dynamics of the non-sgoldstino fields does depend on the sgoldstino field. Care must be taken so that these fields remain stabilized along the full inflationary trajectory. Finally, in subsection 5.2.4 we discuss the special limit of separable Kähler functions (5.1), in which the results of [106] are retrieved.

### 5.2.1 Mass matrix

We start with the general formula for the mass matrix, then specialize to sgoldstino inflation. The scalar potential can be expressed solely in terms of the Kähler function<sup>6</sup>  $G = K + \ln |W|^2$ :

$$V_F = e^G [G_I G^{I\bar{J}} G_{\bar{J}} - 3], \quad (5.3)$$

with  $I, J$  running over all fields  $\Phi_I$ . (Note that we are still working in Planck units  $M_p = 1$ ). The fields span the Kähler manifold with complex metric  $G_{I\bar{J}}$ . The inverse metric  $G^{I\bar{J}}$  is such that  $G_{I\bar{J}} G^{K\bar{J}} = \delta_I^K$  and  $G_{I\bar{J}} G^{I\bar{K}} = \delta_{\bar{J}}^{\bar{K}}$ . The only nonzero connection is  $\Gamma_{I\bar{J}}^K = G_{I\bar{J}\bar{P}} G^{\bar{P}K}$  and its complex conjugate. The nonzero components of the Riemann tensor are  $R_{I\bar{J}K\bar{L}} = G_{S\bar{L}} \partial_{\bar{J}} \Gamma_{IK}^S$  and permutations thereof.

<sup>6</sup>This procedure is ill defined for  $W = 0$ . To cure this, one can use the variable  $\phi \equiv e^G$  instead, which remains well defined [121]. However, in the next section we show that  $W = 0$  at most in isolated points in field space.

The mass matrix is

$$\mathcal{M} = \begin{pmatrix} M_J^I & M_{\bar{J}}^I \\ M_{\bar{J}}^I & M_{\bar{J}}^I \end{pmatrix}, \quad M_J^I = G^{I\bar{K}} \nabla_{\bar{K}} \nabla_J V, \quad M_{\bar{J}}^I = G^{I\bar{K}} \nabla_{\bar{K}} \nabla_{\bar{J}} V, \quad (5.4)$$

with  $\nabla_K v_L = \partial_K v_L - \Gamma_{KL}^M v_M$  the covariant derivative of some vector  $v_L$ . The eigenvalues and eigenvectors of the mass matrix correspond to the  $m^2$ -values and mass eigenstates respectively. The first derivative of the potential is

$$V_K = G_K V + e^G [G^I \nabla_K G_I + G_K] \quad (5.5)$$

where we used metric compatibility  $\nabla_K G_{I\bar{J}} = 0$ ,  $\nabla_K G^I = \delta_K^I$  and introduced the notation  $V_K = \partial_K V$ ,  $G^I = G^{I\bar{J}} G_{\bar{J}}$ . Stationarity is not assumed, as the inflaton field is displaced from its minimum during inflation. The second derivatives of the potential are

$$\begin{aligned} \nabla_{\bar{L}} \nabla_K V &= (G_{K\bar{L}} - G_K G_{\bar{L}}) V + 2G_{(K} V_{\bar{L})} + e^G [G^{I\bar{J}} (\nabla_{\bar{L}} G_{\bar{J}}) (\nabla_K G_I) - R_{I\bar{J}K\bar{L}} G^I G^{\bar{J}} + G_{K\bar{L}}], \\ \nabla_L \nabla_K V &= (\nabla_{(L} G_{K)}) V + 2G_{(K} V_{L)} + e^G [2\nabla_{(K} G_{L)} + G^I \nabla_{(L} \nabla_{K)} G_I], \end{aligned} \quad (5.6)$$

where round brackets denote symmetrization. We used that  $[\nabla_{\bar{L}}, \nabla_K] G_I = \nabla_{\bar{L}} \nabla_K G_I = -R_{K\bar{L}I\bar{J}} G^{\bar{J}}$ . Apart from the terms proportional to  $V_K$ , which are absent for stationary situations, these equations are the same as (2.6, 2.7) of Ref. [122].

Now consider F-term breaking of susy, signaled by a nonzero  $G_X \neq 0$ . Here  $X$  is the scalar component of the chiral superfield which also contains the goldstino. Note that one can always make a field redefinition such that only one linear combination of fields breaks susy. All other fields in the theory, denoted by  $z_i$  (indexed by lower case latin letters), do not break susy. Hence, we split the fields in  $\Phi_I = \{X, z_i\}$ , with

$$G_X|_{z_0} \neq 0, \quad G_i|_{z_0} = 0 \quad (5.7)$$

at some point in field space  $z_0 = \{(z_1)_0, (z_2)_0, \dots\}$ , the so-called susy critical point.

We are interested in a cosmological situation, in which  $X(t)$  is the inflaton rolling along some trajectory with  $V_X \neq 0$ . While the inflaton rolls in the  $X$ -direction, we want all orthogonal fields  $z_i$  to remain extremized at  $z_0$ . To that end we demand that

$$(\partial_X)^m (\partial_{\bar{X}})^n G_i|_{z_0} = 0, \quad \forall m, n \in \mathbb{N}. \quad (5.8)$$

Indeed, from (5.5), we then have that

$$V_i|_{z_0} = G_i V + e^G [G^P \nabla_i G_P + G_i] = e^G G^X \nabla_i G_X = 0. \quad (5.9)$$

For notational convenience we dropped the  $|_{z_0}$  on the right hand side, but the reader should keep in mind that all expressions should be evaluated at  $z = z_0$ . Note that  $i$  labels the  $z_i$  fields, and capital letters label  $\Phi_I$  (i.e. also running over  $X$ ). In the first step we used (5.7), in the second  $\nabla_i G_X|_{z_0} = 0$ , which is a consequence of (5.8).

Thus  $z_i = (z_i)_0$  is an extremum of the potential. To see whether this is a maximum, minimum or saddle point, we must calculate the eigenvalues of the mass matrix, which need to be positive definite for a stable minimum. This analysis is simplified because (5.7) assures the mass matrix is in block diagonal form, i.e.  $M_i^X|_{z_0} = M_i^{\bar{X}}|_{z_0} = 0$ . To prove this last statement, it is enough to show the block diagonal form of the second covariant derivatives, as it follows from (5.8) that the field metric  $G_{I\bar{J}}|_{z_0}$  is block diagonal as well. The first equation in (5.6) gives for mixed indices

$$\begin{aligned} \nabla_{\bar{i}} \nabla_X V|_{z_0} &= (G_{X\bar{i}} - G_X G_{\bar{i}}) V + 2G_{(X} V_{\bar{i})} + e^G [G^{K\bar{L}} (\nabla_{\bar{i}} G_{\bar{L}}) (\nabla_X G_K) - R_{K\bar{L}X\bar{i}} G^K G^{\bar{L}} + G_{X\bar{i}}] \\ &= -e^G G^X G^{\bar{X}} R_{X\bar{X}X\bar{i}} = 0. \end{aligned} \quad (5.10)$$

In the first step we used (5.7) and (5.8) and that  $\nabla_i G_X|_{z_0} = \nabla_X G_i|_{z_0} = 0$ ; in the second step that  $R_{X\bar{X}X\bar{i}}|_{z_0} = G_{j\bar{i}}\partial_{\bar{X}}\Gamma_{XX}^j = 0$  as well, which also follows from (5.8). The second equation in (5.6) likewise vanishes for mixed indices:

$$\nabla_i \nabla_X V|_{z_0} = (\nabla_{(i} G_{X)} - G_{(X} G_{i)})V + 2G_{(X} V_{i)} + e^G [2\nabla_{(X} G_{i)} + G^K \nabla_{(i} \nabla_X) G_K] = 0. \quad (5.11)$$

### 5.2.2 Kähler invariant function for sgoldstino inflation

Let us quickly comment on our use of the Kähler invariant function  $G = K + \ln |W|^2$ , rather than expressing results in terms of the Kähler potential and superpotential. The potential danger in using  $G$  is that it becomes undefined when  $W = 0$ . However, it is easy to show that for sgoldstino inflation we nowhere have  $W = 0$ , except maybe for isolated points in field space. Therefore the Kähler function  $G$  is well defined. To illustrate this, consider a theory with two chiral fields - the extension to more fields is straightforward - with a superpotential  $W = W(X, Z)$ . For sgoldstino inflation, with  $X$  the goldstino superfield, we have

$$D_X W|_{\{X(t), Z_0\}} \neq 0, \quad D_Z W|_{\{X(t), Z_0\}} = 0, \quad (5.12)$$

with  $D_X W = K_X W + W_X$  the Kähler covariant derivative. Setting  $W = 0$  along the *whole* trajectory implies

$$W|_{\{X(t), Z_0\}} = 0 \quad \Rightarrow \quad W_X|_{\{X(t), Z_0\}} = 0 \quad \Rightarrow \quad D_X W|_{\{X(t), Z_0\}} = 0 \quad (5.13)$$

in contradiction with (5.12). Therefore the superpotential can only vanish for sgoldstino inflation at accidental zeroes at isolated points in field space (possibly on the trajectory, but this does not change our conclusions).

As a side remark, note that when the inflaton is identified with the  $Z$  field rather than the sgoldstino field  $X$ , as for example in the models of Ref. [123, 124, 125] that we will study in the next chapter, it is possible to have  $W = 0$ ,  $D_X W|_{\{X_0, Z(t)\}} \neq 0$  and  $D_Z W|_{\{X_0, Z(t)\}} = 0$  along the whole trajectory  $\{X_0, Z(t)\}$ . In this case the Kähler invariant function is not well defined, and a description in terms of  $K$  and  $W$  is needed.

Expanding the Kähler function around the susy critical point  $z^i = z_0^i$ , the most general form for sgoldstino inflation - satisfying (5.7) and (5.8) - can be written in the form

$$G(X, \bar{X}, z_k, \bar{z}_k) = g(X, \bar{X}) + \frac{1}{2} \sum_{i \geq j} \left[ \begin{aligned} & (z_i - (z_i)_0)(z_j - (z_j)_0) f^{(ij)}(X, \bar{X}, z_k, \bar{z}_k) \\ & + (z_i - (z_i)_0)(\bar{z}_j - (\bar{z}_j)_0) h^{(ij)}(X, \bar{X}, z_k, \bar{z}_k) + \text{h.c.} \end{aligned} \right] \quad (5.14)$$

with  $f, h, g$  arbitrary functions of its arguments.

### 5.2.3 Inflationary trajectory

We have seen in subsection 5.2.1 that along the inflationary trajectory all non-sgoldstino fields are extremized at  $z^i = z_0^i$ . Since the mass matrix is block diagonal, we can determine the stability of the  $z_i$  extremum from the sub-block of  $\mathcal{M}$  with  $z_i$  indices. It can easily be shown that the inflaton trajectory itself is independent of the field values of the other fields. Indeed, the potential along the inflationary trajectory only depends on the function  $g(X, \bar{X})$  in (5.14), and is thus independent of the field values of

all other fields. The height  $V_0 \equiv V|_{z_0}$ , slope and second derivatives of the inflaton potential are given by (5.3), (5.5) and (5.6) with  $I, J$  only running over  $X$  and  $G \rightarrow g$ . For example we have

$$V_0 = e^g \left[ g_X g^{X\bar{X}} g_{\bar{X}} - 3 \right], \quad (5.15)$$

$$V_X|_{z_0} = g_X V_0 + e^g \left[ g^X \nabla_X g_X + g_X \right]. \quad (5.16)$$

In contrast, the mass matrix along the orthogonal directions does depend on the inflaton field value. We find

$$\begin{aligned} M_j^i|_{z_0} &= G^{i\bar{k}} \nabla_{\bar{k}} \nabla_j V \\ &= G^{i\bar{k}} \left[ G_{j\bar{k}} V_0 + e^G [G^{l\bar{m}} (\nabla_{\bar{k}} G_{\bar{m}}) (\nabla_j G_l) - R_{X\bar{X}j\bar{k}} G^X G^{\bar{X}} + G_{j\bar{k}}] \right] \\ &= e^g \left[ \delta_j^i (b+1) + x_{\bar{m}}^i x_j^{\bar{m}} + w_j^i \right], \end{aligned} \quad (5.17)$$

and

$$\begin{aligned} M_{\bar{j}}^{\bar{i}}|_{z_0} &= G^{\bar{i}k} \nabla_k \nabla_{\bar{j}} V \\ &= G^{\bar{i}k} \left[ \nabla_{(k} G_{j)} V_0 + e^G [2 \nabla_{(j} G_{k)} + G^X \nabla_{(k} \nabla_{j)} G_X] \right] \\ &= e^g \left[ x_{\bar{j}}^{\bar{i}} (b+2) + y_{\bar{j}}^{\bar{i}} \right]. \end{aligned} \quad (5.18)$$

Here we introduced the notation

$$b = V_0 e^{-g} = g_X g^X - 3 \quad (5.19)$$

$$x_{\bar{j}}^{\bar{i}} = G^{\bar{i}k} \nabla_k G_{\bar{j}} = G^{\bar{i}k} \nabla_{\bar{j}} G_k \quad (5.20)$$

$$w_j^i = -G^{i\bar{k}} G^X G^{\bar{X}} R_{X\bar{X}j\bar{k}} \quad (5.21)$$

$$y_{\bar{j}}^{\bar{i}} = G^{\bar{i}k} G^X \nabla_{(k} \nabla_{\bar{j})} G_X. \quad (5.22)$$

Note that  $b = V_0/m_{3/2}^2$  gives the height of the potential in units of the gravitino mass. During slow-roll this is approximately  $b \sim 3H^2/m_{3/2}^2$ .

The functions  $b, x, y, w$  can be expressed in terms of the functions  $f, g, h$  appearing in the Kähler function (5.14). In general, the constraint that the squared masses should be positive is complicated, but there are two situations in which it simplifies considerably. The first one, discussed in the next section, is if the Kähler invariant function is separable [106, 107]. In this case the matrices  $y$  and  $w$  vanish and the constraint involves the eigenvalues of the  $x$  matrix.

The second case where the constraint simplifies is for a single  $z$  field, i.e.  $i = \{1\}$ , such that there is only one  $f$  and  $h$  function. Then the matrices  $x, y$  and  $w$  become scalars

$$\begin{aligned} b &= g_X g^X - 3 \\ x &= h^{-1} (f - f_{\bar{X}} g^{\bar{X}}), \\ w &= -g^X g^{\bar{X}} h^{-1} (h_{X\bar{X}} - h_X h^{-1} h_{\bar{X}}), \\ y &= h^{-1} g^X \left[ f_X - 2h_X h^{-1} f - f_{\bar{X}} g_{\bar{X}}^{\bar{X}} + (f_{\bar{X}} g_{\bar{X}X}^X + h^{-1} h_X f_{\bar{X}} - f_{X\bar{X}}) g^{\bar{X}} \right]. \end{aligned} \quad (5.23)$$

For a canonically normalized  $z$  field,  $h = 1$ ,  $h_X = h_{X\bar{X}} = 0$  which implies  $w = 0$ .

For single field inflation, or if the matrices  $x, w, y$  can be diagonalized simultaneously, the eigenvalues of the mass matrix are given by

$$m_{\pm}^2 = e^g \left[ (1+b) + |x|^2 + w \pm |(2+b)x + y| \right]. \quad (5.24)$$

The  $z$  eigenstates remain stabilized as long as the smallest mass is positive definite  $m_-^2 > 0$ .

### 5.2.4 Separable Kähler function

The results in the previous section are a generalization of the work [106, 107, 108], who considered a set-up with separable Kähler functions:

$$G(X, \bar{X}, z_i, \bar{z}_i) = g(X, \bar{X}) + \tilde{g}(z_i, \bar{z}_i), \quad (5.25)$$

which is a special limit of the more general function (5.14). For the separable Kähler function above (5.25) all mixed derivatives of  $G$ , such as  $G_{zzX}$ , cancel. With this simplification

$$b = g_X g^X - 3, \quad x_m^{\bar{i}} = \tilde{g}^{\bar{i}k} \tilde{g}_{km}, \quad y_j^{\bar{i}} = w_j^i = 0. \quad (5.26)$$

We now consider the case with only one  $z$  field, which turns  $x_j^{\bar{i}}$  into a scalar. As one can always diagonalize  $x_j^{\bar{i}}$ , this simplification precisely gives the result along one of the eigenvectors, and thus can be straightforwardly be generalized to several  $z$  fields. We recover the system studied in [106]<sup>7</sup>:

$$M_z^z|_{z_0} = e^g [(b+1) + |x|^2], \quad M_z^{\bar{z}}|_{z_0} = e^g (b+2)x, \quad (5.27)$$

which has eigenvalues

$$m_{\pm}^2|_{z_0} = e^g [1 + b + |x|^2 \pm |(2+b)x|] = e^g \left[ \left( |x| \pm \frac{1}{2}|b+2| \right)^2 - \frac{b^2}{4} \right]. \quad (5.28)$$

This result can also be obtained from the general expression for the mass squared eigenvalues (5.24), taking the appropriate limit  $y_j^{\bar{i}} = w_j^i = 0$ . The function  $b$  is bigger, equal or smaller than zero for a dS, Minkowski or AdS universe, respectively. Take  $b \geq 0$ ; in the opposite limit the masses  $m_{-}^2$  and  $m_{+}^2$  are exchanged. The smallest mass eigenstate is positive  $m_{-}^2 > 0$ , i.e., the  $z$  field is stabilized along the inflationary trajectory, for  $|x| < 1$  or  $|x| > (1+b)$ . We will put this analysis in practice for sgoldstino inflation in subsections 5.3.2 (hybrid inflation) and 5.3.3 (small field inflation).

Close to the instability bounds  $|x| \lesssim 1$  or  $|x| \gtrsim (1+b)$  the spectator field  $z$  is lighter than the gravitino mass and/or the Hubble scale, and cannot be integrated out. In a Minkowski vacuum after inflation either  $b = 0$  or  $b \rightarrow \infty$ ; the latter case may occur in a supersymmetric vacuum with  $W \rightarrow 0$ . For  $b = 0$ , the masses reduce to  $m_{\pm}^2 = m_{3/2}^2 (1 \pm |x|)^2$ , with  $m_{3/2}$  the gravitino mass. For  $|x| > 1$ , the lightest scalars from the supersymmetric sector are heavier than the gravitino. However, for  $|x| < 1$  the lightest of the two eigenstates is lighter than the gravitino and cannot be neglected from a low-energy description. This will play an important role later. In the supersymmetric vacuum with  $b \rightarrow \infty$  we find  $m_{\pm}^2 \approx V_0(1 \pm |x|) \rightarrow 0$ , and the spectators are massless. To avoid a plethora of massless fields in the theory, one has to either break the supersymmetry, or else go beyond the simple separable form of the Kähler function (5.25).

## 5.3 Single field sgoldstino inflation

In this paper we focus on effectively single field inflation models, for simplicity. The inflaton  $X$ , a real scalar, is identified with a suitable linear combination of the real and imaginary parts of the sgoldstino field; the orthogonal combination is to remain stabilized at a local minimum of the potential during inflation. As we reviewed in section 1.5, single field inflation can be divided into three classes: small field, large field and hybrid inflation. In the supersymmetric versions of the first two cases, if the model only contains a

<sup>7</sup>Our definition of  $b$  is different from [106], which has  $b \leftrightarrow b - 3$ .

single chiral superfield, the inflaton is automatically the sgoldstino. If several fields are present, as is the case for hybrid inflation, one has to be more careful, as the sgoldstino does not have to coincide with the inflaton direction.

In the remainder of this section we will discuss large field, small field and hybrid sgoldstino inflation, and how (the supersymmetrical version of) the  $\eta$ -problem, discussed in sections 1.5 and 1.6, may or may not be addressed in each case.

### 5.3.1 Large field inflation

In section 1.5 we have seen that in large field inflation, the  $\eta$ -problem should be solved by introducing a symmetry. Tuning the parameters does not work, as the inflationary trajectory spans super-planckian distances in field space  $\Delta\phi > 1$ . Following the considerations in section 1.6, we are thus led to a Kähler function  $G = \mathcal{K}(X - \bar{X})$ , which is symmetric under a shift  $X \rightarrow X + c$  with  $c$  a real constant. Since  $G$  does not depend explicitly on  $\phi \propto \text{Re}(X)$ , the exponent in (1.68) is independent of  $\phi$  and there is no  $\eta$ -problem. In fact, the potential has an exactly flat direction. Since we want the system to end up after inflation in a Minkowski minimum, there is no other option than to set  $V = 0$  along the flat direction, which is incompatible with having inflation.

In order to get a slope for the potential and obtain inflation, the shift symmetry needs to be weakly broken. To assure the breaking does not reintroduce exponential terms that ruin inflation, we add a logarithmic term  $G = \mathcal{K}(X - \bar{X}) + \ln |W(X)|^2$  with  $W$  not growing faster than power law. Without loss of generality we can remove the constant and linear terms in  $\mathcal{K} \ni \alpha(X - \bar{X}) + \beta$ , as they can always be absorbed in  $W$  (by a Kähler transformation<sup>8</sup>). Then the potential along the inflationary trajectory is

$$V_F|_{X=\bar{X}} = W_X G^{X\bar{X}} \bar{W}_{\bar{X}} - 3|W|^2|_{X=\bar{X}}. \quad (5.29)$$

The inverse metric  $G^{X\bar{X}}|_{X=\bar{X}} = -1/\mathcal{K}''(0)$  is a constant along the inflationary trajectory, as it is independent of  $\phi$ ; it just renormalizes the field and can be absorbed by going to canonically normalized fields:  $\phi^2 = -2\mathcal{K}''(0)|X|^2$ . If the superpotential during inflation is dominated by a monomial term  $W \sim \lambda X^n$ , we find

$$V_F|_{X=\bar{X}} \propto n^2 \phi^{2n-2} - 3\phi^{2n} \quad (5.30)$$

which goes negative for large  $\phi > n/\sqrt{3}$ . For field values  $\phi = \mathcal{O}(10)$  as needed for large field inflation, the field will run off to infinity and negative potential, rather than the Minkowski minimum at the origin. This does not give a viable inflation model. The instability occurs for every superpotential that does not grow faster than power law, such that the shift symmetry is only broken softly. Faster growing superpotentials reintroduce the  $\eta$  problem.

Although we did the analysis for a single field, this straightforwardly generalizes to the multifield case. If the inflaton is the sgoldstino, it decouples from the other fields, and its potential can be analysed independently and will always be of the form (5.30). We conclude that large field sgoldstino inflation in a sugra model does not work as it is plagued by an instability in the scalar potential.

We note that it is certainly not impossible to have large field inflation in sugra, only that it does not work with a single chiral superfield. In the next chapter we will consider a class of two field models that avoid the instability by employing a shift symmetry to address the  $\eta$ -problem. However, in these models the inflaton is *not* the sgoldstino (rather the sgoldstino is the field orthogonal to the inflaton).

<sup>8</sup>The function  $G = K + \ln |W|^2$  is invariant under the so-called Kähler transformations  $K \rightarrow K + f + \bar{f}$ ,  $W \rightarrow W e^{-f}$ , where  $f$  is a holomorphic function of the fields. See also section 1.6. In this case  $f = -\alpha X - \beta/2$ , where  $\beta$  is real and  $\alpha$  is purely imaginary since  $\mathcal{K}$  is real.

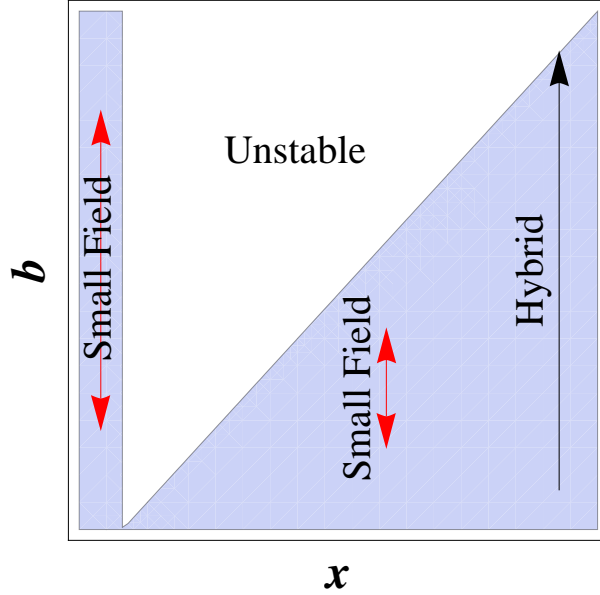


Figure 5.1: (Figure adapted from [106, 108].) Stability diagram for the separable case  $G = g(X, \bar{X}) + \tilde{g}(z, \bar{z})$ . The variables on the axes  $b, x$  are defined in (5.26), with  $x$  one of the degenerate eigenvalues of the  $x_j^i$  matrix. The masses of the spectator fields are positive in the shaded region, while the unstable region signals a tachyonic mode. The black arrow represents the inflationary trajectory for the proposed hybrid set-up, which ends when one of the spectator fields (the waterfall fields) becomes tachyonic. Also shown are possible inflationary trajectories for small field inflation (red arrows).

### 5.3.2 Hybrid inflation

Standard F-term hybrid inflation [126, 28] is an example of sgoldstino inflation. The Kähler function is of the separable form (5.25) discussed in section 5.2.4.

$$G = g(X, \bar{X}) + \tilde{g}(\chi_1, \bar{\chi}_1, \chi_2, \bar{\chi}_2), \quad (5.31)$$

with<sup>9</sup>

$$g = X\bar{X} + k_s(X\bar{X})^2 + \ln |\kappa X|^2 + \dots, \quad \tilde{g} = \chi_1\bar{\chi}_1 + \chi_2\bar{\chi}_2 + \ln |\chi_1\chi_2 - \mu^2|^2 + \dots$$

The model has an R-symmetry, which uniquely fixes the superpotential at the normalized level, and in particular it allows for a linear term in  $X$  but forbids the quadratic and cubic terms in  $W$ . This kills large contributions to the slow-roll parameters, and allows for a flat direction in the inflaton potential, which at tree level is only lifted by higher order terms in the Kähler potential.

The inflaton  $\phi$  is identified with the real direction via the decomposition  $X = (\phi + i\theta)/\sqrt{2}$ . Inflation takes place for large  $\phi > \phi_c = \sqrt{2}\mu$ , and all other fields stabilized at zero field value. The potential along the inflationary trajectory is

$$V = \kappa^2 \mu^4 (1 - 2k_s \phi^2 + \dots) + V_{1\text{-loop}}. \quad (5.32)$$

The flatness of the potential is only lifted by higher order terms in  $K$ , and by the one-loop Coleman-Weinberg potential  $V_{1\text{-loop}}$  [41]. The  $\eta$ -problem is solved via a moderate fine-tuning of  $k_s \lesssim 10^{-2}$ . To

<sup>9</sup>To see that this setup is indeed of the general form (5.14), one can move a factor of  $\ln |\mu^2|^2$  from  $\tilde{g}$  to  $g$  and Taylor expand the remaining  $\ln |\frac{\chi_1\bar{\chi}_2}{\mu^2} - 1|^2$ .

get the correct power spectrum,  $\sqrt{\kappa}\mu$  should be of the grand unified scale or smaller. During inflation  $G_X = \frac{\sqrt{2}}{\phi} + \frac{\phi}{\sqrt{2}} + \frac{k_s\phi^3}{\sqrt{2}}$  and  $G_{\chi_1} = G_{\chi_2} = 0$ . Hence  $\phi$  is indeed the (real part of the) sgoldstino field.

The Minkowski minimum after inflation is at  $X = 0$ , and  $|\chi_1| = |\chi_2| = \mu$ . In the minimum  $G_X = G_{\chi_{\pm}} = 0$  and susy is restored. There is no relation between inflation and low energy susy breaking. The sgoldstino during inflation is unrelated to the sgoldstino today.

The masses of waterfall fields along the inflationary trajectory can be found using the results of section 5.2.4. The mass eigenstates are the linear combinations  $\chi_{\pm} = (\chi_1 \pm \chi_2)/\sqrt{2}$ . Using these as a basis the matrix  $x_n^{\tilde{z}}$  becomes diagonal during inflation. This shows that we can restrict our attention to only one of the complex fields  $\chi_{\pm}$ , the other field will give the same masses for its two real degrees of freedom. Now we can directly compute the masses from (5.28). The stability region as a function of  $b$  and  $|x|$  is plotted in figure 5.1. The inflationary trajectory corresponds to a vertical trajectory in the plot, going upwards as the field rolls down. When it irrevocably hits the instability region (i.e. when the lower mass eigenvalue becomes negative), inflation ends.

We note that a similar stability analysis can be done for all models of sgoldstino inflation. Whereas hybrid inflation critically makes use of the instability regions, for any non-hybrid scenario — being it small or large field inflation — the inflationary trajectory would have to stop before reaching the instability region. This is automatic for  $|x| < 1$ , otherwise the stability conditions place an upper bound on  $b$  during inflation. We will return to this point shortly when discussing small field inflation.

### 5.3.3 Small field inflation

As was already stated in section 1.5, symmetries generically do not help in solving the  $\eta$  problem in the small field models. For example, a shift symmetry  $K = K(X - \bar{X})$ , so useful in large field models, does not do anything in the small field regime. By Taylor expanding the Kähler potential and performing a Kähler transformation, it becomes equivalent to a non shift symmetric  $K = K(X\bar{X})$ . R-symmetries may help in providing a flat potential, but the R-symmetry breaking, which is necessary to obtain a Minkowski vacuum, also tends to spoil the flatness. This is what kills the model proposed in [127], on which we will comment in a bit more detail below. Note that in a sugra model the  $\eta$ -parameter cannot be tuned for arbitrary Kähler geometry [128, 129, 130]. In our example below we will assume an (approximately) canonical Kähler potential, for which there are no obstacles. Ref. [130] considered modular inflation near a maximum; we come back to this model at the end of this section.

We were able to construct a fine-tuned small field inflation model in sugra containing only a single chiral field. In such a set-up the inflaton is automatically the sgoldstino, and our example is an existence proof for small field sgoldstino inflation. Consider a model with<sup>10</sup>

$$K = \sum_n \alpha_n (X\bar{X})^n, \quad W = \sum_n \lambda_n X^n. \quad (5.33)$$

We decompose the complex scalar  $X = (\phi + i\theta)/\sqrt{2}$  with  $\phi$  the inflaton field. The model parameters  $\lambda_n, \alpha_n$  can be tuned in such a way that the potential allows for inflation near an inflection point which, without loss of generality, is located at the origin  $(\phi, \theta) = (0, 0)$ , and a Minkowski minimum at finite field value  $(\phi, \theta) = (\phi_0, 0)$ . In particular, we demand

- Vanishing slope and curvature of the potential at the origin 1)  $V_{\phi}|_{(0,0)} = 0$  and 2)  $V_{\phi\phi}|_{(0,0)} = 0$ , to assure zero slow roll parameters  $\epsilon = \eta = 0$ . The condition on  $\eta$  may be relaxed to  $\eta \lesssim 10^{-2}$ .

<sup>10</sup>This ansatz (5.33) is equivalent to  $G = \sum_{n=1} \alpha_n (X\bar{X})^n + \log |\sum_{n=0} \lambda_n X^n|^2$ .

- The height 3)  $V|_{(0,0)} \equiv V_0$  of the potential at the origin is fixed by the COBE normalization of the inflaton perturbations.
- After inflation the inflaton settles in a local Minkowski minimum with 4)  $V|_{(\phi_0,0)} = 0$  and 5)  $V_\phi|_{(\phi_0,0)} = 0$ . Moreover, the masses are positive definite 6)  $m_i^2|_{(\phi_0,0)} > 0$ .
- Along the whole trajectory, from the extremum to the minimum, the orthogonal field is stabilized 7)  $V_\theta = V_{\phi\theta} = 0$  and 8)  $m_\theta^2 \gtrsim H^2$ .

We consider solutions with canonical kinetic terms, i.e. we set  $\alpha_1 = 1$  and  $\alpha_i = 0$  for  $i \neq 1$ . To satisfy conditions 1-5 we need at least five parameters and choose them accordingly. We take all  $\lambda_i$  real, and consider the first five in the expansion. Tuning is required to satisfy conditions (2) and (4) - the smallness of  $\eta$  parameter and of the cosmological constant - in the usual sense that large contributions should nearly cancel. Conditions 6-8 are then checked for consistency, but do not require any new input. Setting the minimum at  $\phi_0 = 1$  we find two inflationary inflection point solutions<sup>11</sup>

$$\{\lambda_0, \lambda_1, \lambda_2, \lambda_3, \lambda_4\} = \sqrt{\frac{V_0}{23}} \times \{3, -5\sqrt{2}, 3, 0, 2\}, \quad (5.34)$$

and

$$\{\lambda_0, \lambda_1, \lambda_2, \lambda_3, \lambda_4\} = \frac{\sqrt{V_0}}{19\sqrt{73}} \times \left\{ 3\sqrt{39287 - 1464\sqrt{6}}, \sqrt{2(543551 - 19764\sqrt{6})}, 3\sqrt{39287 - 1464\sqrt{6}}, 0, -2\sqrt{4943 - 1152\sqrt{6}} \right\}, \quad (5.35)$$

and all other  $\lambda_i$  are zero.

Both examples above correspond to inflection point inflation, rather than to inflation near a maximum or saddle point. This is unfortunate, as for inflection point inflation the spectral index is bounded to be  $n_s \lesssim 0.92$ , which is by now ruled out by  $\sim 4\sigma$  (see (1.51)). We review this argument in appendix E.

The spectral index can be larger if the cubic term is absent or unnaturally small, as is the case for inflation at a maximum rather than an inflection point. Then the correction to the spectral index (E.4) is set by the quartic term in the Taylor expansion around the extremum, rather than by cubic term, with an upper bound  $n_s \lesssim 0.95$ . In our set-up this would require an extra tuning condition  $V_{\phi\phi\phi} \approx 0$ ; without it we always find a saddle point.

The first solution above (5.34) has a supersymmetric Minkowski minimum. In this scenario the susy breaking observed today is not related to the susy breaking during inflation. The second solution (5.35), however, does end in a susy breaking minimum, and the gravitino mass today can be related to the inflationary scale. The gravitino mass is  $m_{3/2} \sim 10^{-7}$ , see appendix E.

There is a huge difference between the two solutions when combined with other spectator fields. The first solution has a susy preserving vacuum in which  $W \rightarrow 0$ . Although at this exact point our description in terms of a Kähler function  $G$  breaks down, we can nevertheless describe the behavior of the potential as we approach this singular limit. We find that  $b \propto V_0/W_0 \rightarrow \infty$ , with  $b$  defined in (5.23). This implies that if we draw the stability diagram for the simplified case of separable Kähler functions (5.25), see figure 5.3, this inflationary model corresponds to vertical trajectories going upwards to infinity.

The position on the horizontal axis given by  $|x|$  depends on the specifics of the spectator sector, but it is clear that for all  $|x| > 1$  one of the fields becomes tachyonic as the inflaton approaches its minimum, and

<sup>11</sup> $\lambda_3 = 0$  only vanishes for  $\phi_0 = 1$ , but is non-zero for other positions of the minima.

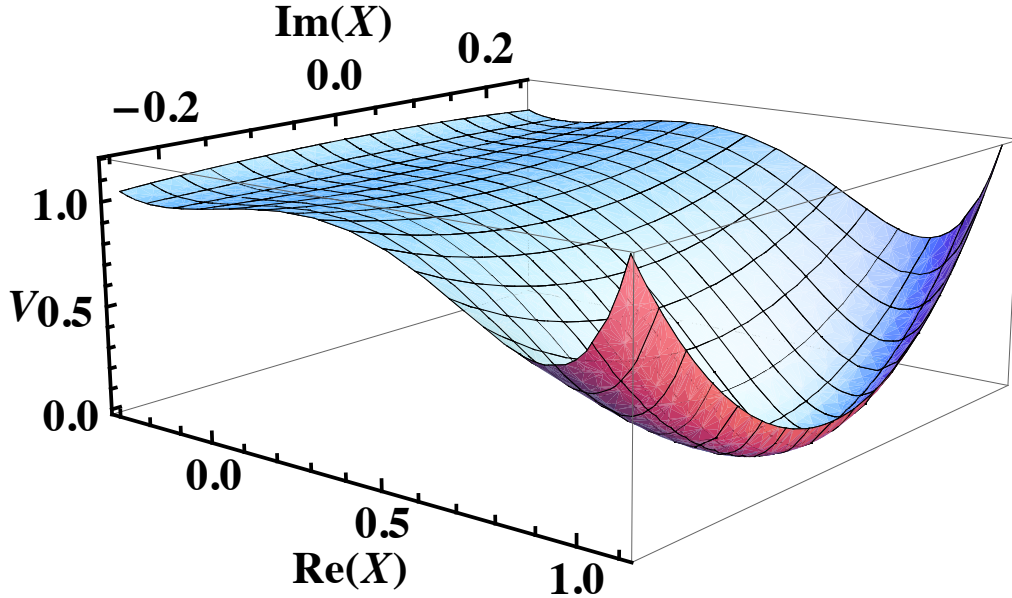


Figure 5.2: *Scalar potential for small field inflation corresponding to the first solution (5.34).*

the potential is unstable. Hence, solution (5.34) with a susy vacuum can only be combined with different fields if this extra sector has  $|x| < 1$  (for several fields the eigenvalues of the  $|x|^2$  matrix should all be less than unity). This puts enormous limitations on the spectator sector. For  $|x| < 1$  the masses of the spectator fields vanish in the vacuum, as discussed at the end of section 5.2.4. However, in a subsequent susy breaking phase transition they may pick up a soft mass term.

This disastrous conclusion may be avoided by going to the most generic Kähler function for sgoldstino inflation (5.14) rather than sticking to the separable case (5.25); it is hard to make a general prediction as in the  $b \rightarrow \infty$  limit also the other quantities  $x, w, y$  in the mass matrix (5.24) may blow up.

In contrast, solution (5.35) has a susy breaking vacuum, and the parameter  $b = V_0/W = 0$  vanishes in the minimum. The inflaton trajectory again corresponds to a vertical trajectory in the stability diagram, but now going downwards. Except for a small region near  $|x| = 1$  there are no instabilities in the potential, and at least for the separable Kähler function (5.25) sgoldstino inflation can straightforwardly be combined with a spectator sector. In the region  $|x| > 1$  the spectator fields are heavy in the vacuum and can be integrated out to get a low energy EFT. In the other limit  $|x| < 1$  the spectator fields are of the same order as the gravitino mass (see the discussion at the end of section 5.2.4), and are relatively light.

Ref. [130] constructed a single-field potential with a maximum, rather than an inflection point, suitable for inflation. As remarked above, this set-up gives a spectral index in better agreement with the Planck data than our inflection point model. The flat maximum was obtained by only allowing odd powers in the superpotential  $W = \sum \lambda_{2n+1} \Phi^{2n+1}$ , and fine-tuning the lowest four  $\lambda_{2n+1}$  parameters. In the absence

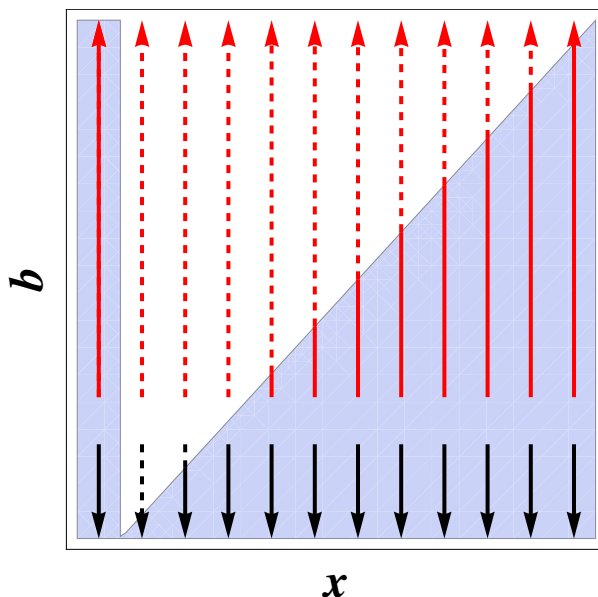


Figure 5.3: *Stability plot of the spectator  $z$ -fields for a separable Kähler function  $G = g(X, \bar{X}) + \tilde{g}(z, \bar{z})$ . The trajectories for small field inflation are vertical lines, going upward (red) to infinity for solution (5.34) which has a susy preserving vacuum, and downward (black) to zero for (5.35) which has a susy breaking vacuum. Dashed lines indicate unstable trajectories. The position on the horizontal axis depends on the specifics of the spectator sector. Solution (5.34) always leads to an instability for  $|x| > 1$ .*

of a symmetry that can guarantee this form of the superpotential, this model is more fine-tuned than the inflection point set-up, as it also requires tuning the even parameters  $\lambda_{2n} = 0$ ; not only the  $\eta$ -parameter is tuned, but also  $V_{\phi\phi\phi}$  at the extremum should vanish. We further note that in this set-up  $W \rightarrow 0$  at the maximum, and thus  $b \rightarrow \infty$ . As discussed above, this puts very strong constraints on the spectator sector, and may make it harder to embed the inflaton model in a larger parent theory.

### Recent proposals for small field sgoldstino inflation

In the recent literature there have been claims for small field sgoldstino inflation, with no or very little fine-tuning of the parameters in the potential. Unless some symmetry principle is invoked, this is not possible as the slow-roll parameters generically blow up in the small field limit. (For example, for  $V \sim \phi^4$  we get  $\epsilon, \eta \sim 1/\phi^2$ .) Indeed we find that these proposals do not work, although the devil is sometimes in the details.

Refs. [119, 120] propose a model of sgoldstino inflation in a single field set-up without tuning of parameters. To address the  $\eta$  problem a logarithmic term is added to the Kähler potential

$$\begin{aligned} K &= X\bar{X} + aX\bar{X}(X + \bar{X}) + b(X\bar{X})^2 + \dots - 2\ln(1 + X + \bar{X}), \\ W &= fX + f_n M. \end{aligned} \tag{5.36}$$

However, in the small field regime the logarithm can simply be expanded and does not alter the qualitative structure of the potential. It also does not enhance the symmetry.

Taking arbitrary parameters, except for the constraint that the minimum at the origin is stable and has zero cosmological constant, both the epsilon- and eta parameter exceed unity throughout the whole field space  $|X| < 1$ . Slow-roll inflation cannot take place. In [119] it is actually claimed that  $\epsilon < 1$ , but what is calculated is  $\epsilon_\theta = g^{\theta\theta}(V_\theta/V)^2$ , where we again decomposed the field  $X = (\phi + i\theta)/\sqrt{2}$  and  $g_{ij}$  is the metric in field space. However, in a situation where the potential falls much steeper in the  $\phi$ -direction than in the  $\theta$ -direction, this is not the relevant slow-roll parameter. Instead, one should use the more general multifield generalization  $\epsilon = g^{ij}V_iV_j/V^2$ .

Ref. [120] shows inflationary trajectories with a large number of e-folds  $N > 60$ . However, their trajectories are calculated in the - non-applicable - slow-roll approximation. For all initial points in field space proposed in [119, 120] we have solved the full two dimensional field equations and the slow-roll approximations to them. In all cases the slow-roll solutions wildly diverge from the full solutions, which can only give inflation for less than an e-fold, confirming once more that this setup does not provide a slow-roll regime.

The only way to get inflation in the set-up of [119, 120] is to tune parameters near an extremum, along the lines of our example (5.33).

Ref. [127] proposes a model with an approximate R-symmetry:

$$K = S\bar{S} + \alpha(S\bar{S})^2, \quad W = W_0 + \mu^2 S - \frac{\lambda}{2(n+1)} S^{n+1}. \quad (5.37)$$

The R-symmetry is only broken by  $W_0$  and the higher order term in the superpotential. In the absence of the constant  $W_0$ , this assures that the potential is nearly flat near the origin, as there is no quadratic and cubic term in the superpotential. The potential is only lifted by the higher order quartic term in the Kähler (which must be tuned  $|\alpha| < 10^{-2}$ ), and the one loop Coleman-Weinberg correction (which vanishes at the origin).

The set-up looks ideal for inflation. However, the  $n$  degenerate minima of the potential are all anti-de Sitter. To get a Minkowski minimum after inflation, the constant  $W_0$  has to be turned on. And although this is a small correction to the potential near the minimum, it is the dominant correction to the inflationary plateau at the origin, and gives rise to non-zero slow roll parameters  $\epsilon$  and  $\eta$ . We find that the resulting potential is too steep to generate 60 e-folds of inflation (at most a single e-fold is possible). Moreover, the tilt of the classical potential (not including the one-loop contribution, which may change this) is such that, unless there is some initial velocity to make it roll uphill, the inflaton will not end in the minimum which is lifted to  $V = 0$ , but rather in one of the other AdS minima.

For concreteness, we can choose to uplift the AdS minimum at positive values of  $\phi$  to a Minkowski minimum (with  $X = (\phi + i\theta)/\sqrt{2}$ ). Moreover, just as [127], we take the parameters in the superpotential real, which simplifies the analysis. The resulting potential will have a positive slope at the origin, as argued above, which kills inflation at the origin. There will however always be a maximum of the potential in between the origin and the minimum. Can we do inflation here? Although the R-symmetry has lost all of its power here (as it can only help to keep the potential flat near the origin), this is still a possibility. However, while the epsilon parameter vanishes at the maximum, the  $\eta$  parameter naturally exceeds unity. Of course,  $\eta$  can be tuned, but as follows from our analysis in section 5.3.3, to satisfy all constraints one needs at least five parameters. The potential of [127] has not enough freedom to do so. Moreover, adding extra, say, higher order terms, and trying to tune  $\eta$ , we find that the maximum morphs into an inflection point (although we did by no means an exhaustive study). This is as expected, there is no reason, no symmetry, assuring that when expanded around the extremum as in (E.1), the cubic term should vanish.

## 5.4 Conclusions

Inflationary models in supergravity, where the inflaton sits in a complex scalar superfield, necessarily involve a multifield analysis. Any extra fields present during inflation must be integrated out to give an effective single field slow-roll dynamics that is consistent with the CMB. However, even very heavy fields can leave a detectable imprint in the spectrum of primordial perturbations, in particular through a reduction in the speed of sound of the adiabatic perturbations. The correct effective field theory for the adiabatic mode has a variable speed of sound that depends on the background trajectory. A necessary condition to recover the standard single field slow-roll description is that the trajectory should have no turns into the heavy directions. In this case, the speed of sound is unity, equal to the speed of light, and integrating out the extra fields gives the same effective action as truncating the heavy fields at their adiabatic minima.

In supersymmetric models there is an extra complication. One has to integrate out whole supermultiplets in order to obtain an effective supergravity description for the remaining superfields. This is only possible if the superfields that are being integrated out are in configurations that do not contribute to susy breaking.

Sgoldstino inflation naturally implements these two conditions. The full inflationary dynamics is confined to the sgoldstino plane. Putting the scalar components of all other superfields at their minima is a consistent truncation of the parent theory. This makes sgoldstino inflationary models extremely attractive, because of their simplicity and robustness.

We have analysed sgoldstino inflation scenarios exploiting the fact that the Kähler invariant function  $G = K + \log |W|^2$  has a relatively simple form (5.14) which allows some aspects to be analysed in a model independent way. We derived a necessary and sufficient condition on the Kähler function (5.24) for the stability of the susy-preserving sector, the spectator fields that are integrated out. Figure 5.1 shows the constraint for a separable Kähler function, in particular for hybrid F-term inflation (which is a well studied case of sgoldstino inflation).

In the case of small field sgoldstino inflation we were able to provide some viable fine-tuned examples around inflection points. The spectral index is rather low, which is problematic in light of the Planck data. A higher spectral index would be possible with additional fine-tuning. Rather surprisingly, the inflationary model can only be straightforwardly combined with a spectator sector if the minimum after inflation breaks susy. In our inflation example with a susy preserving Minkowski vacuum the spectator sector is very constrained by the condition that there should be no tachyonic modes in the system. This is illustrated in figure 5.3. These constraints would also affect the hilltop inflation examples in [130].

One of the motivations for this study was the interesting suggestion, put forward in [119], that a relatively simple supergravity model with a single chiral sgoldstino superfield could account for both inflation and susy breaking in the vacuum. Contrary to claims in [119, 120], our conclusion is that this minimal scenario is very tightly constrained and requires the usual level of fine-tuning that is expected on general grounds. Another interesting model was proposed in [127], in which the flatness of the inflationary plateau follows from an R-symmetry. However we find that the R-symmetry breaking needed to obtain a Minkowski vacuum introduces an unacceptable tilt in the potential, and prevents inflation. It is possible that variations of this model may still work with some extra fine-tuning.

## Chapter 6

# Gauge field production and non-Gaussianity

### 6.1 Introduction

In this chapter we combine a new class of models of chaotic inflation in supergravity with a new mechanism of generating non-Gaussian perturbations from gauge field production during inflation. This combination is very well motivated, as the inflaton-gauge-gauge coupling needed to have reheating in this class of inflation models is the same as the coupling that produces (massless) gauge fields in this new mechanism. However, we also point at a potential problem: the produced gauge fields seem to produce too many primordial black holes to be compatible with current experimental limits. A modification of the original mechanism which employs massive gauge fields provides a safe way to avoid these black hole problems. We show how such a modification could also be embedded in the chaotic inflation models we have in mind. However, the recent Planck results on non-Gaussianity [19] limits the allowed parameter space of this second class of models as well. In this chapter we will work with the WMAP limits [131] on non-Gaussianity and other cosmological parameters (which were the tightest constraints available when this work was carried out), but in the conclusions we will confront the model with the new Planck results. This chapter is based on our work [5].

The broad class of models of chaotic inflation in supergravity that we want to study was developed in a recent series of papers [123, 124, 125]. These models generalize the simplest model of this type proposed long ago in [132]; see also [133, 134, 135, 136, 137, 138, 139, 103, 140, 33, 141, 34, 142, 143, 144, 145] for a partial list of other closely related publications.

The new class of models [123, 124, 125] describes two scalar fields,  $S$  and  $\Phi$ , with the superpotential

$$W = Sf(\Phi) , \tag{6.1}$$

where  $f(\Phi)$  is a real holomorphic function such that  $\bar{f}(\bar{\Phi}) = f(\Phi)$ . Any function which can be represented by Taylor series with real coefficients has this property. The Kähler potential is chosen according to the symmetry considerations in sections 1.5 and 1.6:

$$K = K((\Phi - \bar{\Phi})^2, S\bar{S}). \tag{6.2}$$

In this case, the Kähler potential does not depend on  $\phi = \sqrt{2} \operatorname{Re} \Phi$ . Inflation occurs along the direction

$S = \text{Im } \Phi = 0$ , and the field  $\phi$  plays the role of the inflaton field with the F-term potential, from (1.67),

$$V(\phi) = |f(\phi/\sqrt{2})|^2. \quad (6.3)$$

All scalar fields have canonical kinetic terms along the inflationary trajectory  $S = \text{Im } \Phi = 0$ . Note that in this set-up  $S$  is the sgoldstino field. In the previous chapter, we employed this field as an inflaton. Now it is used as a stabilizer field.

This class of models can be further extended [103, 125] to incorporate a KKLT-type construction with moduli stabilization [102, 146, 147], see also the next chapter, which may have interesting phenomenological consequences and may provide a simple solution to the cosmological moduli and gravitino problems [148, 149].

The generality of the functional form of the inflationary potential  $V(\phi)$  allows one to describe *any* combination of the parameters  $n_s$  and  $r$ . Thus, this rather simple class of models may describe *any* set of observational data which can be expressed in terms of these two parameters by an appropriate choice of the function  $f(\Phi)$  in the superpotential. Meanwhile the choice of the Kähler potential controls masses of the fields orthogonal to the inflationary trajectory [123, 124, 125]. Reheating in this scenario requires considering the scalar-vector coupling  $\sim \phi F_{\mu\nu} F^{\mu\nu}$  [125, 150]. If not only the inflaton but some other scalar field has a mass much smaller than  $H$  during inflation, one may use it as a curvaton field [151] for generation of non-Gaussian perturbations in this class of models [152].

In this chapter, we will study an alternative formulation of this class of models, with the Kähler potential

$$K = K((\Phi + \bar{\Phi})^2, S\bar{S}). \quad (6.4)$$

The simplest version of models of that type, with the Kähler potential

$$K = S\bar{S} + \frac{1}{2}(\Phi + \bar{\Phi})^2 \quad (6.5)$$

was first proposed [132]. In this case, the Kähler potential does not depend on  $\chi = \sqrt{2} \text{Im } \Phi$ , which plays the role of the inflaton field with the potential

$$V(\chi) = |f(\chi/\sqrt{2})|^2. \quad (6.6)$$

The description of inflation in the models (6.2) and (6.4) coincides with each other, up to a trivial replacement  $\phi \rightarrow \chi$ , as long as vector fields are not involved in the process.

The difference appears when one notices that in the model (6.4) the inflaton field is a pseudoscalar, which can have a coupling to vector fields

$$\frac{\alpha}{4} \chi F_{\mu\nu} \tilde{F}^{\mu\nu}, \quad (6.7)$$

where  $\tilde{F}^{\mu\nu} \equiv \epsilon^{\mu\nu\rho\sigma} F_{\rho\sigma}$  and  $\alpha$  is a dimensionful constant. This coupling is expected to be present since it is compatible with all the symmetries, including a shift symmetry in  $\chi$ .

Here we come to the second ingredient of our set-up: the mechanism of generating a non-Gaussian signal from gauge field production during inflation. The study of the phenomenological effects of the coupling (6.7) has received a lot of attention lately [153, 154, 155, 156, 18, 157, 158]. In particular, it has been shown in [156, 18] that, if the constant  $\alpha$  is large enough, such a coupling can lead to a copious production of gauge fields due to the time dependence of  $\chi$ . Through their *inverse decay* into inflaton perturbations, these gauge fields yield an additional contribution to the scalar power spectrum which is

both non-Gaussian and violates scale invariance. In this way it is possible to obtain non-Gaussian and non-scale invariant effects that can be observed by the Planck satellite and has not yet been ruled out yet by WMAP, although the parameter space corresponding to such a signal is relatively small [158]. In addition, gauge fields source tensor modes and lead to a stochastic gravity wave signal that could be detected at interferometers such as Advanced LIGO or Virgo [159, 157] (see also [160]).

Since the new class of inflationary models in supergravity needs a coupling between the inflaton and gauge fields to have successful reheating, we have to consistently take into account the violations of Gaussianity and scale invariance induced by the inverse decay mechanism. This is the topic of section 6.2.

A potential threat in this model is the overproduction of primordial black holes. As we will see in section 6.3, at very small scales, far beyond what is observable by the CMB, the produced gauge quanta largely increase the curvature power spectrum. At some point, various forms of backreaction stops this growth, but by then the power spectrum has reached  $\Delta_\zeta^2 \sim \mathcal{O}(10^{-3})$ . In section 1.4 we have explained that at such high values, a statistical fluctuation might locally increase the density so that primordial black holes are formed. In this way the non-detection of primordial black holes puts an observational upper bound on the power spectrum, which we discuss in section 6.4. Our estimates for the late-time power spectrum land a factor of six above this bound (compare e.g. (6.33) with (6.39)). Since we expect our estimate to be reliable up to factors of order one, we cannot definitively claim that the inverse decay mechanism and its interesting phenomenology is incompatible with current data, but our result on production of primordial black holes highlights a clear tension.

In section 6.5 we describe an alternative mechanism of generation of non-Gaussian perturbations, proposed in [158]. This mechanism requires introduction of a light  $U(1)$  charged field  $h$  with mass  $m_h \ll H$ , where  $H$  is the Hubble constant during inflation. Inflationary perturbations of this field generate a slightly inhomogeneous distribution of a classical scalar field  $h(x)$ . This field induces the vector field mass due to the Higgs effect.

As a result, the vector field mass  $\sim eh(x)$  (with  $e$  the  $U(1)$  coupling constant) takes different values, controlled by fluctuations of the field  $h$ . In the parts of the universe where the value of the vector field mass is small, the vector field fluctuations are easily produced since the gauge mass quenches the tachyonic instability. This in turns leads to a longer stage of inflation because of the additional friction generated by the gauge fields. Meanwhile in the parts of the universe where the fluctuations of the light scalar field  $h$  make this field large, the vector field mass becomes larger and inflation is shorter due to the lack of backreaction. As a result, fluctuations of the light scalar field  $h$  lead to fluctuations of the total number of e-foldings  $\delta N$ , i.e. to adiabatic perturbations of metric. We will show that this effect may generate significant primordial local non-Gaussianity. Also, in the regime of parameters relevant for this scenario the primordial black hole bounds are satisfied parametrically.

To implement this mechanism in our supergravity-based inflationary scenario, one should find a way to guarantee smallness of the mass of the field  $h$  during inflation. We will describe a model where the mass squared of this field during inflation is equal to  $m_h^2 = \gamma H^2$ , where  $\gamma$  can be made small by a proper choice of the Kähler potential.

In section 6.6 we study the evolution of the light field  $h$  during inflation in our scenario, which is similar to the evolution of the curvaton field  $\sigma$  in [152], so we will continue calling this field the curvaton, and use the results of [152] for the description of its evolution. In the original model of [152], just as in any other curvaton model [151], adiabatic perturbations of metric are generated by perturbations of the field  $h$  after a complicated sequence of reheating, expansion of the universe, and the subsequent decay of the curvaton field. In our scenario, adiabatic perturbations are produced due to the modulation of the duration of inflation by the perturbations of the field  $h$ . As we will demonstrate, this mechanism can easily produce local non-Gaussianity in the potentially interesting range  $f_{\text{NL}}$  from  $\mathcal{O}(10)$  to  $\mathcal{O}(100)$ , even

if the coupling constant  $\alpha$  is not very large.

Finally, in section 6.7, we find that typical values of the coupling constant  $\alpha$  considered in this work lead to a relatively high perturbative reheating temperature  $T \sim 10^{10}$  GeV. This should be read as a lower limit, since the copious non-perturbative production of gauge fields already during inflation could lead to and even higher reheating temperature. This could lead to the cosmological gravitino problem [161], but in the class of models with strong moduli stabilization and gravitino mass  $\mathcal{O}(100)$  TeV this problem does not appear [149].

## 6.2 CMB scales: violations of Gaussianity and scale invariance

Recently there has been a lot of interest in the effect of gauge field production in pseudoscalar (axion) inflation [153, 154, 155, 156, 18, 157, 158]. In this section we summarize the main points.

Consider a pseudoscalar inflaton with a potential suitable for inflation. The symmetries of the theory allow for a coupling  $\chi F_{\mu\nu} \tilde{F}^{\mu\nu}$  to some  $U(1)$  gauge sector. This coupling is essential for reheating in the supergravity models we discussed in section 6.1. We will therefore consider the following bosonic part of the action<sup>1</sup>

$$S = - \int d^4x \sqrt{-g} \left[ \frac{1}{2} (\partial\chi)^2 + \frac{1}{4} F^2 + \frac{\alpha}{4} \chi F \tilde{F} + V(\chi) \right].$$

Since all relevant effects arise from the couplings above we can safely neglect the gravitational interaction between perturbations and work with an unperturbed FLRW metric<sup>2</sup>. We organize the perturbation theory based on the equations that we are able to solve. Consider two classical<sup>3</sup> fields  $\vec{A}(x, t)$  and  $\chi(t)$  that solve these two coupled differential equations

$$\ddot{\chi} + 3H\dot{\chi} + \frac{\partial V}{\partial \chi} = \alpha \langle \vec{E} \cdot \vec{B} \rangle, \quad (6.8)$$

$$\vec{A}'' - \nabla^2 \vec{A} - \alpha \chi' \nabla \times \vec{A} = 0, \quad (6.9)$$

where  $\vec{E} \equiv -\dot{\vec{A}}/a$ ,  $\vec{B} \equiv a^{-2} \nabla \times \vec{A}$  and  $\vec{E} \cdot \vec{B} = -F\tilde{F}/4$  are computed from  $\vec{A}$ . As before, dots denote derivatives with respect to  $t$ , primes denote derivatives with respect to conformal time  $\tau$ .

Now let us look at the action expanded around  $\chi$  and  $\vec{A}$ , i.e.  $S[\chi + \delta\chi, \vec{A} + \delta\vec{A}]$ . Organizing the result at various orders in  $\delta\chi$  and  $\delta\vec{A}$  one finds

$$\begin{aligned} S = \text{const} - \int d^4x \sqrt{-g} (\delta\chi) \alpha \left[ \langle \vec{E} \cdot \vec{B} \rangle - \vec{E} \cdot \vec{B} \right] - \int d^4x \sqrt{-g} \left[ \frac{1}{2} (\partial\delta\chi)^2 + \frac{1}{2} \frac{\partial^2 V}{\partial \chi^2} (\delta\chi)^2 + \frac{1}{4} (\delta F)^2 \right. \\ \left. + \frac{\alpha}{4} \chi \delta F \delta \tilde{F} + \frac{\alpha}{2} \delta\chi \delta F \tilde{F} \right] - \int d^4x \sqrt{-g} \left[ \frac{\alpha}{4} \delta\chi \delta F \delta \tilde{F} + \frac{1}{6} (\delta\chi)^3 \frac{\partial^3 V}{\partial \chi^3} \right], \end{aligned}$$

where again the classical background fields  $\chi$  and  $\vec{A}$  solve (6.8) and (6.9). Notice that there is a ‘‘tadpole’’ for  $\delta\chi$  due to the fact that at the background level we solved an inhomogeneous equation for  $\vec{A}$  but just

<sup>1</sup>Notice that in the existing literature, such a coupling is usually associated with interaction of the axion field with vector fields, with a coupling  $-\frac{\alpha}{4f}$ . In our approach it is not necessary to associate the pseudoscalar field with the axion field with the radius of the potential  $\sim f$ , so we normalize the coupling in terms of the reduced Planck mass  $M_p$ , which we then set to one, and consider the following interaction term  $-\frac{\alpha}{4} \chi F_{\mu\nu} \tilde{F}^{\mu\nu}$ . Note also that in this chapter we work in  $(-+++)$  metric.

<sup>2</sup>We are neglecting vector and tensor modes and the slow-roll suppressed interactions coming from the solution of the constraints on the lapse and the shift.

<sup>3</sup>Here we are assuming that the occupation number of the relevant gauge modes is large enough that one can approximate the resulting electromagnetic field with a classical one. This assumption is implicit in all other approaches so far.

a homogeneous one for  $\chi$ . From this term one also sees that  $\delta\chi$  will source  $\delta A^0$ , hence it will modify the constraint (6.12). The equations of motion in Coulomb gauge  $\partial_i A^i = 0$  are

$$a\delta\ddot{A}_i - \frac{\partial_k^2(\delta A_i)}{a} + aH\delta\dot{A}_i - \alpha\dot{\chi}\nabla \times (\delta\vec{A}) = \alpha\delta\dot{\chi}\nabla \times \vec{A} - \alpha(\nabla\delta\chi) \times \vec{A} - \partial_t(a\partial_i(\delta A^0)), \quad (6.10)$$

$$(\delta\ddot{\chi}) + 3H\delta\dot{\chi} - \nabla^2\delta\chi + \frac{\partial^2 V}{\partial\chi^2}\delta\chi = \frac{\alpha}{4} \left( \langle F\tilde{F} \rangle - F\tilde{F} - 2\delta F\tilde{F} \right), \quad (6.11)$$

$$a\partial_i\partial_i(\delta A)^0 = -\alpha\nabla(\delta\chi) \cdot \nabla \times \vec{A}. \quad (6.12)$$

The solution for the constraint equation for  $\delta A^0$  is

$$\delta A^0(x, t) = a^{-1} \int d^3y \frac{\alpha\nabla(\delta\chi) \cdot \nabla \times \vec{A}}{4\pi|x-y|}. \quad (6.13)$$

Unfortunately this coupled system of equations is hard to solve. Hence [156, 18] made the approximation of neglecting all terms quadratic or higher in  $\delta\chi$ ,  $\delta A$  and  $A$ . This is a good approximation as long as  $F\tilde{F}$  (or equivalently  $\langle \vec{E} \cdot \vec{B} \rangle$ ) is not too large (a more quantitative condition is given in (6.29)), which is the regime we will discuss in this section. In the next section we will see that, since  $\langle \vec{E} \cdot \vec{B} \rangle$  grows with time, towards the end of inflation this description is not valid anymore, and one has to take backreaction into account.

Solving the approximated equations of motion

$$a\ddot{A}_i - \frac{\partial_k^2 A_i}{a} + aH\dot{A}_i - \alpha\dot{\chi}\nabla \times \vec{A} = 0 \quad (6.14)$$

$$\delta\ddot{\chi} + 3H\delta\dot{\chi} - \nabla^2\delta\chi + \frac{\partial^2 V}{\partial\chi^2}\delta\chi = \alpha \left( \langle \vec{E} \cdot \vec{B} \rangle - \vec{E} \cdot \vec{B} \right) \quad (6.15)$$

one finds a tachyonic enhancement of the gauge fields. For the growing mode of one of the two polarizations of the gauge field we get

$$A = \frac{1}{\sqrt{2k}} e^{\pi\xi/2} W_{-i\xi, 1/2}(2ik\tau). \quad (6.16)$$

Here  $W_{\lambda, \mu}(x)$  denotes the Whittaker function, and  $\xi$  is defined as<sup>4</sup>

$$\xi \equiv -\frac{\dot{\chi}\alpha}{2H}. \quad (6.17)$$

As we see, the relation between the coupling constant  $\alpha$  and the value of  $\xi$  60 e-foldings before the end of inflation is model dependent, but for our model there is an approximate relation which is valid for the parameters that we are going to explore:

$$\alpha \sim 15\xi. \quad (6.18)$$

For  $\xi > 1$  the new coupling therefore leads to generation of perturbations of the vector fields around horizon scales. The produced gauge fields then change the dynamics of  $\chi$  and  $H$ . The cosmological homogeneous Klein-Gordon equation and the Friedmann equation get extra contributions from the gauge fields and can now be written as

$$\ddot{\chi} + 3H\dot{\chi} + \frac{\partial V}{\partial\chi} = \alpha \langle \vec{E} \cdot \vec{B} \rangle \quad (6.19)$$

$$3H^2 = \frac{1}{2}\dot{\chi}^2 + V + \frac{1}{2} \langle \vec{E}^2 + \vec{B}^2 \rangle. \quad (6.20)$$

<sup>4</sup>Note that we have some minus signs different from [156], but this is a matter of conventions. We will work with a model that has  $\dot{\chi} < 0$  during inflation and define  $\xi$  to be positive. The sign of  $\langle \vec{E} \cdot \vec{B} \rangle$  is always opposite to the sign of  $\dot{\chi}$ . Therefore the physical effect of the tachyonic enhancement is always that inflation is prolonged. To be precise: when  $\dot{\chi}$  is negative, the growing field is actually the opposite polarization, i.e.  $A_-$ , which makes that  $\langle \vec{E} \cdot \vec{B} \rangle > 0$  (see, for example, equation (8) in [154]).

They are computed as

$$\langle \vec{E} \cdot \vec{B} \rangle = \frac{1}{4\pi^2 a^4} \int_0^\infty dk k^3 \frac{\partial}{\partial \tau} |A|^2, \quad (6.21)$$

$$\langle \frac{\vec{E}^2 + \vec{B}^2}{2} \rangle = \frac{1}{4\pi^2 a^4} \int_0^\infty dk k^2 \left[ |A'|^2 + k^2 |A|^2 \right]. \quad (6.22)$$

After renormalization, one can reduce the integration interval to the region  $\frac{1}{8\xi} < \frac{k}{aH} < 2\xi$ , which is where the enhancement in the (derivative of the) gauge field takes place.

From the homogeneous Klein-Gordon equation (6.15) one reads off that the influence of the produced gauge fields on the homogeneous dynamics of  $\chi$  and  $H$  can be safely neglected as long as

$$\frac{\alpha \langle \vec{E} \cdot \vec{B} \rangle}{3H\dot{\chi}} \ll 1, \quad \frac{\frac{1}{2} \langle \vec{E}^2 + \vec{B}^2 \rangle}{3H^2} \ll 1. \quad (6.23)$$

Of these two conditions the first one is always the most stringent. When it stops to hold, backreaction on the homogeneous evolution becomes important and the evolution of  $\chi$  and  $H$  will be slowed down, which makes inflation lasts longer. We will see in the next section that backreaction on the inhomogeneous equation for  $\delta\chi$  happens even earlier. In this section we focus on the regime in which all of these effects are negligible, which e.g. for a quadratic potential corresponds roughly to  $\xi \lesssim 4$ . This is appropriate for the description of CMB scales.

Now we move to the power spectrum. The copiously generated gauge fields may, by inverse decay, produce additional perturbations of the inflaton field  $\delta\chi$ , proportional to the square of the vector field perturbations. As was shown in [156, 18], this can be described (up to backreaction effects to be described in the next section) by using (6.15). The inclusion of the source term leads to an extra contribution to the power spectrum of the curvature perturbation on uniform density hypersurfaces  $\zeta = -\frac{H}{\dot{\chi}}\delta\chi$  (see (1.39)). This has been computed in [156, 18] (we present a quick estimate in appendix F.2)

$$\Delta_\zeta^2(k) = \Delta_{\zeta,\text{sr}}^2(k) \left( 1 + \Delta_{\zeta,\text{sr}}^2(k) f_2(\xi) e^{4\pi\xi} \right). \quad (6.24)$$

Here  $f_2(\xi)$  was defined in [156, 18] and can be computed numerically (a useful large  $\xi$  approximation is given in (F.22)) and

$$\Delta_{\zeta,\text{sr}}^2(k) = \left( \frac{H^2}{2\pi|\dot{\chi}|} \right)^2 \quad (6.25)$$

is the amplitude of the vacuum inflationary perturbations as in standard slow-roll inflaton. WMAP [131] has measured  $\Delta_{\zeta,\text{sr}}^2(k_\star) = 2.43 \cdot 10^{-9}$ , where  $k_\star = 0.002 \text{Mpc}^{-1}$  is the pivot scale that we will take to correspond with  $N = 60$  e-foldings before the end of inflation. The second term in (6.24) violates both scale invariance (and Gaussianity as we will see below), since it comes schematically from  $A^2$ , i.e. the square of a Gaussian which grows with time as in (6.16).

We move to the bispectrum. The produced gauge fields lead to equilateral non-Gaussianity in the CMB [156, 18]

$$f_{NL} = \frac{\Delta_\zeta^6(k)}{\Delta_{\zeta,\text{sr}}^4(k)} e^{6\pi\xi} f_3(\xi), \quad (6.26)$$

where  $f_3(\xi)$  another function defined in [156, 18], which can be computed numerically (see (F.34) for a useful approximation). The amount of non-Gaussianity, therefore, depends exponentially on  $\xi$ . Between  $\xi = 0$  and  $\xi = 3$  it grows from  $\mathcal{O}(1)$  to  $\mathcal{O}(10^4)$  and most of the growth takes place in a small interval around  $\xi \simeq 2.5$ .

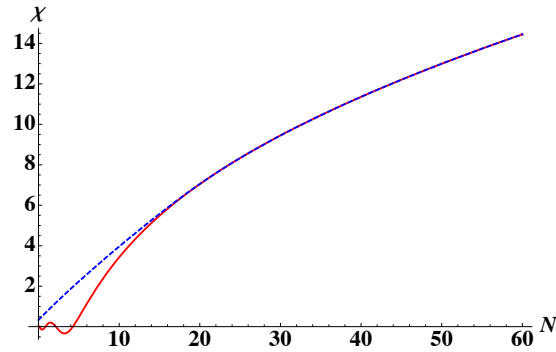


Figure 6.1: *The evolution of the inflaton field  $\chi$ , as a function of the number of e-folds  $N$  left to the end of inflation (time is moving to the left) for  $\xi[N = 60] = 2.2$ . The result in dashed blue does take backreaction from the sources in equations (6.19) and (6.20) into account, the result in red does not. It is clear that backreaction prolongs inflation.*

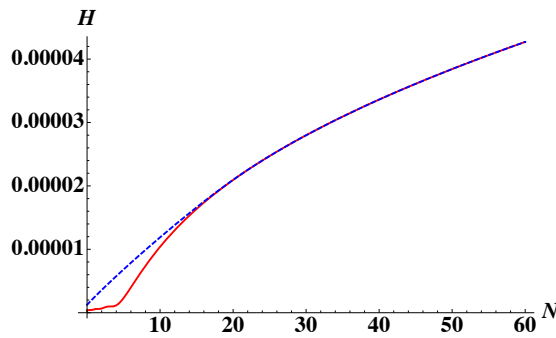


Figure 6.2: *The evolution of the Hubble scale  $H$  as a function of  $N$  for  $\xi[N = 60] = 2.2$ . Again the dashed blue line is the result corrected for backreaction from the sources in equations (6.19) and (6.20).*

The analysis of [158] showed that the bounds coming from the power spectrum (especially from WMAP plus ACT, because of the violation of scale invariance) and from the bispectrum (from WMAP) are compatible, with the former being typically slightly more stringent. Specifying a confidence region in  $\xi$  requires assuming some prior for this parameter. The physically best motivated prior is log-flat in  $\xi$  reflecting the fact the scale of the dimension five coupling  $\chi F \bar{F}$  could be anywhere (with strong indications that it should be below the Planck scale [166]). In this case at 95% CL one finds  $\xi \lesssim 2.2$ . A flat prior on  $\xi$  leads to  $\xi \lesssim 2.4$ .

### 6.3 Very small scales: strong backreaction

In this section we want to estimate the power spectrum and bispectrum towards the end of inflation, i.e. on scales that are too small to be observed in the CMB. The only observational handle available in this regime is the non-detection of primordial black holes, which puts an upper bound on the power spectrum [162, 20, 163, 164, 21, 165].

To make these estimates it is essential to recognize that many of the formulae described in the previous section and given in the literature about inverse decay are valid only in the regime in which backreaction on the inhomogeneous equation for  $\delta\chi$  is small (see (6.29)). As we show in the following, the scales relevant for the production of primordial black holes leave the horizon when backreaction is large. The authors of [167] did not account for backreaction and therefore their conclusion that gauge field production during inflation leads to black hole production might be premature.

For concreteness, we will consider a quadratic potential  $V(\chi) = \frac{1}{2}m^2\chi^2$ , with the mass chosen such that at the pivot scale  $k_*$  (that we take to correspond with  $N = 60$ ) we get  $\Delta_\zeta^2(k_*) = 2.43 \cdot 10^{-9}$ .

Let us first look at the dynamics of  $\chi$  and  $H$ . As we already discussed, when enough gauge field quanta have been produced, the conditions in (6.23) stop to hold (the inequality for  $\langle \vec{E} \cdot \vec{B} \rangle$  is violated first) and  $\chi$  and  $H$  are slowed down. As a result, inflation lasts longer. Let us check this. The behavior of  $\chi$ ,  $H$  and  $\xi$  as functions of  $N$  (the number of e-folds left to the end of inflation) follows from simultaneously solving (6.17), (6.19) and (6.20). In figures 6.1 and 6.2 we have plotted the solutions for  $\chi(N)$  and  $H(N)$ , with and without backreaction taken into account. For  $\xi(N = 60) = 2.2$ , the effect of backreaction becomes 10% around  $N = 11$ .

Now let us consider perturbations. Of course they will be affected by the backreaction on the homogeneous dynamics  $\chi$  and  $H$  that we described above, but there is more. Let us consider (6.10)-(6.12). In the last section we solved for  $A$  in a *homogeneous* background and used that result (6.16) to compute the source term in the equation for  $\chi$  perturbations. But as  $\delta A$  and  $\delta\chi$  grow larger toward the end of inflation (both of them grow as  $e^{2\pi\xi}$ ) the source in the right-hand side of (6.10) can not be neglected anymore. If we were able to solve this equation, we would find that  $\vec{E} \cdot \vec{B}$  now depends on the perturbation  $\delta\chi$ . Expanding  $\vec{E} \cdot \vec{B}$ , which is the source term in (6.11), in powers of  $\delta\chi$  we would find several new terms including additional friction and a modified speed of sound. In [154, 157] it was proposed how to estimate these effects in the regime of strong backreaction by just considering the additional friction term  $\delta\chi$ . The equation of motion for the perturbation  $\delta\chi$  becomes

$$\ddot{\delta\chi} + 3\beta H \dot{\delta\chi} - \frac{\nabla^2}{a^2} \delta\chi + \frac{\partial^2 V}{\partial \chi^2} \delta\chi = \alpha \left[ \vec{E} \cdot \vec{B} - \langle \vec{E} \cdot \vec{B} \rangle \right], \quad (6.27)$$

with the additional friction term

$$\beta \equiv 1 - 2\pi\xi\alpha \frac{\langle \vec{E} \cdot \vec{B} \rangle}{3H\dot{\chi}}. \quad (6.28)$$

Here the new term in  $\beta$  is caused by the dependence of  $\langle \vec{E} \cdot \vec{B} \rangle$  on  $\dot{\chi}$  (via its dependence on  $\xi$ ). The behavior of  $\beta$  has been plotted in figure (6.3). It is always positive<sup>5</sup>.

The new source of backreaction can be neglected as long as

$$2\pi\xi\alpha \frac{\langle \vec{E} \cdot \vec{B} \rangle}{3H\dot{\chi}} \ll 1. \quad (6.29)$$

Note (from comparison with (6.23)) that the factor of  $2\pi\xi$  makes that backreaction on the power spectrum will become significant before backreaction on  $H$  and  $\chi$  does. For  $\xi(N = 60) = 2.2$  we find that backreaction becomes of order 10% ( $\beta = 1.1$ ) at  $N = 22$ .

The modified equation of motion (6.27) suggests that (as was already noted in [157], see also appendix

---

<sup>5</sup>We work with negative  $\dot{\chi}$  which yields positive  $\langle \vec{E} \cdot \vec{B} \rangle$ , while working with  $\dot{\chi} > 0$  gives  $\langle \vec{E} \cdot \vec{B} \rangle < 0$ .

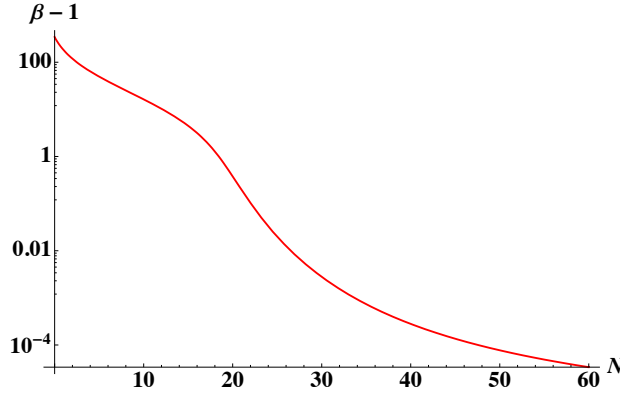


Figure 6.3: Evolution of  $(\beta - 1)$  as function of  $N$ , for  $\xi(N = 60) = 2.2$ .

F.2) we can estimate

$$\delta\chi \approx \frac{\alpha \left( \vec{E} \cdot \vec{B} - \langle \vec{E} \cdot \vec{B} \rangle \right)}{3\beta H^2} \quad (6.30)$$

which leads to the power spectrum

$$\Delta_\zeta^2(k) \simeq \langle \zeta(x)^2 \rangle \simeq \left( \frac{\alpha \langle \vec{E} \cdot \vec{B} \rangle}{3\beta H \dot{\chi}} \right)^2. \quad (6.31)$$

This estimate turns out to be particularly good in the regime in which we can check it, i.e. when  $\xi \lesssim 4$  when the backreaction is negligible and we can compare with (6.24) (see appendix F.2). This gives us confidence to use it also in the strong backreaction regime. It is easy to see that when backreaction becomes large, the second term in (6.28) dominates, and we end up with

$$\Delta_\zeta^2(k) \simeq \left( \frac{1}{2\pi\xi} \right)^2. \quad (6.32)$$

The estimate (6.31) for the power spectrum has been plotted in figure (6.4) together with the formula (6.24), valid only when backreaction is negligible. Indeed, in the regime of strong backreaction the power spectrum asymptotes the estimate in (6.32). At the end of inflation we have  $\xi \simeq 6.7$  (for  $\xi(N = 60) = 2.2$ ), which gives

$$\Delta_\zeta^2(k) \simeq 7.5 \cdot 10^{-4}. \quad (6.33)$$

## 6.4 Bounds from primordial black holes

In section 1.4 we have estimated the upper limit on the power spectrum set by the non-detection of primordial black holes. We found

$$\Delta_{\zeta,c}^2(k) \simeq \langle \zeta(x)^2 \rangle \simeq 0.008 - 0.05, \quad (6.34)$$

depending on the fraction of space  $b$  that can collapse to a black hole. Here we have  $b = 10^{-28} - 10^{-5}$ .

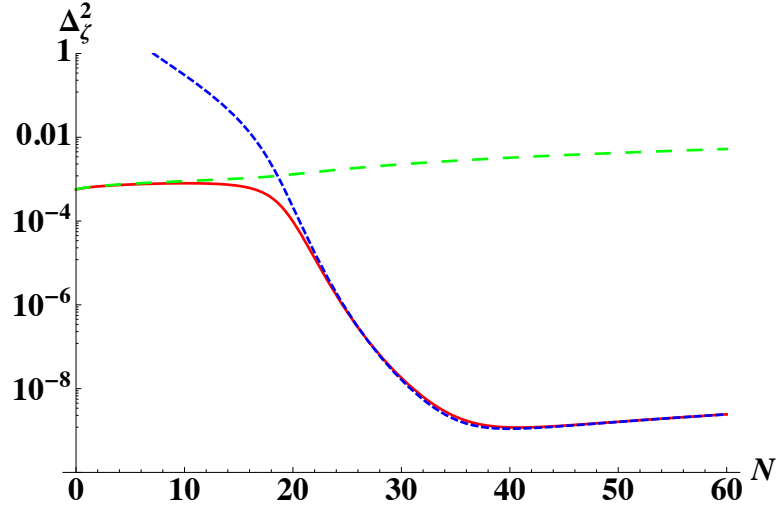


Figure 6.4: Evolution of the power spectrum as function of  $N$ , for  $\xi(N = 60) = 2.2$ . The expression (6.24) that does not take backreaction into account is in finely dashed blue. In solid red is the estimate (6.31). When backreaction becomes significant this estimate coincides with the late-time estimate  $(2\pi\xi[N])^{-2}$ , in largely dashed green.

However, there we worked with a Gaussian distribution for the comoving curvature perturbation  $\zeta$ . In our case  $\zeta$  does not follow a Gaussian distribution. Instead we have (see appendix F.2)

$$\zeta = -\frac{\alpha \left( \vec{E} \cdot \vec{B} - \langle \vec{E} \cdot \vec{B} \rangle \right)}{3\beta H \dot{\chi}}. \quad (6.35)$$

The stochastic properties of the vector field  $A$  are close to those in a free theory, i.e. it has Gaussian perturbations around  $\langle A \rangle = 0$ . As a consequence we can write <sup>6</sup>

$$\zeta = g^2 - \langle g^2 \rangle \quad (6.36)$$

with  $g$  a Gaussian distributed field. This model was studied in [21] and we follow that derivation (see also [163, 164]). The probability distribution function of  $\zeta$  follows from setting  $P(\zeta)d\zeta = P(g)dg$ , and takes the form

$$P(\zeta) = \frac{1}{\sqrt{2\pi(\zeta + \sigma^2)}\sigma} e^{-\frac{\zeta + \sigma^2}{2\sigma^2}}, \quad (6.37)$$

with  $\sigma^2 \equiv \langle g^2 \rangle$ . For a given value of  $b$  we can again infer  $\sigma^2$ . Setting  $t \equiv \frac{\zeta}{\sigma^2} + 1$  (and  $t_c \equiv \frac{\zeta_c}{\sigma^2} + 1$ ) we have  $d\zeta = \sigma^2 dt$  which gives

$$b = \int_{\zeta_c}^{\infty} P(\zeta)d\zeta = \int_{t_c}^{\infty} \frac{e^{-\frac{t}{2}}}{\sqrt{2\pi t}} dt = \text{Erfc} \left( \sqrt{\frac{t_c}{2}} \right), \quad (6.38)$$

where  $\text{Erfc}(x) \equiv 1 - \text{Erf}(x)$  is the complementary error function. Taking again  $b$  in the range  $10^{-28} - 10^{-5}$  one gets a tighter upper bound on the power spectrum than in the Gaussian case:

$$\begin{aligned} \Delta_{\zeta,c}^2(k) &\simeq \langle \zeta(x)^2 \rangle = 2\langle g^2 \rangle^2 \\ &\simeq 1.3 \cdot 10^{-4} - 5.8 \cdot 10^{-3}. \end{aligned} \quad (6.39)$$

<sup>6</sup>Here we can safely neglect the linear term, which is just the standard vacuum slow-roll contribution to  $\zeta$ . See also our estimate for  $f_{NL}$  at small scales in appendix F.4.

Now let us estimate what value of  $b$  is relevant for our investigation.

At the end of inflation, the total mass concentrated in the volume associated with perturbations leaving the horizon  $N$  e-foldings before the end of inflation with the Hubble constant  $H$  can be estimated by

$$M_N \simeq \frac{4}{3}\pi\rho r^3 \simeq \frac{4\pi M_{\text{p}}^2}{H} e^{3N}, \quad (6.40)$$

where we reinserted the reduced Planck mass  $M_{\text{p}}$ , which was set to one in the rest of this chapter, and  $H$  is calculated at the end of inflation. In order to study the subsequent evolution of matter in the comoving volume corresponding to this part of the universe, one should distinguish between two specific possibilities depending on the dynamics of reheating after inflation, discussed in section 6.7.

If reheating is not very efficient, then the universe for a long time remains dominated by scalar field oscillations, with the average equation of state  $p = 0$ . In this case, the total mass in the comoving volume does not change, and therefore at the moment when the black hole forms, its mass  $M_{\text{BH}}$  is equal to  $M_N$  evaluated in (6.40). For the parameters of our model, this gives an estimate (see appendix F.5 for details)

$$M_{\text{BH}} \simeq 10 e^{3N} \text{ g}. \quad (6.41)$$

On the other hand, if reheating is efficient, then the post-inflationary universe is populated by ultra relativistic particles and the energy density in comoving volume scales inversely proportional to the expansion of the universe. In this case, the black hole mass can be estimated as (see appendix F.5)

$$M_{\text{BH}} \simeq 10 e^{2N} \text{ g}. \quad (6.42)$$

In our estimates of the black hole production we will assume the latter possibility, though in general one may have a sequence of the first and the second regime. The final conclusion will only mildly depend on the choice between these two possibilities.

Now, the bounds on  $b$  in terms of the would-be black hole mass  $M_{\text{BH}}$  were given in [162] and updated in [20]. Here we follow the result in [20].<sup>7</sup> Using (6.38) and our estimates of the black hole mass as a function of  $N$ , we can translate this into a bound on the power spectrum as a function of  $N$ . The result is in figure 6.5.

Our estimate (6.33) *violates this bound* for all  $N \lesssim 20$  by a factor of about six. Since we have made some approximations both in deriving the late time power spectrum and in deriving its observational upper bound, our estimate could well be off by some order one factor and therefore we can not draw a definitive conclusion. It is clear though that the parameter values giving rise to an observable but not yet ruled out violation of scale invariance and non-Gaussianity in the CMB-window produce a late time power spectrum that comes at least very close to the primordial black hole bound. A more precise computation is needed to establish whether this bound is actually violated or not.

However, if such a computation revealed that primordial black holes do indeed constrain these models, that would yield a much stronger bound on  $\xi$  as the ones coming from non-Gaussianity and the violation of scale invariance. Since we have seen that the power spectrum has a late-time asymptotic of  $(2\pi\xi[N])^{-1}$ , this problem persists on a wide range of values for  $\xi$ .

For all values of  $\xi$ , our estimate for the power spectrum sharply increases before the end of inflation, the closer to the end the smaller  $\xi$  is. However, if we disregard black hole bounds for  $M_{\text{BH}} \lesssim 10^8$  g, which

<sup>7</sup>However, we do not take the constraints for  $M_{\text{BH}} < 10^8$  g into account, as these are either very model dependent, or assume that black hole evaporation leaves stable relics.

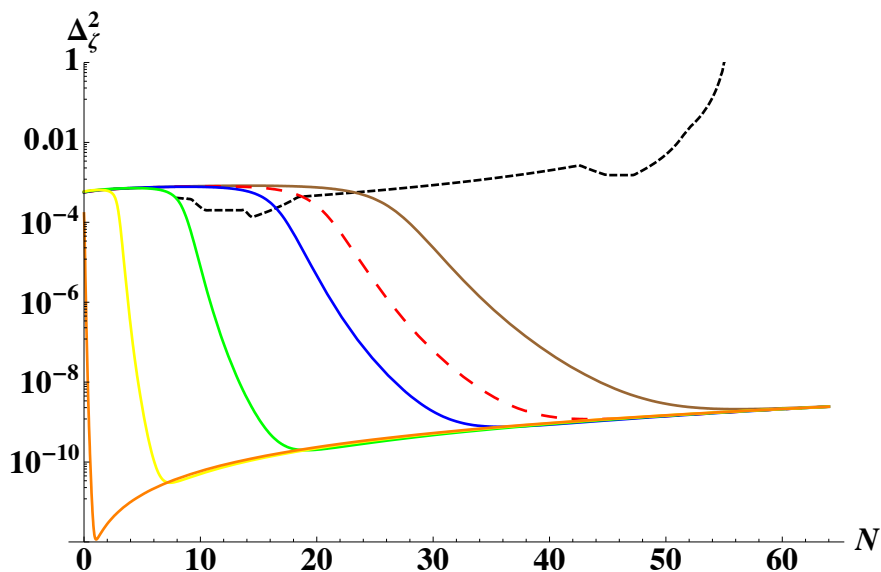


Figure 6.5: *Evolution of our estimate for the power spectrum as a function of  $N$ . In dashed red is the result for  $\xi[N = 64] = 2.2$ . Other lines are for  $\xi[N = 64] = 2.5$  (solid brown),  $\xi[N = 64] = 2$  (solid blue),  $\xi[N = 64] = 1.5$  (solid green),  $\xi[N = 64] = 1$  (solid yellow) and  $\xi[N = 64] = 0.5$  (solid orange). The black hole bound is in dashed black.*

rely on uncertain model dependent assumptions, there are no black hole bounds for  $N \lesssim 8$ . From figure 6.5 we then see that we get

$$\xi(N_{CMB}) \lesssim 1.5 \quad (6.43)$$

for the bound on  $\xi$  at CMB scales from primordial black hole production. In terms of the coupling constant  $\alpha$ , this bound implies the constraint

$$\alpha \lesssim 23. \quad (6.44)$$

This bound is derived using (6.42), i.e. radiation domination right after the end of inflation. This assumption fixes the expansion history of the universe and therefore specifies  $N_{CMB} \simeq 64$ , for the  $N$  corresponding to CMB scales (see appendix F.5 for a derivation). This is required for consistency but changes the numerics very little. Therefore in all other sections we still use  $N_{CMB} = 60$ .

For the matter domination regime, the black hole masses would be greater, for a given  $N$ , see (6.41), and therefore we would have a slightly stronger constraint on  $\xi$  and  $\alpha$ . We find  $\xi \lesssim 1.3$  which corresponds to  $\alpha \lesssim 20$ . Instead of concentrating on it, we will now investigate the model where non-Gaussian perturbations may be generated for much smaller  $\xi$  and  $\alpha$ , without leading to the primordial black hole problem.

## 6.5 Local non-Gaussianity from heavy vector fields

Now let us turn to a scenario, described in [158], in which the produced gauge fields are massive. The production of gauge quanta decreases with the mass of the gauge fields: for  $m_A \sim \xi H$  all production is killed. In this scenario, the gauge fields get their mass via the Higgs mechanism. Fluctuations in the Higgs field  $h$  lead to fluctuations in  $m_A$ , which in turn generate fluctuations in the amount of produced

gauge quanta, and therefore in the amount of extra friction in the dynamics of  $\chi$  and  $H$ . In the end, one has perturbations in  $\Delta N$ , namely the number of extra e-folds of inflation due to gauge field production. This leads to a non-Gaussian signal in the CMB of the local type [158]. Using the  $\delta N$  formalism one finds

$$f_{\text{NL}}^{\text{local}} \sim 10^2 \left( \frac{\Delta N_{\text{max}}^{3/4} e}{\xi 10^{-3}} \right)^4 \left( \frac{m_A}{\xi H} \right)^2. \quad (6.45)$$

Here  $\Delta N_{\text{max}}$  is the increase of the duration of inflation for the case where the vector fields are massless,  $h$  is the Higgs-like field responsible for the mass of the gauge field,  $e$  is its  $U(1)$  charge,  $m_A = eh$  and we assumed a quadratic inflaton potential, so that  $H = \frac{m\chi}{\sqrt{6}}$ .

For a complete description we refer the reader to the original reference [158], section 7. Here we only want to stress that this scenario can also work for  $\xi \sim 1$ . Then it will surely satisfy the bounds from primordial black holes.

Note that the classical field  $h(x)$ , which gives the vector field mass  $eh$ , can be produced either due to the tachyonic mass of the field  $h$  at  $h = 0$ , as in the standard Higgs model, or due to accumulation of long wavelength inflationary perturbations of the field  $h$ . In both cases, the mechanism of [158] requires that the mass of the field  $h$  during inflation should be smaller than the Hubble constant. As a result, even if one assumes that the field has the standard Higgs potential, the value of the field during inflation does not correspond to the position of the minimum of the potential. Instead of that, the field takes different values in different exponentially large parts of the universe. The value of  $f_{\text{NL}}^{\text{local}}$  in this scenario will depend on a typical local value of the field  $h$ , which can be determined by the stochastic approach to investigation of curvaton fluctuations [152].

For simplicity, and to make a clear link to the investigation performed in [152], we will call the light field  $h$  the curvaton, but one should remember that the mechanism of conversion of perturbations of the curvaton field to adiabatic perturbations is different, involving a complicated dynamical processes during reheating. In our case, fluctuations of the field  $h$  lead to fluctuations  $\delta N$  during inflation, and thus to a direct production of adiabatic perturbations of metric.

This scenario can work only if we have a charged scalar field with mass much smaller than  $H$ . At the first glance, one could achieve it by assuming that the relatively light field  $S$  plays the role of the Higgs field. However, the superpotential  $W = mS\Phi$  would break gauge invariance unless we assume that the field  $\Phi$  is also charged. This would be inconsistent with the postulated functional form of the Kähler potential. Therefore we must add to our model at least one charged scalar field  $Q$ .

Fortunately, one can easily do it. Just like in the simplest supersymmetric version of Abelian scalar electrodynamics, one should consider the charged field  $Q$  without any superpotential associated with it. In the global susy limit, the simplest version of this theory with vanishing Fayet-Iliopoulos coefficient would contain a D-term potential  $V_D = \frac{g^2}{2}(\bar{Q}Q)^2$ , but it would not induce any mass of the field  $Q$ .

However, in supergravity, the radial component  $h/\sqrt{2}$  of the scalar field  $Q$  does acquire mass, depending on the choice of the Kähler potential. (The complex phase of the field  $Q = \frac{h}{\sqrt{2}}e^{i\theta}$  is eliminated due to the Higgs effect.) We will consider the following addition to the Kähler potential of our model:

$$\Delta K = Q\bar{Q} + \kappa Q\bar{Q}S\bar{S}. \quad (6.46)$$

Terms of similar functional form were included in many versions of our inflationary scenario for the stabilization of the inflaton trajectory. One can easily find that the resulting mass squared of the field  $h$  during inflation is given by

$$m_h^2 = 3H^2(1 - \kappa). \quad (6.47)$$

Thus in the absence of the term  $\kappa Q\bar{Q}S\bar{S}$  the field  $h$  would be too heavy, but by considering models with  $\gamma \equiv 3(1 - \kappa) \ll 1$  one can have a consistent theory of a light charged scalar field with mass squared  $\gamma H^2$  with  $\gamma \ll 1$ , as required.

Of course, this requires fine-tuning, but this is just a price which one should be prepared to pay for the description of non-Gaussian inflationary perturbations. We will study observational consequences of this model in the next section.

## 6.6 Stochastic approach

In this section we want to find out how fluctuations in the curvaton field  $h$  lead to a variable gauge field mass, and therefore to a non-Gaussian signal in the CMB. We will begin our study with investigation of the behavior of the distribution of the fluctuations in  $h$ , following [152]. During inflation, the long-wavelength distribution of this field generated at the early stages of inflation behaves as a nearly homogeneous classical field, which satisfies the equation

$$3H\dot{h} + V_h = 0, \quad (6.48)$$

which can be also written as

$$\frac{dh^2}{dt} = -\frac{2V_h h}{3H}. \quad (6.49)$$

However, each time interval  $H^{-1}$  new fluctuations of the scalar field are generated, with an average amplitude squared<sup>8</sup>

$$\langle \delta h^2 \rangle = \frac{H^2}{2\pi^2}. \quad (6.50)$$

The wavelength of these fluctuations is rapidly stretched by inflation. This effect increases the average value of the squared of the classical field  $h$  in a process similar to the Brownian motion. As a result, the square of the field  $h$  at any given point with an account taken of inflationary fluctuations changes, in average, with the speed which differs from the predictions of the classical equation of motion by  $\frac{H^3}{4\pi^2}$ :

$$\frac{dh^2}{dt} = -\frac{2V_h h}{3H} + \frac{H^3}{2\pi^2}. \quad (6.51)$$

Using  $3H\dot{\chi} = -V_\chi$ , one can rewrite this equation as

$$\frac{dh^2}{d\chi} = \frac{2V_h h}{V_\chi} - \frac{V^2}{6\pi^2 V_\chi}. \quad (6.52)$$

By solving this equation with different boundary conditions, one can find the most probable value of the locally homogeneous field  $h$ .

Now we will consider the case when the mass of the curvaton field is given by

$$m_h^2 = \gamma H^2 = \frac{\gamma m^2 \chi^2}{6} \quad (6.53)$$

---

<sup>8</sup>For a real massless field we would get  $\langle \delta h^2 \rangle = \frac{H^2}{4\pi^2}$ . An extra coefficient 2 appears in (6.50) because the field  $Q$  is complex, so its absolute value changes faster because of independent fluctuations of its two components. One could argue that in the unitary gauge we only have one scalar degree of freedom. However, unitary gauge is problematic in the description of the Brownian motion and cosmic string formation in the Higgs model. We present the results which should be valid in the regime of small gauge coupling constant  $e$ . Our main conclusions are unaffected by this factor of 2 issue.

with  $\gamma \ll 1$ . This corresponds to the total potential

$$V(\chi, h) = \frac{m^2}{2}\chi^2 + \frac{\gamma}{2}H^2h^2. \quad (6.54)$$

We assume that  $h \ll 1$ , and therefore one can estimate  $H^2 \approx \frac{m^2}{6}\chi^2$ . In this case, (6.52) becomes

$$\frac{dh^2}{d\chi} = \frac{2\gamma\chi h^2}{6} - \frac{m^2\chi^3}{24\pi^2}. \quad (6.55)$$

This equation has a family of different solutions,

$$h^2 = \frac{3m^2}{4\pi^2\gamma^2} \left(1 + \gamma\frac{\chi^2}{6}\right) + A e^{\gamma\chi^2/6}, \quad (6.56)$$

where  $A$  is a constant which could be either positive or negative, depending on initial conditions. During inflation these solutions converge to a simple attractor solution

$$h = \frac{\sqrt{3}m}{2\gamma\pi} \sqrt{1 + \frac{\gamma\chi^2}{6}}. \quad (6.57)$$

We are interested in using this formula to estimate the size of non-Gaussianity, which is produced by the conversion of perturbations in  $h$  into curvature perturbations when the backreaction from gauge fields on the homogeneous evolution becomes substantial, i.e. close to the end of inflation. Hence we should take  $\chi \sim 1$  in (6.57). For  $\gamma \ll 1$ , this solution approaches a constant  $h = \frac{\sqrt{3}m}{2\gamma\pi}$  during the last stages of inflation. Note that this a posteriori justifies the assumption that  $h \ll 1$ , as long as  $\gamma \gg 10^{-6}$ .

To give a particular numerical example, we will use (6.45) for the case  $\xi = 0.5$ . A numerical analysis shows that in this case  $\Delta N_{\max} \sim 0.044$ , and therefore

$$f_{\text{NL}}^{\text{local}} \sim 2.5 \times 10^{11} e^6 \gamma^{-2} \chi^{-2} \quad (6.58)$$

at the end of inflation with  $\gamma\chi^2/6 \ll 1$ .

All our approximations should work fine if the mass of the vector field is much smaller than  $H$ , which leads to a constraint  $e \ll \gamma\chi$ .

Consider for example  $\gamma = 0.1$  and  $\chi = 1$ , which corresponds to the very end of inflation. (We should stress that it would not be consistent to take  $\chi$  much larger than  $\mathcal{O}(1)$  in Planck units since that is its value when curvature perturbations are generated in our scenario. Moreover, the main contribution to  $\Delta N_{\max}$  is given by the last part of the inflationary trajectory where  $\chi = \mathcal{O}(1)$ .) In this case

$$f_{\text{NL}}^{\text{local}} \sim 2.5 \times 10^{13} e^6. \quad (6.59)$$

To have non-Gaussian perturbations with  $f_{\text{NL}}^{\text{local}} = \mathcal{O}(10^2)$  one should take  $e \sim 1.26 \times 10^{-2}$ .

## 6.7 Gauge field production in sugra inflation: reheating

We have found that the coupling  $\chi F\tilde{F}$  needed for reheating in (the pseudoscalar variant of) the new class of sugra inflation models proposed in [123, 124, 125] can as well yield an observable non-Gaussian signal.

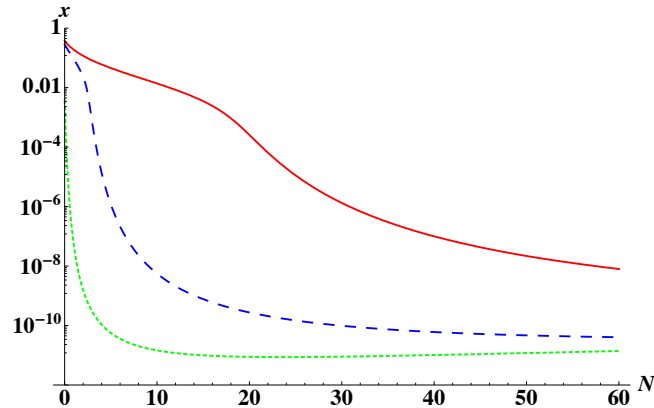


Figure 6.6: Evolution of the normalized energy of the vector field,  $x \equiv \frac{1}{2} (E^2 + B^2) / 3H^2$  as a function of  $N$ , for  $\xi[N = 60] = 2.2$  (solid red),  $\xi[N = 60] = 1.0$  (largely dashed blue) and  $\xi[N = 60] = 0.5$  (finely dashed green).

It only remains to be seen what the effects of the typically needed values for  $\xi$  are for the reheating in the combined model.

In [125] the reheating temperature  $T_R$  for the decay of a scalar inflaton field to two photons due to the interaction  $\frac{\alpha}{4}\phi F^2$  was estimated as

$$T_R \approx \sqrt{2\alpha} \times 10^9 \text{ GeV}. \quad (6.60)$$

A similar estimate is valid in our case. One may also represent it in an equivalent way using the relation  $\frac{\alpha}{4} = -\frac{\xi H}{2\dot{\chi}}$ , and an expression for the slow-roll parameter  $\epsilon = \frac{\dot{\chi}^2}{2H^2}$

$$T_R \approx \frac{2\xi}{\sqrt{\epsilon}} \times 10^9 \text{ GeV}. \quad (6.61)$$

As long as one can describe reheating as a particle by particle decay, reheating in inflationary models of this type does not depend much on whether the inflaton field is a scalar or a pseudoscalar. In both types of models, one may consider interactions with  $\alpha \ll 1$ , which results in reheating temperature  $T_R \lesssim 10^8$  GeV. This solves the cosmological gravitino problem for gravitino in the typical mass range  $m_{3/2} \lesssim 1$  TeV.

However, for  $\alpha \gtrsim 1$ , which is required for production of non-Gaussianity in the models based on the pseudoscalar inflaton, an estimate described above gives  $T_R > 10^9$  GeV. It is good for the theory of leptogenesis, but it could be bad from the point of view of the gravitino problem. Moreover, for  $\alpha \gtrsim 1$  an entirely different mechanism of reheating is operating. At the end of inflation, when the time dependent parameter  $\xi$  grows and becomes large, a significant fraction of the energy of the inflaton field gradually becomes converted to the energy of the vector field (see figure 6.6). This is a very efficient mechanism, which may lead to a very rapid thermalization of energy in the hidden sector. This may exacerbate the gravitino problem. Fortunately, this problem does not appear for superheavy gravitino with mass  $m_{3/2} \gtrsim 10^2$  TeV. Such gravitinos appear in many versions of the models of mini-split supersymmetry, which became quite popular during the last few years, see [168] and references therein.

## 6.8 Conclusions

The new class of chaotic inflation models in supergravity needs a gauge-gauge-inflaton coupling for reheating. The inclusion of this coupling can produce gauge fields and can provide a non-Gaussian signal in the CMB. From an effective point of view, this coupling has to be present, as it respects all symmetries in the model. Therefore it is interesting to see how we can put upper bounds on the coupling constant  $\xi$ .

In this chapter we have studied two possible realizations of this scenario. Taking the parameter  $\xi \simeq 2.2 - 2.5$  ( $\alpha \simeq 32 - 37$ ) produces a large amount of gauge quanta, that by inverse decay give rise to an equilateral non-Gaussianity in the CMB, as studied in [156, 18]. Since the amount of non-Gaussianity  $f_{\text{NL}}^{\text{eq}}$  depends logarithmically on  $\xi$ , and since the Planck bounds on equilateral non-Gaussianity (1.61) are not so much tighter than the WMAP bounds, the constraints on  $\xi$  do not change dramatically. They are still of the same order as the power spectrum constraints studied in [158]. Our main message is and remains that the strongest bound on  $\xi$  may very well come from the non-detection of black holes. We have estimated that towards the end of inflation the power spectrum grows so much that the model may be ruled out because it overproduces primordial black holes. However, as our order-one estimate lands within a factor of six from the critical black hole bound on the power spectrum (with the non-Gaussian nature of the signal taken into account), we need a more precise computation to draw a definitive conclusion.

In the second scenario, where the produced gauge fields are massive due to the Higgs effect in presence of a light curvaton-type field, one can take a smaller value for  $\xi$ , of order 0.5 - 1, corresponding to  $\alpha$  from 8 to 15. Then the model is free of black hole trouble. Also, there will be no observable rise in the power spectrum on CMB scales. In this case, fluctuations in the curvaton field modulate the duration of inflation and can give rise to adiabatic non-Gaussian perturbations of the local type with  $f_{\text{NL}} \sim \mathcal{O}(10 - 100)$ . Then the strongest constraint on  $\xi$  does indeed come from non-Gaussianity. For smaller values of  $\alpha$ , we return to the standard chaotic inflation scenario with Gaussian adiabatic perturbations. In principle, there is enough freedom in the model to lower  $f_{\text{NL}}^{\text{loc}}$  to values consistent with the bounds from Planck (1.61). However, we can not deny that this particular variant of the model looked more promising before Planck than after.



# Chapter 7

## Moduli stabilisation

### 7.1 Introduction

In the previous two chapters, we have tried to embed inflation in the framework of supergravity. In this chapter, based on our work [1], we want to go one step further. For the particular model of inflation in supergravity proposed in [169], we want to study a possible embedding in a higher dimensional Planck-scale theory, for example string theory. In particular, we are after an effective description of the remnants of the extra dimensions that such a theory has on the low scale. After dimensional reduction, the 4D effective field theory will still carry traces of its higher dimensional origin in the form of moduli fields, light scalar fields which parametrize the shapes and sizes of the compactified extra dimensional manifold. For definiteness, we will follow the seminal work of KKLT [170] and assume that all moduli can be fixed at some high scale by fluxes, except for the volume modulus which is to be stabilized at a lower scale by non-perturbative effects. The dynamics of the volume modulus thus enters the low energy effective field theory, and inflation should be studied in conjunction with modulus stabilization. We want to find an effective description of the volume modulus field, and study the conditions under which the modulus dynamics do not ruin the inflationary dynamics of the model.

There are two ways to deal with the moduli fields in the context of inflation. The first is to make the moduli part of the inflaton dynamics. This is for example done in racetrack [171, 172] and Kähler [173, 174] inflation models, where a modulus field is identified with the inflaton field itself. Another approach, the one we follow in this paper, is to decouple the physics of moduli stabilization from the inflationary physics as much as possible. Our set-up is as follows: we have a hybrid inflation sector and a (volume) modulus stabilization sector, which are coupled only gravitationally as dictated by the sugra action. Even though gravitational interactions are usually thought of as being weak, they are generically strong enough to ruin inflation - inflation is UV sensitive, as we already discussed in the introductory sections 1.5 and 1.6. It has indeed been shown that “standard” susy hybrid inflation [175] cannot be combined with a KKLT-like modulus sector [176, 177] (but see [115] for a possible resolution). Instead we will consider a modified model of hybrid inflation [169].

We want to extend the hybrid inflation model of Ref. [169] with a modulus sector. In this set-up the  $\eta$ -problem is solved by a shift symmetry for the inflaton, and in addition by the property that the inflationary superpotential and its first derivative w.r.t. the inflaton field vanishes during inflation. See also the discussion in section 1.6. However, the  $\eta$ -problem is not the only potential difficulty. Making

sure that the modulus field remains stabilized during inflation, implies that the scales appearing in the susy breaking modulus sector are large, resulting in a large gravitino mass. Even though the inflaton direction is protected, large soft corrections to the waterfall masses and other masses may destabilize the inflationary trajectory.

In this chapter we describe an explicit way to stabilize the modulus sector without running into the aforementioned troubles. The trick is to constrain the modulus sector in such a way that its gravitino mass is much smaller than the other scales in the problem. Although this presents some amount of tuning, the result is a phenomenologically favored scenario with low scale susy breaking and high scale inflation. An explicit modulus sector that does the job is the model developed by Kallosh & Linde [102, 178] (we will refer to this as the KL model).

Many sugra or string-derived models of inflation predict a large gravitino mass. In models based on a generic KKLT potential the gravitino mass has to be larger than the Hubble constant during inflation  $m_{3/2} \gtrsim H_*$  [102, 178], whereas in models with a large volume compactification the bound is even stronger  $m_{3/2}^{3/2} \gtrsim H_*$  [179]. It has proven hard to avoid this bound. The KL moduli potential decouples the susy breaking scale from the modulus mass, at the cost of tuning, thereby invalidating the bound. Although it is not automatic that a KL-based inflation scenario with low scale susy breaking can be constructed [176, 177, 103], successful models have been found [180], and the model discussed in this chapter is another example. Other approaches to obtain a light gravitino can be found in Refs. [115, 179, 181, 182, 183].

This chapter is organized as follows. In section 2 we first briefly describe the shift-symmetric super gravitational model of hybrid inflation introduced in Ref. [169]. Then, in section 3, we explain why combining it with a generic KKLT-type modulus sector does not work: it is impossible to find a suitable inflationary trajectory stable in field space. In the fourth section we show that a constrained modulus sector, of which KL is an explicit example, saves inflation. We discuss the inflationary observables, and show some numerical results. We end with a discussion of our results.

## 7.2 The model: sugra hybrid inflation

We briefly describe the supergravitational shift-symmetric model of hybrid inflation, that we want to extend by including a moduli sector in the next sections. For a more detailed introduction we refer to the original paper: Ref. [169].

The model is defined by its superpotential  $W_{\text{inf}}$

$$W_{\text{inf}} = \kappa S (H^2 - M^2) + \frac{\lambda}{\Lambda} N^2 H^2, \quad (7.1)$$

and Kähler potential  $K_{\text{inf}}$

$$\begin{aligned} K_{\text{inf}} = & |H|^2 + |S|^2 + \frac{1}{2} (N + N^*)^2 + \frac{\kappa_H}{\Lambda^2} |H|^4 + \frac{\kappa_S}{\Lambda^2} |S|^4 + \frac{\kappa_N}{4\Lambda^2} (N + N^*)^4 \\ & + \frac{\kappa_{SH}}{\Lambda^2} |S|^2 |H|^2 + \frac{\kappa_{SN}}{2\Lambda^2} |S|^2 (N + N^*)^2 + \frac{\kappa_{HN}}{2\Lambda^2} |H|^2 (N + N^*)^2 + \dots \end{aligned} \quad (7.2)$$

where the ellipses denote higher order terms, and  $\Lambda$  is some cutoff scale. The superfield  $H$  plays the role of waterfall field responsible for ending inflation. The superfield  $S$  is the so-called driving field, as its  $F$ -term provides the energy density that drives inflation. Finally, the imaginary part of  $N$  is the slowly rolling inflaton field. It is hoped that  $N$  can be identified with the right-handed sneutrino superfield, and  $H$  with the grand unified Higgs field that breaks  $B-L$ , thus providing an embedding of the model in a grand unified

theory [184]. The Kähler potential is invariant under a shift of  $N \rightarrow N + i\mu$ ; this is the aforementioned shift symmetry pivotal for keeping the inflaton direction flat. The superfields can be decomposed in real and imaginary components:  $H = (h_r + ih_i)/\sqrt{2}$ ,  $S = (s_r + is_i)/\sqrt{2}$  and  $N = (n_r + in_i)/\sqrt{2}$ .

**Inflation** In this model inflation takes place as the field  $n_i$ , the imaginary part of  $N$ , slowly rolls down to a critical value  $n_i^c$ , while the other fields are in their minimum  $(h_r, h_i, s_r, s_i, n_r) = (0, 0, 0, 0, 0)$ . Let us first check the stability of this minimum and then briefly explain how inflation comes about.

During inflation the  $F$ -term scalar potential

$$V_F = e^K \left[ D_i W K^{i\bar{j}} D_{\bar{j}} \bar{W} - 3|W|^2 \right], \quad (7.3)$$

with  $D_i W = W_i + K_i W$  is constant:

$$V_{\text{tree}} = \kappa^2 M^4, \quad (7.4)$$

and drives inflation with  $H_{\text{inf}}^2 = V_{\text{tree}}/3$ . All non-inflationary fields are at an extremum of the potential independent of the value of  $n_i$ . Hence the inflationary valley is a classically and quantum mechanically stable trajectory provided all masses squared are positive, and the mass exceeds the Hubble scale during inflation. The masses during inflation are

$$\begin{aligned} \{m_{h_r}^2, m_{h_i}^2\} &= \{M^2 \kappa^2 (M^2 (1 - \kappa_{SH}) - 2) + \lambda^2 n_i^4, M^2 \kappa^2 (M^2 (1 - \kappa_{SH}) + 2) + \lambda^2 n_i^4\}, \\ \{m_{s_r}^2, m_{s_i}^2\} &= \{-4M^4 \kappa^2 \kappa_S, -4M^4 \kappa^2 \kappa_S\}, \\ \{m_{n_r}^2, m_{n_i}^2\} &= \{2M^4 \kappa^2 (1 - \kappa_{SN}), 0\}. \end{aligned} \quad (7.5)$$

Here, and from now on, we set  $\Lambda = 1$ . We see that  $h_r$  becomes tachyonic when  $n_i$  drops below the critical value  $(n_i^c)^c \approx \sqrt{2}\kappa M/\lambda$ . This will mark the end of inflation. The  $s_r$ ,  $s_i$  and  $n_r$  directions are stable as long as  $\kappa_{SN} < \frac{5}{6}$  and  $\kappa_S < -\frac{1}{12}$ . This is one of the reasons for including the higher order terms in the Kähler potential (7.2). (The other is that the inflationary observables depend on  $\kappa_{SH}$  [169]; taking  $\kappa_{SH} = \mathcal{O}(10)$  the spectral index can be brought closer to Planck's central value.)

Thanks to the shift symmetry,  $n_i$  itself does not acquire any mass, independent of the higher order terms in the Kähler potential; at tree level it is a flat direction in field space. The slow roll parameter  $\eta = V''/V$  is small, with prime denoting derivative w.r.t. the canonically normalized inflaton field, and there is no  $\eta$ -problem. This is in contrast with “standard” susy hybrid inflation [175] where higher order terms lift the flatness of the potential, and thus must be tuned [28]. The reason for this marked difference is that in our model  $W_{\text{inf}}$  vanishes during inflation (as well as many first and second derivatives of  $W_{\text{inf}}$ ), thereby killing all possible inflaton mass terms. In standard susy hybrid inflation on the other hand  $W_{\text{inf}} \neq 0$ , and the  $\eta$ -problem resurfaces despite the shift symmetry. It is this remarkable property of the inflaton superpotential that led the authors of [169] to suggest that the model can be combined with a modulus sector. In the next sections we will take a closer look at this claim.

The inflaton potential is generated by the 1-loop Coleman-Weinberg potential [41], from the mass splitting between fermions and bosons. Only the waterfall fields have inflaton-dependent mass terms and contribute to the inflaton potential. Writing the mass of the waterfall fields and their fermionic superpartners in the form  $m_{h_{r,i}}^2 = \mu^2(x^2 + y^2 \pm 1)$  and  $\tilde{m}_{h_{r,i}}^2 = \mu^2 x^2$  with

$$\mu^2 = 2\kappa^2 M^2, \quad x = \frac{\lambda^2 n_i^4}{2\kappa^2 M^2}, \quad y = \frac{M^2}{2}(1 - \kappa_{SH}), \quad (7.6)$$

then the loop potential is given by (G.4) in appendix G. We now have the effective potential

$$V_{\text{inf}} = V_{\text{tree}} + V_{\text{loop}}(n_i). \quad (7.7)$$

The  $n_i$ -direction in field space, flat at tree-level, gets slightly lifted at the one-loop level. With a suitable choice of parameters this effective potential can generate inflation. The inflaton field  $n_i$  slowly rolls down until it reaches the critical value  $n_i^c$  where inflation ends. We note that for  $y^2 < 0$ , or equivalently  $\kappa_{SH} > 1$ , the CW-potential has a maximum at  $n_i^{\text{max}}$  given in (G.6). This introduces a constraint on the initial field value of the inflaton field which has to be smaller than  $n_i^{\text{max}}$ , to make sure that the inflaton rolls towards the “right” minimum. On the other hand for  $y^2 > 0$ , the loop potential steadily increases with  $n_i$ , and there is no such problem.

With the potential (7.7) one can calculate the inflaton value  $(n_i)_*$  at horizon-exit, 60 e-folds before the end of inflation, when observable scales leave the horizon. Here the slow-roll parameters  $\epsilon$ ,  $\eta$  and  $\xi^2$  can be evaluated, and consequently the power spectrum  $\Delta_\zeta^2(k_0)$ , the scalar spectral index  $n_s$ , the tensor-to-scalar ratio  $r$ , and the running of the scalar spectral index  $dn_s/d\log k$ .

**After inflation** When the inflation field  $n_i$  reaches its critical value  $n_i^c$ , the waterfall field  $h_r$  becomes tachyonic. Inflation ends with a phase transition during which the waterfall field obtains a non-zero vev. The post-inflationary vacuum field values are  $\{h_r, h_i, s_r, s_i, n_r, n_i\} = \{\pm\sqrt{2}M, 0, 0, 0, 0, 0\}$ , and  $V = 0$  corresponding to zero cosmological constant.

**Numerical results** In Ref. [169] it is shown that in the parameter space

$$\left( \kappa = \mathcal{O}(10^{-1}), M = \mathcal{O}(10^{-3}), \lambda = \mathcal{O}(10^{-1}), \kappa_{SH} = \mathcal{O}(1-10) \right) \quad (7.8)$$

many solutions can be found that satisfy the WMAP  $1\sigma$  range for the power spectrum  $\Delta_\zeta(k_0) = (5.0 \pm 0.1) \times 10^{-5}$  and scalar spectral index  $n_s = 0.960_{-0.013}^{+0.014}$  [185]. The tensor to scalar ratio  $r$  typically becomes of order  $(10^{-5})$  which easily satisfies the WMAP bound  $r < 0.2$ . The model fails on the prediction of  $dn_s/d\log k$ : it typically predicts a value of order  $(10^{-4})$  while WMAP measured  $-0.0032_{-0.020}^{+0.021}$ . As the accuracy of this measurement is rather low, this does not seem to be a serious problem.

Switching from the WMAP5 bounds [185], which were the current ones when this chapter was originally written, to the Planck bounds [15] will not change the results of this chapter.

### 7.3 Adding the modulus sector

The inflaton model described in the previous section is an effective theory, arising as a low-energy effective description of an underlying Planck scale theory. If the UV completion is an extra dimensional theory, we expect moduli fields to appear in the 4D effective action. The moduli fields parametrize the sizes and shapes of the extra dimensions. In case the vacuum manifold is degenerate, the moduli correspond to massless modes appearing in the low energy effective four-dimensional theory.

For definiteness we concentrate in this chapter on a KKLT type moduli sector [170], arising from compactifications in type IIB string theory. KKLT showed that all complex structure moduli (shape moduli) can be stabilized by fluxes. In the simplest case there is only one Kähler modulus (size modulus) left, the volume modulus, which appears in the 4D effective theory. This modulus, in turn, is stabilized

by invoking non-perturbative effects, coming from either gaugino condensation or instantons. Finally, to arrive at a zero cosmological constant, a non-supersymmetric uplifting term is added, generated by an anti-D3 brane located at the bottom of a throat in the compactification manifold.

To combine the inflaton and modulus sector we simply add their respective Kähler- and superpotentials<sup>1</sup>:

$$W = W_{\text{inf}} + W_{\text{mod}}, \quad K = K_{\text{inf}} + K_{\text{mod}} \quad (7.9)$$

with

$$K_{\text{mod}} = -3 \ln(T + \bar{T}). \quad (7.10)$$

### 7.3.1 General approach

The function  $W_{\text{mod}}(T)$  generically contains a constant term  $W_0$  arising from integrating out the stabilized moduli and a non-perturbative potential that is to stabilize  $T$ . In this section we will work with a generic function  $W_{\text{mod}}(T)$  and see what restrictions on this function we get to make inflation work in this moduli-extended framework. We choose a KKLT uplifting potential  $V_{\text{up}} = c/(T + \bar{T})^2$ , with  $c$  a constant tuned to solve the cosmological constant problem. However, its specific form is not so important for our discussion.

As before the modulus fields can be decomposed in real and imaginary parts:  $T = \sigma + i\alpha$ . Choosing the phases in the superpotential judiciously, we can set  $\alpha = 0$  to zero consistently. We define  $\sigma = \sigma_0$  at the minimum of the F-term modulus potential in the absence of the inflaton sector, i.e.

$$\partial_\sigma V_{\text{mod}}^F|_{\sigma=\sigma_0} = 0 \quad \Leftrightarrow \quad D_T W|_{\sigma=\sigma_0} = 0. \quad (7.11)$$

Due to the uplift term and the presence of the inflaton sector,  $\sigma$  is displaced from its F-term minimum both during and after inflation. If the displacement is minimal the inflationary trajectory and the post-inflation minimum are only slightly affected as well, and the moduli sector may be combined with inflation. In this case  $\sigma \approx \sigma_0$  and  $D_T W \approx 0$  are still good approximations. In the rest of this section we discuss the general conditions the moduli sector has to satisfy for this to be the case, followed - in the next section - by an explicit example. There are many pitfalls. When a modulus sector is included, the  $\eta$ -problem may reappear, the vacuum after inflation and/or the inflationary trajectory may be destabilized, and the corrections to the waterfall fields may hamper a successful exit to inflation.

**$\eta$ -problem** We have seen that in the absence of a moduli sector the tree level inflaton mass is zero, as a consequence of the shift symmetry and the fact that  $W_{\text{inf}} = 0$ . Due to the shift symmetry the Kähler potential is independent of  $n_i$ , and thus any mass for  $n_i$  must come from the second derivative of the term in square brackets in (7.3). The fact that the modulus superpotential is non-zero does not change the results, the inflaton potential is still flat at tree level. All terms in  $m_{n_i}^2$  proportional to  $W_{\text{mod}}$  or its derivatives are multiplied by  $(W_{\text{inf}})_{n_i n_i}$ , which is zero during inflation. As the  $\eta$ -problem is usually the main obstacle to embedding inflation in a supergravity theory, this is no small feat.

**Stability of the vacuum** Consider the vacuum after inflation. We suppose the post-inflationary minimum to occur at  $\{h_r, h_i, s_r, s_i, n_r, n_i, \sigma, \alpha\} = \{\pm\sqrt{2}M, 0, 0, 0, 0, 0, \sigma_0, 0\}$ . For the post-inflation scalar potential we find

$$V_{\text{vac}} = \frac{c}{(4\sigma)^2} + V_{\text{mod}}^F + f(M^2), \quad V_{\text{mod}}^F = \frac{-3W_{\text{mod}}^2 + \frac{4}{3}\sigma^2(D_T W_{\text{mod}})^2}{(2\sigma)^3}, \quad (7.12)$$

<sup>1</sup>The Kähler potential does not have to be separable in modulus and inflaton field, e.g.  $K_{\text{inf}}$  can appear inside the log. We checked that its exact form does not affect our qualitative results.

where each term in  $f(M^2)$  is either proportional to  $D_T W$  or to  $W$  (with  $D_T W = -3W/(2\sigma) + W_T$ ). For parameters that keep the modulus stabilized during inflation (discussed below), the  $M$ -dependent corrections  $f(M^2)$  to the modulus potential after inflation are small, and do not destabilize the potential minimum.

The first derivatives of the scalar potential with respect to the eight real fields, evaluated at the postulated potential minimum after inflation, are manifestly zero or involve again small functions of  $M^2$  proportional to  $D_T W$  or  $W$  indicating that the minimum of some of the fields is slightly displaced. One of the displaced fields is the modulus field, which is shifted from its F-term potential minimum  $\sigma_0$  due to the presence of the uplift term. This shift is typically small.

Second derivatives again involve many functions of  $D_T W$ ,  $W$  and  $c$ . The vacuum mass of the field  $n_r$  is most seriously affected by moduli corrections, and runs the risk of going tachyonic:

$$m_{n_r}^2|_{\text{vac}} = \frac{4(D_T W_{\text{mod}})^2 \sigma^2 - 3W_{\text{mod}}^2 + \mathcal{O}(M^2)}{12\sigma^3}. \quad (7.13)$$

Indeed, for  $D_T W_{\text{mod}} \approx 0$  the mass is tachyonic unless  $W_{\text{mod}} \lesssim M$  is sufficiently small, and the  $\mathcal{O}(M^2)$  terms dominate.

**Stability during inflation** The tentative inflationary trajectory is

$$\{h_r, h_i, s_r, s_i, n_r, n_i, \sigma, \alpha\} = \{0, 0, 0, 0, 0, n_i, \sigma_0, 0\}. \quad (7.14)$$

We have to check whether this is still an extremum when the modulus potential is turned on. As before  $n_i$  is the slowly rolling inflaton field. The potential during inflation along this trajectory is then

$$V_{\text{inf}} = \frac{c}{(4\sigma)^2} + V_{\text{mod}}^F + \frac{\kappa^2 M^4}{(2\sigma)^3}, \quad (7.15)$$

with  $V_{\text{mod}}^F$  defined in (7.12). If  $\sigma \approx \sigma_0$  the first two terms in the above expression nearly cancel, and the last term is as before the energy density driving inflation. However, this energy density is now modulus dependent. If this term is too large, the displacement in  $\sigma$  is large, or worse, the barrier separating in the potential disappears and  $\sigma$  rolls off to infinity.

The fields are all at an extremum for the inflationary trajectory, except for the modulus and the  $s_r$  field. The non-vanishing first derivatives are

$$\begin{aligned} \partial_{s_r} V_{\text{inf}} &= \frac{\kappa M^2 ((D_T W_{\text{mod}})\sigma + W_{\text{mod}})}{2\sqrt{2}\sigma^3}, \\ \partial_{\sigma} V_{\text{inf}} &= \frac{-3(3\kappa^2 M^4 + 4c\sigma) + 8\sigma^2 (D_T W_{\text{mod}}) (-2D_T W_{\text{mod}} - \frac{3W_{\text{mod}}}{\sigma} + \sigma W_{\text{mod}}'')}{24\sigma^4}, \end{aligned} \quad (7.16)$$

where primes denote derivatives with respect to  $\sigma$ . We see indeed that during inflation the minimum of the  $\sigma$ -field does not occur at exactly  $\sigma = \sigma_0$ : now it is both the uplift and the inflationary energy density that shifts the minimum away. In addition, the field  $s_r$  is not minimized at  $s_r = 0$ . For  $D_T W_{\text{mod}} \approx 0$ , the first derivative is proportional to  $W_{\text{mod}}$  and is typically large. This can have dramatic consequences, as we will see. The matrix of second derivatives evaluated at the inflationary minimum is not diagonal anymore, as  $V_{s_r \sigma}$  does not vanish. This coupling between  $s_r$  and  $\sigma$  could already be foreseen from (7.16). We also find a similar coupling between  $s_i$  and  $\alpha$ , but as they both have their minimum at zero this coupling will not have any significant consequences.

Just as in the case without moduli fields (*cf.* the discussion below (7.5)), we need some tuning of the  $\kappa$ -parameters in the inflationary Kähler potential to maintain positive definite masses squared. Since expressions are long, we only explicitly give the mass of the field  $h_r$ , that can be compared to (7.5)

$$V_{h_r h_r}^{\text{inf}} = \frac{1}{(2\sigma_0)^3} \left[ \kappa^2 M^2 ((M^2(1 - \kappa_{SH}) - 2) + \lambda^2 n_i^4 - 2W_{\text{mod}}^2 + 2\sigma \lambda n_i^2 D_T W_{\text{mod}} + W_{\text{mod}} (\lambda n_i^2 - 4\sigma D_T W_{\text{mod}}) + \frac{4}{3} \sigma D_T W_{\text{mod}} (\sigma D_T W_{\text{mod}} + 3)) \right]. \quad (7.17)$$

Once again, for  $D_T W_{\text{mod}} \approx 0$ , the corrections — in this case to the waterfall masses — scale with  $W_{\text{mod}}$  and are potentially large.

**Waterfall mechanism and CW-loop** The above expression becomes much more complicated when we take the displacement of  $s_r$  into account, see (7.16). If we allow  $s_r$  to be nonzero we find among many other terms

$$\delta m_{h_r, i}^2 = \frac{\kappa^2 s_r^2}{2\sigma^3} + \dots \quad (7.18)$$

This indicates that the shift in  $s_r$  can do a lot of harm to our model. Once the waterfall masses get dominated by terms like (7.18), the Coleman-Weinberg loop potential changes drastically and inflation is no longer possible. Therefore, we absolutely need the displacement in  $s_r$  to be small.

### 7.3.2 Discussion

As discussed, for a generic superpotential ( $D_T W_{\text{mod}} \approx 0$ ) as this minimizes the F-term superpotential (7.11), and corrections to the inflaton potential scale with  $W_{\text{mod}}$  (which is the only scale in the moduli sector).  $W_{\text{mod}}$  should be large enough to assure the modulus remains stabilized during inflation, yet small enough to ensure that the vacuum and inflationary trajectory is not destabilized. This does not seem to be easy. And indeed, for a KKLT modulus sector, which is of the above described generic form, this is impossible. In the original KKLT paper [170] the non-perturbative potential is a single exponent, and the superpotential is

$$W_{\text{mod}} = -W_0 + A e^{-aT}. \quad (7.19)$$

where the sign in front of  $W_0$  is chosen such that the potential is minimized by  $\alpha = 0$ . The minimum of  $V_{\text{vac}}$  occurs for  $D_T W_{\text{mod}} \approx 0$  and  $W_{\text{mod}} \sim W_0$ . Let us go through all modulus corrections for this specific choice of superpotential.

For the  $n_r$ -direction to be stable in the vacuum after inflation, see (7.13), we have to demand  $W_0 \lesssim \kappa M^2$ . From the perspective of the modulus field, the inflationary energy density  $\kappa^2 M^4$  acts as an additional uplift term (7.15). If this term is too large,  $\sigma$  is destabilized. To avoid this one needs  $\kappa^2 M^4 / (2\sigma)^3 \lesssim V_{\text{up}}$  or

$$\kappa M^2 \lesssim W_0. \quad (7.20)$$

It follows that stabilizing the modulus during inflation plus stabilizing the vacuum are both possible only for a very limited range of parameters:  $W_0 \approx \kappa M^2$ . But what kills the KKLT model are the corrections it gives to the waterfall fields. As anticipated from (7.16) it follows that both  $s_r$  and  $\sigma$  are displaced considerably during inflation. Numerically we find  $s_r \sim \mathcal{O}(10^{-1} - 10^{-2})$  (where we used  $V_{\text{inf}}^{1/4} \sim M_{\text{GUT}}$ ). The corresponding correction to the waterfall field (7.18) is enormous, hampering a graceful exit to inflation.

How to salvage inflation? Taking a look at the modulus corrections ((7.13), (7.15), (7.16), (7.18)), we see they all vanish in the limit in which both

$$D_T W_{\text{mod}}|_{\sigma=\sigma_0} \approx 0 \quad \& \quad W_{\text{mod}}|_{\sigma=\sigma_0} \approx 0. \quad (7.21)$$

The first condition is assured by minimizing of the F-term potential (7.11), but the second constitutes an extra constraint on the modulus potential which can be satisfied by tuning the parameters in the superpotential. Such a tuning is not possible for the one-exponent KKL<sub>T</sub> model. Kallosh & Linde (KL) constructed a modulus sector with two exponents, with the parameters carefully tuned, such that (7.21) is satisfied [102, 178]. We will discuss this model in detail in the next section. The only constraint left is then (7.20), assuring that the modulus remains fixed during inflation.

The fine-tuning required to set  $W_{\text{mod}} \approx 0$  is the same tuning that creates a hierarchy between the gravitino and modulus mass with  $m_{3/2} \ll m_T$ . Since  $H_* \gtrsim m_T$  (from (7.20)), this tuning allows to have low scale susy breaking with high scale inflation — something that seems impossible in non-fine tuned models. This was the motivation behind the KL model. Note that since in hybrid inflation  $V_{\text{inf}} \sim M_{\text{GUT}}^4$ , without this tuning, it is impossible to get the phenomenologically favored TeV scale susy breaking.

Finally we would like to contrast the results with standard susy hybrid inflation [175, 176, 177]. In the standard case, the  $\eta$ -problem reappears once a modulus sector is included; the reason is that in these models the inflaton superpotential is nonzero  $W_{\text{inf}} \neq 0$ , and many terms mixing the modulus and inflaton sector appear in  $V_F$ . In addition, the waterfall masses get large corrections, just as we found above. Although each of these problems can be solved separately by a fine-tuned condition on the modulus potential, they cannot be solved simultaneously. Since in our case, the  $\eta$ -problem has dropped off the list, inflation can be rescued by a single tuning.

## 7.4 Inflation with a KL modulus sector

As discussed in the previous section, hybrid inflation may be combined with a modulus sector provided the latter satisfies (7.21). In this section we work out the details, focusing on the KL modulus sector introduced by Kallosh & Linde in [102, 178]. Augmenting the KKL<sub>T</sub> potential by an additional non-perturbative exponential factor, it is possible (by tuning the parameters) to construct a susy Minkowski minimum with  $D_T W = W_T = 0$ . The superpotential is

$$W_{\text{mod}} = -W_0 + Ae^{-aT} - Be^{-bT} \quad (7.22)$$

with  $W_0$  and  $\sigma_0$ :

$$W_0 = w_0 \equiv A \left( \frac{bB}{aA} \right)^{a/(a-b)} - B \left( \frac{bB}{aA} \right)^{b/(a-b)}, \quad \sigma_0 = \bar{\sigma}_0 \equiv \frac{1}{a-b} \ln \left( \frac{aA}{bB} \right). \quad (7.23)$$

So, at the cost of fixing  $W_0$  and introducing another exponent in the non-perturbative potential, we now explicitly have  $D_T W = W_T = 0$ , and thus  $V_{\text{mod}}^F = 0$ , in the vacuum after inflation  $\{h_r, h_i, s_r, s_i, n_r, n_i, \sigma, \alpha\} = \{\pm\sqrt{2}M, 0, 0, 0, 0, 0, \sigma_0, 0\}$ . No uplift term is needed, and susy is unbroken.

We can get a small but non-zero gravitino mass by perturbing the susy Minkowski solution

$$W_0 = w_0 + \epsilon_w. \quad (7.24)$$

As long as the perturbation is small enough  $D_T W_{\text{mod}} \approx 0$ ,  $W_{\text{mod}} \approx \epsilon_w$  and (7.21) is still satisfied. We will determine below how small  $\epsilon_w$  has to be. With this perturbation the minimum of the F-term potential,

located at  $\sigma_0 = \bar{\sigma}_0 + \mathcal{O}(\epsilon_w)$ , is susy AdS, and a small uplift  $V_{\text{up}} \approx 3W_0^2/(2\sigma_0)^3$  is needed to get zero cosmological constant. Susy is broken in the process. In this set-up there is a large hierarchy between the gravitino  $m_{3/2} = e^K|W| \propto \epsilon_w$  and modulus mass  $m_\sigma \propto \sqrt{V_{\sigma\sigma}} \propto W_0$ .

### 7.4.1 Inflation

Let us see how inflation works for the hybrid inflation model described in section 2 combined with a KL modulus sector.

**Stability of the vacuum** Since the function  $f(M^2) \sim \epsilon^2$  in (7.12) the inflaton corrections to the modulus minimum after inflation are small. Likewise the modulus correction to the inflaton sector are small. The mass of  $n_r$  in (7.13) is manifestly positive definite in the vacuum. We checked numerically the stability of the vacuum.

**Stability during inflation** From (7.15) we see that during inflation we now have

$$V_{\text{inf}} \approx \frac{\kappa^2 M^4 + \mathcal{O}(\epsilon_w^2)}{(2\sigma_0)^3}. \quad (7.25)$$

The inflationary trajectory is slightly shifted from the tentative inflationary trajectory (7.14), as the first derivatives  $V_i$  with  $i = \{s_r, \sigma\}$  are non-zero (7.16). Expanding in small  $\epsilon_w$  this shift is

$$\begin{aligned} \delta\sigma &= -\frac{9\kappa^2 M^4(3-4\kappa_S)}{4a^2 b^2 \kappa_S W_0^2} + \epsilon_w \frac{3(1-2\kappa_S)}{4ab\kappa_S W_0 \sigma_0}, \\ \delta s_r &= -\frac{9\kappa M^2}{8\sqrt{2}abW_0\kappa_S\sigma_0^2} - \epsilon_w \frac{1}{\sqrt{2}\kappa\kappa_S M^2}. \end{aligned} \quad (7.26)$$

The shift due to the inflation sector, which is the  $\epsilon_w$  independent part, is small, and harmless for inflation. The corrections due to the modulus sector scale with  $\epsilon_w$  and can be larger depending on the size of  $\epsilon_w$ . The mass matrix is nearly diagonal. Except for the  $s_r$ -field, the masses for all the inflaton fields are as before (7.5), up to an overall scaling by  $(2\sigma_0)^3$ , and up to order  $\delta m_i^2 = \mathcal{O}(\epsilon_w^2/(2\sigma_0)^3)$  corrections. From the masses of  $s_r$  and  $n_r$  one can deduce constraints on  $\kappa_{SN}$  and  $\kappa_S$ , just as we did before around (7.5):

$$m_{n_r}^2 = \frac{2\kappa^2 M^4(1-\kappa_{SN})}{(2\sigma_0)^3}, \quad m_{s_r}^2 = \frac{\kappa^2 M^4(3-4\kappa_S)}{(2\sigma_0)^3} \quad (7.27)$$

lead to the constraints  $\kappa_{SN} < \frac{5}{6}$  and  $\kappa_S < \frac{2}{3}$ . It follows that for  $\epsilon_w \gtrsim \kappa M^2$  the moduli corrections dominate, and one of the masses, depending on the choice of  $\kappa_i$  parameters in the Kähler potential (7.2), may go tachyonic, thereby destroying inflation.

**Waterfall mechanism and CW-loop** A stronger bound on the value of  $\epsilon_w$  may be obtained by looking at the waterfall masses. Writing the masses of the bosonic waterfall fields and their superpartners in the form  $m^2 = \mu^2(x^2 + y^2 \pm 1)$  and  $\tilde{m}^2 = \mu^2 x^2$ , we find

$$\mu^2 = \frac{2\kappa^2 M^2}{(2\sigma_0)^3} + \mathcal{O}(\epsilon_w), \quad x^2 = \frac{\lambda^2 n_i^4}{2\kappa^2 M^2} + \mathcal{O}(\epsilon_w), \quad y^2 = \frac{M^2}{2}(1-\kappa_{SH}) - \epsilon_w^2 \frac{\kappa_{SH} \lambda^2 n_i^4}{4\kappa^2 \kappa_S^2 M^2}, \quad (7.28)$$

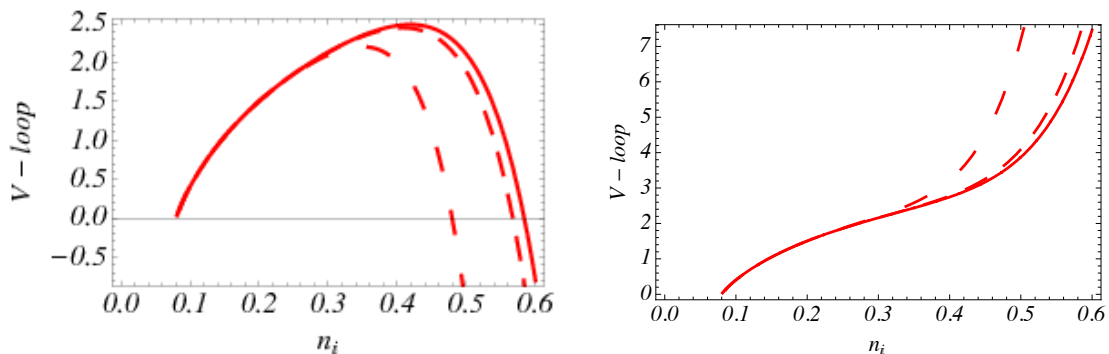


Figure 7.1: The Coleman-Weinberg potential, rescaled by a factor  $10^{15}$ , as a function of  $n_i$  for  $\epsilon_w = \{0, 10^{-7}, 10^{-5}\}$  corresponding to the solid, short dashed and dashed lines respectively. On the left are the results for  $\kappa_{SH} = 1$ , on the right for  $\kappa_{SH} = -1$ .

where the dominant moduli correction for our purposes is the  $\mathcal{O}(\epsilon_w^2)$  correction in  $y^2$ . Although  $y^2 \ll x^2$ , and is an unimportant contribution to the waterfall field mass, it is relevant for the one loop potential. As explained in the appendix G, the reason is that the dominant terms cancel between the bosons and the fermions in the Coleman-Weinberg potential (G.1). Indeed, even in the absence of moduli corrections the term  $\propto M^2(1 - \kappa_{SH})$  in the boson mass causes the loop potential to develop a maximum for  $\kappa_{SH} > 1$  (G.6). If the  $\epsilon_w^2$ -correction in  $y^2$  dominates, the loop potential steepens for large  $n_i$ . In the case of  $\kappa_{SH} > 0$ , this results in the maximum shifting to smaller values of  $n_i$ , until at some point it becomes impossible to get 60 e-folds of inflation. In the opposite limit  $\kappa_{SH} < 0$  it results in a larger spectral index, in contradiction with observations. Either way, inflation is ruined if the moduli corrections get too large. Using (7.28) this gives the bound

$$\epsilon_w \lesssim 0.1 - 0.01\kappa M^2, \quad (7.29)$$

where the exact value depends on the  $\kappa_i$  values, and the precise parameters. This estimate is confirmed by our numerical calculation.

## 7.4.2 Numerical analysis

Adding a modulus sector to inflation, the F-term potential and thus all masses squared are rescaled by a factor  $e^K = (2\sigma)^{-3}$ . We can absorb this factor in the parameters of the superpotential via

$$\bar{\kappa} = \frac{\kappa}{(2\sigma_0)^{3/2}}, \quad \bar{\lambda} = \frac{\lambda}{(2\sigma_0)^{3/2}}, \quad \bar{A} = \frac{A}{(2\sigma_0)^{3/2}}, \quad \bar{B} = \frac{B}{(2\sigma_0)^{3/2}}, \quad \bar{W}_0 = \frac{W_0}{(2\sigma_0)^{3/2}}. \quad (7.30)$$

The barred quantities are the ones that give the effective couplings between the fields, and that can be measured (in principle) in experiments. The rescaling allows to easily compare the parameter space for hybrid inflation without moduli as described in section 7.2 and discussed in detail in Ref. [169], with the set-up where a modulus potential is included. If in the former case the model gives the right predictions for the density perturbations for a given set of parameters, for example  $\{\kappa = 0.14, M = 0.003, \dots\}$ , the same observational results are obtained in the setup up with a modulus field if we choose the same numerical values for the barred quantities  $\{\bar{\kappa} = 0.14, M = 0.003, \dots\}$ . This correspondence works up to  $\mathcal{O}(\epsilon_w)$  corrections. We checked numerically that with the above identification we get the same parameter space for successful inflation, e.g. including the same  $\kappa_{SN}$  dependence, as found in Ref. [169].

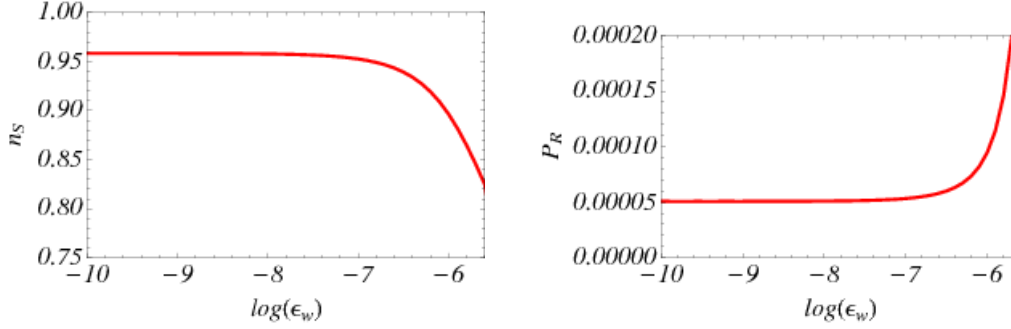


Figure 7.2: The spectral index  $n_s$  (left) and power spectrum  $P_{\mathcal{R}}$  (right) as a function of  $\epsilon_w$  for the parameters mentioned in the text.

Consider an explicit numerical example. For the inflaton sector we choose parameter values

$$\bar{\kappa} = 0.14, \quad M = 0.003, \quad \bar{\lambda} = 0.1, \quad \kappa_{SH} = 1, \quad (7.31)$$

and all other  $\kappa_i$  equal to  $-1$ . As discussed in section 7.2 this assures stability of the inflationary trajectory. For the modulus sector we take

$$\bar{A} = 1, \quad \bar{B} = 1.03, \quad a = \frac{2\pi}{100}, \quad a = \frac{2\pi}{99}. \quad (7.32)$$

which gives  $W_0 = 0.276 + \epsilon_w$  and  $\sigma_0 = 62.41$ . The exact parameter values in (7.32) are not so important, what matters is the resultant value for  $W_0$  and to some lesser extent  $\sigma_0$ .

As anticipated, as we increase  $\epsilon_w$  we see that the moduli corrections first appear in the loop potential. For  $\epsilon_w = \{0, 10^{-7}, 10^{-5}\}$  we get  $\delta\sigma = \{2.06, 2.39, 5.33\} \times 10^{-5}$  and  $\delta s_r = \{3.26, 3.66, 7.28\} \times 10^{-4}$ . These values match our estimates (7.26). Although the increase in  $\delta s_r$  seems quite moderate, the effects are nevertheless visible in the loop potential, where the maximum is shifting to increasingly small  $n_i$ -values. This is plotted in figure 7.1. For  $\epsilon = 10^{-5}$  the loop potential gets modified in such a way that the slow-roll trajectory is not large enough to accommodate 60 e-folds of inflation. Figure 7.1 also shows the equivalent results for  $\kappa_{SH} = -1$  and for the rest the same parameters; now the potential steepens to fast for  $\epsilon_w > 10^{-5}$  pushing the spectral index to values larger than one.

Figure 7.2 shows the spectral index and power spectrum as a function of  $\epsilon_w$ . For small  $\epsilon_w$  the results are identical to those found in the model without a modulus. As  $\epsilon_w$  approaches its critical value (7.29) the results for the spectral index and power spectrum change rapidly, and inflation breaks down abruptly.

## 7.5 Conclusions

In this chapter we combined the hybrid inflation model of [169] with a KKLT like modulus sector. The inflaton mass is protected by a shift symmetry, and remains massless (at tree level) even in the presence of the modulus sector. This is in sharp contrast with standard sugra hybrid inflation.

The vacuum after inflation and the inflationary trajectory are corrected by the modulus sector. These corrections are under control and do not disrupt inflation provided the modulus sector satisfies the constraint  $D_T W_{\text{mod}} \approx W_{\text{mod}} \approx 0$ . The first condition is automatic in the minimum of the potential, the second

condition can be satisfied by fine-tuning the parameters in the potential. This is the same fine-tuning needed to get a hierarchy between the gravitino and modulus mass, and which allows for low scale susy breaking yet high scale inflation. As explicit examples, the original KKLT modulus stabilization scheme [170] does not satisfy the above condition, whereas the fine-tuned model of Kallosh & Linde [102, 178] does.

Why inflation works for a modulus sector with small scale susy breaking can be easily understood by considering the relevant scales in the system.

1. The modulus mass  $m_T \propto W_0$  which sets the height of the barrier in the modulus potential. It has to be larger than the inflationary scale for the modulus to be stabilized during inflation; this implies the condition (7.20).
2. The energy density during inflation  $V_{\text{inf}} = \bar{\kappa}^2 M^4$ , which determines the size of the density perturbations. To get the observed amplitude we find  $V_{\text{inf}}^{1/4} \sim M_{\text{GUT}}$  is of the order of the grand unified scale.
3. The vacuum gravitino mass  $m_{3/2} = e^{K/2}|W| \propto \epsilon_W$ , which sets the scale of the moduli corrections to the inflationary potential. It cannot be too large, the bound (7.29) translates in a bound on the gravitino mass  $m_{3/2} \lesssim 10^9 - 10^{10} \text{GeV}/\sigma_0^{3/2}$ .

In summary, we find that it is possible to extend the, in itself already very promising, model of supersymmetric hybrid inflation proposed in Ref. [169] with a moduli sector. It is absolutely necessary to have a modulus sector that does not break susy too badly. Therefore we need to tune the parameters in the superpotential. As a bonus, however, we find that our extended model can accommodate TeV-scale susy breaking.

**Part IV**

**Outlook**



# Outlook

In this thesis we have provided effective descriptions of various cosmological processes. Here, in this last part, we offer some conclusions, and point to new roads for research based on our work. We will also discuss some implications of the Planck data.

In chapters 3 and 4 we have found the unrenormalized divergent contributions to the effective action for the Abelian Higgs model in an expanding universe. After all subtleties involving gauge invariance, Goldstone bosons and the use of unitary gauge, the final answer (4.59) seems very clear and intuitive. While the use of effective theories in time dependent backgrounds has only just begun, and deserves much more devotion, see for example [186, 187], certain physical applications of our work can already be conceived.

The first option that comes to mind is the one that inspired us to do our computations in the first place: Higgs inflation, introduced in subsection 1.7. Apart from renormalizing our result (4.59), we should take the non-minimal Higgs-graviton coupling into account. This is work in progress. The corrections to the effective action that one would not naively expect are proportional to  $V_{\theta\theta} \sim \partial V / \partial \phi_{\text{cl}}$  and therefore small during inflation, but grow during reheating. (In the renormalized effective action they show up as the wave function renormalization.) Note that Higgs inflation, with the few input parameters it requires, matches the Planck results very well. Its largest observational threat is coming from the relatively low Higgs mass measured at the LHC. A more precise measurement of the top mass, perhaps in a new  $e^+e^-$ -collider, and of the tensor-to-scalar ratio, by Planck, can further test or rule out Higgs inflation.

Another possible application is the description of flat directions in the MSSM and its extensions [188], which are lifted by the one-loop quantum corrections. This may affect inflation models or Affleck-Dine baryogenesis models using flat directions [189, 190].

The study of single field inflation in supergravity, done in chapter 5, has shown to what extent inflationary dynamics can be decoupled from all other “matter” dynamics present. We have shown that a maximal decoupling is achieved when the inflaton field direction coincides with that of supersymmetry breaking. A logical next topic to study would be the inclusion of moduli fields to such a model. In the meantime, since sgoldstino inflation cannot be of the large field type, a possible detection of tensor waves would, by the Lyth bound (1.65), rule out this scenario. Hybrid variants and especially small field scenarios are still experimentally viable. In this last scenario it is possible that supersymmetry breaking happens once and for all when inflation takes place. The non-detection of susy particles at the LHC so far confirms this model, but there is a very long way to go.

Since Planck has not found any trace of (primordial) non-Gaussianity, the models presented in chapter 6 are still experimentally viable, with some changed parameter input, but have undoubtedly lost some of their appeal. What remains is that we have shown that the coupling  $\chi F\tilde{F}$ , compatible with all symmetries in the problem, is actually more constrained by primordial black holes than by non-Gaussianity

or the breaking of scale invariance. However, this is still an estimate and it would be very interesting to (numerically) study the precise evolution of the small inflaton modes in the regime where backreaction from the gauge fields is large. Furthermore, we have revealed the close connection to the supergravity models studied in [123, 124, 125]. The flexibility of these models has by now been extended to a possible inclusion of cosmic strings as well [191].

Chapter 7, finally, has shown how KL moduli stabilization can be done in the particular hybrid sneutrino inflation model of [169]. This model is perfectly compatible with the Planck data.

All in all, we see that Planck's first release of cosmological results has affected the models studied in this thesis in various ways. More drama is expected from the second release, where tensor waves will either be seen (ruling out Higgs inflation) or been put under a much stronger bound (ruling out  $m^2\phi^2$ -inflation). Here the theoretical cosmologist can only wait. It is clear, however, that the increasing precision in cosmology forces, or invites, the theorist to prepare precise effective descriptions. In particular, spelling out the subtle effects of time dependence in background fields brings about a whole new field of study whose subtleties we have just begun to explore.

## Appendix A

# Mode functions for the time dependent scalar field

This appendix is dedicated to solving

$$\ddot{g}_{\vec{k}} - 2i\bar{E}_{\vec{k}}\dot{g}_{\vec{k}} = -V(t)(1 + g_{\vec{k}}), \quad g_{\vec{k}}(0) = 0, \quad \dot{g}_{\vec{k}}(0) = 0, \quad (\text{A.1})$$

for  $g_{\vec{k}}(t)$  up to order  $(\bar{E}_{\vec{k}})^{-2}$ . We want to prove that equation (2.68) indeed leads to (2.69).

First we calculate an integral that we will need soon:

$$\begin{aligned} \int_0^t dt' e^{2i\bar{E}_{\vec{k}}(t-t')} \alpha(t') &= \frac{ie^{2i\bar{E}_{\vec{k}}(t-t')}}{2\bar{E}_{\vec{k}}} \alpha(t') \Big|_{t'=0}^{t'=t} - \int_0^t dt' \frac{e^{2i\bar{E}_{\vec{k}}(t-t')}}{-2i\bar{E}_{\vec{k}}} \dot{\alpha}(t') \\ &= \frac{i[\alpha(t) - \alpha(0)e^{2i\bar{E}_{\vec{k}}t}]}{2\bar{E}_{\vec{k}}} + \frac{\dot{\alpha}(t) - \dot{\alpha}(0)e^{2i\bar{E}_{\vec{k}}t}}{4\bar{E}_{\vec{k}}^2} + \mathcal{O}(\bar{E}_{\vec{k}}^{-3}). \end{aligned} \quad (\text{A.2})$$

Now back to the original problem. We are first going to calculate the Green's function  $G(t, t')$  from

$$\ddot{G}_{\vec{k}} - 2i\bar{E}_{\vec{k}}\dot{G}_{\vec{k}} = \delta(t - t'), \quad (\text{A.3})$$

and then we get  $g_{\vec{k}}^{(n)}(t)$  order by order in  $V(t)$  from

$$g_{\vec{k}}^{(n)}(t) = \int_0^\infty dt' G(t, t') \left[ -V(t')(1 + g_{\vec{k}}^{(n-1)}(t')) \right]. \quad (\text{A.4})$$

$G(t, t')$  is just the retarded propagator, hence the integration from 0 to  $\infty$ . 1 is factored out such that  $g^{(0)}(t) = 0$ .

To solve (A.3) we insert the Fourier expansion  $G(t, t') = \frac{1}{2\pi} \int_{-\infty}^\infty d\omega e^{-i\omega(t-t')} \tilde{G}(\omega)$ . This gives easily (also expand the delta function as  $\delta(t - t') = \frac{1}{2\pi} \int_{-\infty}^\infty d\omega e^{-i\omega(t-t')}$ )

$$-\omega^2 \tilde{G}(\omega) - 2\bar{E}_{\vec{k}} \tilde{G}(\omega) = 1, \quad \rightarrow \quad \tilde{G}(\omega) = -\frac{1}{\omega(\omega + 2\bar{E}_{\vec{k}})}. \quad (\text{A.5})$$

So now we find  $G(t, t')$  from

$$G(t, t') = \frac{1}{2\pi} \int_{-\infty}^{\infty} d\omega e^{-i\omega(t-t')} \cdot \frac{1}{\omega(\omega + 2\bar{E}_{\vec{k}})}. \quad (\text{A.6})$$

The integrand has poles at  $\omega = 0$  and  $\omega = -2\bar{E}_{\vec{k}}$ . For  $t > t'$  ( in the integral the dummy variable  $t'$  is going to run from zero up) we have to close the contour in the lower half plane. Therefore we run the contour clockwise, so we get a factor of  $(-2\pi i)$ . All in all the residue theorem gives

$$\begin{aligned} G(t, t') &= -2\pi i \frac{1}{2\pi} \left[ -\frac{1}{2\bar{E}_{\vec{k}}} + -\frac{1}{-2\bar{E}_{\vec{k}}} e^{2i\bar{E}_{\vec{k}}(t-t')} \right] \theta(t-t') \\ &= i \left[ \frac{1}{2\bar{E}_{\vec{k}}} \left( 1 - e^{2i\bar{E}_{\vec{k}}(t-t')} \right) \right] \theta(t-t'). \end{aligned} \quad (\text{A.7})$$

Now we can begin to solve (A.4). Inserting  $g_{\vec{k}}^{(0)}(t) = 0$  we find for  $g_{\vec{k}}^{(1)}(t)$

$$\begin{aligned} g_{\vec{k}}^{(1)}(t) &= \int_0^{\infty} dt' G(t, t') \left[ -V(t')(1 + g_{\vec{k}}^{(0)}(t')) \right] \\ &= \int_0^t dt' \left[ -\frac{i}{2\bar{E}_{\vec{k}}} \left( 1 - e^{2i\bar{E}_{\vec{k}}(t-t')} \right) V(t') \right] \\ &= \frac{-i \int_0^t dt' V(t')}{2\bar{E}_{\vec{k}}} + \frac{i}{2\bar{E}_{\vec{k}}} \int_0^t dt' e^{2i\bar{E}_{\vec{k}}(t-t')} V(t') \\ &= \frac{-i \int_0^t dt' V(t')}{2\bar{E}_{\vec{k}}} + \frac{i}{2\bar{E}_{\vec{k}}} \left[ \frac{i \left[ V(t) - V(0)e^{2i\bar{E}_{\vec{k}}t} \right]}{2\bar{E}_{\vec{k}}} + \mathcal{O}(\bar{E}_{\vec{k}}^{-2}) \right] \\ &= \frac{-i \int_0^t dt' V(t')}{2\bar{E}_{\vec{k}}} - \frac{V(t) - V(0)e^{2i\bar{E}_{\vec{k}}t}}{4\bar{E}_{\vec{k}}^2} + \mathcal{O}(\bar{E}_{\vec{k}}^{-3}). \end{aligned} \quad (\text{A.8})$$

Now to get  $g_{\vec{k}}^{(2)}(t)$  we plug into the right hand side:

$$\begin{aligned} g_{\vec{k}}^{(2)}(t) &= \int_0^{\infty} dt' G(t, t') \left[ -V(t')g_{\vec{k}}^{(1)}(t') \right] \\ &= \int_0^t dt' \frac{i}{2\bar{E}_{\vec{k}}} \left( 1 - e^{2i\bar{E}_{\vec{k}}(t-t')} \right) \cdot -V(t') \left[ \frac{-i \int_0^{t'} dt'' V(t'')}{2\bar{E}_{\vec{k}}} - \frac{V(t') - V(0)e^{2i\bar{E}_{\vec{k}}t'}}{4\bar{E}_{\vec{k}}^2} + \mathcal{O}(\bar{E}_{\vec{k}}^{-3}) \right] \\ &= -\frac{1}{4\bar{E}_{\vec{k}}^2} \int_0^t dt' V(t') \int_0^{t'} dt'' V(t'') + \mathcal{O}(\bar{E}_{\vec{k}}^{-3}) \end{aligned} \quad (\text{A.9})$$

We perform these integrals in turn.

For (A.9) we get, denoting the primitive function of  $V$  by  $\tilde{V}$  (irrelevant integration constant set to zero)

$$\begin{aligned}
-\frac{1}{4\bar{E}_k^2} \int_0^t dt' V(t') \int_0^{t'} dt'' V(t'') &= \frac{1}{4\bar{E}_k^2} \int_0^t dt' V(t') [\tilde{V}(t') - \tilde{V}(0)] \\
&= -\frac{1}{4\bar{E}_k^2} \left[ \frac{1}{2} \tilde{V}^2(t') \Big|_{t'=0}^{t'=t} - \tilde{V}(0) (\tilde{V}(t) - \tilde{V}(0)) \right] \\
&= -\frac{1}{4\bar{E}_k^2} \left[ \frac{1}{2} \tilde{V}^2(t) + \frac{1}{2} \tilde{V}^2(0) - \tilde{V}(0) \tilde{V}(t) \right] \\
&= -\frac{1}{8\bar{E}_k^2} \left[ (\tilde{V}(t) - \tilde{V}(0))^2 \right] \\
&= -\frac{1}{8\bar{E}_k^2} \left[ \int_0^t dt' V(t') \right]^2. \tag{A.10}
\end{aligned}$$

So we end up with:

$$g_{\vec{k}}(t) = \frac{-i \int_0^t dt' V(t')}{2\bar{E}_{\vec{k}}} - \frac{V(t) - V(0)e^{2i\bar{E}_{\vec{k}}t}}{4\bar{E}_{\vec{k}}^2} - \frac{1}{8\bar{E}_{\vec{k}}^2} \left[ \int_0^t dt' V(t') \right]^2 + \mathcal{O}(\bar{E}_{\vec{k}}^{-3}). \tag{A.11}$$

### Application to scalar fields

For the time dependent scalar field we have  $V(t) = \delta m^2(t)$  and we are interested in  $|U_{\vec{k}}(t)|^2$  up to order  $(\bar{E}_{\vec{k}})^{-2}$ . So we have (upon using that  $\delta m^2(0) = 0$ )

$$\begin{aligned}
|U_{\vec{k}}(t)|^2 = |1 + g_{\vec{k}}(t)|^2 &= 1 + \frac{\left[ \int_0^t dt' \delta m^2(t') \right]^2}{4\bar{E}_{\vec{k}}^2} - \frac{\delta m^2(t)}{2\bar{E}_{\vec{k}}^2} - \frac{\left[ \int_0^t dt' \delta m^2(t') \right]^2}{4\bar{E}_{\vec{k}}^2} + \mathcal{O}(\bar{E}_{\vec{k}}^{-3}) \\
&= 1 - \frac{\delta m^2(t)}{2\bar{E}_{\vec{k}}^2} + \mathcal{O}(\bar{E}_{\vec{k}}^{-3}). \tag{A.12}
\end{aligned}$$



## Appendix B

# Abelian Higgs model

In this appendix we will drop the subscript of the field  $A_0$ .

### B.1 Mixed propagator

The defining equation for the propagator is (3.47):

$$\begin{pmatrix} -\left(\partial_{(x)}^\mu \partial_\mu^{(x)} + m_A^2\right) & \delta m_{A\theta}^2 \\ \delta m_{A\theta}^2 & \partial_{(x)}^\mu \partial_\mu^{(x)} + m_\theta^2 \end{pmatrix} \begin{pmatrix} \Delta_{AA}^{++}(x-y) & \Delta_{A\theta}^{++}(x-y) \\ \Delta_{\theta A}^{++}(x-y) & \Delta_{\theta\theta}^{++}(x-y) \end{pmatrix} = -i\delta^{(4)}(x-y) \begin{pmatrix} 1 & 0 \\ 0 & 1 \end{pmatrix}. \quad (\text{B.1})$$

and we claim that it is solved by (3.48):

$$\begin{aligned} \Delta_{kn}^{++}(x-y) &= \theta(x^0 - y^0) \int \frac{d^3k}{(2\pi)^3} \left[ -\frac{1}{2\bar{E}_A} U_k^1(x^0) U_n^{1*}(y^0) + \frac{1}{2\bar{E}_\theta} U_k^2(x^0) U_n^{2*}(y^0) \right] e^{i\vec{k}\cdot(\vec{x}-\vec{y})} \\ &\quad + \theta(y^0 - x^0) \int \frac{d^3k}{(2\pi)^3} \left[ -\frac{1}{2\bar{E}_A} U_k^{1*}(x^0) U_n^1(y^0) + \frac{1}{2\bar{E}_\theta} U_k^{2*}(x^0) U_n^2(y^0) \right] e^{-i\vec{k}\cdot(\vec{x}-\vec{y})} \end{aligned} \quad (\text{B.2})$$

Let us first compute  $\partial_{x^0}^2 (\Delta_{AA}^{++}(x-y))$ . The double time derivative gives three contributions on the  $\theta(x^0 - y^0)$  part and three ones on the  $\theta(y^0 - x^0)$  part. We get

$$\begin{aligned} \partial_{x^0}^2 &\left[ \theta(x^0 - y^0) \int \frac{d^3k}{(2\pi)^3} \left[ \frac{1}{2\bar{E}_A} U_A^1(x^0) U_A^{1*}(y^0) - \frac{1}{2\bar{E}_\theta} U_A^2(x^0) U_A^{2*}(y^0) \right] e^{i\vec{k}\cdot(\vec{x}-\vec{y})} \right. \\ &\quad \left. + \theta(y^0 - x^0) \int \frac{d^3k}{(2\pi)^3} \left[ \frac{1}{2\bar{E}_A} U_A^{1*}(x^0) U_A^1(y^0) - \frac{1}{2\bar{E}_\theta} U_A^{2*}(x^0) U_A^2(y^0) \right] e^{-i\vec{k}\cdot(\vec{x}-\vec{y})} \right] \end{aligned}$$

$$\begin{aligned}
&= \partial_{x^0} \left[ \delta(x^0 - y^0) \delta(\vec{x} - \vec{y}) \int \frac{d^3 k}{(2\pi)^3} \left( \frac{1}{2\bar{E}_A} U_A^1(x^0) U_A^{1*}(y^0) - \frac{1}{2\bar{E}_\theta} U_A^2(x^0) U_A^{2*}(y^0) \right) e^{i\vec{k}\cdot(\vec{x}-\vec{y})} \right] \\
&\quad - \partial_{x^0} \left[ \delta(x^0 - y^0) \delta(\vec{x} - \vec{y}) \int \frac{d^3 k}{(2\pi)^3} \left( \frac{1}{2\bar{E}_A} U_A^1(y^0) U_A^{1*}(x^0) - \frac{1}{2\bar{E}_\theta} U_A^2(y^0) U_A^{2*}(x^0) \right) e^{-i\vec{k}\cdot(\vec{x}-\vec{y})} \right] \\
&\quad + \delta(x^0 - y^0) \delta(\vec{x} - \vec{y}) \int \frac{d^3 k}{(2\pi)^3} \left( \frac{1}{2\bar{E}_A} \dot{U}_A^1(x^0) U_A^{1*}(y^0) - \frac{1}{2\bar{E}_\theta} \dot{U}_A^2(x^0) U_A^{2*}(y^0) \right) e^{i\vec{k}\cdot(\vec{x}-\vec{y})} \\
&\quad - \delta(x^0 - y^0) \delta(\vec{x} - \vec{y}) \int \frac{d^3 k}{(2\pi)^3} \left( \frac{1}{2\bar{E}_A} U_A^1(y^0) \dot{U}_A^{1*}(x^0) - \frac{1}{2\bar{E}_\theta} U_A^2(y^0) \dot{U}_A^{2*}(x^0) \right) e^{-i\vec{k}\cdot(\vec{x}-\vec{y})} \\
&\quad + \theta(x^0 - y^0) \int \frac{d^3 k}{(2\pi)^3} \left[ \frac{1}{2\bar{E}_A} \left( -E_A^2 U_A^1(x^0) + \delta m_{A\theta}^2 U_\theta^1(x^0) \right) U_A^{1*}(y^0) \right. \\
&\quad \quad \quad \left. - \frac{1}{2\bar{E}_\theta} \left( -E_A^2 U_A^2(x^0) + \delta m_{A\theta}^2 U_\theta^2(x^0) \right) U_A^{2*}(y^0) \right] e^{i\vec{k}\cdot(\vec{x}-\vec{y})} \\
&\quad + \theta(y^0 - x^0) \int \frac{d^3 k}{(2\pi)^3} \left[ \frac{1}{2\bar{E}_A} \left( -E_A^2 U_A^{1*}(x^0) + \delta m_{A\theta}^2 U_\theta^{1*}(x^0) \right) U_A^1(y^0) \right. \\
&\quad \quad \quad \left. - \frac{1}{2\bar{E}_\theta} \left( -E_A^2 U_A^{2*}(x^0) + \delta m_{A\theta}^2 U_\theta^{2*}(x^0) \right) U_A^2(y^0) \right] e^{-i\vec{k}\cdot(\vec{x}-\vec{y})}. \quad (\text{B.3})
\end{aligned}$$

Now the first pair of lines cancels off against each other. The second pair gives  $-i\delta^{(4)}(x - y)$  once we impose the Wronskian relations

$$\begin{aligned}
U_\alpha^1 \dot{U}_\beta^{1*} - \dot{U}_\gamma^1 U_\delta^{1*} &= 2i\bar{E}_A \delta_{\alpha A} \delta_{\beta A} \delta_{\gamma A} \delta_{\delta A} \\
U_\alpha^2 \dot{U}_\beta^{2*} - \dot{U}_\gamma^2 U_\delta^{2*} &= 2i\bar{E}_\theta \delta_{\alpha\theta} \delta_{\beta\theta} \delta_{\gamma\theta} \delta_{\delta\theta}. \quad (\text{B.4})
\end{aligned}$$

These Wronskian follow from demanding the correct equal time commutation relations between each field and its associated momentum. Using the equations of motion one can show that the Wronskians are time independent.

To get the third pair of lines we have used the equation of motion (3.45). When we act with the remainder of the operator  $-(\partial_\mu \partial^\mu + m_A^2)$  on  $\Delta_{AA}^{++}(x - y)$  we will see that the factors of  $-E_A^2$  inside the integrals become  $(-E_A^2 + \vec{k} \cdot \vec{k} + m_A^2) = 0$ . So we are only left with the parts that involve  $U_\theta$ 's.

Now we compute  $\delta m_{A\theta}^2 \Delta_{\theta A}^{++}(x - y)$ . This gives

$$\begin{aligned}
&\theta(x^0 - y^0) \int \frac{d^3 k}{(2\pi)^3} \left[ -\frac{1}{2\bar{E}_A} \delta m_{A\theta}^2 U_\theta^1(x^0) U_A^{1*}(y^0) + \frac{1}{2\bar{E}_\theta} \delta m_{A\theta}^2 U_\theta^2(x^0) U_A^{2*}(y^0) \right] e^{i\vec{k}\cdot(\vec{x}-\vec{y})} \\
&\quad + \theta(y^0 - x^0) \int \frac{d^3 k}{(2\pi)^3} \left[ -\frac{1}{2\bar{E}_A} \delta m_{A\theta}^2 U_\theta^{1*}(x^0) U_A^1(y^0) + \frac{1}{2\bar{E}_\theta} \delta m_{A\theta}^2 U_\theta^{2*}(x^0) U_A^2(y^0) \right] e^{-i\vec{k}\cdot(\vec{x}-\vec{y})}, \quad (\text{B.5})
\end{aligned}$$

which cancels the third pair of lines we discussed just before. So we indeed find that

$$-\left( \partial_\mu^{(x)} \partial_\mu^{(x)} + m_A^2 \right) \Delta_{AA}^{++}(x - y) + \delta m_{A\theta}^2 \Delta_{\theta A}^{++}(x - y) = -i\delta^{(4)}(x - y), \quad (\text{B.6})$$

which is just the upper left index of the matrix equation (B.1) that we are trying to verify.

To prove the lower right index of (B.1) we can proceed along exactly the same lines. Now for the lower left index. First we compute  $\partial_t^2 \Delta_{\theta A}^{++}(x - y)$ . This gives again three pairs of lines. The first pair cancels

just as before. The second pair cancels upon using the Wronskian relations (B.4). For the third pair we get

$$\begin{aligned} & \theta(x^0 - y^0) \int \frac{d^3k}{(2\pi)^3} \left[ -\frac{1}{2\bar{E}_A} \left( -E_\theta^2 U_\theta^1(x^0) - \delta m_{A\theta}^2 U_A^1(x^0) \right) U_A^{1*}(y^0) \right. \\ & \quad \left. + \frac{1}{2\bar{E}_\theta} \left( -E_\theta^2 U_\theta^2(x^0) - \delta m_{A\theta}^2 U_\theta^2(x^0) \right) U_A^{2*}(y^0) \right] e^{i\vec{k}\cdot(\vec{x}-\vec{y})} \\ & + \theta(y^0 - x^0) \int \frac{d^3k}{(2\pi)^3} \left[ -\frac{1}{2\bar{E}_A} \left( -E_\theta^2 U_\theta^{1*}(x^0) - \delta m_{A\theta}^2 U_A^{1*}(x^0) \right) U_A^1(y^0) \right. \\ & \quad \left. + \frac{1}{2\bar{E}_\theta} \left( -E_\theta^2 U_\theta^{2*}(x^0) - \delta m_{A\theta}^2 U_A^{2*}(x^0) \right) U_A^2(y^0) \right] e^{-i\vec{k}\cdot(\vec{x}-\vec{y})}. \end{aligned} \quad (\text{B.7})$$

Again we have used (3.45), and again the factors  $(-E_\theta^2)$  will become  $(-E_\theta^2 + \vec{k}\cdot\vec{k} + m_\theta^2) = 0$  when we act with the remainder of  $\partial_\mu^{(x)} \partial_{(x)}^\mu + m_\theta^2$ .

When we now compute  $\delta m_{A\theta}^2 \Delta_{AA}^{++}(x-y)$  we find

$$\begin{aligned} & \theta(x^0 - y^0) \int \frac{d^3k}{(2\pi)^3} \left[ -\frac{1}{2\bar{E}_A} \delta m_{A\theta}^2 U_A^1(x^0) U_A^{1*}(y^0) + \frac{1}{2\bar{E}_\theta} \delta m_{A\theta}^2 U_A^2(x^0) U_A^{2*}(y^0) \right] e^{i\vec{k}\cdot(\vec{x}-\vec{y})} \\ & + \theta(y^0 - x^0) \int \frac{d^3k}{(2\pi)^3} \left[ -\frac{1}{2\bar{E}_A} \delta m_{A\theta}^2 U_A^{1*}(x^0) U_A^1(y^0) + \frac{1}{2\bar{E}_\theta} \delta m_{A\theta}^2 U_A^{2*}(x^0) U_A^2(y^0) \right] e^{-i\vec{k}\cdot(\vec{x}-\vec{y})} \end{aligned} \quad (\text{B.8})$$

which exactly cancels the remaining terms in (B.7). So we find that

$$\delta m_{A\theta}^2 \Delta_{AA}^{++}(x-y) + \left( \partial_\mu^{(x)} \partial_{(x)}^\mu + m_\theta^2 \right) \Delta_{A\theta}^{++}(x-y) = 0, \quad (\text{B.9})$$

which proves the lower left index of (B.1).

Proving its upper right index, finally, is straightforward now.

## B.2 Mode functions

We set

$$\begin{aligned} U_A^1 &= e^{-i\bar{E}_A t} (1 + f_A^1), & U_\theta^1 &= e^{-i\bar{E}_\theta t} f_\theta^1, \\ U_\theta^2 &= e^{-i\bar{E}_\theta t} (1 + f_\theta^2), & U_A^2 &= e^{-i\bar{E}_A t} f_A^2. \end{aligned} \quad (\text{B.10})$$

and we want to solve equation (3.47)

$$\begin{aligned} \ddot{f}_A^1 - 2i\bar{E}_A \dot{f}_A^1 &= -\delta m_A^2 (1 + f_A^1) + \delta m_{A\theta}^2 e^{i(\bar{E}_A - \bar{E}_\theta)t} f_\theta^1 \\ \ddot{f}_A^2 - 2i\bar{E}_A \dot{f}_A^2 &= -\delta m_A^2 f_A^2 + \delta m_{A\theta}^2 e^{i(\bar{E}_A - \bar{E}_\theta)t} (1 + f_\theta^2) \\ \ddot{f}_\theta^1 - 2i\bar{E}_\theta \dot{f}_\theta^1 &= -\delta m_\theta^2 f_\theta^1 - \delta m_{A\theta}^2 e^{-i(\bar{E}_A - \bar{E}_\theta)t} (1 + f_A^1) \\ \ddot{f}_\theta^2 - 2i\bar{E}_\theta \dot{f}_\theta^2 &= -\delta m_\theta^2 (1 + f_\theta^2) - \delta m_{A\theta}^2 e^{-i(\bar{E}_A - \bar{E}_\theta)t} f_A^2. \end{aligned} \quad (\text{B.11})$$

In appendix A we have computed the Green's function  $G(t, t')$  of the operator  $\ddot{f} - 2i\bar{E}\dot{f}_A$ :

$$G(t, t') = \theta(t - t') \frac{i}{2\bar{E}} \left( 1 - e^{2i\bar{E}(t-t')} \right). \quad (\text{B.12})$$

With this we showed that the equation  $\ddot{f} - 2i\bar{E}f_A = g(t)$  is solved by

$$f(t) = \frac{i \int_0^t dt' g(t')}{2\bar{E}} + \frac{g(t) - g(0)e^{2i\bar{E}t}}{4\bar{E}^2} + \mathcal{O}(\bar{E}^{-3}). \quad (\text{B.13})$$

So there we go. At “zeroth” order we have

$$f_A^{1(0)} = f_A^{2(0)} = f_\theta^{1(0)} = f_\theta^{2(0)} = 0. \quad (\text{B.14})$$

We insert that into (B.11) to find the first order solutions:

$$\begin{aligned} \ddot{f}_A^{1(1)} - 2i\bar{E}_A \dot{f}_A^{1(1)} &= -\delta m_A^2 \\ \ddot{f}_A^{2(1)} - 2i\bar{E}_A \dot{f}_A^{2(1)} &= \delta m_{A\theta}^2 e^{i(\bar{E}_A - \bar{E}_\theta)t} \\ \ddot{f}_\theta^{1(1)} - 2i\bar{E}_\theta \dot{f}_\theta^{1(1)} &= -\delta m_{A\theta}^2 e^{-i(\bar{E}_A - \bar{E}_\theta)t} \\ \ddot{f}_\theta^{2(1)} - 2i\bar{E}_\theta \dot{f}_\theta^{2(1)} &= -\delta m_\theta^2. \end{aligned} \quad (\text{B.15})$$

To solve the first equation we only have to copy (B.13):

$$f_A^{1(1)} = -\frac{i \int_0^t dt' \delta m_A^2(t')}{2\bar{E}_A} - \frac{\delta m_A^2(t) - \delta m_A^2(0)e^{2i\bar{E}_A t}}{4\bar{E}_A^2} + \mathcal{O}(\bar{E}_A^{-3}). \quad (\text{B.16})$$

For the second equation we get

$$\begin{aligned} f_A^{2(1)} &= \frac{i \int_0^t dt' \delta m_{A\theta}^2(t') e^{i(\bar{E}_A - \bar{E}_\theta)t'}}{2\bar{E}_A} + \frac{\delta m_{A\theta}^2(t) e^{i(\bar{E}_A - \bar{E}_\theta)t} - \delta m_{A\theta}^2(0) e^{2i\bar{E}_A t}}{4\bar{E}_A^2} + \mathcal{O}(\bar{E}_A^{-3}) \\ &= \frac{\delta m_{A\theta}^2(t) e^{i(\bar{E}_A - \bar{E}_\theta)t} - \delta m_{A\theta}^2(0)}{2\bar{E}_A (\bar{E}_A - \bar{E}_\theta)} + \frac{\delta m_{A\theta}^2(t) e^{i(\bar{E}_A - \bar{E}_\theta)t} - \delta m_{A\theta}^2(0) e^{2i\bar{E}_A t}}{4\bar{E}_A^2} + \mathcal{O}(\bar{E}_A^{-3}) \end{aligned} \quad (\text{B.17})$$

where in the second line we did the usual partial integration trick on the first term. The extra terms induced are order  $(\bar{E}_A)^{-3}$ .

In the same way the third equation gives

$$\begin{aligned} f_\theta^{1(1)} &= -\frac{i \int_0^t dt' \delta m_{A\theta}^2(t') e^{-i(\bar{E}_A - \bar{E}_\theta)t'}}{2\bar{E}_\theta} - \frac{\delta m_{A\theta}^2(t) e^{-i(\bar{E}_A - \bar{E}_\theta)t} - \delta m_{A\theta}^2(0) e^{2i\bar{E}_\theta t}}{4\bar{E}_\theta^2} + \mathcal{O}(\bar{E}_\theta^{-3}) \\ &= \frac{\delta m_{A\theta}^2(t) e^{-i(\bar{E}_A - \bar{E}_\theta)t} - \delta m_{A\theta}^2(0)}{2\bar{E}_\theta (\bar{E}_A - \bar{E}_\theta)} - \frac{\delta m_{A\theta}^2(t) e^{-i(\bar{E}_A - \bar{E}_\theta)t} - \delta m_{A\theta}^2(0) e^{2i\bar{E}_\theta t}}{4\bar{E}_\theta^2} + \mathcal{O}(\bar{E}_\theta^{-3}). \end{aligned} \quad (\text{B.18})$$

The fourth equation is just like the first and gives

$$f_\theta^{2(1)} = -\frac{i \int_0^t dt' \delta m_\theta^2(t')}{2\bar{E}_\theta} - \frac{\delta m_\theta^2(t) - \delta m_\theta^2(0) e^{2i\bar{E}_\theta t}}{4\bar{E}_\theta^2} + \mathcal{O}(\bar{E}_\theta^{-3}). \quad (\text{B.19})$$

Now we want to go to second order. However,  $f_A^{2(1)}$  and  $f_\theta^{1(1)}$  are already of order  $(\bar{E})^{-2}$ . Their second order contributions will be of order  $(\bar{E})^{-3}$ , which is beyond our interest for now. So we focus on  $f_A^{1(2)}$  and  $f_\theta^{2(2)}$ :

$$\begin{aligned} \ddot{f}_A^{1(2)} - 2i\bar{E}_A \dot{f}_A^{1(2)} &= -\delta m_A^2 f_A^{1(1)} + \delta m_{A\theta}^2 e^{i(\bar{E}_A - \bar{E}_\theta)t} f_\theta^{1(1)} \\ \ddot{f}_\theta^{2(2)} - 2i\bar{E}_\theta \dot{f}_\theta^{2(2)} &= -\delta m_\theta^2 f_\theta^{2(1)} - \delta m_{A\theta}^2 e^{-i(\bar{E}_A - \bar{E}_\theta)t} f_A^{2(1)}. \end{aligned} \quad (\text{B.20})$$

Now we only need the first term of (B.13):

$$\begin{aligned} f_A^{1(2)} &= \frac{i}{2\bar{E}_A} \int_0^t dt' \left[ -\delta m_A^2(t') f_A^{1(1)} + \delta m_{A\theta}^2(t') e^{i(\bar{E}_A - \bar{E}_\theta)t'} f_\theta^{1(1)}(t') \right] + \mathcal{O}(\bar{E}_A^{-3}) \\ f_\theta^{2(2)} &= \frac{i}{2\bar{E}_A} \int_0^t dt' \left[ -\delta m_\theta^2(t') f_\theta^{2(1)} - \delta m_{A\theta}^2(t') e^{-i(\bar{E}_A - \bar{E}_\theta)t'} f_A^{2(1)}(t') \right] + \mathcal{O}(\bar{E}_\theta^{-3}) \end{aligned} \quad (\text{B.21})$$

Of both expressions we only keep the first term, which is just the usual result. The second term is actually order  $(\bar{E}_A)^{-4}$ : one from the overall denominator, two from the f-functions and one from the exponent that comes down once we integrate by parts. So we are left with the usual result (see appendix A):

$$\begin{aligned} f_A^{1(2)} &= -\frac{1}{8\bar{E}_A^2} \left[ \int_0^t dt' \delta m_A^2(t') \right]^2 + \mathcal{O}(\bar{E}_A^{-3}) \\ f_\theta^{2(2)} &= -\frac{1}{8\bar{E}_\theta^2} \left[ \int_0^t dt' \delta m_\theta^2(t') \right]^2 + \mathcal{O}(\bar{E}_\theta^{-3}). \end{aligned} \quad (\text{B.22})$$

Now we have all the pieces we need, so we can compute all the products we need. We set  $\delta m_A^2(0) = \delta m_\theta^2(0) = \delta m_{A\theta}^2(0) = 0$ . First two products that are just as before in appendix A:

$$|U_A^1|^2 = |1 + f_A^1|^2 = 1 - \frac{\delta m_A^2(t)}{2\bar{E}_A^2} + \mathcal{O}(\bar{E}_A^{-3}) \quad (\text{B.23})$$

$$|U_\theta^2|^2 = |1 + f_\theta^2|^2 = 1 - \frac{\delta m_\theta^2(t)}{2\bar{E}_\theta^2} + \mathcal{O}(\bar{E}_\theta^{-3}). \quad (\text{B.24})$$

Now two products that are actually too small to consider:

$$|U_A^2|^2 = |f_A^2|^2 = \mathcal{O}(\bar{E}^{-4}) \quad (\text{B.25})$$

$$|U_\theta^1|^2 = |f_\theta^1|^2 = \mathcal{O}(\bar{E}^{-4}). \quad (\text{B.26})$$

Now for something new:

$$\begin{aligned} U_A^1 U_\theta^{1*} &= e^{-i\bar{E}_A t} e^{i\bar{E}_\theta t} \left( 1 - \frac{i \int_0^t dt' \delta m_A^2(t')}{2\bar{E}_A} - \frac{\delta m_A^2(t)}{4\bar{E}_A^2} - \frac{1}{8\bar{E}_A^2} \left[ \int_0^t dt' \delta m_A^2(t') \right]^2 + \mathcal{O}(\bar{E}^{-3}) \right) \\ &\quad \left( \frac{\delta m_{A\theta}^2(t) e^{i(\bar{E}_A - \bar{E}_\theta)t}}{2\bar{E}_\theta (\bar{E}_A - \bar{E}_\theta)} - \frac{\delta m_{A\theta}^2(t) e^{i(\bar{E}_A - \bar{E}_\theta)t}}{4\bar{E}_\theta^2} + \mathcal{O}(\bar{E}^{-3}) \right) \\ &= \delta m_{A\theta}^2 \left( \frac{1}{2\bar{E}_\theta (\bar{E}_A - \bar{E}_\theta)} - \frac{1}{4\bar{E}_\theta^2} \right) + \mathcal{O}(\bar{E}^{-3}) \\ &= U_A^{1*} U_\theta^1. \end{aligned} \quad (\text{B.27})$$

$$\begin{aligned} U_A^2 U_\theta^{2*} &= e^{-i\bar{E}_A t} e^{i\bar{E}_\theta t} \left( \frac{\delta m_{A\theta}^2(t) e^{i(\bar{E}_A - \bar{E}_\theta)t}}{2\bar{E}_A (\bar{E}_A - \bar{E}_\theta)} + \frac{\delta m_{A\theta}^2(t) e^{i(\bar{E}_A - \bar{E}_\theta)t}}{4\bar{E}_A^2} + \mathcal{O}(\bar{E}^{-3}) \right) \\ &\quad \left( 1 + \frac{i \int_0^t dt' \delta m_\theta^2(t')}{2\bar{E}_\theta} - \frac{\delta m_\theta^2(t)}{4\bar{E}_\theta^2} - \frac{1}{8\bar{E}_\theta^2} \left[ \int_0^t dt' \delta m_\theta^2(t') \right]^2 + \mathcal{O}(\bar{E}^{-3}) \right) \\ &= \delta m_{A\theta}^2 \left( \frac{1}{2\bar{E}_A (\bar{E}_A - \bar{E}_\theta)} + \frac{1}{4\bar{E}_A^2} \right) + \mathcal{O}(\bar{E}^{-3}) \\ &= U_A^{2*} U_\theta^2. \end{aligned} \quad (\text{B.28})$$



# Appendix C

## Vector loops

### C.1 Minkowski

The  $D^{(4)}(k)$  propagator for a vector field with time independent mass can be written, for arbitrary  $\xi$ , as

$$D_{\mu\nu}^{(4)}(x-y) = -i \int \frac{d^4k}{(2\pi)^4} \left[ \frac{1}{k^2 - m^2} \left( \eta_{\mu\nu} - \frac{k_\mu k_\nu}{k^2} \right) + \frac{\xi}{k^2 - \xi m^2} \frac{k_\mu k_\nu}{k^2} \right] e^{-ik \cdot (x-y)}. \quad (\text{C.1})$$

It satisfies

$$\left[ \eta^{\alpha\beta} \partial_\alpha \partial_\beta \eta^{\mu\nu} + \left( \frac{1}{\xi} - 1 \right) \partial^\mu \partial^\nu + m^2 \eta^{\mu\nu} \right] D_{\nu\rho}^{(4)}(x-y) = i \delta^{(4)}(x-y) \delta_\rho^\mu. \quad (\text{C.2})$$

Note the difference in sign between the propagator (C.1) and its scalar analogue (2.7). Consequently there is also a sign difference between (C.2) and (2.6).

Now there are some useful expressions to be computed with this propagator that we need in sections 3.3 and 4.3.

In (3.24) we need the contraction

$$\begin{aligned} \eta^{\mu\nu} D_{\mu\nu}^{(4)}(x-y) &= -i \int \frac{d^4k}{(2\pi)^4} \left[ \frac{1}{k^2 - m^2} \left( \eta^{\mu\nu} \eta_{\mu\nu} - \frac{\eta^{\mu\nu} k_\mu k_\nu}{k^2} \right) + \frac{\xi}{k^2 - \xi m^2} \frac{\eta^{\mu\nu} k_\mu k_\nu}{k^2} \right] e^{-ik \cdot (x-y)} \\ &= -i \int \frac{d^4k}{(2\pi)^4} \left[ \frac{1}{k^2 - m^2} (4 - 1) + \frac{\xi}{k^2 - \xi m^2} \right] e^{-ik \cdot (x-y)} \\ &= -3D_A^{(4)}(x-y) - \xi D_\xi^{(4)}(x-y), \end{aligned} \quad (\text{C.3})$$

where  $D_A^{(4)}$  denotes the propagator for a scalar field with mass squared  $m^2$ , and  $D_\xi^{(4)}$  the propagator for a scalar field with mass squared  $\xi m^2$  (compare with (2.7)).

The other expressions we are after are only valid on the level of  $D^{(3)}$  propagators. Therefore we should first do a contour integration over  $k^0$ . This yields exactly the same structure for propagators as in the

scalar case (see (2.51)). However, in the vector case the Wightman function is given by

$$D_{\mu\nu}(x-y) = - \int \frac{d^3k}{(2\pi)^3} \frac{1}{2E_{\vec{k}}^{(A)}} \left( \eta_{\mu\nu} - \frac{k_\mu k_\nu}{k^2} \right) e^{-ik \cdot (x-y)} \Big|_{k^0=E_{\vec{k}}^{(A)} \equiv \sqrt{\vec{k} \cdot \vec{k} + m^2}} \\ - \xi \int \frac{d^3k}{(2\pi)^3} \frac{1}{2E_{\vec{k}}^{(\xi)}} \frac{k_\mu k_\nu}{k^2} e^{-ik \cdot (x-y)} \Big|_{k^0=E_{\vec{k}}^{(\xi)} \equiv \sqrt{\vec{k} \cdot \vec{k} + \xi m^2}}. \quad (\text{C.4})$$

The second expression that we will need, in (3.30) follows rightaway

$$D_{00}(x-y) = - \left( 1 - \frac{\left( E_{\vec{k}}^{(A)} \right)^2}{m^2} \right) D_A(x-y) - \xi \frac{\left( E_{\vec{k}}^{(\xi)} \right)^2}{\xi m^2} D_\xi(x-y), \quad (\text{C.5})$$

with  $D_A$  the Wightman function for a scalar field of mass squared  $m^2$  and  $D_\xi$  the Wightman function for a scalar field of mass squared  $\xi m^2$ .

In (3.27) we need to work out

$$\mathcal{A}_{A\mu}^{(2)} = -\frac{i}{2} (\partial_{\phi_{\text{cl}}} m_A^2(x^0)) \int d^4y \eta^{\mu\nu} \eta^{\rho\sigma} \left[ \bar{\Delta}_{A\nu A\rho}^{++}(x-y) \delta m_A^2(y^0) \bar{\Delta}_{A\sigma A\mu}^{++}(y-x) \right. \\ \left. - \bar{\Delta}_{A\nu A\rho}^{+-}(x-y) \delta m_A^2(y^0) \bar{\Delta}_{A\sigma A\mu}^{-+}(y-x) \right]. \quad (\text{C.6})$$

Just as in the scalar case, when writing the propagators in terms of Wightman functions the terms multiplying  $\theta(y^0 - x^0)$  cancel. After the standard integration over  $d^3y$  that gives a three momentum delta function we find

$$\mathcal{A}_{A\mu}^{(2)} = -\frac{i}{2} (\partial_{\phi_{\text{cl}}} m_A^2(x^0)) \int dy^0 \theta(x^0 - y^0) \delta m_A^2(y^0) \times \\ \left[ \int \frac{d^3k}{(2\pi)^3} \frac{1}{4 \left( \bar{E}_{\vec{k}}^{(A)} \right)^2} \delta(\vec{k} - \vec{p}) \eta^{\mu\nu} \eta^{\rho\sigma} \left( \eta_{\nu\rho} - \frac{k_\nu k_\rho}{k^2} \right) \left( \eta_{\sigma\mu} - \frac{p_\sigma p_\mu}{p^2} \right) \times \right. \\ \left. \left( e^{-i(k^0+p^0)(x^0-y^0)} - e^{i(k^0+p^0)(x^0-y^0)} \right) \Big|_{k^0=p^0=\bar{E}_{\vec{k}}^{(A)}} \right. \\ + \xi \int \frac{d^3k}{(2\pi)^3} \frac{1}{4 \bar{E}_{\vec{k}}^{(A)} \bar{E}_{\vec{k}}^{(\xi)}} \delta(\vec{k} - \vec{p}) \eta^{\mu\nu} \eta^{\rho\sigma} \left( \eta_{\nu\rho} - \frac{k_\nu k_\rho}{k^2} \right) \left( \frac{p_\sigma p_\mu}{p^2} \right) \times \\ \left. \left( e^{-i(k^0+p^0)(x^0-y^0)} - e^{i(k^0+p^0)(x^0-y^0)} \right) \Big|_{k^0=\bar{E}_{\vec{k}}^{(A)}, p^0=\bar{E}_{\vec{k}}^{(\xi)}} \right. \\ + \xi \int \frac{d^3k}{(2\pi)^3} \frac{1}{4 \bar{E}_{\vec{k}}^{(A)} \bar{E}_{\vec{k}}^{(\xi)}} \delta(\vec{k} - \vec{p}) \eta^{\mu\nu} \eta^{\rho\sigma} \left( \frac{k_\nu k_\rho}{k^2} \right) \left( \eta_{\sigma\mu} - \frac{p_\sigma p_\mu}{p^2} \right) \times \\ \left. \left( e^{-i(k^0+p^0)(x^0-y^0)} - e^{i(k^0+p^0)(x^0-y^0)} \right) \Big|_{k^0=\bar{E}_{\vec{k}}^{(\xi)}, p^0=\bar{E}_{\vec{k}}^{(A)}} \right. \\ \left. + \xi^2 \int \frac{d^3k}{(2\pi)^3} \frac{1}{4 \left( \bar{E}_{\vec{k}}^{(\xi)} \right)^2} \delta(\vec{k} - \vec{p}) \eta^{\mu\nu} \eta^{\rho\sigma} \left( \frac{k_\nu k_\rho}{k^2} \right) \left( \frac{p_\sigma p_\mu}{p^2} \right) \times \right. \\ \left. \left( e^{-i(k^0+p^0)(x^0-y^0)} - e^{i(k^0+p^0)(x^0-y^0)} \right) \Big|_{k^0=p^0=\bar{E}_{\vec{k}}^{(\xi)}} \right]. \quad (\text{C.7})$$

Now we need some contractions

$$\begin{aligned}
\eta^{\mu\nu}\eta^{\rho\sigma}\eta_{\nu\rho}\eta_{\sigma\mu} &= 4 \\
\eta^{\mu\nu}\eta^{\rho\sigma}\frac{k_\nu k_\rho}{k^2}\eta_{\sigma\mu} &= 1 \\
\eta^{\mu\nu}\eta^{\rho\sigma}\frac{k_\nu k_\rho}{k^2}\frac{p_\sigma p_\mu}{p^2} &= 1 + \frac{(k^0)^2(p^i)^2 + (k^i)^2(p^0)^2 - 2k^0 p^0 k^i p^i}{k^\mu k_\mu p^\nu p_\nu}.
\end{aligned} \tag{C.8}$$

Using these and the three momentum delta function we find

$$\begin{aligned}
\mathcal{A}_{A\mu}^{(2)} &= -\frac{1}{4}(\partial_{\phi_{\text{cl}}}m_A^2(x^0))\int_0^{x^0}dy^0\delta m_A^2(y^0)\times \\
&\left[ \int \frac{d^3k}{(2\pi)^3}\frac{1}{(\bar{E}_{\vec{k}}^{(A)})^2}\left(3 + \frac{4(\bar{E}_{\vec{k}}^{(A)})^2\vec{k}\cdot\vec{k}}{m_A^4}\right)\sin\left[2\bar{E}_{\vec{k}}^A(x^0-y^0)\right] \right. \\
&-2\xi\int \frac{d^3k}{(2\pi)^3}\frac{1}{\bar{E}_{\vec{k}}^{(A)}\bar{E}_{\vec{k}}^{(\xi)}}\frac{(\bar{E}_{\vec{k}}^{(A)}+\bar{E}_{\vec{k}}^{(\xi)})^2\vec{k}\cdot\vec{k}}{m_A^2m_\xi^2}\sin\left[(\bar{E}_{\vec{k}}^A+\bar{E}_{\vec{k}}^{(\xi)})(x^0-y^0)\right] \\
&\left. +\xi^2\int \frac{d^3k}{(2\pi)^3}\frac{1}{(\bar{E}_{\vec{k}}^{(\xi)})^2}\left(1 + \frac{4(\bar{E}_{\vec{k}}^{(\xi)})^2\vec{k}\cdot\vec{k}}{m_\xi^4}\right)\sin\left[2\bar{E}_{\vec{k}}^\xi(x^0-y^0)\right] \right].
\end{aligned} \tag{C.9}$$

Now we perform the standard integration over  $y^0$ :

$$\begin{aligned}
\int_0^{x^0}dy^0f(y^0)\sin[A(x^0-y^0)] &= \left[f(y^0)\frac{\cos[A(x^0-y^0)]}{A}\right]_{y^0=0}^{y^0=x^0} \\
&- \int_0^{x^0}dy^0(\partial_{y^0}f(y^0))\frac{\cos[A(x^0-y^0)]}{A} \\
&= \frac{f(x^0)}{A} + \dots,
\end{aligned} \tag{C.10}$$

where the terms on the dots will only contribute to the finite terms. Now we have

$$\begin{aligned}
\mathcal{A}_{A\mu}^{(2)} &= -\frac{1}{4}(\partial_{\phi_{\text{cl}}}m_A^2(x^0))\delta m_A^2(x^0)\times \\
&\left[ \int \frac{d^3k}{(2\pi)^3}\frac{1}{2(\bar{E}_{\vec{k}}^{(A)})^3}\left(3 + \frac{4(\bar{E}_{\vec{k}}^{(A)})^2\vec{k}\cdot\vec{k}}{m_A^4}\right) -2\xi\int \frac{d^3k}{(2\pi)^3}\frac{1}{\bar{E}_{\vec{k}}^{(A)}\bar{E}_{\vec{k}}^{(\xi)}}\frac{(\bar{E}_{\vec{k}}^{(A)}+\bar{E}_{\vec{k}}^{(\xi)})\vec{k}\cdot\vec{k}}{m_A^2m_\xi^2} \right. \\
&\left. +\xi^2\int \frac{d^3k}{(2\pi)^3}\frac{1}{2(\bar{E}_{\vec{k}}^{(\xi)})^3}\left(1 + \frac{4(\bar{E}_{\vec{k}}^{(\xi)})^2\vec{k}\cdot\vec{k}}{m_\xi^4}\right) \right]
\end{aligned} \tag{C.11}$$

$$\begin{aligned}
&= -\frac{1}{4} (\partial_{\phi_{\text{cl}}} m_A^2(x^0)) \delta m_A^2(x^0) \times \\
&\quad \left[ 3 \int \frac{d^3 k}{(2\pi)^3} \frac{1}{2 \left(\bar{E}_{\vec{k}}^{(A)}\right)^3} + \xi^2 \int \frac{d^3 k}{(2\pi)^3} \frac{1}{2 \left(\bar{E}_{\vec{k}}^{(\xi)}\right)^3} \right. \\
&\quad \left. + \int \frac{d^3 k}{(2\pi)^3} \frac{\vec{k} \cdot \vec{k}}{m_A^4} \left( \frac{2}{\bar{E}_{\vec{k}}^{(A)}} - 2\xi \cdot \frac{1}{\bar{E}_{\vec{k}}^{(\xi)} \xi} - 2\xi \cdot \frac{1}{\bar{E}_{\vec{k}}^{(A)} \xi} + \xi^2 \cdot \frac{2}{\bar{E}_{\vec{k}}^{(\xi)} \xi^2} \right) \right] \\
&= -\frac{1}{4} (\partial_{\phi_{\text{cl}}} m_A^2(x^0)) \delta m_A^2(x^0) \times \left( 3 \int \frac{d^3 k}{(2\pi)^3} \frac{1}{2 \left(\bar{E}_{\vec{k}}^{(A)}\right)^3} + \xi^2 \int \frac{d^3 k}{(2\pi)^3} \frac{1}{2 \left(\bar{E}_{\vec{k}}^{(\xi)}\right)^3} \right). \tag{C.12}
\end{aligned}$$

Here we have used that  $m_\xi^2 = \xi m_A^2$ . We use this result in (3.28). The two remaining integrals are the standard ones covered already in chapter 2.

Let us at this point introduce some shorthand notation, to prevent very lengthy equations when we get to the vector diagrams in FLRW in the next section. The manipulations done between (C.7) and (C.9) can be summarized as

$$\eta^{\mu\nu} \eta^{\rho\sigma} \bar{D}_{\mu\rho}(\vec{k}) \bar{D}_{\sigma\nu}(\vec{p}) \Big|_{\vec{k}=-\vec{p}} = C_{IJ}(k) \bar{D}_I \bar{D}_J \tag{C.13}$$

$$= \left( 3 + \frac{4\vec{k}^2 \bar{E}_A^2}{\bar{m}_A^4} \right) \bar{D}_A(\vec{k})^2 + \xi^2 \left( 1 + \frac{4\vec{k}^2 \bar{E}_\xi^2}{\bar{m}_\xi^4} \right) \bar{D}_\xi(\vec{k})^2 - 2\xi \frac{\vec{k}^2 (\bar{E}_A + \bar{E}_\xi)^2}{\bar{m}_A^2 \bar{m}_\xi^2} \bar{D}_A(\vec{k}) \bar{D}_\xi(\vec{k}), \tag{C.14}$$

with  $I, J = A, \xi$ , and  $\bar{D}_{I,ab} = (2\bar{E}_I)^{-1} e^{-i\bar{E}_I(t_a - t_b)}$  the Wightman function of the field  $I$ , Fourier transformed with respect to three momentum.

## C.2 FLRW

In this section we show the computation of the extra vector diagrams in FLRW, absent in Minkowski.

### C.2.1 $\mathcal{A}_{\text{mass}}^{(2)}$

In (4.35) we compute the contribution of the vector loop with an  $\delta m_{A_0 A_0}^2$  insertion at spacetime point  $y$ . We have

$$\begin{aligned}
\mathcal{A}_{\text{mass}}^{(2)} &= i \int d^4 y \frac{1}{2} \lambda_{h_{A_\mu A_\nu}}^+(x^0) \left[ \bar{\Delta}_{A_\nu A_0}^{++}(x-y) \lambda_{\delta_{A_0 A_0}}^+(y^0) \bar{\Delta}_{A_0 A_\mu}^{++}(y-x) \right. \\
&\quad \left. + \bar{\Delta}_{A_\nu A_0}^{+-}(x-y) \lambda_{\delta_{A_0 A_0}}^-(y^0) \bar{\Delta}_{A_0 A_\mu}^{-+}(y-x) \right] \\
&= i \int d^4 y \frac{1}{2} (i \partial_{\phi_{\text{cl}}} m_A^2(x^0)) \eta^{\mu\nu} \left[ \bar{\Delta}_{A_\nu A_0}^{++}(x-y) (i \delta m_{A_0 A_0}^2(y^0)) \bar{\Delta}_{A_0 A_\mu}^{++}(y-x) \right. \\
&\quad \left. + \bar{\Delta}_{A_\nu A_0}^{+-}(x-y) (-i \delta m_{A_0 A_0}^2(y^0)) \bar{\Delta}_{A_0 A_\mu}^{-+}(y-x) \right].
\end{aligned} \tag{C.15}$$

Now when we again rewrite the propagators in terms of Wightman functions, we will need the propagator combination (using the shorthand notation introduced in (C.14))

$$\begin{aligned}
\eta^{00} \eta^{\mu\nu} \bar{D}_{\mu 0}(\vec{k}) \bar{D}_{0\nu}(\vec{p}) \Big|_{\vec{k}=-\vec{p}} &= \sum C_{IJ} \bar{D}_I(\vec{k}) \bar{D}_J(\vec{k}) \\
&= \frac{\vec{k}^2 (2\vec{k}^2 + \bar{m}_A^2)}{\bar{m}_A^4} \bar{D}_A(\vec{k})^2 + \xi^2 \frac{(\bar{\omega}_\xi^2 + \vec{k}^2) \bar{\omega}_\xi^2}{\bar{m}_\xi^4} \bar{D}_\xi(\vec{k})^2 - 2\xi \frac{\vec{k}^2 \bar{\omega}_\xi (\bar{\omega}_\xi + \bar{\omega}_A)}{\bar{m}_A^2 \bar{m}_\xi^2} \bar{D}_A(\vec{k}) \bar{D}_\xi(\vec{k}),
\end{aligned} \tag{C.16}$$

with as before  $I, J = A, \xi$ , and  $\bar{D}_I(-\vec{k}) = \bar{D}_I(\vec{k}) = 1/(2\bar{\omega}_i) e^{-i\bar{\omega}_I(\tau - \tau_b)}$ . (Note that now we are working with conformal energy  $\omega$  and conformal time  $\tau$ .)

Setting  $x^0 = \tau$  and  $y^0 = \tau_y$  this gives

$$\mathcal{A}_{\text{mass}}^{(2)} = -\partial_{\phi_{\text{cl}}} m_A^2(\tau) \int_0^\tau d\tau_y \delta m_{A_0 A_0}^2(\tau_y) \int \frac{d^3 k}{(2\pi)^3} \sum \frac{C_{IJ}}{(2\bar{\omega}_I)(2\bar{\omega}_J)} \sin[(\bar{\omega}_I + \bar{\omega}_J)(\tau - \tau_y)] \tag{C.17}$$

which by the by now standard manipulations yields

$$\mathcal{A}_{\text{mass}}^{(2)} = -(\partial_{\phi_{\text{cl}}} m_A^2(\tau)) \delta m_{A_0 A_0}^2(\tau) \frac{(3 + \xi^2)}{64\pi^2} \ln(\Lambda/\bar{m}) + \text{finite}. \tag{C.18}$$

### C.2.2 $\mathcal{A}_{\text{mix}}^{(2)}$

Now we begin from (4.36):

$$\begin{aligned}
\mathcal{A}_{\text{mix}}^{(2)} &= i \int d^4 y \lambda_{hA_\mu A_\nu}^+(x^0) \left[ \bar{\Delta}_{A_\nu A_0}^{++}(x-y) \lambda_{\delta A_0 A_i}^+(y^0) \bar{\Delta}_{A_i A_\mu}^{++}(y-x) \right. \\
&\quad \left. + \bar{\Delta}_{A_\nu A_0}^{+-}(x-y) \lambda_{\delta A_0 A_i}^-(y^0) \bar{\Delta}_{A_i A_\mu}^{-+}(y-x) \right] \\
&= i \partial_{\phi_{\text{cl}}} m_A^2(\tau) \int d^4 y (\delta m_{A_0 A_i}^2)(\tau_b) \eta^{\mu\nu} \left[ \bar{\Delta}_{A_\nu A_0}^{++}(x-y) \bar{\Delta}_{A_i A_\mu}^{++}(y-x) - \bar{\Delta}_{A_\nu A_0}^{+-}(x-y) \bar{\Delta}_{A_i A_\mu}^{-+}(y-x) \right] \\
&= -\frac{2}{\xi} \partial_{\phi_{\text{cl}}} m_A^2(\tau) \int_0^\tau d\tau_y \mathcal{H}(\tau_y) \int \frac{d^3 k}{(2\pi)^3} p^i \eta^{\mu\nu} \left[ \bar{D}_{xy, \mu 0}(\vec{k}) \bar{D}_{xy, i\nu}(\vec{p}) + \bar{D}_{yx, \mu 0}(\vec{k}) \bar{D}_{yx, i\nu}(\vec{p}) \right]_{\vec{k}=-\vec{p}} \\
&= -\frac{2}{\xi} \partial_{\phi_{\text{cl}}} m_A^2(\tau) \int_0^\tau d\tau_y \mathcal{H}(\tau_y) \int \frac{d^3 k}{(2\pi)^3} \frac{C_{IJ}}{(2\bar{\omega}_I)(2\bar{\omega}_J)} 2 \cos[(\bar{\omega}_I + \bar{\omega}_J)(\tau - \tau_y)] \\
&= -\frac{2}{\xi} \partial_{\phi_{\text{cl}}} m_A^2(\tau) \int \frac{d^3 k}{(2\pi)^3} \frac{2\mathcal{H}'(\tau)}{(2\bar{\omega}_I)(2\bar{\omega}_J)(\bar{\omega}_I + \bar{\omega}_J)^2} C_{IJ} + \text{finite} \\
&= \partial_{\phi_{\text{cl}}} m_A^2(\tau) \frac{3\mathcal{H}'(\tau)(1-\xi)^2}{32\pi^2 \xi} \ln(\Lambda/\bar{m}) + \text{finite}. \tag{C.19}
\end{aligned}$$

As we now have a cosine instead of a sine in the expression on the third line above (caused by the spatial derivative contained in  $\delta m_{A_0 A_i}^2$ ), we integrate by parts twice to isolate the leading term in the UV limit. This is why the result is proportional to  $\mathcal{H}'$ . The relevant propagator contribution is defined by

$$\begin{aligned}
p^i \eta^{\mu\nu} \bar{D}_{\mu 0}(\vec{k}) \bar{D}_{i\nu}(\vec{p}) \Big|_{\vec{k}=-\vec{p}} &\equiv \sum C_{IJ} \bar{D}_I \bar{D}_J \\
&= -\frac{\vec{k}^2 \bar{\omega}_A (2\vec{k}^2 + \bar{m}_A^2)}{\bar{m}_A^4} \bar{D}_A^2 - \frac{\vec{k}^2 \bar{\omega}_\xi (2\vec{k}^2 + \bar{m}_\xi^2)}{\bar{m}_A^4} \bar{D}_\xi^2 + \frac{\vec{k}^2 (\bar{\omega}_A + \bar{\omega}_\xi) (\vec{k}^2 + \bar{\omega}_A \bar{\omega}_\xi)}{\bar{m}_A^4} \bar{D}_A \bar{D}_\xi.
\end{aligned}$$

### C.2.3 $\mathcal{A}_{\text{mix}}^{(3)}$

At third order the only contribution is from the diagram with two  $\delta m_{A_0 A_i}^2$  insertions. From (C.20) we have

$$\begin{aligned}
\mathcal{A}_{\text{mix}}^{(3)} &= i \int d^4 y \int d^4 z \frac{1}{2} \lambda_{hA_\mu A_\nu}^+(x^0) \times \\
&\quad \sum \bar{\Delta}_{A_\nu A_\rho}^{+a}(x-y) \lambda_{\delta A_\rho A_\sigma}^a(y^0) \bar{\Delta}_{A_\sigma A_\kappa}^{ab}(y-z) \lambda_{\delta A_\kappa A_\tau}^b(z^0) \bar{\Delta}_{A_\tau A_\mu}^{b+}(z-x) \\
&= i \int d^4 y \int d^4 z \frac{1}{2} i \eta^{\mu\nu} (\partial_{\phi_{\text{cl}}} m_A^2(x^0)) \times \\
&\quad \sum \bar{\Delta}_{A_\nu A_\rho}^{+a}(x-y) \left( -is(a) \delta m_{A_\rho A_\sigma}^2(y^0) \right) \bar{\Delta}_{A_\sigma A_\kappa}^{ab}(y-z) \times \\
&\quad \left( -is(b) \delta m_{A_\kappa A_\tau}^2(z^0) \right) \bar{\Delta}_{A_\tau A_\mu}^{b+}(z-x). \tag{C.20}
\end{aligned}$$

The sum is over the four possibilities for the Lorentz indices:

$$(\rho, \sigma, \kappa, \tau) = (i, 0, j, 0), (0, i, 0, j), (0, i, j, 0), (i, 0, 0, j). \tag{C.21}$$

The spacetime points  $y$  and  $z$  can be on the positive or on the negative branch, which gives four possibilities that we should sum over as well :

$$(a, b) = (++) , (-+), (+-), (--) . \quad (\text{C.22})$$

We used the sign function  $s(a)$  which we define as  $s(+)=1, s(-)=-1$ .

The propagator between a  $(\pm)$ -vertex and a  $(\pm)$ -vertex is  $\bar{\Delta}^{\pm\pm}$ , and we write them out in terms of Fourier transformed Wightman functions using the notation introduced around (C.14). Taking the action of the spatial derivatives in  $\delta m_{A_0 A_i}^2$  will then bring down powers of momentum. Finally, the  $\vec{y}$  and  $\vec{z}$  integrals give delta functions encoding momentum conservation. At the end of the day we find

$$\begin{aligned} \mathcal{A}_{\text{mix}}^{(3)} &= \frac{2}{\xi^2} \partial_{\phi_{cl}} m_A^2(\tau) \int_0^\tau d\tau_y \int_0^\tau d\tau_z \mathcal{H}(\tau_y) \mathcal{H}(\tau_z) \int \frac{d^3 k}{(2\pi)^3} \sum_\rho k^i k^j s_\rho \\ &\times \left[ \left( \bar{D}_{yx}(\vec{k}) \bar{D}_{yz}(\vec{p}) \bar{D}_{xz}(\vec{q}) + \text{c.c.} \right)_{\vec{k}=\vec{q}=-\vec{p}} - 2\theta_{yz} \left( \bar{D}_{xy}(\vec{k}) \bar{D}_{yz}(\vec{p}) \bar{D}_{xz}(\vec{q}) + \text{c.c.} \right)_{\vec{k}=\vec{p}=-\vec{q}} \right], \end{aligned} \quad (\text{C.23})$$

where the sum  $\sum_\rho$  is now only over the Lorentz indices (C.21), which we suppressed in the above formula. The sign  $s_\rho = (1, 1, -1, -1)$  for the four possibilities (C.21). The relevant propagator combinations, putting Lorentz indices back in, are

$$\begin{aligned} \sum s_m k^i k^j \bar{D}_{yx}(\vec{k}) \bar{D}_{yz}(\vec{p}) \bar{D}_{xz}(\vec{q}) \Big|_{\vec{k}=\vec{q}=-\vec{p}} &= k^i k^j \eta^{\mu\nu} \left[ \bar{D}_{\mu i}(\vec{k}) \bar{D}_{0j}(\vec{p}) \bar{D}_{0\nu}(\vec{q}) + \bar{D}_{\mu 0}(\vec{k}) \bar{D}_{i0}(\vec{p}) \bar{D}_{j\nu}(\vec{q}) \right. \\ &\quad \left. - \bar{D}_{\mu 0}(\vec{k}) \bar{D}_{ij}(\vec{p}) \bar{D}_{0\nu}(\vec{q}) - \bar{D}_{\mu i}(\vec{k}) \bar{D}_{00}(\vec{p}) \bar{D}_{j\nu}(\vec{q}) \right]_{\vec{k}=\vec{q}=-\vec{p}} \\ &= \sum C_{IJK}(\vec{k}) \bar{D}_I(\vec{k}) \bar{D}_J(\vec{k}) \bar{D}_K(\vec{k}), \end{aligned} \quad (\text{C.24})$$

and

$$\begin{aligned} \sum s_m k^i k^j \bar{D}_{xy}(\vec{k}) \bar{D}_{yz}(\vec{p}) \bar{D}_{xz}(\vec{q}) \Big|_{\vec{k}=\vec{p}=-\vec{q}} &= k^i k^j \eta^{\mu\nu} \left[ \bar{D}_{\mu i}(\vec{k}) \bar{D}_{0j}(\vec{p}) \bar{D}_{0\nu}(\vec{q}) + \bar{D}_{\mu 0}(\vec{k}) \bar{D}_{i0}(\vec{p}) \bar{D}_{j\nu}(\vec{q}) \right. \\ &\quad \left. - \bar{D}_{\mu 0}(\vec{k}) \bar{D}_{ij}(\vec{p}) \bar{D}_{0\nu}(\vec{q}) - \bar{D}_{\mu i}(\vec{k}) \bar{D}_{00}(\vec{p}) \bar{D}_{j\nu}(\vec{q}) \right]_{\vec{k}=\vec{p}=-\vec{q}} \\ &= \sum D_{IJK}(\vec{k}) \bar{D}_I(\vec{k}) \bar{D}_J(\vec{k}) \bar{D}_K(\vec{k}), \end{aligned} \quad (\text{C.25})$$

with  $I, J, K = A, \xi$ , and  $C_{IJK}, D_{IJK} \sim k^2$ . Using  $\bar{D}_{I,xy}(\vec{k}) = (2\bar{\omega}_I)^{-1} e^{-i\bar{\omega}_I(\tau_x - \tau_y)}$  we have

$$\begin{aligned} \mathcal{A}_{\text{mix}}^{(3)} &= \frac{4}{\xi^2} \partial_{\phi_{cl}} m_A^2(\tau) \int_0^\tau d\tau_y \int_0^\tau d\tau_z \mathcal{H}(\tau_y) \mathcal{H}(\tau_z) \int \frac{d^3 k}{(2\pi)^3} \sum \frac{1}{(2\bar{\omega}_I)(2\bar{\omega}_J)(2\bar{\omega}_K)} \\ &\times \left[ C_{IJK} \cos((\bar{\omega}_K - \bar{\omega}_I)\tau + (\bar{\omega}_I + \bar{\omega}_J)\tau_y - (\bar{\omega}_J + \bar{\omega}_K)\tau_z) \right. \\ &\quad \left. - 2\theta_{bc} D_{IJK} \cos((\bar{\omega}_I + \bar{\omega}_K)\tau - (\bar{\omega}_I - \bar{\omega}_J)\tau_y - (\bar{\omega}_J + \bar{\omega}_K)\tau_z) \right]. \end{aligned} \quad (\text{C.26})$$

Now use integration by parts with respect to  $\tau_y$  and  $\tau_z$  to write

$$\begin{aligned} &\int_0^\tau d\tau_y \mathcal{H}(\tau_y) \int_0^\tau d\tau_z \mathcal{H}(\tau_z) \cos[(\bar{\omega}_I + \bar{\omega}_J)\tau_y - (\bar{\omega}_J + \bar{\omega}_K)\tau_z + (\bar{\omega}_K - \bar{\omega}_I)\tau] \\ &= \frac{\mathcal{H}(\tau)^2}{(\bar{\omega}_J + \bar{\omega}_K)(\bar{\omega}_I + \bar{\omega}_J)} + \dots \end{aligned} \quad (\text{C.27})$$

where we used the initial conditions (4.67). And similarly

$$\begin{aligned}
& \int_0^\tau d\tau_y \mathcal{H}(\tau_y) \int_0^\tau d\tau_z \mathcal{H}(\tau_z) \theta_{bc} \cos [(\bar{\omega}_I + \bar{\omega}_K)\tau - (\bar{\omega}_I - \bar{\omega}_J)\tau_y - (\bar{\omega}_J + \bar{\omega}_K)\tau_z] \\
&= - \int_0^\tau d\tau_y \frac{\mathcal{H}(\tau_y)^2}{(\bar{\omega}_J + \bar{\omega}_K)} \sin [(\bar{\omega}_I + \bar{\omega}_K)\tau - (\bar{\omega}_I + \bar{\omega}_K)\tau_y] \\
&= - \frac{\mathcal{H}(\tau)^2}{(\bar{\omega}_J + \bar{\omega}_K)(\bar{\omega}_I + \bar{\omega}_K)}. \tag{C.28}
\end{aligned}$$

The end result is

$$\begin{aligned}
\mathcal{A}_{\text{mix}}^{(3)} &= \frac{4}{\xi^2} \partial_{\phi_{\text{cl}}} m_A^2(\tau) \mathcal{H}^2(\tau) \int \frac{d^3k}{(2\pi)^3} \sum \frac{1}{(2\bar{\omega}_I)(2\bar{\omega}_J)(2\bar{\omega}_K)} \\
&\quad \times \left[ \frac{C_{IJK}}{(\bar{\omega}_I + \bar{\omega}_J)(\bar{\omega}_J + \bar{\omega}_K)} + \frac{2D_{IJK}}{(\bar{\omega}_J + \bar{\omega}_K)(\bar{\omega}_I + \bar{\omega}_K)} \right] \\
&= \partial_{\phi_{\text{cl}}} m_A^2(\tau) \mathcal{H}^2(\tau) \frac{(1 - 3\xi - 3\xi^2 + \xi^3) - (1 + \xi)^3}{64\pi^2 \xi^2} \ln(\Lambda/\bar{m})^2 + \text{finite} \\
&= \partial_{\phi_{\text{cl}}} m_A^2(\tau) \mathcal{H}^2(\tau) \frac{-6(1 + \xi)}{32\pi^2 \xi} \ln(\Lambda/\bar{m}) + \text{finite}. \tag{C.29}
\end{aligned}$$

## Appendix D

# Action for Abelian Higgs model in FLRW

Here we work out the explicit form of the action (4.15) to fourth order in quantum fluctuations. Using conformal coordinates the overall volume factor is  $\sqrt{-g} = a^4$ , and  $g^{\mu\nu} = a^{-2}\eta^{\mu\nu}$ . Unless otherwise stated, all indices below are raised and lowered using the Minkowski metric.

Start with the kinetic term for the gauge field. The connection cancels in the field strength, and thus

$$-\frac{1}{4} \int d^4x \sqrt{-g} F^2 = -\frac{1}{4} \int d^4x F^{\mu\nu} F_{\mu\nu} = \frac{1}{2} \int d^4x A_\mu (\partial_\rho \partial^\rho \eta^{\mu\nu} - \partial^\mu \partial^\nu) A_\nu. \quad (\text{D.1})$$

As expected, the result is invariant under a conformal transformation of the metric. The kinetic terms and potential for the Higgs field are expanded as

$$\begin{aligned} & \int d^4x \sqrt{-g} (|D\Phi|^2 - V) \\ &= \int d^4x \sqrt{-g} \left( \left| (\partial_\mu + igA_\mu) \frac{1}{\sqrt{2}} (\phi_R + i\theta) \right|^2 - V \right) \\ &= \int d^4x \left\{ \frac{a^2}{2} \left[ \sum_{\varphi=\phi_R, \theta} (\partial_\mu \varphi \partial^\mu \varphi + g^2 A^2 \varphi^2) + 2gA^\mu (-\theta \partial_\mu \phi_R + \phi_R \partial_\mu \theta) \right] - a^4 V \right\} \\ &= \int d^4x \left\{ \sum_{\hat{\varphi}=\hat{\phi}_R, \hat{\theta}} \left[ -\frac{1}{2} \left( \hat{\varphi} (\partial_\mu \partial^\mu - \frac{a''}{a} + a^2 V_{\varphi\varphi}) \hat{\varphi} - g^2 A^2 \hat{\varphi}^2 \right) - \frac{1}{3!} a V_{\varphi\varphi\varphi} \hat{\varphi}^3 - \frac{1}{4!} V_{\varphi\varphi\varphi\varphi} \hat{\varphi}^4 \right] \right. \\ & \quad \left. + gA^\mu \left[ -a\hat{\theta} \partial_\mu \left( \frac{\hat{\phi}_R}{a} \right) + a\hat{\phi}_R \partial_\mu \left( \frac{\hat{\theta}}{a} \right) \right] \right\}, \quad (\text{D.2}) \end{aligned}$$

with  $\phi_R = \phi_{\text{cl}} + h$ . The factor of  $a^2$  in the third line comes from  $\sqrt{-g} = a^4$  times  $a^{-2}$  coming from changing the inner product with respect to the conformal metric to a Minkowski inner product. The prime denotes derivative with respect to conformal time  $\tau$ . We rescaled the scalar fields  $\hat{\varphi}_\alpha = a\varphi_\alpha$  as in (4.16). The term in between two factors of  $\varphi$  in the last line is just the standard FLRW scalar result that we found already in (4.6). The expansion of  $V$  in its derivatives with respect to  $\varphi$ , and the subsequent conversion into  $\hat{\varphi}$ , is straightforward.

The gauge fixing action is

$$\begin{aligned} S_{\text{GF}} &= -\frac{1}{2\xi} \int d^4x \sqrt{-g} \left[ (\nabla_\mu A^\mu - \xi g \phi_R \theta)^2 \right] \\ &= -\frac{1}{2\xi} \int d^4x \sqrt{-g} \left[ (g^{\mu\nu} \nabla_\mu A_\nu)^2 - (g^{\mu\nu} \nabla_\mu A_\nu) 2\xi g \phi_R \theta + \xi^2 g^2 \phi_R^2 \theta^2 \right]. \end{aligned} \quad (\text{D.3})$$

The first term becomes

$$\begin{aligned} \frac{-1}{2\xi} \int d^4x (\partial_\mu A^\mu - \eta^{\mu\nu} \Gamma_{\mu\nu}^\rho A_\rho)^2 &= \frac{1}{2\xi} \int d^4x A_\mu \left[ \partial^\mu \partial^\nu + 2\eta^{\alpha\beta} \Gamma_{\alpha\beta}^\mu \partial^\nu - \eta^{\alpha\beta} \Gamma_{\alpha\beta}^\mu \eta^{\rho\sigma} \Gamma_{\rho\sigma}^\nu \right] A_\nu \\ &= \frac{1}{\xi} \int d^4x \left[ \frac{1}{2} A_\mu \partial^\mu \partial^\nu A_\nu + A_0 (\mathcal{H}' - 2\mathcal{H}^2) A_0 - A_0 2\mathcal{H} \partial^i A_i \right]. \end{aligned} \quad (\text{D.4})$$

The second term in (D.3) we can partially integrate using (with  $\tilde{A}^\mu \equiv g^{\mu\nu} A_\nu$  to indicate the index is raised with  $g^{\mu\nu}$ )

$$\int d^4x \sqrt{-g} (\nabla_\mu \tilde{A}^\mu) B = - \int d^4x \sqrt{-g} \tilde{A}^\mu \partial_\mu B. \quad (\text{D.5})$$

This follows from the fact that we have a covariant volume and a covariant derivative. Note also that  $\nabla_\mu g_{\mu\nu} = 0$ , and it is therefore irrelevant whether the raised index is on  $A$  or on  $\nabla$ . Thus the second term in (D.3) can be written as (note again the factor of  $a^{-2}$  coming from changing to an inner product with respect to Minkowski metric)

$$- \int d^4x a^2 g A^\mu (\theta \partial_\mu \phi_R + \phi_R \partial_\mu \theta) = - \int d^4x g A^\mu \left[ a \hat{\theta} \partial_\mu \left( \frac{\hat{\phi}_R}{a} \right) + a \hat{\phi}_R \partial_\mu \left( \frac{\hat{\theta}}{a} \right) \right]. \quad (\text{D.6})$$

The second term above will cancel with the last term in (D.2). The complete gauge-fixing term is

$$\begin{aligned} S_{\text{GF}} &= \int d^4x \left\{ \frac{1}{\xi} \left[ \frac{1}{2} A_\mu \partial^\mu \partial^\nu A_\nu + A_0 (\mathcal{H}' - 2\mathcal{H}^2) A_0 - A_0 2\mathcal{H} \partial^i A_i \right] \right. \\ &\quad \left. - g A^\mu \left[ \hat{\theta} \left( \partial_\mu - \frac{a'}{a} \delta_\mu^0 \right) \hat{\phi}_R + \hat{\phi}_R \left( \partial_\mu - \frac{a'}{a} \delta_\mu^0 \right) \hat{\theta} \right] - \frac{1}{2} \xi g^2 \hat{\phi}_R^2 \hat{\theta}^2 \right\}. \end{aligned} \quad (\text{D.7})$$

Finally the Faddeev-Popov term is (compare with (3.14))

$$S_{\text{FP}} = \int d^4x a^4 \bar{\eta} [-\nabla^2 + \xi g^2 (\theta^2 - \phi_R^2)] \eta. \quad (\text{D.8})$$

Now use  $\Gamma_{\mu\rho}^\mu = \partial_\rho \sqrt{-g} / \sqrt{-g}$  to write the first term in (D.8) as

$$- \int d^4x \sqrt{-g} \bar{\eta} \nabla^2 \eta = - \int d^4x \sqrt{-g} \bar{\eta} \left( \frac{1}{\sqrt{-g}} \partial_\mu \sqrt{-g} g^{\mu\nu} \partial_\nu \right) \eta = - \int d^4x \hat{\eta} \left[ \partial^2 - \frac{a''}{a} \right] \hat{\eta}, \quad (\text{D.9})$$

where in the last step we rescaled the anti-commuting scalars  $\hat{\eta} = a\bar{\eta}$ . Hence

$$S_{\text{FP}} = - \int d^4x \hat{\eta} \left[ \partial^2 - \frac{a''}{a} + \xi g^2 (\hat{\phi}_R^2 - \hat{\theta}^2) \right] \hat{\eta}. \quad (\text{D.10})$$

Putting it all together, we write the action as  $S = \sum S^{(i)}$  with  $i$  denoting the number of quantum fields each term in  $S^{(i)}$  contains. Then

$$S^{(0)} = \int d^4x \left\{ \frac{1}{2} (\hat{\phi}'_{\text{cl}})^2 - \frac{1}{2} (\partial_i \hat{\phi}_{\text{cl}})^2 + \frac{1}{2} \frac{a''}{a} \hat{\phi}_{\text{cl}}^2 - a^4 V \right\}, \quad (\text{D.11})$$

$$S^{(1)} = \int d^4x \left\{ -\hat{h} \left( (\partial^2 - \frac{a''}{a}) \hat{\phi}_{\text{cl}} + a^3 V_{\phi_{\text{cl}}} \right) \right\}, \quad (\text{D.12})$$

$$\begin{aligned} S^{(2)} = \frac{1}{2} \int d^4x \left\{ A_\mu \left[ (\partial_\rho \partial^\rho + g^2 \hat{\phi}_{\text{cl}}^2) \eta^{\mu\nu} - (1 - \frac{1}{\xi}) \partial^\mu \partial^\nu \right] A_\nu \right. \\ \left. + \frac{2}{\xi} [A_0 (\mathcal{H}' - 2\mathcal{H}^2) A_0 - A_0 2\mathcal{H} \partial^i A_i] \right. \\ \left. - \hat{\theta} (\partial^2 - \frac{a''}{a} + a^2 V_{\theta\theta} + \xi g^2 \hat{\phi}_{\text{cl}}^2) \hat{\theta} - 4gA^0 \hat{\theta} \left( \partial_\tau - \frac{a'}{a} \right) \hat{\phi}_{\text{cl}} \right. \\ \left. - \hat{h} (\partial^2 - \frac{a''}{a} + a^2 V_{hh}) \hat{h} - 2\hat{\eta} \left[ \partial^2 - \frac{a''}{a} + \xi g^2 \hat{\phi}_{\text{cl}}^2 \right] \hat{\eta} \right\}, \quad (\text{D.13}) \end{aligned}$$

$$S^{(3)} = \int d^4x \left\{ -S_{\alpha\beta\gamma} a V_{\alpha\beta\gamma} \hat{\varphi}_\alpha \hat{\varphi}_\beta \hat{\varphi}_\gamma - 2gA^\mu \hat{\theta} \left( \partial_\mu - \frac{a'}{a} \delta_\mu^0 \right) \hat{h} + g^2 (A^2 - \xi \hat{\theta}^2 - 2\xi \hat{\eta} \hat{\eta}) \hat{\phi}_{\text{cl}} \hat{h} \right\}, \quad (\text{D.14})$$

$$S^{(4)} = \int d^4x \left\{ -S_{\alpha\beta\gamma\delta} V_{\alpha\beta\gamma\delta} \hat{\varphi}_\alpha \hat{\varphi}_\beta \hat{\varphi}_\gamma \hat{\varphi}_\delta + \frac{1}{2} g^2 A^2 (\hat{h}^2 + \hat{\theta}^2) - g^2 \xi \hat{\eta} (\hat{\theta}^2 - \hat{h}^2) \hat{\eta} - \frac{1}{2} g^2 \xi \hat{\theta}^2 \hat{h}^2 \right\}, \quad (\text{D.15})$$

with  $\varphi_\alpha = \{h, \theta\}$ , and  $S_{\alpha\beta\gamma(\delta)}$  symmetry factors. Note that  $V$  and its derivatives should be evaluated at  $\Phi = \phi_{\text{cl}}$  (we have made a Taylor expansion of  $V(\phi + h + i\theta)$ ). For a quartic Higgs potential

$$a^4 V \Big|_{\Phi=\phi_{\text{cl}}} = a^4 \left[ \frac{1}{2} m^2 \phi_{\text{cl}}^2 + \frac{\lambda}{4!} \phi_{\text{cl}}^4 \right] = \frac{1}{2} \hat{m}^2 \hat{\phi}_{\text{cl}}^2 + \frac{\lambda}{4!} \hat{\phi}_{\text{cl}}^4. \quad (\text{D.16})$$



## Appendix E

# Small spectral index for inflection point inflation

In subsection 5.3.3 we stated that in inflection point inflation the spectral index is bounded to be  $n_s \lesssim 0.92$ . In this appendix we review this argument. We derive the spectral index and power spectrum for inflection point inflation, following the work of Refs. [117, 118]. To a very good approximation the inflationary observables only depend on the  $\eta$ -parameter at the extremum and on the number of e-folds.

Expanding the potential around the inflection point gives:

$$V = V_0(1 + 1/2\eta_0\phi^2 + C_3\phi^3 + C_4\phi^4 + \dots), \quad (\text{E.1})$$

with  $\eta, C_3 < 0$  so that the field rolls towards the minimum at positive  $\phi$  values. Inflation ends when the  $C_3$  term becomes important, and  $\epsilon \approx 1$ , which occurs for field values  $\phi_f^2 \sim \sqrt{2}/(3|C_3|)$ . We can calculate the number of e-folds

$$N \approx \int_{\phi_f}^{\phi_N} \frac{V}{V'} = \frac{1}{\eta} \log \left[ \frac{\phi}{3C_3\phi + \eta} \right]_{\phi_f}^{\phi_N}, \quad (\text{E.2})$$

where we used  $V \approx V_0$  above. The above expression can be inverted to obtain the value of the inflaton field  $N$  e-folds before the end of inflation  $\phi_N$ :

$$\phi_N = \frac{e^{N\eta_0}\eta_0/C_3}{-3(e^{N\eta_0} - 1) - \eta_0/(\phi_f C_3)} \approx \frac{e^{N\eta_0}\eta_0}{-3C_3(e^{N\eta_0} - 1)}, \quad (\text{E.3})$$

where in the second step we used  $\eta_0/(\phi_f|C_3|) \ll 1$ . This is a good approximation as  $\eta_0 \ll 1$  is fine-tuned, whereas  $C_3$ , and thus  $\phi_f$ , is naturally of order one<sup>1</sup>. Note that in this limit, the number of e-folds is independent of the end of inflation, as  $\phi_f$  has dropped out of the equation. As a result the inflationary observables are insensitive to the precise coefficients of the higher order terms in (E.1). The spectral index is

$$n_s \approx 1 + 2\eta \approx 1 + 2\eta_0 + 12C_3\phi_N \approx 1 - 2\eta_0 \frac{(e^{\eta_0 N} + 1)}{(e^{\eta_0 N} - 1)}, \quad (\text{E.4})$$

---

<sup>1</sup>To be precise,  $C_3 = \mathcal{O}(1)$  for  $\phi_0 \sim 1$ . For minima at smaller field values generically  $C_3$  increases, as a sharper turnover of the potential is needed. We do not find valid solutions for minima for  $\phi_0 \gg 1$  much larger, as then other local minima at smaller field values appear.

where we used that  $\epsilon \ll \eta$ . For  $N < 50 - 60$  one finds  $n_s < 0.92 - 0.93$  for the whole range of  $|\eta_0| \lesssim 10^{-2}$ . The power spectrum is

$$\Delta_\zeta^2(k_0) = \frac{V}{150\pi^2\epsilon} = \frac{3C_3^2 e^{-4N\eta_0} (e^{N\eta_0} - 1)^4 V_0}{25\pi^2\eta_0^4} \quad (\text{E.5})$$

with  $\Delta_\zeta^2(k_0) = 4 \times 10^{-10}$  measured by WMAP. (Note that with the current Planck results [15] we would get slightly different results.)

For the first example (5.34) in the text  $\eta_0 = 0$  and  $C_3 = -2.39$ . For  $\eta_0 = 0$ , the expressions simplify to

$$n_s - 1 = -\frac{4}{N}, \quad \Delta_\zeta^2(k_0) = \frac{3C_3^2 N^4 V_0}{25\pi^2}, \quad (\text{for } \eta_0 = 0). \quad (\text{E.6})$$

Choosing  $N = 50$  this gives  $n_s = 0.92$  and  $V_0 = 9 \times 10^{-16}$ . The second example (5.35) has  $C_3 = -3.69$ , and gives the same spectral index and similar  $V_0 = 4 \times 10^{-16}$ . The gravitino mass today is related to the inflationary scale via  $m_{3/2} = e^{K/2} W|_{\min} \sim 10^2 \sqrt{V_0} \sim 10^{-7}$ , far above the electroweak scale.

## Appendix F

# Effects of gauge field production in the CMB

This appendix contains some explicit computations left out in chapter 6. We want to estimate the effect that the produced gauge fields have on the two- and three point function, and to translate that into numerical values for the power spectrum and for  $f_{\text{NL}}$ . To compare the power spectrum estimate with the bounds set by primordial black hole production, as we have done in the main text, we also need an estimate of the mass of such a black hole. This is the subject of the last section of this appendix.

### F.1 Variance of $\vec{E} \cdot \vec{B}$

The variance of  $\vec{E} \cdot \vec{B}$  is defined as

$$\begin{aligned}\sigma^2 &\equiv \langle (\vec{E} \cdot \vec{B})^2 \rangle - \langle \vec{E} \cdot \vec{B} \rangle^2 \\ &= \langle E_i E_j \rangle \langle B_i B_j \rangle + \langle E_i B_j \rangle \langle B_i E_j \rangle.\end{aligned}\tag{F.1}$$

We find

$$\begin{aligned}\langle E_i E_j \rangle \langle B_i B_j \rangle &= \frac{1}{a^8} \int \frac{dkdq}{(2\pi)^6} |A'(k)|^2 |A(q)|^2 q^4 k^2 \int d^2\Omega_k d^2\Omega_q \epsilon_i(k) \epsilon_j^*(k) \epsilon_j^*(q), \\ \langle E_i B_j \rangle \langle B_i E_j \rangle &= \frac{1}{a^8} \int \frac{dkdq}{(2\pi)^6} A(k) A'^*(k) A'(q) A^*(q) q^3 k^3 \int d^2\Omega_k d^2\Omega_q \epsilon_i(k) \epsilon_i(q) \epsilon_j^*(k) \epsilon_j^*(q).\end{aligned}\tag{F.3}$$

Here we use the polarization tensor conventions given in [18]:

$$\begin{aligned}\vec{k} \cdot \vec{\epsilon}_\pm(\vec{k}) &= 0 \\ \vec{k} \times \vec{\epsilon}_\pm(\vec{k}) &= \mp ik \vec{\epsilon}_\pm(\vec{k}) \\ \vec{\epsilon}_\pm(-\vec{k}) &= \vec{\epsilon}_\pm(\vec{k})^*,\end{aligned}\tag{F.4}$$

which are normalized via  $\vec{\epsilon}_\lambda(\vec{k})^* \cdot \vec{\epsilon}_{\lambda'}(\vec{k}) = \delta_{\lambda\lambda'}$ . Given our conventions we are dealing with  $\vec{\epsilon}_-$  here.

The angular integral gives  $(4\pi)^2/3$ , i.e. a third of the whole sphere. The integrals over the modulus are similar to the one in [18] and are computed in the same way

$$I_2 = \frac{1}{a^4} \int \frac{dk}{(2\pi)^3} |A'(k)|^2 k^2 \simeq 2.2 \cdot 10^{-5} \frac{H^4}{\xi^3} e^{2\pi\xi}, \quad (\text{F.5})$$

$$I_3 = \frac{1}{a^4} \int \frac{dk}{(2\pi)^3} \frac{\partial_\tau}{2} |A(k)|^2 k^3 \simeq 1.9 \cdot 10^{-5} \frac{H^4}{\xi^4} e^{2\pi\xi}, \quad (\text{F.6})$$

$$I_4 = \frac{1}{a^4} \int \frac{dk}{(2\pi)^3} |A(k)|^2 k^4 \simeq 1.9 \cdot 10^{-5} \frac{H^4}{\xi^5} e^{2\pi\xi}. \quad (\text{F.7})$$

Putting things together one finds

$$\sigma = \sqrt{\frac{(4\pi)^2}{3} (I_3^2 + I_2 I_4)} = 2.0 \cdot 10^{-4} \frac{H^4}{\xi^4} e^{2\pi\xi} \simeq \langle \vec{E} \cdot \vec{B} \rangle. \quad (\text{F.8})$$

The last comparison follows from (F.18).

## F.2 Power spectrum estimate

In [156, 18] the power spectrum (6.24) has been obtained by the Green's function method. In [157] a quick estimate was introduced to compute the power spectrum in the case of large backreaction ( $\beta \gg 1$ ). Here we want to review and further explore this estimate, showing how it leads to (6.31) and also how, in the case of negligible backreaction, it approximates the precise result (6.24) within a factor of two.

The full equation of motion for the perturbation  $\delta\chi$  is (in real space)

$$\delta\ddot{\chi} + 3\beta H \delta\dot{\chi} - \frac{\nabla^2}{a^2} \delta\chi + m^2 \delta\chi = \alpha \left[ \vec{E} \cdot \vec{B} - \langle \vec{E} \cdot \vec{B} \rangle \right], \quad (\text{F.9})$$

with

$$\beta \equiv 1 - 2\pi\xi \alpha \frac{\langle \vec{E} \cdot \vec{B} \rangle}{3H\dot{\chi}}. \quad (\text{F.10})$$

Near horizon crossing we can estimate  $\partial \sim H$ . Since we have, near horizon crossing,  $H^2 = \frac{k^2}{a^2}$ , the first term cancels the third one. The second term can be approximated as  $3\beta H^2 \delta\chi$ . The last term on the left hand side is just a slow-roll correction and can be discarded. This directly gives

$$\delta\chi \approx \frac{\alpha \left( \vec{E} \cdot \vec{B} - \langle \vec{E} \cdot \vec{B} \rangle \right)}{3\beta H^2} \quad (\text{F.11})$$

and therefore we have

$$\zeta \equiv -\frac{H}{\dot{\chi}} \delta\chi \approx -\frac{\alpha \left( \vec{E} \cdot \vec{B} - \langle \vec{E} \cdot \vec{B} \rangle \right)}{3\beta H \dot{\chi}}. \quad (\text{F.12})$$

For the position space two point function of  $\zeta$  we then get

$$\langle \zeta(x)^2 \rangle \equiv \frac{H^2}{\dot{\chi}^2} \langle \delta\chi^2 \rangle \approx \frac{H^2}{\dot{\chi}^2} \left( \frac{\alpha\sigma}{3\beta H^2} \right)^2 = \left( \frac{\alpha \langle \vec{E} \cdot \vec{B} \rangle}{3\beta H \dot{\chi}} \right)^2 \quad (\text{F.13})$$

with  $\sigma$  the variance computed in the previous subsection.

To compare the position space power spectrum with the momentum space power spectrum we use

$$\begin{aligned}\langle \zeta(\vec{k})\zeta(\vec{k}') \rangle &\equiv (2\pi)^3 \delta^3(\vec{k} + \vec{k}') P(k), \quad P(k) \equiv \frac{2\pi^2 \Delta_\zeta^2(k)}{k^3}, \\ \langle \zeta(x)^2 \rangle &= \int d \ln k \Delta_\zeta^2(k) \simeq \mathcal{O}(1) \Delta_\zeta^2(k).\end{aligned}\tag{F.14}$$

This gives the result (6.31):

$$\Delta_\zeta^2(k) \simeq \langle \zeta(x)^2 \rangle = \left( \frac{\alpha \langle \vec{E} \cdot \vec{B} \rangle}{3H\dot{\chi}} \right)^2.\tag{F.15}$$

This expression has been plotted in figure 6.4.

Now when backreaction is strong we can approximate  $\beta \approx -2\pi\xi\alpha\frac{\langle \vec{E} \cdot \vec{B} \rangle}{3H\dot{\chi}}$ , which immediately gives the approximation (6.32)

$$\Delta_\zeta^2(k) = \frac{1}{(2\pi\xi)^2}.\tag{F.16}$$

We can as well make an approximation for the case where  $\beta \approx 1$  (negligible backreaction) and compare the result with the precise result (6.24), just to see how well this whole approximation works. For  $\beta = 1$  we have

$$\Delta_\zeta^2(k) = \left( \frac{\alpha \langle \vec{E} \cdot \vec{B} \rangle}{3H\dot{\chi}} \right)^2.\tag{F.17}$$

Upon using the estimate for  $\langle \vec{E} \cdot \vec{B} \rangle$  found in [156, 18]

$$\langle \vec{E} \cdot \vec{B} \rangle \approx 2.4 \times 10^{-4} \frac{H^4}{\xi^4} e^{2\pi\xi}\tag{F.18}$$

and

$$\alpha \equiv -\frac{2H\xi}{\dot{\chi}}\tag{F.19}$$

we find

$$\begin{aligned}\Delta_\zeta^2(k) &= \frac{4H^2\xi^2}{\dot{\chi}^2} \times 5.76 \times 10^{-8} \times \frac{H^8}{\xi^8} e^{4\pi\xi} \times \frac{1}{9H^2\dot{\chi}^2} \\ &= 2.56 \times 10^{-8} \times \frac{H^8}{\dot{\chi}^4} \times \frac{e^{4\pi\xi}}{\xi^6} \\ &= 2.56 \times 10^{-8} \times \left( \frac{H^2}{2\pi\dot{\chi}} \right)^4 \times (2\pi)^4 \times \frac{e^{4\pi\xi}}{\xi^6} \\ &= 4.0 \times 10^{-5} \times \Delta_{\zeta,\text{sr}}^4(k) \times \frac{e^{4\pi\xi}}{\xi^6}.\end{aligned}\tag{F.20}$$

This can be compared with the more precise result computed in [156, 18] that uses the Green's function approach

$$\Delta_\zeta^2(k) = \Delta_{\zeta,\text{sr}}^4(k) \times f_2(\xi) \times e^{4\pi\xi}\tag{F.21}$$

$$\simeq \Delta_{\zeta,\text{sr}}^4(k) \frac{7.5 \times 10^{-5}}{\xi^6} \times e^{4\pi\xi}.\tag{F.22}$$

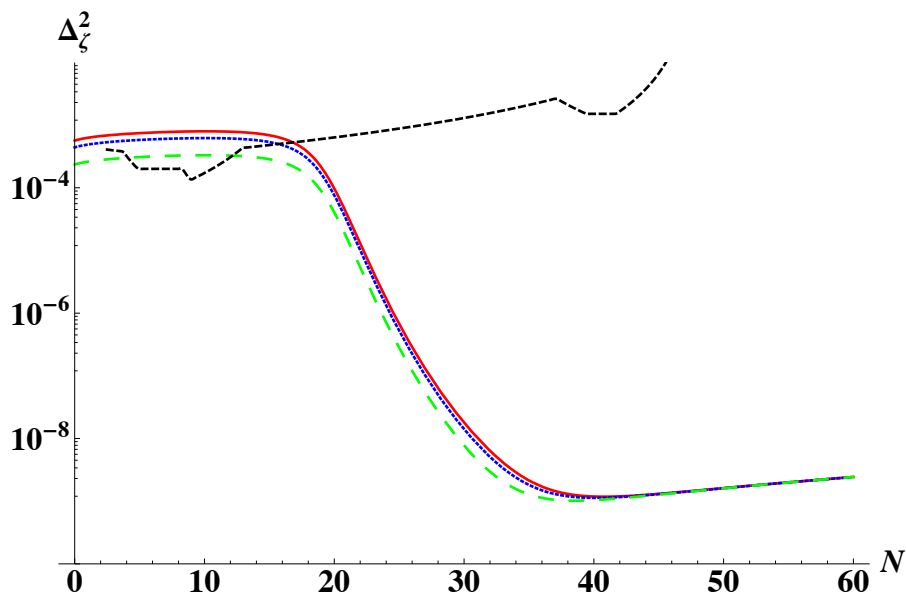


Figure F.1: Evolution of the power spectrum as in figure 6.4, still for  $\xi[N = 60] = 2.2$ . The red solid line is our estimate. The blue, finely dashed line is our estimate corrected with a fudge factor of 1.3. The green, largely dashed line is our estimate corrected with a fudge factor of 2.5. All signals remain within an order one factor from the black hole bounds in dashed black.

where in the second line we used the large  $\xi$  limit for  $f_2$ . We infer that this quick estimate is off by a factor less than two.

Actually, for some  $\xi$  the estimate comes even closer than this ratio  $\frac{7.5}{4}$ . Let us examine the situation at  $\xi = 3$  (which, for  $\xi(N = 60) = 2.2$ , corresponds to  $N \approx 35$ ). Above, we approximated the numerical function  $f_2(\xi)$  by  $\frac{7.5 \times 10^{-5}}{\xi^6}$  which yields an overestimate by a factor of 1.3. At the other hand, we also approximated the numerically found result for  $\langle \vec{E} \cdot \vec{B} \rangle$  by the estimate (F.18), which is an underestimate, that for  $\xi = 3$  only captures a fraction of 0.73 of the true  $\langle \vec{E} \cdot \vec{B} \rangle$ . Putting everything together one finds that, at  $\xi = 3$  ( $N = 35$ ), our estimate (F.15) with  $\beta$  set to one overestimates the precisely computed numerical result (F.21) by a factor of

$$\frac{4}{7.5} \times \frac{1.3}{(0.73)^2} \approx 1.3. \quad (\text{F.23})$$

At  $\xi=2.2$  ( $N=60$ ) we find that our estimate (F.15) overestimates the precisely computed result by a factor of 2.5.

Now one might introduce a fudge factor such that at some preferred value for  $\xi$  our approximation precisely matches the numerically computed result. However, we have just seen that the inclusion of such a fudge factor will induce only a small shift in our estimate that we anyway only trust up to corrections of order one. Besides, the fudge factor would always be arbitrary, as it depends on the preferred value of  $\xi$  where it makes both signals match. Therefore it seems safe to neglect it altogether. In figure F.1 we have for once plotted how the total power spectrum (including the standard slow-roll contribution) would shift from such a correction. In the rest of the chapter 6 we work with our uncorrected estimate for the power spectrum.

N.B. This estimate involves only the gauge field contribution to the power spectrum. Apart from that there is always the standard slow-roll component  $\Delta_{\zeta, \text{sr}}^2(k)$ . This is the dominant contribution on CMB scales. That is why any estimate of the total power spectrum matches the precise result so well on CMB scales, whatever order one fudge factor one chooses.

### F.3 Skewness of $\vec{E} \cdot \vec{B}$

Now we want to compute

$$\tau^3 \equiv \langle (\vec{E} \cdot \vec{B} - \langle \vec{E} \cdot \vec{B} \rangle)^3 \rangle = \langle (\vec{E} \cdot \vec{B})^3 \rangle - 4\langle \vec{E} \cdot \vec{B} \rangle^3 \simeq \langle (\vec{E} \cdot \vec{B})^3 \rangle_c + 3\langle \vec{E} \cdot \vec{B} \rangle^3, \quad (\text{F.24})$$

where we used that  $\langle (\vec{E} \cdot \vec{B})^2 \rangle \simeq 2\langle \vec{E} \cdot \vec{B} \rangle^2$  from the previous section and in the last step we recognized that there are  $1 + 3 \times 2 = 7$  non-connected diagrams in  $\langle (\vec{E} \cdot \vec{B})^3 \rangle$ , each one equal to  $\langle \vec{E} \cdot \vec{B} \rangle^3$ . Using Wick's theorem we find many terms. All of them have the same angular integral

$$\int d^2\Omega_{k_1} d^2\Omega_{k_2} d^2\Omega_{k_3} \epsilon_i(k_1) \epsilon_i(k_2) \epsilon_j^*(k_1) \epsilon_j(k_3) \epsilon_j^*(k_2) \epsilon_j^*(k_3) = \frac{2\pi^5}{3}. \quad (\text{F.25})$$

Counting all the possible pairwise contractions one finds

$$\langle (\vec{E} \cdot \vec{B})^3 \rangle_c = -\frac{2\pi^5}{3} (2I_3^3 + I_2 I_3 I_4) = \left[ -2.4 \cdot 10^{-4} \frac{H^4}{\xi^4} e^{2\pi\xi} \right]^3 \simeq -\langle \vec{E} \cdot \vec{B} \rangle^3 \quad (\text{F.26})$$

and therefore

$$\tau^3 \simeq 2\langle \vec{E} \cdot \vec{B} \rangle^3. \quad (\text{F.27})$$

### F.4 Bispectrum and $f_{\text{NL}}$ estimate

The position space three point function of  $\zeta$  can be directly generalized from (F.13):

$$\langle \zeta(x)^3 \rangle \equiv -\frac{H^3}{\dot{\chi}^3} \langle \delta\chi^3 \rangle \approx -\frac{H^3}{\dot{\chi}^3} \left( \frac{\alpha\tau}{3\beta H^2} \right)^3 = -2 \left( \frac{\alpha \langle \vec{E} \cdot \vec{B} \rangle}{3\beta H \dot{\chi}} \right)^3, \quad (\text{F.28})$$

where we used the definition of the skewness  $\tau^3$  (F.24) and its estimate (F.27).  $\langle \zeta(x)^3 \rangle$  is positive. (Again: we work with negative  $\dot{\chi}$  which yields positive  $\langle \vec{E} \cdot \vec{B} \rangle$ , while working with  $\dot{\chi} > 0$  would give  $\langle \vec{E} \cdot \vec{B} \rangle < 0$ .)

Let us first analyze this result in the regime where backreaction is negligible, i.e.  $\beta = 1$ . Using (F.18) and (F.19) we get

$$\langle \zeta(\vec{x})^3 \rangle \simeq 2 \frac{8}{27} (2.4 \times 10^{-4})^3 \frac{H^{12} e^{6\pi\xi}}{\xi^9 \dot{\chi}^6} \simeq 8.2 \times 10^{-12} \frac{H^{12} e^{6\pi\xi}}{\xi^9 \dot{\chi}^6}. \quad (\text{F.29})$$

Now we want to compare this with the momentum space bispectrum  $B(k)$ , defined via

$$\langle \zeta(\vec{k}_1) \zeta(\vec{k}_2) \zeta(\vec{k}_3) \rangle \equiv (2\pi)^3 \delta^3(k_1 + k_2 + k_3) B(\vec{k}_1, \vec{k}_2, \vec{k}_3) \quad (\text{F.30})$$

for which we can write

$$\langle \zeta(\vec{x})^3 \rangle = \int \frac{d^3 k_1}{(2\pi)^3} \int \frac{d^3 k_2}{(2\pi)^3} B(\vec{k}_1, \vec{k}_2, -\vec{k}_1 - \vec{k}_2). \quad (\text{F.31})$$

When non-Gaussianity is large mostly on equilateral triangles, the integral is supported in the region  $k_2 \simeq k_1$  and  $\theta_{12} \simeq \pi/3$ . Hence we estimate

$$\langle \zeta(\vec{x})^3 \rangle = \int d \log k \frac{8\pi^2}{(2\pi)^6} k^6 B_{\text{eq}}(k) \simeq \frac{8\pi^2}{(2\pi)^6} k^6 B_{\text{eq}}(k) \mathcal{O}(1), \quad (\text{F.32})$$

where  $B_{\text{eq}}(k)$  is the bispectrum evaluated on equilateral triangles. Now we can compare our estimate (F.29) with the precisely computed result using the Green's function approach, that we take from result (2.8) of [158],

$$B_{\text{eq}}(k) = \frac{1}{(2\pi)^3} \langle \zeta(\vec{k}_1) \zeta(\vec{k}_2) \zeta(\vec{k}_3) \rangle \simeq \frac{3 \times 3 \times 2.8 \times 10^{-7}}{10(2\pi)^2} \frac{H^{12} e^{6\pi\xi}}{\xi^9 \dot{\phi}^6} \frac{1}{k^6}, \quad (\text{F.33})$$

where we have used the large  $\xi$  estimate

$$f_3(\xi) = \frac{2.8 \cdot 10^{-7}}{\xi^9}. \quad (\text{F.34})$$

This last result leads to

$$\langle \zeta(\vec{x})^3 \rangle \simeq \frac{8\pi^2}{(2\pi)^6} k^6 B_{\text{eq}}(k) \simeq 8.2 \times 10^{-12} \frac{H^{12} e^{6\pi\xi}}{\xi^9 \dot{\phi}^6} \quad (\text{F.35})$$

which agrees (surprisingly) well with (F.29).

In the regime of strong backreaction we can write  $\beta \approx -2\pi\xi\alpha \frac{\langle \vec{E} \cdot \vec{B} \rangle}{3H\dot{\chi}}$  and the estimate (F.28) directly gives the generalization of (F.16)

$$\langle \zeta(\vec{x})^3 \rangle \simeq \frac{1}{4\pi^3 \xi^3}. \quad (\text{F.36})$$

Finally we want to convert these results into a value for  $f_{\text{NL}}$ . From 1.60 we have

$$\begin{aligned} f_{\text{NL}}^{\text{eq}} &= B_{\text{eq}}(\vec{k}) \frac{10}{3} \frac{1}{(2\pi)^4} \frac{1}{\Delta_\zeta^4(k)} \frac{k^9}{3k^3} = \frac{(2\pi)^6}{8\pi^2} \frac{1}{k^6} \langle \zeta(\vec{x})^3 \rangle \times \frac{10}{3} \frac{1}{(2\pi)^4} \frac{1}{\Delta_\zeta^4(k)} \frac{k^9}{3k^3} \\ &= \frac{10}{9} \frac{(2\pi)^2}{8\pi^2} \frac{\langle \zeta(\vec{x})^3 \rangle}{\Delta_\zeta^4(k)}. \end{aligned} \quad (\text{F.37})$$

In the regime of negligible backreaction we can then take our estimate (F.29), and conclude that

$$f_{\text{NL}}^{\text{eq}} = \frac{2.8 \cdot 10^{-7}}{\xi^9} \frac{e^{6\pi\xi} \Delta_{\zeta, \text{sr}}^6(k)}{\Delta_\zeta^4(k)}. \quad (\text{F.38})$$

This again matches the result obtained in [156, 18] by a more precise computation. (Of course, after that we had found that the expressions for  $\langle \zeta(\vec{x})^3 \rangle$  match so well, this is only a consistency check.)

In the regime of strong backreaction, finally, we need to insert (F.36) into (F.37). Using our power spectrum estimate (F.16) we find

$$f_{\text{NL}}^{\text{eq}} = \frac{10}{9} \frac{(2\pi)^2}{8\pi^2} \frac{(2\pi\xi)^4}{4\pi^3 \xi^3} = \frac{10}{9} 2\pi\xi \simeq 42 \quad (\text{F.39})$$

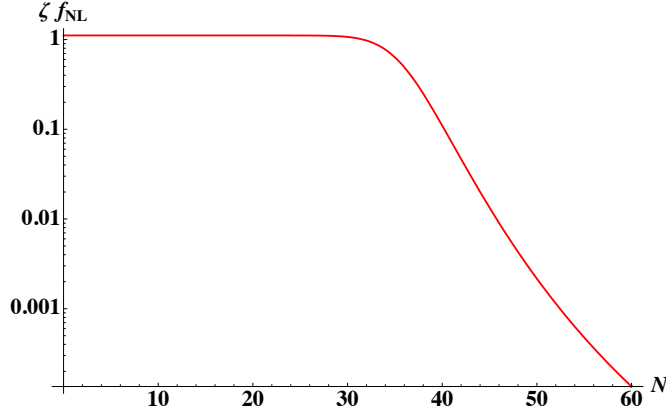


Figure F.2: Evolution of  $f_{\text{NL}} \times \zeta$  as a function of  $N$ , for  $\xi[N = 60] = 2.2$

where we have used that towards the end of inflation we have  $\xi \simeq 6$ .

Notwithstanding the precise match between (F.29) and (F.35), there is still an order one factor between the estimate for the three point function (and for  $f_{\text{NL}}$ ) and its precisely computed numerical value. Again: to arrive at (F.29) we have used the estimate (F.18) for  $\langle \vec{E} \cdot \vec{B} \rangle$ , and to arrive at (F.35) we have inserted the large  $\xi$  approximation  $\frac{2.8 \cdot 10^{-7}}{\xi^9}$  for  $f_3(\xi)$ . When using precise numerical prescriptions rather than estimates for  $\langle \vec{E} \cdot \vec{B} \rangle$  and  $f_3(\xi)$  we find that our estimates overshoots the precisely computed  $f_{\text{NL}}$  by a factor of 9.5 at  $\xi = 2.2$  ( $N = 60$ ), and by a factor of 3.8 at  $\xi = 3$  ( $N \approx 35$ ).

Again we will not bother introducing a fudge factor to close this gap at some preferred value of  $\xi$ . Anyway, when backreaction is large  $f_{\text{NL}}$  is not a suitable indicator for the amount of non-Gaussianity anymore. In figure F.2 we plot our estimate for a more meaningful quantity: the skewness, which is equivalent to  $f_{\text{NL}}\zeta$ . When backreaction becomes important, it saturates at a value of about one, which a posteriori justifies our approach (6.36).

## F.5 Black hole masses

In this appendix we give some details about the derivation of (6.42) for the black hole mass and about the total number of efoldings enforced by a specific expansion history.

Suppose the universe is radiation dominated right after the end of inflation. Then the expansion proceeds as  $a \sim (t/t_0)^{1/2}$ , so  $H(t) = \frac{1}{2t}$ . This regime starts at  $t_0$ , which is not the time since the beginning of Big Bang, but simply the constant  $t_0 = \frac{1}{2H}$ , where  $H$  is the Hubble constant at the end of inflation. We distinguish it from the decreasing  $H(t) = \frac{1}{2t}$ . The wavelength  $l_{t_0} = H^{-1}e^N$  grows as  $l_t = H^{-1}(t/t_0)^{1/2}e^N = H^{-1}(2Ht)^{1/2}e^N$ . The horizon size  $1/H(t) = 2t$  grows and becomes equal to  $l_t$  (and black holes form) at

$$2t = H^{-1}(2Ht)^{1/2}e^N$$

i.e. at

$$(2Ht)^{1/2} = (t/t_0)^{1/2} = e^N.$$

In other words, the black holes form after the universe expands by a factor  $e^N$  since the end of inflation.

The initial energy stored inside the volume  $H^{-1}e^N$  was  $M_N \simeq 10e^{3N}$  g, but during this extra expansion it scales down (redshifts) by the factor  $e^N$ , so it becomes

$$M_{BH} \simeq 10e^{2N}g.$$

It should be stressed that specifying the energy density at the end of inflation and at reheating, directly determines the number of efoldings corresponding to any scale (and in particular CMB scales) according to [192]

$$N(k) = 62 - \log \frac{k}{a_0 H_0} - \log \frac{10^{16} \text{GeV}}{V_*^{1/4}} + \log \frac{V_*^{1/4}}{V_{end}^{1/4}} - \frac{1}{3} \log \frac{V_{end}^{1/4}}{\rho_{reh}^{1/4}},$$

where  $V_*$  is the energy density during inflation when the mode  $k$  left the horizon,  $V_{end}$  is the energy density at the end of inflation,  $\rho_{reh}$  is the energy density at reheating and the subscript 0 refers to today's value. Taking for example  $\rho_{reh} = V_{end} = m^2 M_p^2/2$  and  $V_k = m^2 15^2 M_p^2/2$  with  $m = 6 \times 10^6 M_p$  gives  $N_{CMB} = N(a_0 H_0) \simeq 64$ . We use this value in our discussion of primordial black holes, but since the difference between 60 and 64 changes very little in our numerics, for simplicity we use  $N_{CMB} = 60$  in the rest of chapter 6.

## Appendix G

# Sugra Coleman-Weinberg potential

In this appendix we study the standard Coleman-Weinberg potential, that we derived and generalized in chapters 3 and 4, in the supergravitational context of chapter 7. We begin with the standard expression (note that now that we consider a gauge singlet field, we do not have the extra term proportional to  $\ddot{\phi}$  that we found in chapters 3 and 4)

$$V_{\text{CW}} = \frac{1}{64\pi^2} \sum_i (-1)^F m_i^4 \ln \left( \frac{m_i^2}{\Lambda^2} \right) \quad (\text{G.1})$$

where the sum is over all masses, with  $F = 1$  for bosons and  $F = -1$  for fermions, and  $\Lambda$  is the cut-off scale. Only the  $n_i$ -dependent mass terms lift the inflaton potential, in our case these are the waterfall field masses and their fermionic partners. They can be written in the form

$$m_{h_r,i}^2 = \mu(x^2 + y^2 \pm 1), \quad \tilde{m}_{h_r,i}^2 = \mu^2 x^2 \quad (\text{G.2})$$

with  $\mu, x, y$  given for inflation without and with a modulus field respectively by (7.6) and (7.28). The waterfall field  $h_r$  becomes tachyonic and inflation ends for  $x^c = 1$ .

Even though  $y^2 \ll x^2$  is clearly subdominant in the expression for the mass terms (G.2), they are important for the shape of the loop potential. This is because the dominant contributions of the boson mass cancels with that of the fermion mass in (G.1). The loop potential becomes

$$V_{\text{CW}} = \left( \frac{\mu^4}{32\pi^2} \right) \left[ 2(1 + x^2 y^2 + y^4) \ln \left( \frac{x^2 \mu^2}{Q^2} \right) + (x^2 + y^2 + 1)^2 \ln \left( 1 + \frac{y^2 + 1}{x^2} \right) + (x^2 + y^2 - 1)^2 \ln \left( 1 + \frac{y^2 - 1}{x^2} \right) \right], \quad (\text{G.3})$$

with  $Q$  the renormalization scale which we fix to  $Q = \mu = \tilde{m}_{h_r,i}|_{x=1}$ . For negative values  $y^2 < 0$  the potential develops a maximum at large  $x$ . Inflation has to take place on the left of the maximum, for the inflaton field to roll towards the “right” minimum. This also means that if the maximum is too close to the critical value, it is impossible to get 60 e-folds of inflation. To see the maximum appearing, we can take the large  $x$  limit of the potential

$$\lim_{x \rightarrow \infty} \left( \frac{32\pi^2}{\mu^4} \right) V_{\text{CW}} = 3 + 4 \ln(x) + 2y^2 x^2 (1 + 4 \ln(x)). \quad (\text{G.4})$$

The slope of the potential at large  $x$  gets a positive contribution from the  $y^0$ -term, and a positive or negative contribution from the  $y^2$  correction; if the latter is negative, the potential has a maximum. The slope is

$$\lim_{x \rightarrow \infty} \partial_x V_{\text{CW}} = \frac{4}{x} + 4xy^2(3 + 4 \log(x)), \quad (\text{G.5})$$

which vanishes for

$$x_{\text{max}}^2 = -(y^2(3 + 4 \ln(x_{\text{max}})))^{-1} \quad (\text{G.6})$$

which is only a solution for  $y^2 < 0$ . Numerically we find for  $\kappa_{SH} = \mathcal{O}(1)$  that  $x_{\text{max}} = 50 - 100$  in the absence of moduli corrections (i.e. using (7.6)).

# Bibliography

- [1] S. Mooij and M. Postma, JCAP **1006**, 012 (2010) [arXiv:1001.0664 [hep-ph]].
- [2] S. Mooij and M. Postma, JCAP **1109**, 006 (2011) [arXiv:1104.4897 [hep-ph]].
- [3] A. Achucarro, S. Mooij, P. Ortiz and M. Postma, JCAP **1208**, 013 (2012) [arXiv:1203.1907 [hep-th]].
- [4] D. P. George, S. Mooij and M. Postma, JCAP **1211**, 043 (2012) [arXiv:1207.6963 [hep-th]].
- [5] A. Linde, S. Mooij and E. Pajer, Phys. Rev. D **87**, 103506 (2013) [arXiv:1212.1693 [hep-th]].
- [6] A. Riotto, hep-ph/0210162.
- [7] D. Baumann, arXiv:0907.5424 [hep-th].
- [8] T. Biswas, A. Notari and W. Valkenburg JCAP **1011**, 030 (2010) [arXiv:1007.3065 [astro-ph.CO]].
- [9] K. Land and J. Magueijo, Phys. Rev. Lett. **95**, 071301 (2005) [astro-ph/0502237].
- [10] S. M. Carroll, San Francisco, USA: Addison-Wesley (2004) 513 p
- [11] P. A. R. Ade *et al.* [ Planck Collaboration], arXiv:1303.5062 [astro-ph.CO].
- [12] A. H. Guth, Phys. Rev. D **23**, 347 (1981).
- [13] P. A. R. Ade *et al.* [ Planck Collaboration], arXiv:1303.5076 [astro-ph.CO].
- [14] V. F. Mukhanov, H. A. Feldman and R. H. Brandenberger, Phys. Rept. **215**, 203 (1992).
- [15] P. A. R. Ade *et al.* [ Planck Collaboration], arXiv:1303.5082 [astro-ph.CO].
- [16] J. M. Maldacena, JHEP **0305**, 013 (2003) [astro-ph/0210603].
- [17] M. Alishahiha, E. Silverstein, D. Tong and , Phys. Rev. D **70**, 123505 (2004) [hep-th/0404084].
- [18] N. Barnaby, R. Namba and M. Peloso, JCAP **1104**, 009 (2011) [arXiv:1102.4333 [astro-ph.CO]].
- [19] P. A. R. Ade *et al.* [Planck Collaboration], arXiv:1303.5084 [astro-ph.CO].
- [20] B. J. Carr, K. Kohri, Y. Sendouda and J. 'i. Yokoyama, Phys. Rev. D **81**, 104019 (2010) [arXiv:0912.5297 [astro-ph.CO]].
- [21] D. H. Lyth, JCAP **1205**, 022 (2012) [arXiv:1201.4312 [astro-ph.CO]].
- [22] A. D. Linde, Phys. Lett. B **108** (1982) 389.

- [23] A. Albrecht and P. J. Steinhardt, Phys. Rev. Lett. **48** (1982) 1220.
- [24] A. D. Linde, Phys. Lett. B **129** (1983) 177.
- [25] A. D. Linde, Phys. Rev. D **49** (1994) 748 [astro-ph/9307002].
- [26] D. H. Lyth, Phys. Rev. Lett. **78** (1997) 1861 [arXiv:hep-ph/9606387].
- [27] A. Achucarro, J. O. Gong, S. Hardeman, G. A. Palma and S. P. Patil, JCAP **1101**, 030 (2011) [arXiv:1010.3693 [hep-ph]].
- [28] A. D. Linde and A. Riotto, Phys. Rev. D **56** (1997) 1841 [hep-ph/9703209].
- [29] F. L. Bezrukov, M. Shaposhnikov, Phys. Lett. **B659** (2008) 703-706. [arXiv:0710.3755 [hep-th]].
- [30] F. Bezrukov, A. Magnin, M. Shaposhnikov and S. Sibiryakov, JHEP **1101** (2011) 016 [arXiv:1008.5157 [hep-ph]].
- [31] F. Bezrukov, M. Y. Kalmykov, B. A. Kniehl and M. Shaposhnikov, JHEP **1210**, 140 (2012) [arXiv:1205.2893 [hep-ph]].
- [32] S. Alekhin, A. Djouadi and S. Moch, Phys. Lett. B **716**, 214 (2012) [arXiv:1207.0980 [hep-ph]].
- [33] S. Ferrara, R. Kallosh, A. Linde, A. Marrani and A. Van Proeyen, Phys. Rev. D **82** (2010) 045003 [arXiv:1004.0712 [hep-th]].
- [34] S. Ferrara, R. Kallosh, A. Linde, A. Marrani and A. Van Proeyen, Phys. Rev. D **83** (2011) 025008 [arXiv:1008.2942 [hep-th]].
- [35] S. V. Ketov and A. A. Starobinsky, JCAP **1208**, 022 (2012) [arXiv:1203.0805 [hep-th]].
- [36] J. Garcia-Bellido, J. Rubio, M. Shaposhnikov and D. Zenhausern, Phys. Rev. D **84**, 123504 (2011) [arXiv:1107.2163 [hep-ph]].
- [37] M. E. Peskin and D. V. Schroeder, Reading, USA: Addison-Wesley (1995) 842 p
- [38] A. Zee, Princeton, UK: Princeton Univ. Pr. (2010) 576 p
- [39] S. Coleman, Cambridge, UK: Cambridge Univ. Pr. (1985) 402 p
- [40] E. Calzetta and B. L. Hu, Phys. Rev. D **35** (1987) 495
- [41] S. R. Coleman, E. J. Weinberg, Phys. Rev. **D7** (1973) 1888-1910.
- [42] S. Weinberg, Phys. Rev. D **7**, 2887 (1973).
- [43] S. Weinberg, Phys. Rev. D **9** (1974) 3357.
- [44] J. S. Schwinger, J. Math. Phys. **2** (1961) 407-432.
- [45] L. V. Keldysh, Zh. Eksp. Teor. Fiz. **47** (1964) 1515 [Sov. Phys. JETP **20** (1965) 1018].
- [46] R. D. Jordan, Phys. Rev. **D33** (1986) 444-454.
- [47] P. M. Bakshi, K. T. Mahanthappa, J. Math. Phys. **4** (1963) 1-11.
- [48] P. M. Bakshi, K. T. Mahanthappa, J. Math. Phys. **4** (1963) 12-16.
- [49] J. P. Paz, Phys. Rev. **D42** (1990) 529-542.

- [50] S. Weinberg, Phys. Rev. **D72** (2005) 043514. [hep-th/0506236].
- [51] J. Baacke, K. Heitmann and C. Patzold, Phys. Rev. D **55** (1997) 7815 [arXiv:hep-ph/9612264].
- [52] J. Goldstone, Nuovo Cim. **19** (1961) 154-164.
- [53] J. Goldstone, A. Salam, S. Weinberg, Phys. Rev. **127** (1962) 965-970.
- [54] J. Baacke, K. Heitmann, Phys. Rev. **D60** (1999) 105037. [hep-th/9905201].
- [55] K. Heitmann, Phys. Rev. **D64** (2001) 045003. [hep-ph/0101281].
- [56] K. Heitmann, Master's Thesis, Universität Dortmund, 1996.
- [57] K. Heitmann, PhD Thesis, Universität Dortmund, 2000.
- [58] B. Clauwens, R. Jeannerot, JCAP **0803** (2008) 016. [arXiv:0709.2112 [hep-ph]].
- [59] L. A. Dolan, R. Jackiw, Phys. Rev. **D9** (1974) 3320-3341.
- [60] C. Grosse-Knetter and R. Kogerler, Phys. Rev. D **48** (1993) 2865 [hep-ph/9212268].
- [61] T. Anderberg, arXiv:0804.2284 [physics.gen-ph].
- [62] P. B. Arnold, E. Braaten, S. Vokos, Phys. Rev. **D46** (1992) 3576-3586.
- [63] S. H. H. Tye and Y. Vtorov-Karevsky, Int. J. Mod. Phys. A **13**, 95 (1998) [hep-th/9601176].
- [64] N. K. Nielsen, Nucl. Phys. B **101** (1975) 173.
- [65] R. Fukuda, T. Kugo, Phys. Rev. **D13** (1976) 3469.
- [66] D. Boyanovsky, D. Brahm, R. Holman and D. S. Lee, Phys. Rev. D **54** (1996) 1763 [arXiv:hep-ph/9603337].
- [67] N. D. Birrell and P. C. W. Davies, Cambridge, Uk: Univ. Pr. ( 1982) 340p
- [68] P. Candelas and D. J. Raine, Phys. Rev. D **12** (1975) 965.
- [69] A. Ringwald, Annals Phys. **177** (1987) 129.
- [70] A. Ringwald, Z. Phys. C **34**, 481 (1987).
- [71] P. B. Greene and L. Kofman, Phys. Lett. B **448** (1999) 6 [hep-ph/9807339].
- [72] J. Baacke, K. Heitmann, C. Patzold, "Nonequilibrium dynamics of fermions in a spatially homogeneous scalar background field," Phys. Rev. **D58** (1998) 125013. [hep-ph/9806205].
- [73] J. Baacke, K. Heitmann, C. Patzold, Phys. Rev. **D57** (1998) 6398-6405. [hep-th/9711144].
- [74] J. Baacke, D. Boyanovsky and H. J. de Vega, Phys. Rev. D **63**, 045023 (2001) [hep-ph/9907337].
- [75] G. M. Shore, Annals Phys. **128** (1980) 376.
- [76] B. Allen, Nucl. Phys. B **226** (1983) 228.
- [77] K. Ishikawa, Phys. Rev. D **28** (1983) 2445.
- [78] B. Garbrecht, Nucl. Phys. B **784**, 118 (2007) [hep-ph/0612011].

- [79] C. Gordon, D. Wands, B. A. Bassett and R. Maartens, *Phys. Rev. D* **63** (2001) 023506 [arXiv:astro-ph/0009131].
- [80] S. Groot Nibbelink and B. J. W. van Tent, [arXiv:hep-ph/0011325].
- [81] S. Groot Nibbelink and B. J. W. van Tent, *Class. Quant. Grav.* **19** (2002) 613 [arXiv:hep-ph/0107272].
- [82] D. Wands, N. Bartolo, S. Matarrese and A. Riotto, *Phys. Rev. D* **66**, 043520 (2002) [arXiv:astro-ph/0205253].
- [83] K. A. Malik and D. Wands, *Phys. Rept.* **475**, 1 (2009) [arXiv:0809.4944 [astro-ph]].
- [84] C. M. Peterson and M. Tegmark, *Phys. Rev. D* **83**, 023522 (2011) [arXiv:1005.4056 [astro-ph.CO]].
- [85] A. Achucarro, J. -O. Gong, S. Hardeman, G. A. Palma and S. P. Patil, *Phys. Rev. D* **84** (2011) 043502 [arXiv:1005.3848 [hep-th]].
- [86] S. Cespedes, V. Atal and G. A. Palma, *JCAP* **1205**, 008 (2012) [arXiv:1201.4848 [hep-th]].
- [87] G. Shiu and J. Xu, *Phys. Rev. D* **84**, 103509 (2011) [arXiv:1108.0981 [hep-th]].
- [88] D. Baumann and D. Green, *JCAP* **1109**, 014 (2011) [arXiv:1102.5343 [hep-th]].
- [89] C. Cheung, P. Creminelli, A. L. Fitzpatrick, J. Kaplan and L. Senatore, *JHEP* **0803** (2008) 014 [arXiv:0709.0293 [hep-th]].
- [90] S. Weinberg, *Phys. Rev. D* **77** (2008) 123541 [arXiv:0804.4291 [hep-th]].
- [91] A. J. Tolley and M. Wyman, *Phys. Rev. D* **81**, 043502 (2010) [arXiv:0910.1853 [hep-th]].
- [92] J. Garriga and V. F. Mukhanov, *Phys. Lett. B* **458**, 219 (1999) [hep-th/9904176].
- [93] C. P. Burgess, J. M. Cline and R. Holman, *JCAP* **0310**, 004 (2003) [hep-th/0306079].
- [94] A. Achucarro, J. -O. Gong, S. Hardeman, G. A. Palma and S. P. Patil, *JHEP* **1205**, 066 (2012) [arXiv:1201.6342 [hep-th]].
- [95] P. Binetruy, G. Dvali, R. Kallosh and A. Van Proeyen, *Class. Quant. Grav.* **21** (2004) 3137 [hep-th/0402046].
- [96] Képa Sousa, PhD Thesis, Leiden University, 2012.
- [97] X. Chen and Y. Wang, *JCAP* **1004**, 027 (2010) [arXiv:0911.3380 [hep-th]].
- [98] C. M. Peterson and M. Tegmark, arXiv:1111.0927 [astro-ph.CO].
- [99] S. Cremonini, Z. Lalak and K. Turzyski, *JCAP* **1103**, 016 (2011) [arXiv:1010.3021 [hep-th]].
- [100] A. Avgoustidis, S. Cremonini, A. -C. Davis, R. H. Ribeiro, K. Turzyski and S. Watson, *JCAP* **1202**, 038 (2012) [arXiv:1110.4081 [astro-ph.CO]].
- [101] S. Hardeman, J. M. Oberreuter, G. A. Palma, K. Schalm and T. van der Aalst, *JHEP* **1104** (2011) 009 [arXiv:1012.5966 [hep-ph]].
- [102] R. Kallosh and A. D. Linde, *JHEP* **0412** (2004) 004 [hep-th/0411011].
- [103] S. C. Davis and M. Postma, *JCAP* **0803** (2008) 015 [arXiv:0801.4696 [hep-ph]].
- [104] S. P. de Alwis, *Phys. Lett. B* **626**, 223 (2005) [hep-th/0506266].

- [105] S. P. de Alwis, *Phys. Lett. B* **628**, 183 (2005) [hep-th/0506267].
- [106] A. Achúcarro, K. Sousa, *JHEP* **0803**, 002 (2008). [arXiv:0712.3460 [hep-th]].
- [107] A. Achúcarro, S. Hardeman, K. Sousa, *JHEP* **0811**, 003 (2008). [arXiv:0809.1441 [hep-th]].
- [108] A. Achúcarro, S. Hardeman and K. Sousa, *Phys. Rev. D* **78** (2008) 101901 [arXiv:0806.4364 [hep-th]].
- [109] D. Gallego and M. Serone, *JHEP* **0901**, 056 (2009) [arXiv:0812.0369 [hep-th]].
- [110] D. Gallego and M. Serone, *JHEP* **0906**, 057 (2009) [arXiv:0904.2537 [hep-th]].
- [111] Diego Gallego, *JHEP* **1106**, 087 (2011). [arXiv:1103.5469 [hep-th]].
- [112] L. Brizi, M. Gomez-Reino and C. A. Scrucca, *Nucl. Phys. B* **820**, 193 (2009) [arXiv:0904.0370 [hep-th]].
- [113] A. Achúcarro, S. Hardeman, J. M. Oberreuter, K. Schalm and T. van der Aalst, *JCAP* **1303**, 038 (2013) [arXiv:1108.2278 [hep-th]].
- [114] P. Binetruy and M. K. Gaillard, *Nucl. Phys. B* **254**, 388 (1985).
- [115] S. C. Davis and M. Postma, *JCAP* **0804** (2008) 022 [arXiv:0801.2116 [hep-th]].
- [116] L. Boubekeur and D. H. Lyth, *JCAP* **0507** (2005) 010 [arXiv:hep-ph/0502047].
- [117] P. Brax, S. C. Davis and M. Postma, *JCAP* **0802** (2008) 020 [arXiv:0712.0535 [hep-th]].
- [118] A. D. Linde and A. Westphal, *JCAP* **0803** (2008) 005 [arXiv:0712.1610 [hep-th]].
- [119] L. Álvarez-Gaumé, C. Gómez and R. Jiménez, *JCAP* **1103** (2011) 027 [arXiv:1101.4948 [hep-th]].
- [120] L. Alvarez-Gaume, C. Gomez and R. Jimenez, *JCAP* **1203**, 017 (2012) [arXiv:1110.3984 [astro-ph.CO]].
- [121] Riccardo Barbieri, E. Cremmer, S. Ferrara, *Phys. Lett. B* **163** (1985) 143.
- [122] L. Covi, M. Gómez-Reino, C. Gross, G. A. Palma, C. A. Scrucca, *JHEP* **0903** (2009) 146 [arXiv:0812.3864 [hep-th]].
- [123] R. Kallosh and A. Linde, *JCAP* **1011**, 011 (2010) [arXiv:1008.3375 [hep-th]].
- [124] R. Kallosh, A. Linde and T. Rube, *Phys. Rev. D* **83**, 043507 (2011) [arXiv:1011.5945 [hep-th]].
- [125] R. Kallosh, A. Linde, K. A. Olive and T. Rube, *Phys. Rev. D* **84**, 083519 (2011) [arXiv:1106.6025 [hep-th]].
- [126] G. R. Dvali, Q. Shafi and R. K. Schaefer, *Phys. Rev. Lett.* **73** (1994) 1886 [hep-ph/9406319].
- [127] M. Dine and L. Pack, *JCAP* **1206**, 033 (2012) [arXiv:1109.2079 [hep-ph]].
- [128] L. Covi, M. Gomez-Reino, C. Gross, J. Louis, G. A. Palma and C. A. Scrucca, *JHEP* **0806** (2008) 057 [arXiv:0804.1073 [hep-th]].
- [129] L. Covi, M. Gomez-Reino, C. Gross, J. Louis, G. A. Palma and C. A. Scrucca, *JHEP* **0808** (2008) 055 [arXiv:0805.3290 [hep-th]].
- [130] I. Ben-Dayan, R. Brustein and S. P. de Alwis, *JCAP* **0807**, 011 (2008) [arXiv:0802.3160 [hep-th]].

- [131] E. Komatsu *et al.* [WMAP Collaboration], *Astrophys. J. Suppl.* **192** (2011) 18 [arXiv:1001.4538 [astro-ph.CO]].
- [132] M. Kawasaki, M. Yamaguchi and T. Yanagida, *Phys. Rev. Lett.* **85** (2000) 3572 [hep-ph/0004243].
- [133] M. Yamaguchi and J. Yokoyama, *Phys. Rev. D* **63**, 043506 (2001) [arXiv:hep-ph/0007021].
- [134] M. Yamaguchi, *Phys. Rev. D* **64**, 063502 (2001) [arXiv:hep-ph/0103045].
- [135] M. Kawasaki and M. Yamaguchi, *Phys. Rev. D* **65**, 103518 (2002) [arXiv:hep-ph/0112093].
- [136] M. Yamaguchi and J. Yokoyama, index," *Phys. Rev. D* **68** (2003) 123520 [arXiv:hep-ph/0307373].
- [137] P. Brax and J. Martin, *Phys. Rev. D* **72**, 023518 (2005) [arXiv:hep-th/0504168].
- [138] R. Kallosh, arXiv:hep-th/0702059.
- [139] K. Kadota and M. Yamaguchi, *Phys. Rev. D* **76**, 103522 (2007) [arXiv:0706.2676 [hep-ph]].
- [140] M. B. Einhorn and D. R. T. Jones, *JHEP* **1003**, 026 (2010) [arXiv:0912.2718 [hep-ph]].
- [141] H. M. Lee, 'JCAP **1008**, 003 (2010) [arXiv:1005.2735 [hep-ph]].
- [142] F. Takahashi, arXiv:1006.2801 [hep-ph];
- [143] K. Nakayama and F. Takahashi, arXiv:1008.2956 [hep-ph].
- [144] E. Silverstein and A. Westphal, *Phys. Rev. D* **78**, 106003 (2008) [arXiv:0803.3085 [hep-th]].
- [145] L. McAllister, E. Silverstein and A. Westphal, arXiv:0808.0706 [hep-th].
- [146] J. J. Blanco-Pillado, R. Kallosh and A. D. Linde, *JHEP* **0605**, 053 (2006) [hep-th/0511042];
- [147] R. Kallosh and A. D. Linde, *JCAP* **0704**, 017 (2007) [arXiv:0704.0647 [hep-th]].
- [148] A. Linde, Y. Mambrini and K. A. Olive, *Phys. Rev. D* **85**, 066005 (2012) [arXiv:1111.1465 [hep-th]].
- [149] E. Dudas, A. Linde, Y. Mambrini, A. Mustafayev and K. A. Olive, *Eur. Phys. J. C* **73**, 2268 (2013) [arXiv:1209.0499 [hep-ph]].
- [150] S. Ferrara and R. Kallosh, *JHEP* **1112**, 096 (2011) [arXiv:1110.4048 [hep-th]].
- [151] A. D. Linde and V. Mukhanov, *Phys. Rev. D* **56**, 535 (1997) [arXiv:astro-ph/9610219]; K. Enqvist and M. S. Sloth, *Nucl. Phys. B* **626**, 395 (2002) [arXiv:hep-ph/0109214]; D. H. Lyth and D. Wands, *Phys. Lett. B* **524**, 5 (2002) [arXiv:hep-ph/0110002]; T. Moroi and T. Takahashi, *Phys. Lett. B* **522**, 215 (2001) [Erratum-ibid. B **539**, 303 (2002)] [arXiv:hep-ph/0110096].
- [152] V. Demozzi, A. Linde and V. Mukhanov, *JCAP* **1104**, 013 (2011) [arXiv:1012.0549 [hep-th]].
- [153] M. M. Anber and L. Sorbo, *JCAP* **0610**, 018 (2006) [astro-ph/0606534].
- [154] M. M. Anber and L. Sorbo, *Phys. Rev. D* **81**, 043534 (2010) [arXiv:0908.4089 [hep-th]].
- [155] R. Durrer, L. Hollenstein and R. K. Jain, *JCAP* **1103**, 037 (2011) [arXiv:1005.5322 [astro-ph.CO]].
- [156] N. Barnaby and M. Peloso, *Phys. Rev. Lett.* **106** (2011) 181301 [arXiv:1011.1500 [hep-ph]].
- [157] N. Barnaby, E. Pajer and M. Peloso, *Phys. Rev. D* **85**, 023525 (2012) [arXiv:1110.3327 [astro-ph.CO]].

- [158] P. D. Meerburg and E. Pajer, *JCAP* **1302**, 017 (2013) [arXiv:1203.6076 [astro-ph.CO]].
- [159] J. L. Cook and L. Sorbo, *Phys. Rev. D* **85** (2012) 023534 [Erratum-ibid. *D* **86** (2012) 069901] [arXiv:1109.0022 [astro-ph.CO]].
- [160] M. M. Anber and L. Sorbo, *Phys. Rev. D* **85** (2012) 123537 [arXiv:1203.5849 [astro-ph.CO]].  
N. Barnaby, J. Moxon, R. Namba, M. Peloso, G. Shiu and P. Zhou, *Phys. Rev. D* **86** (2012) 103508 [arXiv:1206.6117 [astro-ph.CO]].
- [161] P. Fayet, Talk at the XVIIth Rencontre de Moriond, Ecole Normale Superieure preprint LPTENS 82/10 (1982); S. Weinberg, *Phys. Rev. Lett.* **48**, 1303 (1982); J. R. Ellis, A. D. Linde and D. V. Nanopoulos, *Phys. Lett. B* **118**, 59 (1982); L. M. Krauss, *Nucl. Phys.* **B227**, 556 (1983); J. R. Ellis, J. S. Hagelin, D. V. Nanopoulos, K. A. Olive and M. Srednicki, *Nucl. Phys. B* **238**, 453 (1984); M. Y. Khlopov, A. D. Linde, *Phys. Lett.* **B138**, 265-268 (1984).
- [162] A. S. Josan, A. M. Green and K. A. Malik, *Phys. Rev. D* **79** (2009) 103520 [arXiv:0903.3184 [astro-ph.CO]].
- [163] C. T. Byrnes, E. J. Copeland and A. M. Green, *Phys. Rev. D* **86**, 043512 (2012) [arXiv:1206.4188 [astro-ph.CO]].
- [164] E. Bugaev and P. Klimai, *JCAP* **1111**, 028 (2011) [arXiv:1107.3754 [astro-ph.CO]]. E. Bugaev and P. Klimai, *Phys. Rev. D* **85**, 103504 (2012) [arXiv:1112.5601 [astro-ph.CO]]. P. A. Klimai and E. V. Bugaev, arXiv:1210.3262 [astro-ph.CO].
- [165] S. Shandera, A. L. Erickcek, P. Scott and J. Y. Galarza, arXiv:1211.7361 [astro-ph.CO].
- [166] T. Banks, M. Dine, P. J. Fox and E. Gorbatov, *JCAP* **0306** (2003) 001 [hep-th/0303252].
- [167] C. -M. Lin and K. -W. Ng, *Phys. Lett. B* **718**, 1181 (2013) [arXiv:1206.1685 [hep-ph]].
- [168] N. Arkani-Hamed and S. Dimopoulos, *JHEP* **0506**, 073 (2005) [arXiv:hep-th/0405159]; G. F. Giudice and A. Strumia, *Nucl. Phys. B* **858**, 63 (2012) [arXiv:1108.6077 [hep-ph]]; M. Ibe, S. Matsumoto and T. T. Yanagida, *Phys. Rev. D* **85**, 095011 (2012) [arXiv:1202.2253 [hep-ph]]; E. Dudas, A. Linde, Y. Mambrini, A. Mustafayev and K. A. Olive, arXiv:1209.0499 [hep-ph].
- [169] S. Antusch, K. Dutta and P. M. Kostka, *Phys. Lett. B* **677** (2009) 221 [arXiv:0902.2934 [hep-ph]].
- [170] S. Kachru, R. Kallosh, A. D. Linde and S. P. Trivedi, *Phys. Rev. D* **68** (2003) 046005 [arXiv:hep-th/0301240].
- [171] J. J. Blanco-Pillado *et al.*, *JHEP* **0411** (2004) 063 [arXiv:hep-th/0406230].
- [172] J. J. Blanco-Pillado *et al.*, *JHEP* **0609** (2006) 002 [arXiv:hep-th/0603129].
- [173] J. P. Conlon and F. Quevedo, *JHEP* **0601**, 146 (2006) [arXiv:hep-th/0509012].
- [174] M. Cicoli, C. P. Burgess and F. Quevedo, *JCAP* **0903**, 013 (2009) [arXiv:0808.0691 [hep-th]].
- [175] G. R. Dvali, Q. Shafi and R. K. Schaefer, *Phys. Rev. Lett.* **73** (1994) 1886 [arXiv:hep-ph/9406319].
- [176] P. Brax, C. van de Bruck, A. C. Davis and S. C. Davis, *JCAP* **0609** (2006) 012 [arXiv:hep-th/0606140].
- [177] Ph. Brax, C. van de Bruck, A. C. Davis, S. C. Davis, R. Jeannerot and M. Postma, *JCAP* **0701** (2007) 026 [arXiv:hep-th/0610195].

- [178] R. Kallosh and A. D. Linde, JHEP **0702** (2007) 002 [arXiv:hep-th/0611183].
- [179] J. P. Conlon, R. Kallosh, A. D. Linde and F. Quevedo, JCAP **0809** (2008) 011 [arXiv:0806.0809 [hep-th]].
- [180] H. Y. Chen, L. Y. Hung and G. Shiu, JHEP **0903** (2009) 083 [arXiv:0901.0267 [hep-th]].
- [181] M. Badziak and M. Olechowski, JCAP **1002**, 026 (2010) [arXiv:0911.1213 [hep-th]].
- [182] M. Badziak and M. Olechowski, JCAP **0902** (2009) 010 [arXiv:0810.4251 [hep-th]].
- [183] M. Badziak and M. Olechowski, JCAP **0807** (2008) 021 [arXiv:0802.1014 [hep-th]].
- [184] S. Antusch, M. Bastero-Gil, S. F. King and Q. Shafi, Phys. Rev. D **71** (2005) 083519 [arXiv:hep-ph/0411298].
- [185] E. Komatsu *et al.* [WMAP Collaboration], Astrophys. J. Suppl. **180** (2009) 330 [arXiv:0803.0547 [astro-ph]].
- [186] H. Collins, R. Holman and A. Ross, JHEP **1302**, 108 (2013) [arXiv:1208.3255 [hep-th]].
- [187] T. Markkanen and A. Tranberg, arXiv:1303.0180 [hep-th].
- [188] K. Enqvist and A. Mazumdar, Phys. Rept. **380** (2003) 99 [hep-ph/0209244].
- [189] I. Affleck and M. Dine, Nucl. Phys. B **249** (1985) 361.
- [190] M. Dine, L. Randall and S. D. Thomas, Nucl. Phys. B **458** (1996) 291 [hep-ph/9507453].
- [191] A. Linde, arXiv:1303.4435 [hep-th].
- [192] A. R. Liddle and D. H. Lyth, Phys. Rept. **231** (1993) 1 [astro-ph/9303019].

# Summary

I take it as a great privilege that for four years and a half already I have been around in this “Big Bang business”. On these pages I would like to clarify what this has been about for me: from a general introduction to cosmology to the research described in this thesis. Every now and then some corners are cut short, but then again I do not intend to keep the reader busy with this for four years and a half...

## Man in an expanding universe

As we cannot simply step out of it for a second, the universe should be studied from within. In this first paragraph I want to explain briefly how man, despite its modest place in the universe, manages to extract quantitative information from the night sky.

First of all we need a method to determine distances in the cosmos. In everyday life we perceive depth when our brain compares the separate images caught by our left and right eye. The so-called “parallax method” applies this same principle in astronomy. Two measurements, with an interval of six months, are made of the angle that a star makes with the horizon. In these six months the earth changes its position: she completes half of her orbit around the sun. Just like we do not see exactly the same with our left and right eye, the two measurements of the position of the star yield two different results. From their difference follows the distance to the star.

A second method makes use of the brightest light source we know in the universe: type IA supernovas. These are enormous explosions that occur in some binary systems (two stars orbiting each other). They are perfect to be used as lighthouses in the cosmos as, to a very good approximation, they are all equally bright. That is to say: if they had all been equally distant. By comparing a supernova’s brightness with those of another supernova whose distance to us we know, we find the distance to the first one.

Apart from the distance to a star we would also like to measure its velocity relative to us. This can for example be done by employing the Doppler effect. Anyone who has ever seen a fire truck passing knows this phenomenon. When the truck is approaching us the distance between two consecutive sound waves shrinks, and we hear the siren at a higher tone than the firemen do themselves. Once the fire truck has passed, its sound of waves reaching us are somewhat stretched out, and we perceive a lower tone.

This same effect also happens in the light waves that a star emits. When the star is moving towards us, its light waves seem to be closer to each other. When she is moving from us, we measure a larger distance between two consecutive wave fronts. By comparing a star’s emitted pattern to what we would measure had she been at rest, we find its velocity.

In this same way Edwin Hubble measured the distances and relative velocities of many stars in the

'20s of the last century. He found not only that all stars are moving from us, but also that their velocities are proportional to their distances from us. A star that is three times further from us than another one, is moving three times as fast from us. How is that possible? Hubble thought and concluded “Because they all started in the same point!” The Big Bang theory had been born. Everything began at the same point in space and time. Had this one star not been moving three times faster, it would not have got three times further from us. We are observing the consequences of a cosmic explosion: after 13.8 billion years pieces are still flying around.

## The background radiation

After Hubble the picture of the expanding, cooling universe has been refined much further. Increasingly precise measurements have yielded an ever more accurate model. This section is about one of the most important observations, indispensable for this thesis: the cosmic microwave background (CMB) radiation. When the universe was about 380,000 years old, the temperature decreased such that free electrons could no longer exist. Instead they got caught inside protons to form hydrogen. As a consequence, travelling light particles (photons) did no longer scatter off electrons, and their (straight) path through the cosmos was no longer disturbed. These photons are still travelling and produce a signal that we know as the CMB. It was discovered in the '60s by Penzias and Wilson in the US. Looking for something totally different, they tried their very best to get rid of this “noise” signal. They even checked their telescope for pigeon droppings, but the signal persisted to be there. At this point they were made aware of the work by George Gamow, who was the first to speculate about the CMB. By chance Penzias and Wilson turned out to have made a Nobelprize-worthy discovery: a baby picture of the universe. As the photons in the CMB have travelled freely to us since 380,000 years after the Big Bang<sup>1</sup>, they contain a lot of information about the early universe.

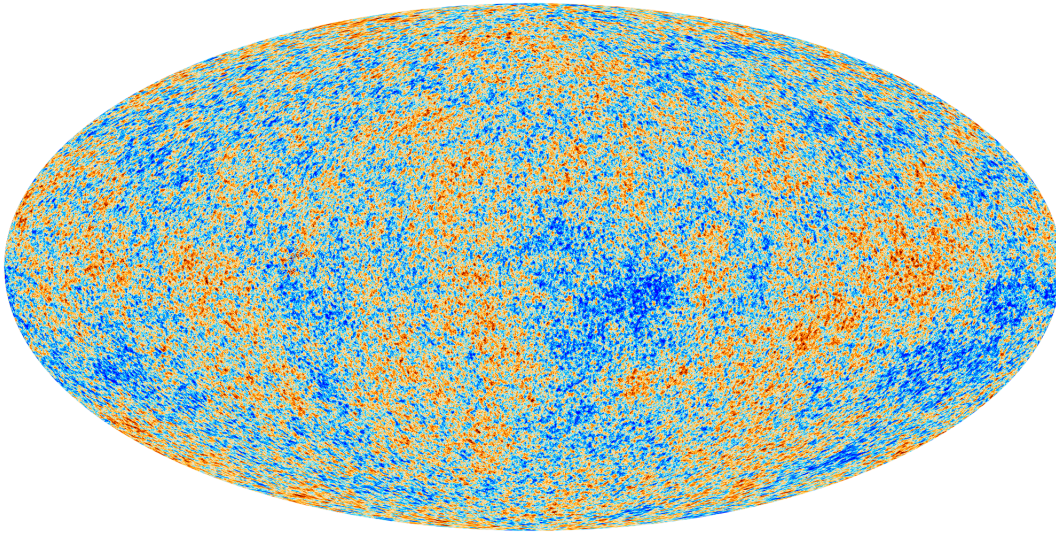
## Symmetry on large scales...

Then what do we see in the CMB? In two words: complete symmetry. The CMB's temperature is 2.73 Kelvin ( $\approx -270^\circ\text{C}$ ), in all directions. This is a very surprising result. Two photons reaching a telescope on earth from opposite directions, were very distant from each other when they began their journey. In 13.8 billion years such a photon travels 13.8 billion light years (not even taking into account the expansion of the universe). At the start of their straight flight they were therefore more than 27 billion light years apart. Now, Einstein prescribes that information can not travel faster than the speed of light. When the CMB was emitted, the universe was about 380,000 years old. At that moment we expect that information (like a temperature) can have travelled over 380,000 light years at most. It is therefore very surprising that two photons that were more than ten thousand times further apart, still had managed apparently to adjust to the same temperature.

The uniform CMB temperature fits in well with our general picture of the universe on large scales. (Note that by “large” we here mean cosmologically large: length scales of  $10^{24}$  meter and larger.) At such scales the visible universe looks the same everywhere and in all directions. Again the question rises: what caused all that homogeneity and isotropy?

---

<sup>1</sup>Note that the CMB was produced everywhere in the universe. Therefore there is no end to the CMB-bombardment. A CMB photon that arrives on earth today was simply produced a bit further away than one that was detected last year.



*Projection of the temperature of the CMB. Red areas are a fraction warmer than the general background temperature of 2.73 Kelvin, blue areas are somewhat colder. The difference between the warmest and coldest spots is one thousandth of a degree. (esa.int/planck)*

### **... perturbations on small scales**

On smaller scales the universe is of course not at all that homogeneous. The closer we look, the more “perturbations” of the cosmological equilibrium situation manifest themselves: from star clusters to this booklet. This leads us to a second interesting question: what causes these perturbations? How do the first lumps come about in the originally perfectly symmetric primordial soup? The answer is partly in the background radiation. It turns out that on top of the universal background temperature of 2.73 Kelvin there exist tiny temperature fluctuations: a photon from the one area is just one thousandth part of a degree colder than a photon from another area. This indicates that when the CMB was emitted gravity in such an area was just a tiny bit stronger than the global average<sup>2</sup>. At such a place the soup gets pulled a bit more and a little clump is formed, which in turn pulls the rest a bit harder. With this principle the structures in the current universe can be explained quite easily.

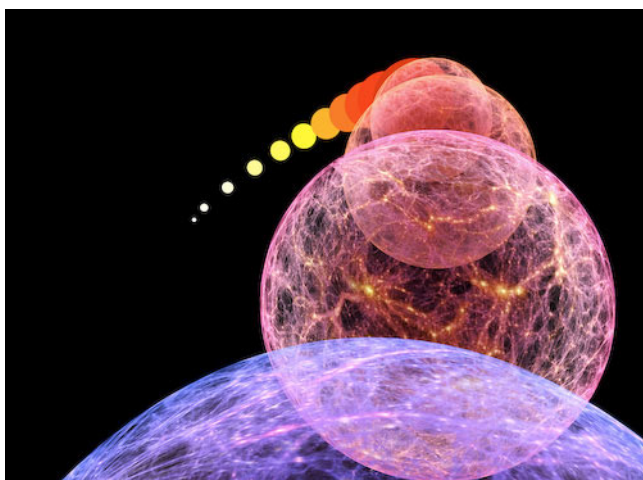
This answer to the question how structure formation begins instantly points to a new one: what causes the temperature fluctuations in the CMB? How come that already when the universe was only 380,000 years old, gravity was not totally homogeneous anymore?

## **Cosmological inflation**

The paradigm of cosmological inflation, proposed by Alan Guth in 1980 and further developed by (among many others) Slava Mukhanov and Andrei Linde, solves both of the problems sketched above in one go.

---

<sup>2</sup>A stronger gravitational force at some place attracts more particles and therefore leads to a higher temperature. However, it takes more energy now for a photon to escape. This is a stronger effect. The net result therefore is that we measure a somewhat lower temperature.



*Cosmological inflation: an explosion of space itself. This artist's impression shows what an "observer outside the universe" would see. (scienceblogs.com)*

Or better: in one explosion. The hypothesis is that when the universe was (much) younger than one second, it has undergone an enormous expansion. This adds to the "standard" expansion measured by Hubble. Guth demonstrated that if in a fraction of the first second the universe increases its size by a factor of  $10^{26}$  at least<sup>3</sup>, we can explain why it looks so homogeneous. According to Guth initially the universe does not have to be that homogeneous. The consequence of the enormous expansion (inflation) of the universe is that everything that we can see today, was confined to a very small space before inflation took place. At such small scales it is not difficult to imagine homogeneity.

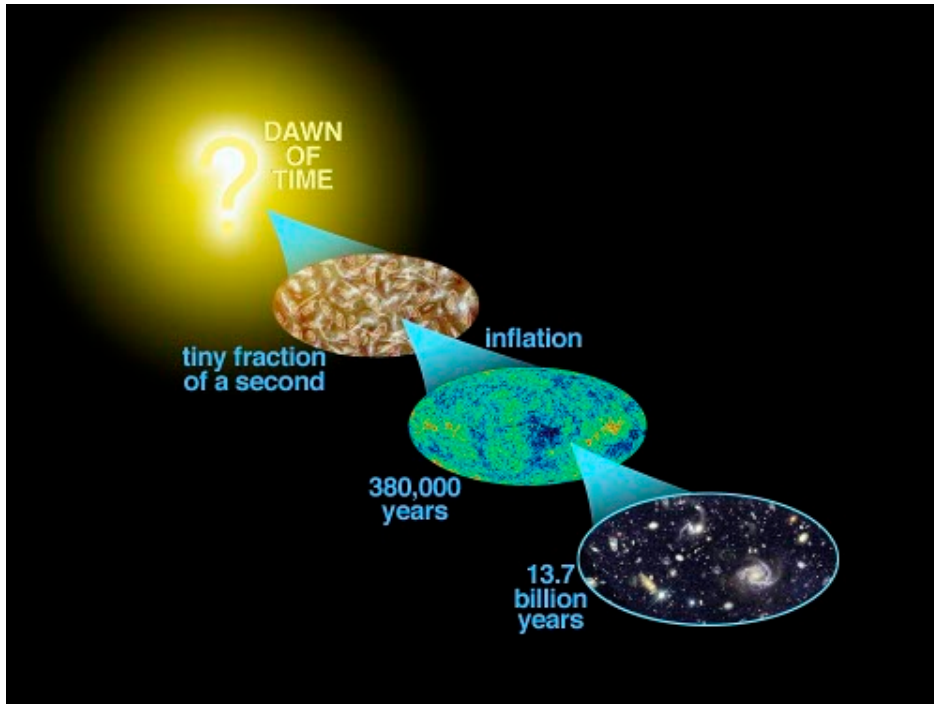
To understand how inflation solves the problem of structure formation as well, a bit more background knowledge is needed. Einstein has shown by his famous formula  $E = mc^2$  that to create a particle with mass  $m$  out of nothing, one needs an amount of energy of  $mc^2$ . At the other hand there is quantum mechanics stating that on the smallest length scales (the order of the size of an atom, about  $10^{-10}$  meter) there is always some uncertainty in the amount of energy. Even in the vacuum there can be some energy for some short time. And where there is energy, there can be particles! Merging Einstein's (special) relativity with quantum mechanics shows that even in the vacuum two particles can be created out of nothing, which after a short time collide and disappear in thin air again. The vacuum therefore is not really empty. It is more like a boiling pot, with bubbles of the size of an atom.

The work done by Mukhanov has shown that during inflation this process of particle creation and annihilation is hampered. Because of the very rapid expansion of the universe, both particles do not get back to each other anymore. The bubbles in the vacuum do not disappear anymore, but are blown up to sizes that exceed quantummechanical scales and that can influence the "big" world. In his famous calculation, partly sketched in chapter 1, Mukhanov showed that blown up quantum bubbles precisely form the seeds that (over the next 380,000 years) grow into the tiny temperature fluctuations in the CMB. Ultimately all structure that we know originates from a pot of primordial soup that is boiling over!

In the last 30 years hundreds of models of inflation have been proposed. The most influential model builder is probably Andrei Linde, who is also co-author of article [5] on which this thesis is based. Every

---

<sup>3</sup>This expansion is faster than the speed of light, but there is no violation of special relativity. It is space itself that is expanding, there is no information travelling faster than light through space.



*The history of the universe. Before (and during) the Big Bang we know nothing. Inflation blows up a small, causally connected part of space thereby generating the homogeneous universe that we observe. Quantum bubbles (of the inflaton field) are stretched out and lead to the temperature fluctuations in the background radiation. These evolve further to all structures we observe in the universe today. (scienceblogs.com)*

model is characterized by the properties of the “inflaton” (the particle that causes inflation to happen) and the forces that act on it. This leads to precise predictions of the statistical properties of the CMB fluctuations that can be tested experimentally.

## Inflation with the Higgs field

Recently there has been much attention for models that make the Higgs particle (discovered at CERN in Geneva last year) responsible for inflation. This has the advantage that there is no need to postulate a new particle (all other known particles are fundamentally incapable). Therefore the number of new parameters to be determined experimentally is minimal. Even better: by combining the results of the LHC (like the mass of the Higgs particle) with cosmological measurements of the CMB, the theory can really be tested. At the moment the Higgs mass seems a tiny bit too small for the model to work. However there are still too many issues not well understood, theoretical as well as experimental, to be able to draw a definitive conclusion.

The chapters 3 and 4 of this thesis describe our research of one of these not well understood elements of Higgs inflation. When the Higgs particle is used in the early universe as an inflaton, it has more freedom of movement than when it is measured at CERN. The vibrations of the quantum field associated to the Higgs particle follow a pattern that is more dynamical. That is why the usual Higgs theory needs to

be generalized. In a simplified model we have precisely shown what are the consequences of these extra dynamics, and shown how the theory is still “gauge invariant” (invariant under modification of certain parameters).

## Superinflation

Since the early '70s there has been a lot of interest for supersymmetry, supergravitation and superstring-theory. These “supertheories” have in common that, by proposing (many) new particles, some theoretical shortcomings of the current standard theorem can be overcome. The ultimate goal: a theory that describes gravity on quantum scales, has still not been found. However, the validity of standard theorems can be stretched out to higher energy scales. Experimentally, however, no postulated new “superparticle” has been found. Another problem is that the huge number of unknown parameters in these new theorems drastically reduces their predictability.

The chapters 5 and 7 of this thesis describe how inflation can work in such a “super context”. Chapter 5 tries to decouple the dynamics of inflation as much as possible from the model’s other dynamics. In this way inflation’s predictability can be maintained, even if there is so little quantitative information available about the other (super)particles in the model. Chapter 7 shows how an existing model of inflation can be made compatible with superstringtheory. This last theory requires the existence of extra spatial dimensions, which are only observable on extremely high (experimentally unaccessible) energy scales. Still these extra dimensions have some indirect influence on the physics on lower energy scales, and we have shown under which conditions these new effects do not spoil inflation.

## Particle production during inflation

Chapter 6 looks at a model in which during inflation extra particles are produced. It follows from adding one new particle and one new coupling (between that particle and the inflaton) to the most standard model of inflation. The question is now: which observable quantity is most sensitive to this new coupling, and can therefore be used to constrain it? We have pointed out that, contrary to what was claimed in literature, for once this observable was not to be found in the CMB. It turns out that the very limited presence of a certain type of black holes in the universe puts the most stringent pressure on this proposed coupling. We show as well how these same models can still work in an “superenvironment” (embedded in a model of supergravitation).

## Future research

So what is next now? I know more than four years and a half ago, but I have more questions as well. At this point my first goal is to work out the model of Higgs inflation in much further detail. Different research groups have different opinions on the theory’s precise predictions, and I first of all want to work out how the effects studied by us further influence this debate. But there is so much more to do, also because the new measurements of the PLANCK satellite constrain the existing models ever further. Less than a hundred years after Hubble’s discovery cosmology has become a precision science. I am happy that I will have three more years at least to work on that, at a place where the sun shines in daytime and the stars light up at night...

# Samenvatting

Ik vind het een groot voorrecht dat ik al vier en een half jaar in het “oerknalwereldje” heb mogen meelopen. Op deze pagina's licht ik graag toe wat dat tot nu toe voor mij behelst heeft: van een algemene inleiding in de kosmologie tot aan het in dit proefschrift beschreven onderzoek. Af en toe worden er wat bochtjes kort afgesneden, maar ik wil de lezer ook geen vier en een half jaar bezig houden...

## De mens in het uitdijend universum

Aangezien we er niet even uit kunnen stappen, moet het heelal van binnenuit bestudeerd worden. In deze eerste sectie wil ik kort uitleggen hoe de mens er, ondanks zijn bescheiden positie in het universum, in slaagt om kwantitatieve informatie uit de sterrenhemel af te leiden.

Allereerst hebben we een manier nodig om afstanden te bepalen in het heelal. In ons dagelijks leven zien wij diepte doordat onze hersenen de door beide ogen opgevangen beelden met elkaar vergelijken. De zogenaamde “parallaxmethode” past ditzelfde principe toe in de sterrenkunde. Met een tussenpoos van een half jaar wordt tweemaal de hoek gemeten die een bepaalde ster maakt met de horizon. In dit half jaar verandert de aarde van plaats: zij legt een halve baan om de zon af. Precies zoals we met ons linkeroog niet precies hetzelfde zien als met ons rechteroog, leveren de twee metingen van de positie van de ster twee verschillende resultaten op. Uit het verschil volgt de afstand tot de ster.

Een tweede methode maakt gebruik van de helderste lichtbron die we kennen in het heelal: type IA supernova's. Dit zijn enorme explosies die optreden in sommige dubbelstersystemen (twee sterren die om elkaar heen draaien). Ze zijn ideaal te gebruiken als vuurtorens in het heelal omdat ze bij zeer goede benadering allemaal even helder zijn. Dat wil zeggen: als ze allemaal even ver weg zouden staan. Door de helderheid van een supernova te vergelijken met die van een andere waarvan de afstand bekend is vindt men de afstand tot de eerste supernova.

Behalve de afstand tot een ster willen we ook haar relatieve snelheid ten opzichte van ons meten. Dit kan bijvoorbeeld door gebruik te maken van het Dopplereffect. Iedereen die op straat wel eens een brandweerwagen voorbij heeft horen rijden kent dit verschijnsel. Wanneer de brandweerwagen op ons af komt rijden daalt de afstand tussen opeenvolgende geluidsgolven en horen we de sirene daarom op een hogere toon dan de brandweermannen zelf. Eenmaal gepasseerd zijn de geluidsgolven die bij ons komen juist wat uitgerekt en horen we een lagere toon.

Hetzelfde effect treedt op in de lichtgolven die een ster uitzendt. Beweegt de ster naar ons toe, dan lijken haar lichtgolven wat dichter bij elkaar te liggen. Beweegt ze van ons af, dan meten we een wat grotere afstand tussen twee opeenvolgende golffronten. Door het uitgezonden patroon van lichtgolven van een ster te vergelijken met wat we zouden meten als zij stil zou staan, vinden we de snelheid van de ster.

Op deze manier mat Edwin Hubble in de jaren '20 van de vorige eeuw van vele sterren hun afstanden en relatieve snelheden. Niet alleen vond hij dat alle sterren van ons af bewegen, maar ook dat deze snelheid recht evenredig is met haar afstand tot ons. Als een ster drie keer zo ver weg staat als een andere, beweegt zij ook drie keer zo snel van ons af. Hoe kan dat? Hubble dacht na en zei "Omdat ze allemaal in hetzelfde punt begonnen zijn!" De oerknaltheorie was geboren. Alles is op hetzelfde punt in ruimte en tijd begonnen. Als die ene ster niet driemaal zou hard zo gaan, was ze niet driemaal zo ver bij ons vandaan geraakt. Wij kijken naar de gevolgen van een kosmische explosie: na 13,8 miljard jaar vliegen de brokstukken nog steeds in het rond.

## De achtergrondstraling

Na Hubble is het beeld van het uitdijend, afkoelend universum veel verder ingekleurd. Steeds preciezere metingen hebben een immer accurater model opgeleverd. Deze paragraaf gaat over één van de belangrijkste observaties, onmisbaar voor dit proefschrift: de kosmische achtergrondstraling. Toen het heelal ongeveer 380.000 jaar oud was, zakte de temperatuur zodanig dat electronen niet meer vrij voor konden komen, maar door protonen ingevangen werden om waterstof te vormen. Als gevolg hiervan botsten rondreizende lichtdeeltjes (fotonen) niet meer voortdurend op electronen, maar konden ze ongestoord hun rechte weg vervolgen, als Mozes door de Rode Zee. Deze fotonen reizen nog steeds en vormen een signaal dat de "achtergrondstraling" genoemd wordt, of CMB (Cosmic Microwave Background) radiation. In de jaren '60 werd de achtergrondstraling ontdekt door Penzias en Wilson in de USA. Op zoek naar iets heel anders deden ze alle moeite om deze "ruis" weg te werken. Ze controleerden hun telescoop zelfs op duivenpoep, maar het signaal bleef aanwezig. Op dit punt werden ze gewezen op het theoretisch werk van George Gamow, die als eerste over de CMB gesproken had. Bij toeval bleken Penzias en Wilson een ontdekking gedaan te hebben die de Nobelprijs waard was: een babyfoto van het universum. Omdat de fotonen in de CMB sinds 380.000 jaar na de oerknal vrijwel onverstoord hun enorme weg naar de aarde af hebben kunnen leggen<sup>4</sup>, zijn zij uitstekend geschikt om inzicht te krijgen in het vroege heelal.

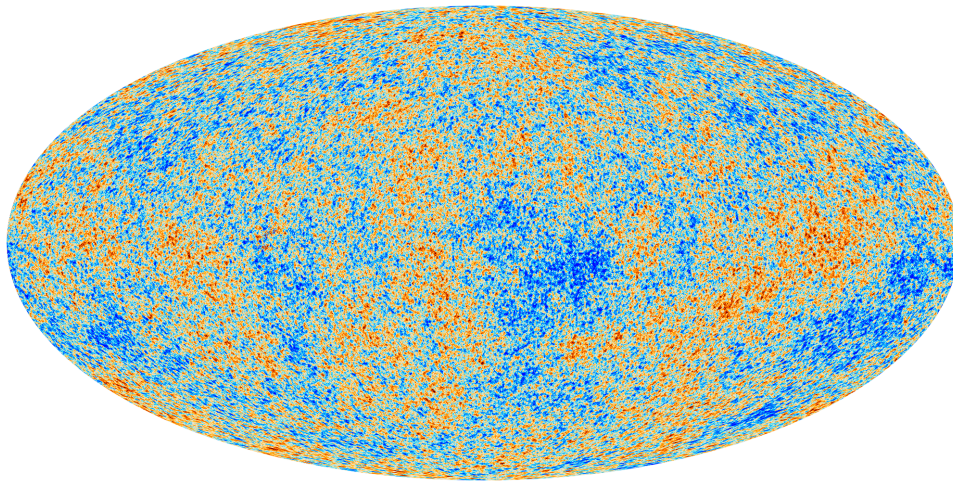
## Symmetrie op grote schalen...

Wat zien we dan in de CMB? In twee woorden: totale symmetrie. De temperatuur van de CMB is 2,73 Kelvin ( $\approx -270^\circ\text{C}$ ), in alle richtingen. Dit is een zeer verrassend resultaat. Twee fotonen die uit tegengestelde richting in een aardse telescoop belanden, zijn zeer ver van elkaar aan hun reis begonnen. Ga maar na: in 13,8 miljard jaar legt zo'n foton 13,8 miljard lichtjaar af (en dan hebben we de expansie van het heelal nog niet eens meegerekend). Aan het begin van hun reis waren ze dus een dikke 27 miljard lichtjaar van elkaar verwijderd. Nu, Einstein schrijft voor dat informatie niet sneller dan het licht kan reizen. Toen de CMB uitgezonden werd, was het heelal 380.000 jaar oud. Op dat moment verwachten we dat informatie (zoals over een temperatuur) over maximaal 380.000 lichtjaar gereisd kan hebben. Het is dus zeer verrassend dat twee fotonen die meer dan tienduizend maal verder van elkaar afstonden, blijkbaar toch al kans hadden gezien om hun temperatuur op elkaar af te stemmen.

De uniforme CMB temperatuur past precies in het beeld dat we hebben van het universum op grote schalen. (Let op, met "groot" wordt hier kosmologisch groot bedoeld: lengteschalen van  $10^{24}$  meter en groter.) Op zulke schalen ziet het zichtbare heelal er overal en in alle richtingen hetzelfde uit. Opnieuw is de vraag: waar komt al die homogeniteit en isotropie vandaan?

---

<sup>4</sup>Merk op dat de CMB van overal in het universum uitgezonden werd. Er komt dus geen eind aan het CMB-bombardement. Wel zijn de CMB-fotonen die nu binnenkomen dus nog iets verder weg geproduceerd dan die die vorig jaar gemeten werden.



*Projectie van de temperatuur van de kosmologische achtergrondstraling. Rode gebiedjes zijn een fractie warmer dan de uniforme achtergrondtemperatuur van 2,73 Kelvin, blauwe gebiedjes zijn iets kouder. Het verschil tussen de warmste en de koudste plek is één duizendste graad. (esa.int/planck)*

## ... verstoringen op kleine schalen

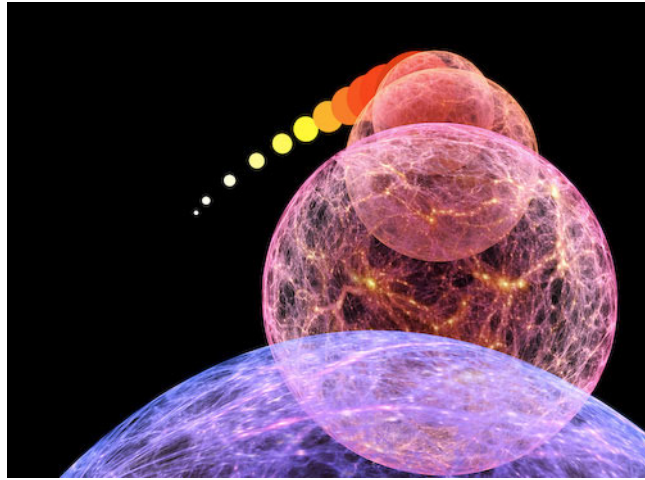
Op kleinere schalen is het heelal natuurlijk helemaal niet zo homogeen. Hoe dichterbij we kijken, hoe meer “verstoringen” van de kosmologische evenwichtssituatie in beeld komen: van sterrenstelsels tot dit boekje. Dit levert een tweede interessante vraag op: waar komen die verstoringen vandaan? Hoe ontstaan de eerste klonten in de aanvankelijk perfect symmetrische kosmologische oersoep? Het antwoord is deels in de achtergrondstraling te vinden. Het blijkt namelijk dat bovenop de uniforme achtergrondtemperatuur van 2,73 Kelvin nog minieme temperatuurfluctuaties zitten: een foton uit het ene gebiedje is net een duizendste deel van een graad kouder dan een foton uit het andere. Dit betekent dat toen de CMB uitgezonden werd de zwaartekracht in zo'n gebiedje net iets sterker was dan verderop<sup>5</sup>. Op zo'n plek wordt dan iets harder aan de soep getrokken en ontstaat er een klontje dat dan vervolgens weer iets harder aan de rest trekt. Zo kunnen de structuren in het huidige heelal vrij eenvoudig verklaard worden.

Dit antwoord op de vraag hoe structuurgroei begint leidt direct tot een nieuwe vraag: waar komen de temperatuurfluctuaties in de achtergrondstraling dan vandaan? Wat heeft ervoor gezorgd dat toen het heelal pas 380.000 jaar oud was, de zwaartekracht al niet meer helemaal homogeen was?

## Kosmologische inflatie

Het paradigma van kosmologische inflatie, voorgesteld door Alan Guth in 1980 en verder uitgewerkt door (o.a.) Slava Mukhanov en Andrei Linde, lost beide problemen in één klap op. Of beter: in één explosie. De hypothese is dat toen het universum nog (veel) minder dan een seconde oud was, het een enorme uitdijning ondergaan heeft. Deze komt dus bovenop de “standaard” uitdijning die Hubble gemeten heeft.

<sup>5</sup>Een sterkere zwaartekracht op een bepaalde plaats leidt tot meer deeltjes op en daardoor tot een hogere temperatuur. Echter: het kost een foton meer energie om te ontsnappen. Dit is een sterker effect. Netto meten we daarom juist een iets lagere temperatuur.



*Kosmologische inflatie: een explosie van de ruimte zelf. Deze artist's impression geeft weer wat een "waarnemer buiten het universum" zou zien. (scienceblogs.com)*

Guth rekende voor dat als het universum in een fractie van de eerste seconde minimaal  $10^{26}$  groter wordt<sup>6</sup>, we kunnen verklaren waarom het zo homogeen lijkt. Volgens Guth hoeft het heelal aanvankelijk helemaal niet zo homogeen te zijn. Het gevolg van de enorme uitdijing (inflatie) van het heelal is dat alles wat wij vandaag de dag kunnen zien, voor inflatie een enorm kleine ruimte innam. Op zulke kleine afstanden is het niet moeilijk om homogeniteit voor te stellen.

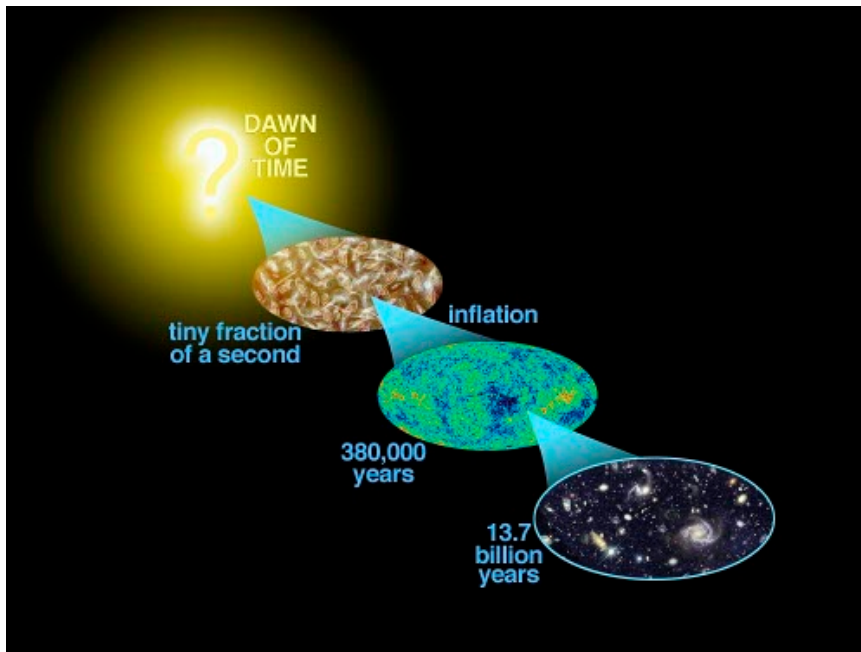
Om in te zien hoe inflatie ook het probleem van structuurvorming oplost, is iets meer achtergrondkennis nodig. Einstein heeft via zijn beroemde formule  $E = mc^2$  laten zien dat om een deeltje met massa  $m$  uit het niets te creëren, een energiebedrag van  $mc^2$  nodig is. Aan de andere kant leert de quantummechanica dat er op de kleinste lengteschalen (op de orde van de afmetingen van een atoom, circa  $10^{-10}$  meter) altijd een onzekerheid in de hoeveelheid energie is. Zelfs in het vacuüm kan er eventjes wat energie zijn. En wie energie zegt, zegt deeltjes! Wie Einstein en de quantummechanica samenvoegt, snapt dat zelfs in het vacuüm twee deeltjes uit het niets kunnen ontstaan, om kort daarna in een botsing met elkaar weer in het niets op te lossen. Het vacuüm is daarom niet echt leeg. Het is meer een borrelend vat, met bubbeltjes ter grootte van een atoom.

Het werk van Mukhanov heeft aangetoond dat tijdens inflatie dit proces van deeltjescreatie en -annihilatie gedwarsboomd wordt. Doordat het heelal zo snel uitdijt, vinden beide deeltjes elkaar niet meer terug. De bubbeltjes in het vacuüm verdwijnen niet meer, maar worden opgeblazen tot groottes die de quantumschalen overstijgen en de "grote" wereld kunnen beïnvloeden. In zijn beroemde berekening, deels geschetst in hoofdstuk 1, liet Mukhanov zien dat het precies de opgeblazen quantumbubbels zijn die (in 380.000 jaar) uitgroeien tot de minieme temperatuurfluctuaties in de CMB. Zo vindt alle structuur die wij kennen haar oorsprong in een pannetje overkokende oersoep!

In de afgelopen dertig jaar zijn er honderden modellen van inflatie voorgesteld. De meest invloedrijke modelbouwer is waarschijnlijk Andrei Linde, tevens co-auteur van artikel [5] waarop hoofdstuk 6 gebaseerd is. Elk model wordt gekarakteriseerd door de eigenschappen van het "inflaton" (het deeltje dat inflatie veroorzaakt) en de krachten die op dat deeltje werken. Dit leidt tot precieze voorspellingen van de

---

<sup>6</sup>Deze uitdijing gaat sneller dan het licht, maar is niet in strijd met de speciale relativiteitstheorie. Het is de ruimte zelf die uitdijt, er reist geen informatie sneller dan het licht door de ruimte.



*De geschiedenis van het universum. Voor (en tijdens) de oerknal weten we niks. Inflatie blaast een klein, causaal verbonden gedeelte van de ruimte op en genereert zo het homogene heelal dat wij waarnemen. Quantumbubbels (van het inflatonveld) worden opgeblazen en leiden tot de temperatuurfuctuaties in de achtergrondstraling. Deze groeien uit tot alle structuren die we nu waarnemen in het heelal. (scienceblogs.com)*

statistische eigenschappen van de CMB temperatuurfuctuaties die experimenteel getoetst kunnen worden.

## Inflatie met het Higgsveld

Recent is er veel aandacht geweest voor modellen die het Higgsdeeltje (vorig jaar ontdekt op CERN in Genève) verantwoordelijk maken voor inflatie. Dit heeft als voordeel dat er geen nieuw deeltje gepostuleerd hoeft te worden (alle andere bekende deeltjes zijn fundamenteel ongeschikt). Hierdoor is het aantal nieuwe, experimenteel te bepalen parameters ook minimaal. Sterker nog: door meetgegevens van de LHC (zoals de Higgsmassa) te combineren met kosmologische metingen aan de CMB kan de theorie echt getest worden. Op dit moment lijkt de Higgsmassa een fractie te klein om het model te laten werken, maar er zijn nog teveel onbegrepen elementen, zowel theoretisch als experimenteel, om tot een definitieve conclusie te komen.

De hoofdstukken 3 en 4 van dit proefschrift beschrijven ons onderzoek naar één van deze onbegrepen elementen van Higgs inflatie. Wanneer het Higgsdeeltje in het vroege heelal als inflaton gebruikt wordt, heeft het meer bewegingsmogelijkheden dan wanneer het in CERN gemeten wordt. De trillingen van het aan het Higgsdeeltje geassocieerde quantumveld volgen een patroon dat meer dynamisch is. Daarom moet de gangbare Higgstheorie gegeneraliseerd worden. In een versimpeld model hebben wij precies de effecten van deze extra dynamica laten zien, en toegelicht hoe de theorie nog steeds “ijkinvariant” (onverschillig

onder verandering van bepaalde parameters) is.

## Superinflatie

Sinds de vroege jaren '70 is er veel aandacht geweest voor supersymmetrie, supergravitatie en supersnaartheorie. Deze “supertheorieën” hebben gemeen dat ze door het introduceren van (vele) nieuwe deeltjes theoretische onvolkomenheden van de heersende “standaardtheorie” overkomen. Het ultieme doel: een theorie die de zwaartekracht tot op de quantumschalen beschrijft, is echter nog steeds niet gevonden. Wel kan de geldigheid van standaardtheorieën tot hogere energieschalen worden uitgerekt. Experimenteel echter is er op het moment van schrijven nog steeds geen nieuw voorspeld “superdeeltje” gevonden. Het enorm aantal onbekende parameters in deze nieuwe theorieën zorgt daarnaast voor een drastische reductie van hun voorspelbaarheid.

De hoofdstukken 5 en 7 van dit proefschrift beschrijven hoe inflatie kan werken in zo'n “superomgeving”. Hoofdstuk 5 probeert om de dynamica van inflatie zoveel mogelijk los te koppelen van alle andere dynamica in het model. Zo kan de voorspelbaarheid van de inflatietheorie overeind blijven, ook als er zo weinig kwantitatieve informatie is over de andere deeltjes in het model. Hoofdstuk 7 laat zien hoe een bestaand model van inflatie compatibel gemaakt kan worden met supersnaartheorie. Deze laatste theorie beschrijft het bestaan van extra ruimtelijke dimensies, die alleen toegankelijk zijn op extreem hoge (experimenteel onbereikbare) energieschalen. Toch hebben deze extra dimensies indirect ook invloed op de fysica op lagere energieschalen, en wij hebben laten zien onder welke voorwaarden inflatie nog steeds plaats kan vinden.

## Deeltjesproductie tijdens inflatie

Hoofdstuk 6 kijkt naar een model waarin tijdens inflatie nog extra deeltjes worden geproduceerd. Aan het meest standaard inflatiemodel wordt één extra deeltje en één extra koppeling (tussen dat deeltje en het inflaton) toegevoegd. De vraag is nu: welke observabele grootte geeft de scherpste eisen op de grootte van deze extra koppeling? Wij hebben laten zien dat, in tegenstelling tot wat algemeen beweerd werd in de literatuur, deze observabele voor de verandering eens niet in de CMB te vinden is. Het blijkt dat de beperkte aanwezigheid van een bepaald type zwarte gaten in het universum de nieuw voorgestelde koppeling het meest onder druk zet. Ook laten we zien hoe deze zelfde modellen in een “superomgeving” (ingebed in een supergravitatie model) kunnen blijven werken.

## Toekomstig onderzoek

En nu? Ik weet meer dan vier en een half jaar geleden, maar ik heb ook veel meer vragen. Mijn eerste doel op dit moment is om het model van Higgs inflatie veel preciezer uit te werken. Verschillende onderzoeksgroepen verschillen van mening over de precieze voorspellingen van de theorie, en ik wil als eerste uitwerken hoe de door ons onderzochte effecten hier verder invloed op hebben. Maar er is zoveel meer te doen, ook omdat de nieuwe metingen van de PLANCK satelliet de bestaande modellen steeds verder inperken. Minder dan honderd jaar na de ontdekkingen van Hubble is kosmologie een precisiewetenschap geworden. Ik ben blij dat ik daar nog minstens drie jaar aan verder mag werken op een plek waar overdag de zon schijnt en 's nachts de sterren oplichten...

# Acknowledgments

This is the end of my thesis, and the end of four and a half years in the theory group at Nikhef. I was expecting to be at the top of the mountain I saw ahead of me in 2009. Well, I have gained some height for sure, but I cannot say that the top seems any nearer now. However, it has been a beautiful trip, and I am eager to continue. At this point I want to thank the people who helped me come up to here.

First and for all comes my daily advisor Marieke Postma. Sharp but patient while working, and so relaxed to hang out with on the balcony, on a frozen lake, on the road or wherever: I could not have wished for a better supervisor. Thank you for making these years such a pleasure.

My official promotor is Eric Laenen. In day-to-day life Marieke took care of all supervision, but I want to thank you for convincing me to come here, and especially for providing the opportunity to do an internship at Stanford.

Next I want to thank all the collaborators I have had so far. I have enjoyed and shamelessly benefited from discussing and working with Ana Achúcarro, Damien George, Andrei Linde, Pablo Ortiz and Enrico Pajer, and I hope that there still is a lot more to come. I also want to thank my “cosmolega” Jan Weenink for all our discussions and good times we had roaming through cosmology.

I like the life in our theory group a lot and for that I want to thank all of its (ex-)members. The interference between daily (lunch, coffee, balcony), weekly (windmill), monthly (theorists invading Nikhef) and yearly (day out and especially Sinterklaas) rhythms produces a very pleasantly resonating vibe in the group, where physics, metaphysics and all life in between is discussed.

I thank my parents for all their support and stimulation, and also for leaving me free to study whatever I choose. I want to thank my uncles and aunt Jan, Bernard and Hetty for introducing me to the beauty of physics and my uncle Wolf for introducing me to the art of survival in science.

Les dernières paroles de cette thèse sont pour mon amour Stéphanie Moy avec qui la vie est tellement plus belle. Merci BA pour être là, pour être ouverte à tout, pour me montrer une vie riche et chaude, pour ta patience quand ma tête est perdue dans l’univers et surtout pour vouloir vivre ta vie avec moi!